Thesis

Interactions of Radionuclides with Cellulose Degradation Products

By Charlotte Rebecca Heath

SUBMITTED IN PARTIAL FULFILMENT OF THE REQUIREMENTS FOR THE AWARD OF

DOCTOR OF PHILOSOPHY

Loughborough University

September 2008

Research Supervisor Professor Peter Warwick

ABSTRACT

The aim of this work was to determine the solubility of radionuclides in solutions of cellulose degradation products (CDP) and isosaccharinic acid (ISA) the main product of cellulose degradation. Thorium was the main radionuclide investigated as the solubility of tetravalent actinides in the near field of a nuclear waste repository at high pH and low Eh has been shown to increase in the presence of such ligands. The measurement of thorium solubility was achieved by using different methods e.g. liquid scintillation counting, gamma spectrometry, ICP-MS and ICP-OES. ICP-OES was shown to be the most accurate method for this analysis. Various methods have been used to obtain solubility values e.g. undersaturation and oversaturation, and these have been investigated to determine whether the values obtained from these methods differ. Solubility studies were carried out at different pHs (6, 8 and 12). The kinetics of the complexation of thorium with ISA and with CDP were investigated at these pHs. The concentration of ISA in a solution of synthesised 10% CDP was approximately 0.01 mol dm^{-3}. In high pH solutions, the solubility of thorium was found to be 31 times greater in a solution of CDP compared to a solution of ISA at the same ISA concentration. No significant differences in thorium solubilities were found in similar solutions at pH 6 and 8.

The solubilities of cobalt, nickel and cadmium were measured in the presence of 10% CDP and an equivalent concentration of ISA. The solubilities of all the metals studied in a CDP solution increased when compared to solubilities in ISA. These findings suggest that there are other complexing ligands present in the CDP other than ISA. The CDP mixture was investigated by LC-ICP-MS to determine what other complexing agents were increasing the metal's solubility. Preliminary results suggested that most of the thorium was complexed in the CDP mixture as there was little evidence for the presence of free thorium in solution and that thorium was complexed with a number of different components in the CDP solution.

Solid state NMR studies and Gaussian modelling of M:ISA complexes was carried out to investigate the bonding mechanisms of metals to ISA when ISA was in either the lactone or open chain form. Measurement of chemical shift changes on a ^{13}C spectrum using solid state NMR at pH 7 showed that there was little complexation of ligand with the metal. Cadmium, europium and iron showed the biggest change in chemical shift in high pH conditions at the carboxylate end of the ISA ligand suggesting that this was where the metal was most likely to

be bound. Gaussian modelling was carried out on the Cd:ISA complexes, investigating 1:1 monodentate and bidentate binding of the metal to the ISA and 2:1 M:ISA complexes. These results supported the results obtained from the experimental work although further modelling is needed to obtain firm conclusions as to where and how metal is bound to ISA.

ACKNOWLEDGEMENTS

Throughout my PhD there have been a number of people who have been a great support for me over the three years. Firstly I would like to thanks my supervisor Professor Peter Warwick for his constant support and guidance, for being an excellent mentor and a real inspiration to me.

I am grateful to Professor Warwick and to Loughborough University for financially supporting my PhD studies.

For their technical help I would like to thank like to thank Dr Mark Edgar for all his time and effort with the NMR work, Dr Sandie Dann for her XRD expertise, Dave Wilson for always being on hand when there was an HPLC problem, Dr George Weaver, Professor Roger Smith, Dr Caroline Kirk, Trevor Brown, Claire Maskell, Dhinesh Asogan, Dr Tamer Shoeib, Dr Sam Kerr and Dr Mark Cowper and Professor Francis Livens for allowing me to work alongside them at Serco and Manchester respectively.

Special thanks should go to the Radiochemistry Group at Loughborough and friends in the department, Dr Nick Evans, Linda Sands, Adam Douglas, Ricky Hallam, Anumaija Leskinen, Silvia Anton Gascon, Fidelis Sameh Ebong, Katie Titley, Dhinesh Asogan, Amber Lowe, Tom Varley and especially Dr Tara Lewis for not only helping me professionally but also being a great support and always listening to my constant chatter!

I would also like to thank Alexia, Dan, my fellow Amigo's and the girls of 61 Storer Road for keeping me sane, always managing to make me laugh and putting up with my moaning and a few tears along the way!

Finally the biggest thanks should go to my parents for always believing in me, never letting me give up on myself and providing much needed manicures, facials, petrol in my car etc... when needed!

TABLE OF ABBREVIATIONS

Chemical agents and terminology

CDP – Cellulose Degradation Products

Da MWCO – Dalton Molecular Weight Cut Off

DI - Deionised

HOMO – Highest Occupied Molecular Orbital

HSAB – Hard Soft Acid Base Theory

ISA – Isosaccharinic Acid

LUMO – Lowest Unoccupied Molecular Orbital

M:ISA – Metal:ISA Complex

M:L – Metal:Ligand Complex

NRVB – Nirex Reference Vault Backfill

OPC – Ordinary Portland Cement

PCM – Plutonium Contaminated Material

PFA – Pulverised Fuel Ash

THPA – Tetrahydroxypentanoic Acid

Analytical methods

CE – Capillary Electrophoresis

CP – Cross Polarisation

CSA – Chemical Shift Anisotropy

FTIR – Fourier Transform Infra Red

HPAEC – High Performance Anion Exchange Chromatography

HPIEC – High Performance Ion Exchange Chromatography

HPLC – High Performance Liquid Chromatography

ICP – Inductively Coupled Plasma

LC – Liquid Chromatography

LCR – Low Count Reject

LOD – Limit of Detection

LSC – Liquid Scintillation Counting

MAS – Magic Angle Spinning

MS – Mass Spectrometry

NMR – Nuclear Magnetic Resonance

OES – Optical Emission Spectroscopy

REDOR – Rotational Echo Double Resonance

SS NMR – Solid State NMR

SSB – Spinning Side Bands

XRD – X Ray Diffraction

Nuclear Industry Terminology

BNFL – British Nuclear Fuel Ltd

CoRWM – Committee on Radioactive Waste Management

HLW – High Level Waste

ILW – Intermediate Level Waste

LLW – Low Level Waste

NDA – Nuclear Decommissioning Agency

VLLW – Very Low Level Waste

TABLE OF CONTENTS

TABLE OF FIGURES

LIST OF TABLES

AIMS AND OBJECTIVES

There were two main aims throughout this project based on the solubility of tetravalent metals and the complexation mechanisms of isosaccharinic acid (ISA). The first was to determine the solubility of thorium, used as an analogue for plutonium in the +4 state, in the presence of cellulose degradation products (CDP) and ISA, the main product from the alkaline anaerobic degradation of CDP, at a range of pH values. One task within this was to determine a robust experimental method for the study as previous studies demonstrated many discrepancies when comparing results. Complexation of the thorium in CDP was studied by ICP-MS to determine the components that complexed with the thorium.

The second main objective was to examine the complexation mechanism of ISA in the solid form, with metals, focussing on cadmium. This was studied using solid state NMR and Gaussian modelling and the experimental and modelled data were compared to attempt to elucidate where the metal was bound on the ligand. Different stoichiometries and coordination numbers were modelled for the complexation of cadmium to ISA and NMR ^{13}C chemical shifts were calculated and compared to experimental data.

INTRODUCTION

The Nuclear Decommissioning Authority, NDA, is charged with developing methods for the disposal of radioactive wastes produced from nuclear reactions. There are a number of criteria that must be met to ensure the safe disposal of the waste that include ensuring the long term protection of people and the environment, carrying out the research and the conception of ideas in an open and transparent way, basing the work on sound science and using public monies effectively [1].

Research has been carried out for a long period of time on the disposal of radioactive waste produced from nuclear reactions spanning a period of 50 years [2]. Many options for the safe management of this waste have been suggested such as disposal at sea, in subduction zones, in ice sheets and in space [3]. For wastes that pose a long term risk, the committee on radioactive waste management, CoRWM, decided that interim storage, geological disposal and phased geological disposal were the three main areas to focus on [4].

The focus throughout this thesis was on the deep geological disposal of intermediate level waste, ILW and some low level waste, LLW, which will be buried in a nuclear waste repository underground at a depth between 300 and 1000 metres down [5]. During closure, a backfill material will be used to surround the waste. In the UK, the surrounding material will be cement. After closure, the near-field (the engineered part of the repository) porewater chemistry will be of high pH and low Eh caused by contact of the water with the cement and the rusting of steel containers encapsulating the waste. The movement of groundwater means that radionuclides could potentially migrate from the inside of the repository and the near field, into the surrounding areas, termed the far field.

The movement of radionuclides from the near field to the far field is determined predominantly by their solubility in the near field porewater and also their sorption from solution onto any solid components present. Therefore anything that affects these factors, i.e. the presence of ligands which could potentially complex to the radionuclides, must be considered in the safety assessment of the repository. The ILW and LLW are likely to contain cellulose in the form of paper, wood and cloth. Cellulose degrades under the alkaline

anaerobic conditions created in the near field of the repository to form highly complexing ligands, which can increase the solubility of several radionuclides enabling them to be transported to the far field [6][7]. The main component from the degradation of cellulose is isosaccharinic acid, which makes up approximately 80% of the total organic carbon in the resulting mixture [8]. ISA is a six carbon carboxylic acid molecule with sites available for complexation with metals. Studies have found that M:ISA complexes do exist, subsequently increasing the metal solubility that would make them more mobile in the repository. This effect has been noted to have the largest increase of solubility with tetravalent actinides and, in particular, plutonium in the 4+ oxidation state [7]. Other radionuclides studied were nickel, technetium, tin, uranium, and europium. The choice of radionuclides to study comes from either their presence in nuclear waste or their use as analogues for other radionuclides such as europium for americium.

Thorium is often used as an analogue for plutonium 4+ and can also be present in nuclear waste. Previous studies have shown that there are discrepancies when comparing thorium solubility at high pH with solubilities ranging from ranging from $10^{-7} - 10^{-10}$ mol dm^{-3} [9]. This could be largely due to the structure of the solid form of thorium created, i.e. whether it is amorphous or crystalline, and how well it has been defined, but can also be due to the preparation method and pre-treatment of the thorium, the temperature and the inclusion of colloids in the final solution [10]. The aim of the work presented in this thesis was to determine the solubility of thorium by using two different experimental methods to establish if this caused any differences in the results. The methods investigated were oversaturation and undersaturation and the effect of the experimental method chosen on the solubility data was established.

To determine how a ligand complexes with a metal can provide useful information on possible future interactions of that ligand with other metals, and could enable predictions to be made about further complexes and reactions the ligand could undergo. For this reason, complexes of ISA (in the lactone and open chain form), and metals, were studied using solid state nuclear magnetic resonance, SS NMR, to determine the metal binding site of the ligand. When attempting to characterise a complex, it is important not to rely solely on one method of analysis, so this work set out to demonstrate the uses of SS NMR and Gaussian molecular modelling of the complexes for such characterisations.

1 BACKGROUND

The disposal of radioactive waste is subject to a number of specific requirements, enforced due to safety assessments. The risk to an individual at any time must not exceed a specified limit [11]. Any movement of radionuclides through repository walls into soils is hazardous, especially if the movement occurs before the waste has been left a significant time in order to decay. Because of these issues, there are a number of important aspects to consider when researching the disposal of the waste from the contents of the waste, ranging from the method of disposal and responsibilities [12] to the site location itself [13].

1.1 Low and Intermediate level wastes

Radioactive wastes are placed into four categories depending on their specific activity. These categories are very low level wastes, VLLW, which can be disposed of with ordinary refuse, LLW, which are wastes other than those disposable by VLLW methods but with an activity of less than 4 GBq per tonne of alpha or 12 GBq per tonne of beta/gamma activity; ILW, which are wastes exceeding the upper boundaries for LLW but are not affected by heat or produce heat themselves; and high level waste, HLW, which are wastes where the internal temperature could rise as a result of their radioactivity [3]. The focus of this thesis is on the disposal of the LLW and ILW. LLW tends to arise from the operation and decommissioning of nuclear facilities and consist of lightly contaminated miscellaneous waste comprising mainly of paper, plastic and metal [5]. ILW arise mainly from the reprocessing of spent fuel and from operation, maintenance and decommissioning of nuclear plants. The major components are for example nuclear fuel cladding and reactor components, graphite from reactor cores and sludges from the treatment of radioactive liquid effluents [5]. The LLW category may also contain significant amounts of organic material. The amounts of all these wastes present can be seen in Table 1

Table 1 Waste inventory, 2007 [14]

Material	Mass (tonnes)		
METALS:	HLW	ILW	LLW
Stainless steel	3.2	27,000	160,000
Other steel	5.3	45,000	870,000
Magnox	0	7,800	130
Aluminium	0	1,200	30,000
Zircaloy	0	1,500	40
Other metals	91	3,200	90,000
ORGANICS:			
Cellulosics	0	1,900	90,000
Plastics	0	5,600	80,000
Rubbers	0	1,200	23,000
Other organics	0	1,400	24,000
INORGANICS:			
Concrete, cement, sand & rubble	0	58,000	1,700,000
Graphite	0	79,000	20,000
Glass & Ceramics	2,200	1,000	15,000
Sludges, flocs & liquids	0	32,000	19,000
Other inorganics	640	2,800	31,000
SOIL	0	86	330,000
UNSPECIFIED	0	4,100	130,000
TOTAL	2,900	270,000	3,600,000

1.2   Repository Design

The proposed design of a waste repository can be seen in Figure 1 [3]. There will be a multi barrier concept in place, the barriers being both physical and chemical, for the retardation of movement of radionuclides through the repository and ultimately into the surrounding soils and geosphere.
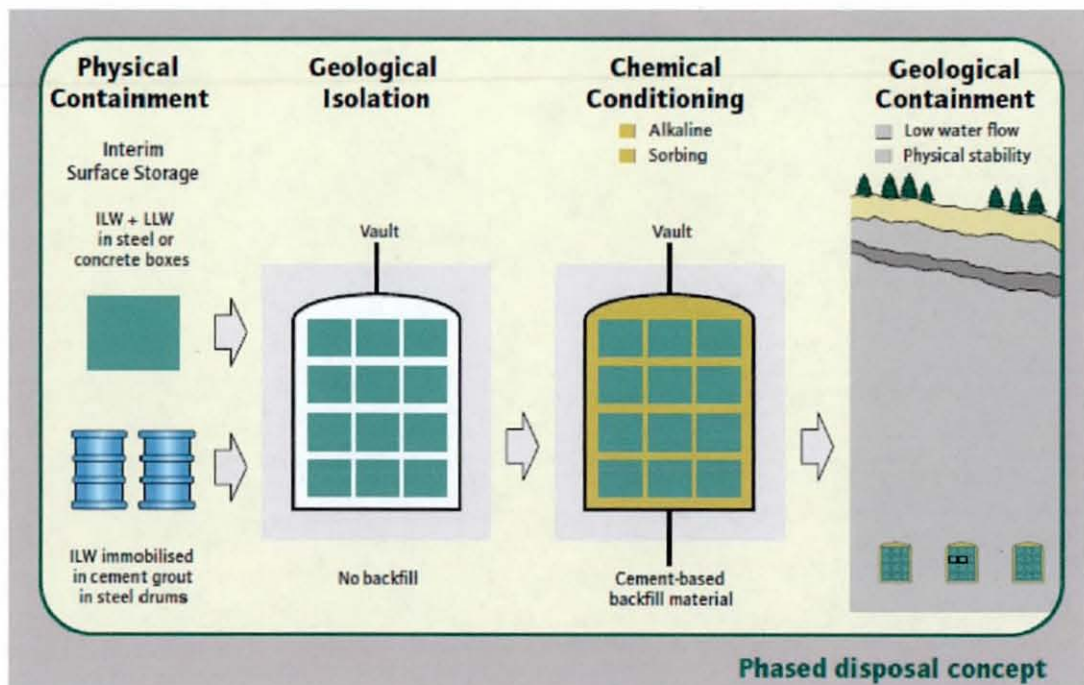
Figure 1   A Schematic representing a proposed waste repository design for the disposal of LLW and ILW [3]

The physical barriers are in the form of waste packaging and the cement backfill used in the repository. The conditions formed when groundwater flows through the cement and into the repository create chemical barriers. The environment created will be at high pH and low Eh due to the cement components and the rusting of the steel containers respectively [3]. Different cement backfills exist such as Nirex Reference Vault Backfill, NRVB, and Ordinary Portland Cement, OPC. Other materials considered for the backfill include non cementitious products such as clays.

1.2.1 Nirex Reference Vault Backfill

A form of cementitious material that can be used in a repository is called NRVB. This material is water permeable and will allow groundwater to pass through it and emerge with a pH of at least 10.5 [15]. As well as producing a high pH environment the backfill will also provide abundant surfaces for the sorption of radionuclides, subsequently reducing their mobility [3]. The NRVB is essentially made up of calcium hydroxide and calcium silicate hydrate gel formed by the hydration of Portland cement and/or lime. The NRVB has been engineered to fulfil a number of requirements as listed below [16]:

- Long term maintenance of the alkaline conditions

- Long term maintenance of high active surface area for sorption of radionuclides

- High permeability and porosity to achieve homogeneous chemical conditions and to allow the escape of gases created from reactions within the repository after closure.

1.2.2 Lime

Lime, (CaO), comes from $CaCO_3$, which is abundant in nature as limestone. Lime itself occurs sparingly in the environment and is usually in the hydrated form $Ca(OH)_2$, produced after the lime reacts with water. Lime produces the aqueous conditions of approximately pH 12.5 as the product $Ca(OH)_2$ is partly soluble [17]. The production of mortar or concrete comes from the mixture of the lime with sand or coarser material. Lime based materials are porous and will slowly re-carbonate over time in the presence of moisture and CO_2.

1.2.3 Portland Cement

Portland cement, sometimes referred to as ordinary Portland cement, can provide higher compressive strengths than lime based products and gains strength in the presence of water. The selected raw materials, shown in Table 2, are blended together and reacted in a rotary kiln at temperatures exceeding 1400°C. The resulting product is finely ground before use.

Table 2 Chemical composition of Portland cement [17]

Oxide	Weight %
CaO	61-67
SiO$_2$	17-24
Al$_2$O$_3$	3-8
Fe$_2$O$_3$	1-6
MgO	0.1-4
Na$_2$O + K$_2$O	0.5-1.5
SO$_3$	1.3

1.2.4 PCM Grout

Later in this thesis some comparative studies are carried out which compare different cementitious materials used to encase ILW and HLW. The proposed cement for some HLW is a 3:1 mixture of pulverised fine ash, PFA:OPC. This is an encapsulating matrix expected to be used for BNFL plutonium contaminated material, PCM streams, PCM, (combustible and non-combustible PCM) PCM incinerator-ash, and actinide-recovery flocs (actually 1:1 PFA:OPC) [18]. The PFA is a pozzolanic substance as it combines with lime to form additional hydration products. It is produced as a fine ash separated from the flue gas of a power station burning pulverised coal. The compositions of PFA depend on the burning conditions and on the compositions of the minerals associated with the coal. Approximately 60-90% of the PFA consists of spherical glass particles, the remainder consists of quartz, mullite, hematite and magnetite crystals within the glass. The glass is made up of silica and alumina with some iron oxide, lime, alkalis and magnesia [18].

1.3 Waste Containers and Packaging

The waste is packaged in steel containers which, when they corrode in the presence of groundwater, will produce reducing conditions affecting the reactions of any materials present. The following reactions will occur when the containers in the repository come into contact with water. These reactions are accounted for in the safety assessment of the repository and, as with the cement backfill, actually facilitate the inhibition of the mobility of redox sensitive radionuclides, particularly actinides, by creating a low Eh environment. The reaction requires water and oxygen for the material to rust. The steel surface will not be uniform therefore there will be areas with low electrode potential acting as anodes and areas acting as cathodes [19]. With the depletion of oxygen and the production of hydrogen a reducing environment will be produced creating a low Eh environment in the groundwater.

1.4 Cellulose Degradation

Cellulose, and particularly its degradation products, are of importance in the design and safety assessment of a radioactive waste repository for ILW and LLW [20],[21]. The alkaline degradation of solid organic polymers present in the ILW and LLW can form water soluble complexants. The degradation can occur via radiolytic [22],[23], microbial or chemical degradation [24]. Of these three processes chemical degradation has been shown to be the most significant, as radiolytic effects cause no significant changes in the solubility of radionuclides over that of chemical [25],[26] and it is not certain as to whether microbes will survive the repository conditions.

1.4.1 Radiolytic Degradation of Cellulose

Radiation effects may only be significant for ILW in the repository although it is possible that mixed disposal of ILW and LLW could expose LLW forms to significant gamma doses [27]. The radiolysis of organic materials can yield several products [28]

- A carbonaceous residue which could be present as a hydrocarbon gel. This will eventually degrade to carbon with prolonged irradiation

- Hydrogen gas

- Carbon containing volatile species such as CH_4, CO_2 and CO

- Acidic species, for example those with halogen atoms as HCl or HF

- Small organic molecules

The radiolytic degradation of cellulose was carried out on samples of polymers in the presence of cementitious materials [25],[26] and both alpha and gamma irradiation were employed. The solubility of plutonium was investigated and the conclusion was that the radiation decomposition experiments gave similar results to the chemical decomposition experiments. The solubility of the plutonium was increased in the radiolytic degradation products but never significantly more than the products from chemical degradation. Within these experiments the extent of chemical degradation occurring was not controlled so some of the solubility enhancement may have arisen from this process.

1.4.2 Microbial Degradation of Cellulose

The effects of microorganisms cannot be excluded from the planned disposal of radioactive waste [29],[30]. Groundwater will contain various sub-classes of microorganisms [30], however the conditions in the near field of a radioactive waste repository will provide a very different environment from those normally experienced by soil microorganisms. Most studies in this area conclude that the extent of microbial activity is likely to be limited under near field conditions, however the effects should not be ignored entirely [24]. There does seem to be an uncertainty as to how widespread the microbial activity will be and it is expected that chemical degradation will still dominate under the high pH conditions [31]. The activity of microbes could be increased by the heterogeneity of the near field environment. In areas where pore water has not penetrated but water vapour has caused the surface to be damp, microbes will be given a better chance of survival and growth [24].

The effect of microbes on the performance of a radioactive waste repository can be detrimental but in some instances positive. The microbial oxidation of organic material could reduce the pH of the pore water hence increasing the solubility of many radionuclides, and gas production, from these processes [31] could cause fractures in the NRVB, both detrimental effects. The microbes could also degrade the soluble organic products from cellulose

degradation before they enhance any metal solubility [24], which would obviously be a positive side effect of microbial degradation.

1.5 Chemical Degradation of Cellulose

Out of the three degradation processes, chemical degradation of cellulose and its products was the focus of this thesis. There have been many studies that have shown that, when cellulose degrades chemically under alkaline anaerobic or aerobic conditions, a number of soluble products are formed which enhance the solubility and reduce the sorption of certain radionuclides [32],[33],[34]. The main mechanism behind the alkaline degradation of cellulose is fairly well understood and is described in the literature, [35],[36],[6]. Cellulose is a linear condensation polymer made up of D-anhydroglucopyranose units, often referred to as glucose units. These are linked by β-1,4-glycosidic bonds and are shown in Figure 2.
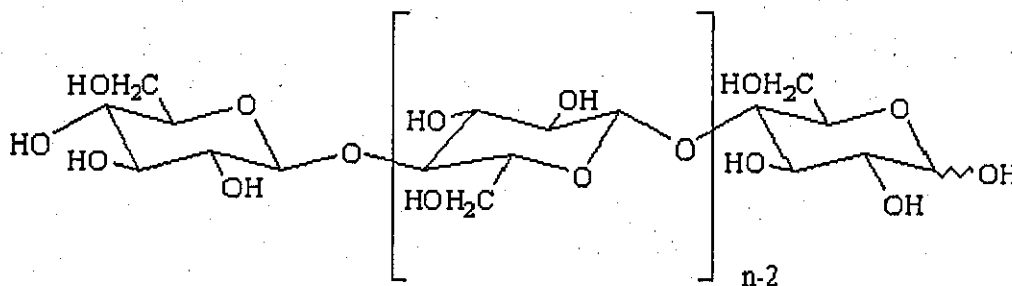
Figure 2 The structure of cellulose

Under the conditions of the near field the main degradation is by a beta-alkoxycarbonyl elimination which breaks the 1,4-glycosidic linkage. One hexose monomer unit is split off from the cellulose molecule and the next glucose end group can take part in the reactions. This process is often referred to as the "peeling reaction" and releases glucose units one by one from the cellulose molecule, resulting in a depolymerisation [37]. The peeling reaction is shown in Figure 3.
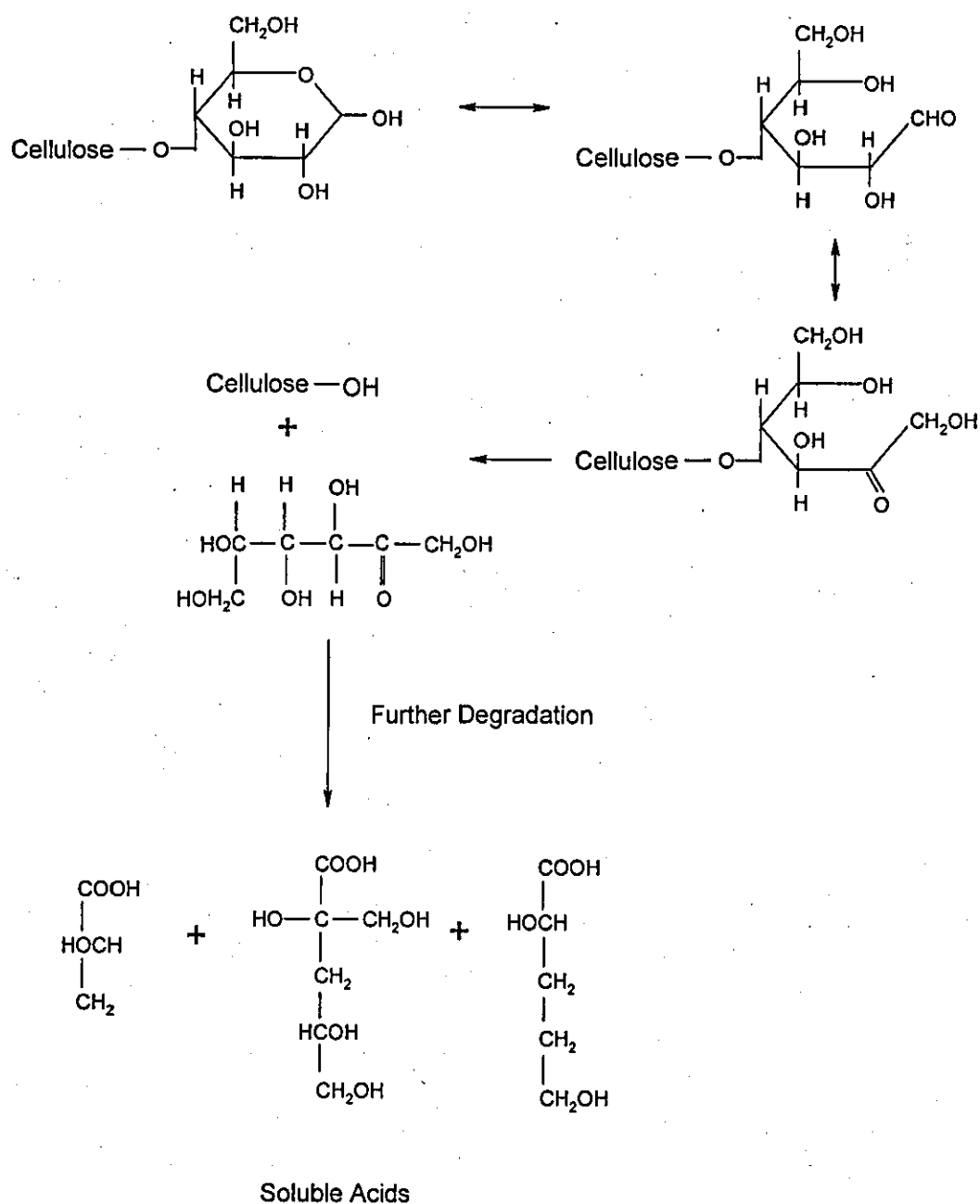
Figure 3 The peeling reaction of Cellulose [6]

If no other reactions occurred then the cellulose would degrade completely by the peeling reaction scheme. However the β-elimination can occur at different positions which results in the hexose unit remaining attached to the cellulose molecule, therefore terminating the depolymerisation. This is called the "stopping" reaction. Physical stopping reactions can also

occur inhibiting the degradation of cellulose. This is where a reducing end group reaches an inaccessible crystalline region of the cellulose, [38],[8],[39],[40]. The final forms of the degradation products come from either reaction as a diketone is formed which undergoes benzilic acid rearrangement.

1.5.1.1 Identification of Products from the Chemical Degradation of Cellulose

The type of cellulosic material degraded has been shown to change the concentrations of various products produced [8]. The main degradation products of pure cellulose are α-isosaccharinic acid and β-isosaccharinic acid, which accounted for approximately 80% of the total dissolved organic carbon formed [8],[39],[41]. When other forms of cellulose were degraded such as tela tissues, cotton and recycled paper the degradation yielded higher proportions of the simple aliphatic acids, especially acetic acid [8], although the ISA was still the dominant species present. A study by Pourchez et al. also detected alcohols after the degradation of cellulose ethers although the concentrations of hydroxyl acids was ten times higher than the alcohol concentration [42]. There have been many studies on identifying the main products from the degradation of cellulose using many different methods. The main analytical methods employed were HPLC [43],[34], CE [34],[44], GC-MS [34],[8],[45], HPIEC and HPAEC [8]. A comprehensive study carried out by Greenfield et al. lists the main products produced under various different conditions and using different types of cellulose [6] and a review of the commonly detected alkaline degradation products has been written by Knill and Kennedy [46]. Among many others the ligands produced of highest concentration are listed below [43]:

Formic acid	3,4-dihydroxy-butanoic acid
Acetic acid	2-C-(hydroxyl-butanoic acid
Glycolic acid	3-deoxy-D-pentonic acid
Lactic acid	

1.5.1.2 Kinetics of Chemical Degradation of Cellulose

It is important to consider the kinetics of cellulose degradation so an accurate value for the concentration of complexing ligands produced from the process can be estimated. There have been a number of studies on the kinetics of cellulose degradation and factors controlling the depolymerisation reaction [39],[34],[41]. Experiments carried out by Van Loon et al. indicate that complete degradation of cellulose would occur after approximately 10^7 years [40]. Other studies have indicated a more rapid initial degradation of cellulose that later levelled out when analysed over 3 years. Long term prediction models based on this work found that lower concentrations of ISA and less degradation of the cellulose had actually occurred after 7 years than was predicted from the three year study [41],[39]. The degradation rate is determined by the peeling mechanism and depends on the concentration of available reducing end groups. As the degradation continues, alkaline hydrolysis of glycosidic linkages becomes the rate limiting step and is not dependant on the degradation products themselves [46]. This means that inaccessible end groups, which would be higher in concentration the more crystalline the cellulose is, will slow the rate of degradation down significantly [39],[43].

1.5.1.3 Solubility effects of cellulose degradation products

The solubility of various radionuclides has been determined in solutions of cellulose degradation products, CDP. The solubility of the metals is usually increased significantly as expected due to the presence of many complexing ligands. As the main component of CDP is ISA, it was thought that this was the ligand that was responsible for increasing the solubilities of the radionuclides but studies have shown that the solubility is enhanced in a solution of CDP when compared to the solubility in ISA at a comparable concentration[7],[47], see Table 3.

Table 3 The solubility of metals in the presence of complexing ligands in high pH solutions. Each column in the table has a reference where the data was collected from. The results in NRVB equilibrated water show baseline solubilities for the metals.

Metal	In CDP (moldm^{-3}) [7]	In erythro ISA(10^{-3} M) (moldm^{-3}) [7]	In erythro ISA(10^{-3} M) (moldm^{-3}) [47]	In NRVB Equilibrated Water (moldm^{-3}) [7]
Ni	2×10^{-4}			2×10^{-8}
Sn	1×10^{-3}			9×10^{-8}
Th(Na ISA)	2×10^{-6}	9.2×10^{-8}	9.3×10^{-8}	$<2 \times 10^{-10}$
U (IV) (Na ISA)	2×10^{-4}	9.1×10^{-6}	9.2×10^{-6}	8×10^{-7}
U (VI) (Na ISA)	1×10^{-4}	1.7×10^{-4}	1.7×10^{-4}	4×10^{-6}
Pu (Na ISA)	7×10^{-5}	4.8×10^{-5}	4.7×10^{-5}	4×10^{-10}
Pu (Ca ISA)	7×10^{-5}	2×10^{-7}	2×10^{-7}	4×10^{-10}
Am	2×10^{-6}			4×10^{-10}

Table 4 includes the solubility enhancement factors, defined as the increase in solubility of the metal ion in leachates compared to ISA, all calculated using the data from Table 3, and demonstrates how large the difference is between the solubilities particularly the plutonium result.

Table 4 Solubility enhancement factors from the data in Table 3

Metal	Solubility Enhancement Factor
Th	21.7
U (IV)	22.0
U (VI)	0.59
Pu	350.0

Similar studies have been carried out which support these results [34]. The solubility of certain radionuclides is increased in the presence of degradation products when compared to an analogue of ISA, tetrahydroxypentanoic acid, THPA. The solubility of Sm and Eu was increased in the degradation mixture more than when in pure THPA whereas the solubility of Cu and Co stayed the same. This indicates that there is another complexing agent present in the waste as previously thought, that complexes with trivalent metal cations but not divalent. As ISA is the main product formed from the degradation of cellulose it is likely that whatever else is in the solution enhancing metal solubility is a minor component [25]. The solubility of metals has been found to increase in some other components from the degradation of cellulose but the complexing agents have never been found at high enough concentrations in the CDP to have such an effect [7],[48],[33].

1.6 Isosaccharinic acid

Regardless of whether the CDP enhances the solubility of certain radionuclides or not, ISA is still an important complexing agent present in the wastes that does have a significant effect on metal solubility. For this reason it is important to understand the complexation of the ligand and the different ways in which it can retard, or aid, radionuclide migration throughout a nuclear waste repository.

As discussed previously ISA is formed from the alkaline anaerobic degradation of cellulose, section 1.5. The degradation of cellulose yields two diastereoisomers, α- and β-D-isosaccharinic acids in approximately equal concentrations [49], see Figure 4.
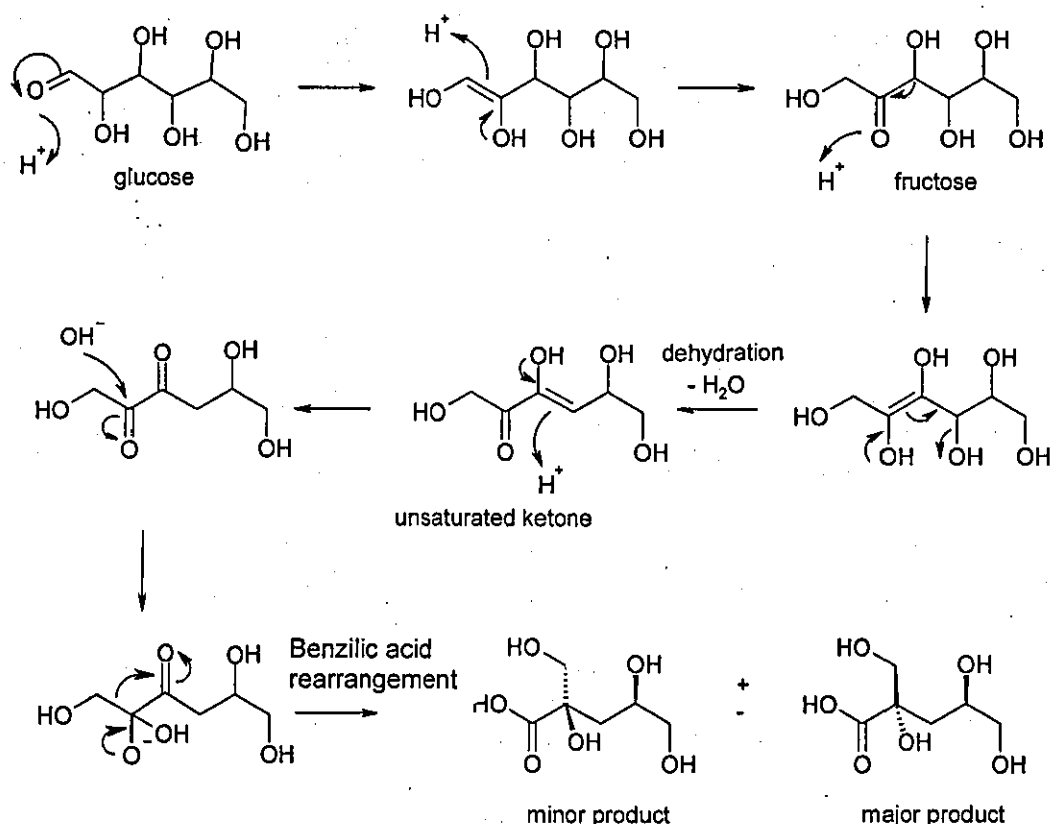
Figure 4 Proposed degradation of glucose to form ISA

Each diastereomer then has two enantiomeric lactone conformations [50],[8]. The dominant form at high pH is the isosaccharinate form, [51],[52] which is the deprotonated carboxylic acid end group. The two diastereoisomers, α-ISA and β-ISA, can be seen in Figure 5 and the lactone form can be seen in Figure 6. The two isomers of ISA exhibit different solubilities and this can depend on whether the calcium or sodium salt is being measured. β-isosaccharinate forms a highly soluble calcium salt whereas α-isosaccharinate has only a sparingly soluble calcium salt. The sodium salt solubility is approximately two orders of magnitude higher than the calcium salt [27],[53],[54]. Throughout this work the α-isosaccharinic

acid is formed and the sodium salt is used. The solubility for the sodium form has been found to be pH independent in the range 4.5 to 10 [55].
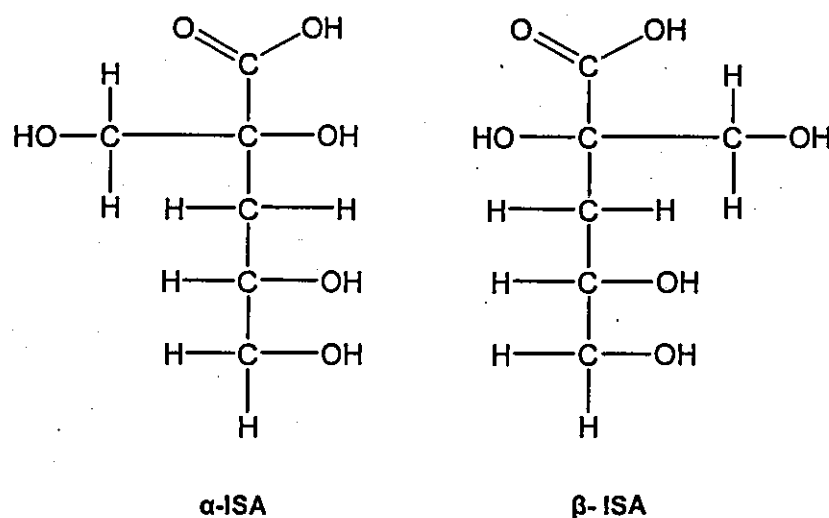
Figure 5 Structure of the isosaccharinic acid diastereoisomers
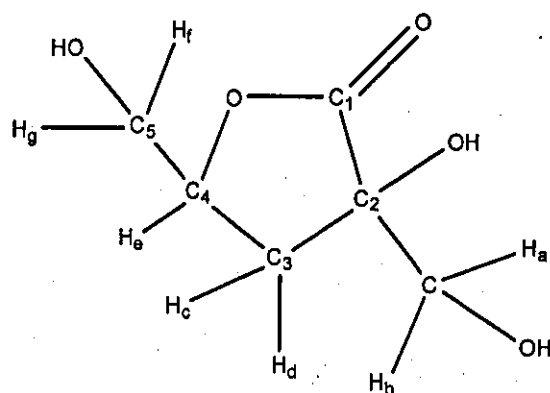
Figure 6 α-D-isosaccharino-1,4-lactone

The crystal structure of sodium ISA has been characterised by single crystal X-ray diffraction methods, despite it being difficult to produce a crystalline solid, and the 3D structure is shown in Figure 7 [55].
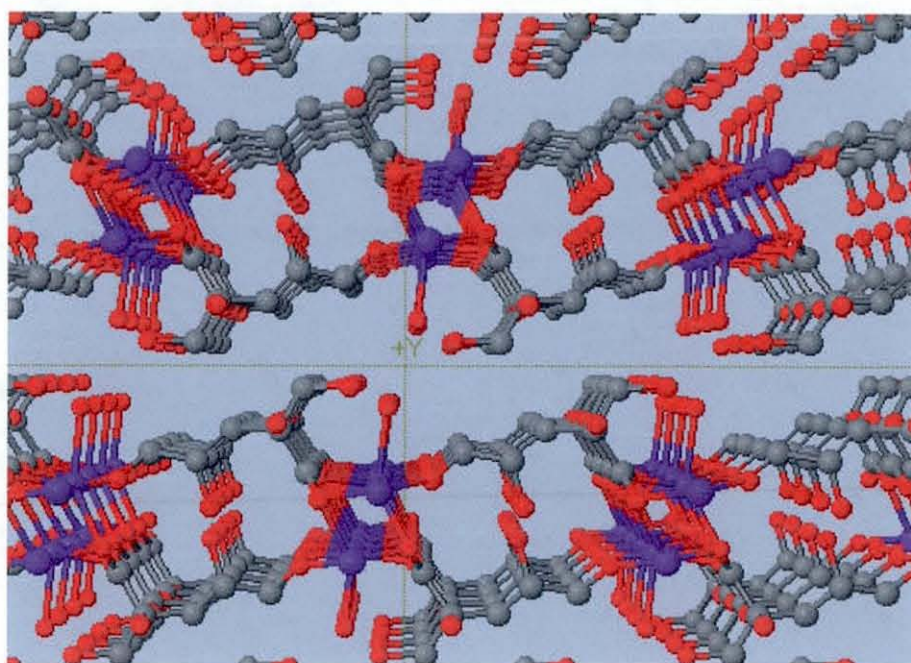
Figure 7 The modelled X-ray structure of sodium isosaccharinic acid

An important consideration when looking at ISA structures at the pHs used throughout this thesis is the conversion from the open chain to the lactone form. Although only the open chain structures are produced in the alkaline degradation of cellulose, if the pH is lowered the ISA changes structure into the lactone form [51]. Below pH 6 the lactone form dominates and above pH 10 the open chain dominates. In between these two pH's both forms may exist although above pH 7 the lactone form concentration is negligible compared to the open chain. This change in structure is also affected by kinetics as the move from the lactone to the open chain takes only 8 minutes whereas the reverse reaction takes approximately 1000 minutes [51]. This work also indicates that, when moving from an acid to an alkaline pH, the lactone may have an initial fast transformation to the open chain form but then a slow transformation back to the lactone conformation may follow. These changes in structure will almost definitely change the complex formed with metals and therefore could affect the solubility. Previous work has demonstrated the importance of considering the lactone form of the ISA when determining the solubility of Np(IV) at pH's ranging from 5-14, [56]. With the changes in structure, the availability of the groups involved in complexation will change.

1.6.1 Stability and Degradation of ISA

The stability of the ISA in repository conditions needs to be taken into consideration as this could affect the solubility results over time. Studies have shown that ISA is stable in these high pH, anaerobic conditions for at least 60 days [57],[58] although there has been contrasting research which suggested otherwise where the rate of production of ISA was calculated to be slower than the rate of degradation after several years of exposure time [39],[31]. For the ISA to degrade microbially, there must be organisms present under repository conditions, which means they must be active under alkaline, anaerobic conditions. There have been a number of these types of organisms recovered from alkaline sites where cellulose would have been present [31]. The conclusions from this study were that the probability of large numbers of ISA degrading microbes being present in the repository to make a significant effect on the ISA concentration was very low. It is possible however that these microbes could develop over time.

1.6.2 ISA Sorption

ISA can affect a metal's solubility in solution but can also effect its sorption, or the ligand can be sorbed to a surface itself. Numerous studies have found that ISA has a high affinity to sorb onto cement [41],[57] and the sorption has been seen to increase with increasing degradation of the cementitious material. At long contact times the sorption of the ligand onto the cement was seen to decrease, possibly due to carbonation of the cements surface over time [57]. This theory is backed up by another study where no sorption of ISA or gluconic acid was found on calcite at high pH, so calcite formed on the surface of the cement may retard the sorption process [59]. Research by Van Loon et al. actually studied the sorption under a wide range of different liquid to solid ratios and found that the sorption of ISA onto cement reached equilibrium after only one day [58].

ISA can also affect metals sorption onto cement by forming soluble complexes with sorbed metals, increasing the metals mobility in the repository by decreasing their sorption to the cement. This effect has been seen in numerous studies where ISA increased the concentration of metal in solution by decreasing its sorption to cementitious material [7],[43],[59],[57].

1.6.3 Effects of ISA on Metal Solubility and M:ISA complexation

Some solubility studies of ISA and various cations have already been discussed and the results can be seen in Table 3. Many other studies have also been carried out which support the theory that ISA is an important complexant in a nuclear waste repository as it increases the cations concentrations in solution. Some of the results can be seen in Table 5 and a summary of other solubility studies can be found in a review [60]. Some of these findings will be important to consider later in this thesis for comparison purposes.

Table 5 Results from solubility studies with ISA

Cations studied	Important findings	Reference
Pb, Zn, Cr, Cu, Cd	Concentrations of Cd were below the detection limit of the instrument Ca(ISA)$_2$ had no effect on the solubility of Cr, Zn or Pb but did increase the Cu concentration in solution.	Malin et al. [48]
Ca(II), Np(IV)	Significant complexation of ISA with Np and Ca was shown at low and high pH.	Rai et al. [56]
U(IV)	pH independent stability constants were determined for the U:ISA and gluconate:U complexes.	Warwick et al. [61]
Ni(III)	Measurements at pH's ranging from 7-13.3 show the different stoichiometries of the ISA:Ni complexes formed.	Warwick et al. [62]
Np(IV)	The solubility of Np was significantly increased in the presence of ISA	Rai et al. [63]
Pu(IV)	The solubility was increased and sorption of Pu to cement was reduced in the presence of ISA.	Greenfield et al. [7]

An understanding of the complexation involved between the ISA and cations could aid predictions on how the ligand will affect metal behaviour in the repository. A large section of this thesis concentrates on the mechanistic interactions of ISA and cations using NMR techniques.

NMR has long been used as an analytical tool for structural determination of complexes formed with ligands, for example gluconate and gluconolactone complexes [64],[65],[66] and with ISA [52],[67]. From such studies, many possible structures of M:sugar complexes have been put forward as well as the different stoichiometries formed at different pHs (Table 6). The structures proposed for many of these complexes often involve not only bonding of the carboxyl group but also the hydroxyl groups [68],[64],[69],[70], and show the possibility of chelate complexes being formed [71].

Table 6 Metal:Ligand complex stoichiometries at different pH's in solution

Metal Complex	< pH 7.9	pH 7.9-11	> pH 11
Cd Glu [72]	Cd:Glu 1:1	Cd:OH 1:2 Cd:Glu 1:1 and 3:1	Cd:OH 1:2 Cd:Glu 1:1 and 3:1
Ni Glu [72]	Ni:Glu 1:1	Ni:OH 1:1.5 Ni:Glu 2:1	Ni:Glu 2:1 Ni:OH 1:2
Cd ISA [72]	Cd:ISA 2:1 and 1:1	Cd:OH 1:2 Cd:ISA 1:1 and 3:1	Cd:OH 1:2 Cd:ISA 1:1
Eu ISA [72]	Eu:ISA 1:1		Eu:OH 1:3 Eu:ISA 1:1
Fe(II) ISA [72]	Fe(II):ISA 1:1		Fe(II):OH between 1:2 and 1:3 Fe(II):ISA 1:1
Np(IV) ISA [63]	Np(OH)$_3$ISA Np(OH)$_2$ISA$_2$		
Th ISA [67]		3 ISA ligands were involved in the complexation at pH 8	
Th-ISA/Glu-Ca [73]			1:2:1 Th:ISA:Ca 1:2:1 Th:Glu:Ca

Th ISA Ca [54]			1:1 Th:ISA In the absence of Ca 1:2:1 Th:ISA:Ca
Eu ISA [54]			1:1 Eu ISA
Eu ISA/Glu [73]			Eu:ISA 1:1 Eu:Glu 1:1
Ni ISA [72]		Ni:OH 1:1.5	Ni:ISA 2:1
	Ni:ISA 1:1	Ni:ISA 2:1	Ni:OH 1:2

The complexation reactions could involve the bonding of the cation to the hydroxyl groups as well as the carboxyl. A study by Rai et al. [56], indicated that deprotonation of some of the hydroxyl groups on the ISA could be induced at lower pHs than expected due to the presence of a metal. This hypothesis is supported in a study of the coordination of aldonic acids towards copper [68]. Depending at what pH deprotonation occurred, this could greatly affect the complexes formed at the pHs used in this thesis. Studies have shown that even at high pH there is only one deprotonation that occurs and that is of the carboxyl group, as is expected [52],[57]. The pKa of the carboxyl group on the ISA has been reported as 3.87 and has been found to be almost completely deprotonated at pH ≥ 5.3 so deprotonation of this group should be well defined at the pHs used throughout this work [74],[52]. Even if any of the hydroxyl groups were not deprotonated, as the pH increased the deprotonation of the carboxyate group could initiate a change in the conformation of the ISA molecule, which could affect the hydrogen bonding environments of some of the hydroxyl groups [71]. One possible structure that could be formed has been presented in previous work where there is an insertion of a hydrogen bond between the carboxylate anion and the hydroxyl group on the secondary alcohol. This would create a six membered ring, which is not dissimilar to the lactone structure, in which a hydrogen bond closes the ring as opposed to a covalent ester linkage [52]. This change was noticed as the pH was increased from 5 to 13 and was determined by looking at the change in proton NMR chemical shifts as a result of increasing pH.

1.6.4 Solid State NMR Studies

A reoccurring point with a number of the ISA complexation and stoichiometry studies is the importance of using a number of different analytical techniques to confirm a structure [68]. This is one of the reasons SS NMR is used in this work to investigate whether it can provide extra information regarding the complexation of ISA with various metals and also to see if it can be used with amorphous solids which may be difficult to obtain structural information from. SS NMR can also provide some advantages over solution NMR such as those listed below [75]:

- No solvent effects are observed so there is no interference that might be seen from water for example.

- Minimal sample preparation is needed, just a solid that can be ground into a powdered form to be sampled.

- Cross Polarisation-Magic Angle Spinning, CP-MAS, is used. This means that ^{13}C spectra, which would usually have poor signal to noise ratio and long relaxation times due to the nuclei being of low abundance, can be recorded clearly and relatively quickly. The effect of the cross polarisation is to transfer magnetization from the abundant proton spins in the sample to the ^{13}C spin via the dipolar coupling between the two nuclei.

- Chemical Shift Anisotropy, CSA, can be obtained and this gives extra information on the carbons orientation in space. Each chemical shift is made up of the sum of the shielding tensors XX, YY and ZZ along the 3 axes of the 3D nuclei. When an atom is completely symmetrical in orientation, no CSA is observed but when differences occur with the orientation of the atom, CSA is seen in the form of spinning side bands, SSB. These SSB appear equidistance from the main peak on opposite sides but will be of different intensities depending on the orientation of the particular atom being analysed. This technique has been used on carbohydrates before with success [76].

SS NMR has been used in previous studies to aid crystal structure determination [77],[78]. It has also been used alongside solution NMR to assign peaks to specific carbons and protons in a

complex [77],[79]. Gaussian modelling is also used to compare to experimental data, again to aid the assignment of the structures of the ISA:metal complexes formed. This has been successful in previous studies where calculated chemical shifts from the Gaussian software and experimental shifts were compared [80],[81].

1.7 Thorium Background

The CDP discussed previously has been shown to increase the solubility of a number of radionuclides but the tetravalent elements seem to experience a larger increase in their solubility than other cations. Thorium is a relatively small highly charged cation which undergoes extensive interaction with water and with many anions. The aqueous chemistry of thorium is simplified somewhat as it only exists in the 4+ oxidation state and is therefore not redox sensitive. Because of its high charge, thorium ions have a strong tendency to hydrolyse in water and this can lead to the formation of polymeric and colloidal species [82]. Thorium can form many complexes in solution, one of which is the insoluble thorium hydroxide but this can become more soluble in the presence of carbonate species which will need to be considered throughout this report [83],[84].

1.7.1 Thorium Solubility experiments

Solid phase thorium may exist as amorphous thorium hydroxide or crystalline thorium oxide but is more likely to be a mixture of hydroxide and oxide. The solubility of thorium is critically dependent on whether the hydroxide (solubility approximately 10^{-8} mol dm^{-3}) or the oxide (solubility approximately 10^{-15} mol dm^{-3}) is the solubility limiting phase. Neck et al. have reported the solubility of crystalline thorium dioxide [9] and the solubility of amorphous thorium hydroxide [10] and Neck and Kim have reviewed the solubility and hydrolysis of tetravalent actinides [85]. The measured solubility of thorium is usually in the region of 10^{-8} mol dm^{-3} and no difference is observed above pH 7 in the solubility of thorium dioxide or thorium hydroxide [82],[9],[85]. This is thought to be because at this point the solubility is not controlled by bulk crystalline solid but by amorphous fractions on the surface. Not having a single, well defined, solid phase could be one of the reasons for differences in reported solubilities. Other reasons may be the method of preparation of the solid phase, pre-treatment, alteration and temperature. In addition, the presence of colloids can greatly affect measured

solubility [10]. Elapsed time before the measurement of solubility (so called equilibrium time) also affects solubility, particularly when a complexing ligand is present. An investigation by Vercammen et al. showed that solubilites measured after 5 days were significantly higher than those measured after 25 days although X-ray diffraction studies showed that this was not down to the different crystallinities of the thorium solid phase [86]. According to the hydrolysis constants of Th(IV), the complex Th(OH)$_4$ (aq) is the predominant species in near neutral and alkaline conditions [9]. Studies have found that drying the precipitate of thorium hydroxide before use in a solubility experiment rather than just washing it can result in solubilities 3-4 orders of magnitude lower [87]. The drying of the thorium removes the water and hydroxide ions which may be complexed with the cation and this process can also occur as the precipitates ages. The differences in the results are unlikely to be due to ionic strength differences because, in neutral and alkaline solutions of low ionic strength, the solubility of thorium is independent of the medium, and ionic strength, as the water activity and the activity coefficients of Th(OH) $_4$ (aq) are approximately equal to 1 [85].

In the presence of calcium, thorium can coprecipitate with calcium and this may be important in this work as some of the solubility measurements have been made using saturated solutions of calcium hydroxide [88]. The presence of calcium can also effect the stoichiometry of complexes formed. For example, when ISA complexes with thorium in the absence of calcium a 1:1 Th:ISA complex is formed but a 1:2:2 Th:Ca:ISA complex is formed in the presence of calcium [88],[86].

1.7.2 Methods of thorium analysis

The method of detecting and analysing thorium was given a lot of consideration when planning this work as this could also be a possible source of the discrepancies of the results obtained from different experiments. Alpha spectrometry is a widely used method with low detection limits but usually involves the pre-treatment, solubilisation and extraction of the thorium prior to analysis [89]. Other techniques that have been used are neutron activation analysis and energy dispersive X-ray techniques but the most common are inductively coupled plasma techniques used in conjunction with mass spectrometry or atomic emission spectroscopy [89]. These are the preferred techniques as they are usually faster and more accurate [90].

1.8 Plan

The literature review suggested that the following areas of work should be investigated:

- Development of a reproducible method for investigating thorium solubility using over and undersaturation methods at a range of pH values.

- Kinetic studies for the precipitation and complexation of thorium.

- Investigation of the solubilities of thorium, nickel, cobalt and cadmium in the presence of CDP and ISA at different cellulose loadings and ISA concentrations.

- Identification of components in CDP, other than ISA, which increase metal solubilities.

- Investigation of the complexation of ISA with different cations to determine the mechanism of metal binding using SSNMR and Gaussian modelling.

The above areas of work are described in the following chapters.

2 EXPERIMENTAL

2.1 Materials and Equipment

Deionised water, produced from a Barnstead NANOpure water purification system and AR reagents were used throughout. Calcium hydroxide 95+ %, potassium phosphate monobasic 99%, tetramethylammonium hydroxide 25% in water and α-D-lactose monohydrate 99.5+ % were purchased from Acros Organics, Loughborough. Nitric acid, formic acid, acetic acid, lactic acid, hydrochloric acid, all the metal chlorides used and sodium hydroxide, 2 mol dm^{-3} carbonate free, were purchased from Fischer Scientific, Loughborough. Thorium nitrate hydrate batch 1 was purchased from Fluka, Schweiz, at a specific activity of 3.93 kBq g^{-1}, Thorium nitrate hydrate batch 2 was purchased from Hopkin and Williams Ltd, London. Kimwipe® tissues were purchased from Kimtech Science, Kimberley Clarke Professional, Kent. Whatman centrifuge filters (vectra spin) and 10 k Da MWCO polysulphane 3 cm^3 filters were used to filter the solubility experiment solutions. The cation exchange resin in section 2.2.3 was purchased from Lancaster, Lancashire. The liquid scintillation cocktail used in the thorium method development study was Goldstar Meridian, Surrey. NRVB and PCM samples were sent from WMT at Winfrith.

2.1.1 Instrument specifications

Table 7 details all the instruments used throughout and the conditions that were applied to each analysis.

Table 7 Instrument specifications and uses

Instrument	Purpose	Method Specifications
Packard TRI-CARB 2750 TR/LL Liquid Scintillation Counter GMI Inc Minnesota	Thorium investigations.	Region A set as: lower limit 5.0 – upper limit 2000 with a LCR of 50 and region B set as: lower limit 250 - upper limit 2000
Hewlett Packard Series II 1090 HPLC with Diode Array Detector	Characterisation of CDP and quantitation by comparison with ISA. Characterisation of ISA	Chem Station Software ©
Bruker DPX 400 MHz Nuclear Magnetic Resonance machine, Coventry	Characterisation of ISA	The proton NMR was run at 400.13 MHz and the carbon NMR was run at 100.61 MHz. A high resolution HX probe was used.
FTIR – Shimadzu, Pettreson Scientific, Luton	Characterisation of ISA	FTIR-8300 Fourier Transform Infrared Spectrophotometer coupled with Hyper IR 1.51 software
Eh Probe – Orion 9678 BNWP Thermo electron corporation, Fisher, Loughborough Sure Flow combo Redox/ORP	Measurement of solution Eh	Calibrated using solution A and B. Solution A – 4.22 g potassium ferrocyanide and 1.65 g potassium ferricyanide in 100 cm^3 water gives an Eh value of 240 mV. Solution B – 0.422 g potassium ferrocyanide, 1.65 g potassium ferricyanide and 3.39 g potassium fluoride in 100 cm^3 water gives an Eh value of 300 mV.
Jenway pH meter and probe, Thermo electron corporation, Fisher, Loughborough	Measurement of all solution pH.	Calibrated using standards (typically pH 4, 7, and 10). Used only if calibration slope $\geq$ 97%.
Bruker DPX-500 MHz SS NMR spectrometer, Coventry	Mechanistic studies of ISA:Metal interactions – For extra techniques used in this analysis see section 2.6.1.	For ^{13}C analysis - Operated at 125.77 MHz for carbon and 500.13 MHz for proton decoupling employing a 4 mm MAS HX probe. Unless otherwise stated a spin rate of 8 KHz was used to spin the samples. D1 delay – 360 s. Pulse programme - cp.av.
ICP-OES Perkin-Elmer Optima 5300 dual view	Thorium method development and solubility studies	Argon gas used. Glass cyclonic spray chamber, nebuliser used was a cross-flow design with GemTips. 40 MHz, free-running solid-state RF generator, adjustable from 750 to 1500 watts, in 1 watt increments
ICP-MS	Identification of	Argon gas used, tuned daily with 1 ppb In. Glass conical nebuliser,

Element 2 XR instrument from Thermo-Finnigan	components in the CDP	low resolution used for thorium and cadmium and medium resolution for cobalt and nickel.
	Solubility studies	
Reverse Nierh Johnson MS	Thorium measurement investigations – slightly different parameters used for this analysis, see section 2.4.4.1.3.	
HPLC for LC-ICP-MS – see previous specifications	Identification of components in the CDP	Conditions as before but with 0.1 % acetic acid as the mobile phase.
Gamma Spectrometry, Ortec, Advanced Measurement Technology, Wokingham	Thorium measurement investigations	Ge-Li detector used with maestro computer software. The instrument was calibrated with Cs^{137}, which has a known gamma photon energy at 662 keV. Water was measured for 60 hours for background subtraction.
Gaussian modelling	Theoretical solid state NMR work	Gaussian 03 model [91]
X-Ray Diffractrometer	XRD of solid state ISA:Metal samples	Bruker D8 Advance diffractometer which operates with monochromatised Cu Kα radiation over the 2 θ range 5-60 using a 0.014 2 θ step.
Nitrogen atmosphere MBraun Glovebox, Germany	All the thorium solubility studies	UNILAB (1250/780) W system with integrated gas purifier (1 column), water cooled, single phase input. The system has a chemical combi analyser and mini antechamber attached.

2.2 Preparation of α – Isosaccharinic acid

ISA is not commercially available and therefore must be made in a laboratory. The calcium salt was initially prepared [92] then converted to the sodium salt [6].

2.2.1 Preparation of Ca-ISA

Alpha lactose monohydrate (500 g) was dissolved in 5 dm^{-3} of distilled water. Calcium hydroxide (135 g) was then added and the flask was sparged with oxygen-free nitrogen for six hours, whereupon it was stoppered, and left at room temperature for 3 days. The resulting brown solution was refluxed for 10 hours and filtered whilst hot. The solution was then evaporated in a stream of moving air until the volume was down to approximately 1500 cm^3. The mixture was refrigerated overnight and the white solid removed by filtration. The solid was then washed with cold water, ethanol and propanone. Recrystallisation of the calcium salt

was performed by dissolving calcium ISA (1.19 g) in hot water (100 g). The hot solution was then filtered free of calcium carbonate. The liquid phase was then evaporated under reduced pressure in a Büchi RE11 Rotavapor.

2.2.2 Preparation of Na-ISA

The calcium salt was converted to the sodium salt by the use of an ion exchange method [6]. Calcium isosaccharinate (8 g) was added to Chelex-100 (BioRad) resin (200 g) in one litre of deionised water and the suspension mixed for three hours. The resin was filtered off with a Millipore 0.2 μm membrane filter. The solution concentrate was then reduced by boiling down to about 100 cm^3. It was then evaporated further in an oven at 80 °C until a thick syrup was obtained. The syrup was then removed from the oven and left at room temperature (20 °C) to crystallise. The crystals were titurated in the presence of water-free diethylether and then filtered.

2.2.3 Preparation of ISA Lactone

To a suspension of calcium isosaccharinate (74 g), in hot water (400 cm^3), a solution of oxalic acid dehydrate (20 g), in hot water (200 cm^3), was added. The mixture was filtered whilst hot and the filtrate was passed through a column (3.5 x 45 cm) of Amberlite IR-120 (H$^+$) cation-exchange resin. The column effluent and washings were concentrated under reduced pressure at 50-60 °C to a thick, partly crystalline, syrup. This semi-crystalline syrup was dissolved in refluxing ethanol (500 cm^3). After the crystals had dissolved, ethyl ethanoate (2 dm^3) and petroleum ether (1 dm^3, b.p. 65-67) were added, and the hot solution was filtered. After cooling to room temperature, the solution was seeded, (seed crystals may be obtained by crystallizing a portion of the syrup from hot ethyl ethanoate) and placed in a refrigerator for several days. Filtration removed approximately 40 g of wet crystals, which were recrystallised by dissolution in the minimum amount of refluxing ethyl ethanoate. Cooling, seeding, and holding at approximately 5 °C for several days gave crystalline α-D-isosaccharino-1,4-lactone.

2.2.4 ISA Characterisation and Analysis

All batches of ISA made were analysed by a number of techniques and compared to previous batches created and analysed at Loughborough University [93].

2.2.4.1 FTIR

A solid sample of sodium isosaccharinate (0.5 mg) was pressed into a potassium bromide discs using potassium bromide (100 mg), before recording the IR absorption spectrum.

2.2.4.2 NMR

Sodium isosaccharinate (20-30 mg) was dissolved in deuterium oxide and the pH of the solution was adjusted to 12 by adding deuterated sodium hydroxide (0.1 mol dm^{-3}). The solution was then placed into a NMR tube before recording the proton and carbon spectrum.

2.2.4.3 HPLC

Samples of sodium isosaccharinate were filtered through centrifuge filters (10 000 Da MWCO) and pH adjusted to a pH of ~ 4 using nitric acid and sodium hydroxide solutions. These samples were run on the HPLC and the retention time was compared to a standard of ISA made up at 0.01 mol dm^{-3}.

Column:	Waters resolve C18, 5 µm, 90 Å, 3.9 x 300 mm column, part no: WAT 011740
Runtime:	20 min
Mobile Phase:	0.1 M Potassium dihydrogen orthophosphate, adjusted to pH 3.2 $\pm$ 0.1 with concentrated orthophosphoric acid.
Detector:	UV diode array detector
Wavelength:	210 nm
Temperature:	Room temperature
Injection Volume:	20 µl
Flow Rate:	0.7 ml/min

2.3 CDP preparation

The method used for preparing 1% (w/w of solids) and 10% (w/w of solids) CDP samples was that reported by Serco Assurance [94]. For example, for the 10% loading, DI water (750 cm^3), was placed into a stainless steel can and then sparged with nitrogen. Kimwipe® Tissues (30 g), were cut into small squares with an approximate size of 2 cm^2 and added to the steel container. Calcium hydroxide (270 g), was then added to the container and the solution was mixed and re purged with nitrogen. Calcium hydroxide was chosen instead of using cementitious material for ease of use and to save time. The container was then closed tightly, weighed and placed in an oven at 80 °C for 30 days. After this time the container was allowed to cool and then was re-weighed to check for evaporation. The solution was then filtered under vacuum through Fisherbrand QL 100 filter papers and then refiltered through 30,000 MWCO centrifuge filters before use in the experiments. The CDP solution was analysed by HPLC. A 1 % loading used 3 g of tissues and 297 g of calcium hydroxide in 750 cm^3 DI water.

2.3.1 NRVB

A study was carried out to investigate the effects that different cellulose loadings would have on the resulting species in the CDP and the ISA concentration. This was carried out with NRVB instead of the calcium hydroxide so it could be compared accurately to PCM grout which was also used. The same method was used as in section 2.3. The NRVB was broken up into small pieces of approximately 1 cm^2 in size. Loadings of 1, 10, 20, 50 and 100 % cellulose were used. The first batch used in section 3.2.1.1, the 10% solution, was made up in glass containers. When the different loadings were investigated the steel containers were used.

2.3.2 PCM Grout

See section 2.3.1. The only change is that PCM grout was used instead of NRVB and steel containers were used throughout this study.

2.3.2.1 HPLC of CDP

All prepared batches of cellulose degradation products were analysed by HPLC. The samples were filtered through 10 000 Da MWCO centrifuge filters and pH adjusted to ~ 4 using nitric acid and sodium hydroxide solutions. Dilution of the samples was not necessary. Sodium isosaccharinate solutions were prepared at concentrations of 0.01, 0.001 and 0.0001 mol dm^{-3} to determine the concentrations of ISA in the samples of CDP. Standards of formic acid, lactic acid and acetic acid were also made up at 0.02 mol dm^{-3} and the retention times were compared to those in the CDP.

2.4 Solubility Studies

The solubility of various different metals in the presence of CDP and ISA was determined by ICP-MS unless stated otherwise.

2.4.1 Nickel solubility

A nickel chloride solution was made up in 0.001 mol dm^{-3} hydrochloric acid at a concentration of 4×10^{-3} mol dm^{-3}. Aliquots of this (6 cm^{-3}) were put into thirty 15 cm^{-3} plastic centrifuge tubes. The pH of the samples was then adjusted to 12 with tetramethylammonium hydroxide, all except five C_0 samples which were left at the acidic pH so as to measure the initial nickel concentration. The samples were left 48 hours to precipitate. After this time, 6 cm^{-3} of 0.001 mol dm^{-3} hydrochloric acid was added to five of the thirty vials to make the C_0 samples, (the same samples that were left at acidic pH previously,) 6 cm^{-3} of tetramethylammonium hydroxide at pH 12 was added to five vials to make the C12 samples and 6 cm^{-3} of filtered NRVB equilibrated water was added to five vials. These were the controls. The other vials had ligands added to them. The ligands were 10 % CDP (filtered) and ISA at 10^{-3} and 10^{-4} mol dm^{-3}. The CDP and NRVB equilibrated water was filtered prior to addition through 10000 Da MWCO. Aliquots of each ligand, 6 cm^{-3}, were added to five vials each. The samples were then left for a period of 3 days to equilibrate before being centrifuged. The supernatant was then filtered through 0.22 μm Millipore filters. The samples were acidified by adding 0.5 cm^{3} of 2 mol dm^{-3} hydrochloric acid to each vial. The NRVB and CDP samples then had to be diluted by 10 and 250 times respectively to reduce the sodium content entering the ICP. The samples were then analysed by ICP-MS.

2.4.2 Cadmium Solubility

The samples for this analysis were made up as outlined in section 2.4.1. Cadmium chloride was used instead of nickel chloride.

2.4.3 Cobalt Solubility

The samples for this analysis were made up as outlined in section 2.4.1. Cobalt chloride was used instead of nickel chloride. The samples were filtered through 10,000 Da MWCO filters instead of 0.22 μm filters as cobalt was observed coming through the latter.

2.4.4 Thorium solubility

This section is in two parts. In the first part, the method of measurement of thorium is investigated and in the second part, the solubility of thorium in the presence of different complexing ligands is determined.

2.4.4.1 Measurement of Thorium

A number of different methods were employed to investigate the measurement of thorium including liquid scintillation counting, gamma spectroscopy, ICP-MS and ICP-OES.

2.4.4.1.1 Liquid Scintillation Counting

Liquid scintillation cocktail, 10 cm^3, was added to 1 cm^3 of each sample for analysis by LSC in glass vials.

2.4.4.1.1.1 Thorium in water

A stock solution of thorium nitrate was made up with each thorium batch at 0.2 mol dm^{-3} in boiled and nitrogen purged deionised water. In duplicate, each batch was diluted by a factor of 40 into deionised water. The solutions were left 48 hours before they were filtered through 0.45 μm supatop syringe filters.

2.4.4.1.1.2 Thorium in Calcium Hydroxide

A saturated calcium hydroxide solution was made by adding 0.4 g of calcium hydroxide to 100 cm^3 of boiled and nitrogen purged water. This solution was left to stand for 24 hours before being filtered through 0.45 µm supatop syringe filters. The solutions of both batches of thorium in calcium hydroxide were then made up from the stock solution as described in section 2.4.4.1.1.1 but calcium hydroxide was used to dilute the samples instead of water.

2.4.4.1.1.3 Thorium in Carbonate and chloride tests

Solutions of sodium chloride and sodium carbonate (0.1 mol dm^{-3}) were prepared in sodium hydroxide at a pH of approximately 13. The samples were then made up from the stock solution of thorium, only batch 2, as described in section 2.4.4.1.1.1 but these solutions of sodium chloride and sodium carbonate were used instead of the water for the dilution.

2.4.4.1.1.4 Thorium Colloid Interferences

To test for the effects of colloids the solutions made up in section 2.4.4.1.1.2 were re filtered through the 0.45 µm supatop syringe filters, after the 1 cm^3 had been removed for counting. The resulting solution was counted and then this process was then repeated a final time. This was carried out with nine solutions of only batch 2 thorium nitrate.

2.4.4.1.1.5 Thorium in Fresh Calcium hydroxide

Calcium nitrate (3.19 g), was added to sodium hydroxide (1.09 g), dissolved in deionised water (100 cm^3). This was then left to stand for 24 hours before being filtered under suction, washed with water and air-dried. The product of calcium hydroxide (0.4 g), was added to deionised water (100 cm^3), and left to stand for 24 hours. This then was used in the same way as in section 2.4.4.1.1.1 but this new solution of calcium hydroxide was used instead of the water for dilution.

2.4.4.1.1.6 Thorium in Sodium Hydroxide

This solution was made up as in section 2.4.4.1.1.1 from the stock solutions of thorium but a solution of sodium hydroxide at pH 13 was used for the dilution step instead of the water.

2.4.4.1.1.7   Thorium in NRVB

This solution was made up as in section 2.4.4.1.1.1 from the stock solutions of thorium but a solution of NRVB equilibrated water at pH 13 was used for the dilution step instead of the water.   The NRVB equilibrated water was made by breaking NRVB into small pieces of approximately 1 x 1 cm, adding them to deionised water (270 g to 750 cm^3), purging with nitrogen then leaving at 80 $\square$ C for 30 days to equilibrate. The solution is then filtered under vacuum through Fisherbrand QL 100 filter papers and then refiltered through 30,000 MWCO centrifuge filters before use in the experiments.

2.4.4.1.2 Gamma Spectrometry

The samples used to investigate the measurement of thorium by gamma spectrometry were those outlined in sections 2.4.4.1.1.1, 2.4.4.1.1.2 and 2.4.4.1.1.6. After the 1 cm^3 was taken for the LSC, the remainder was weighed and counted in a glass vial by gamma spectrometry for 60 hours.

2.4.4.1.3 ICP-MS

The solutions analysed by ICP-MS were the thorium in water, section 2.4.4.1.1.1, and thorium in calcium hydroxide, section 2.4.4.1.1.2. The samples were acidified by adding concentrated nitric acid (0.02 cm^3), to 5 cm^3 of sample before analysis. The calcium hydroxide sample was diluted by 100 times before the analysis to reduce the salt content of the sample. The ICP for this analysis was used in Escan mode, start mass 0 mass units, stop mass 300 mass units, settle time 0.001 seconds, sample time 0.005 seconds, seg time 1 second, detector mode triple, scan duration 60 seconds.

2.4.4.2 Comparison of thorium solubilities

Solubility studies were performed using over and undersaturation techniques. Oversaturation is where a sufficient amount of thorium nitrate is added to the solution of interest, the pH is then adjusted to produce a precipitate of thorium hydroxide. Undersaturation is where thorium precipitate is first formed before the solution of interest is added to the precipitate at the required pH.

2.4.4.2.1 Undersaturation

The kinetics of the precipitation of thorium was studied before the solubility experiments were carried out.

2.4.4.2.1.1 Kinetic Studies

The first stage in the measurement of solubility by the undersaturation method is to prepare a precipitate of thorium hydroxide. The kinetics and the stability of the precipitate were investigated by firstly preparing a solution of thorium nitrate (4×10^{-3} mol dm^{-3}), in sodium chloride solution (0.1 mol dm^{-3}). Aliquots (12 cm^3), of this solution were pipetted into 30 centrifuge tubes and the pH adjusted to the required values of 6, 8 or 12 by using sodium hydroxide (2 mol dm^{-3}), or concentrated nitric acid solutions. Four sample tubes were left for different time period of 2, 7, 14, 21 and 28 days. The extra 10 samples for each pH were used to ensure the pHs had not drifted too much. After the allotted time period, the samples were filtered through pre-conditioned centrifuge filters (10,000 Da MWCO), pre conditioned with sodium chloride solutions (0.1 mol dm^{-3}), at the same pH as the samples. To reduce filter blockage, one filter was used for every two samples filtered. The filtered samples were then acidified by adding concentrated nitric acid (0.02 cm^3), before the concentration of thorium in each solution was determined by ICP-OES analysis.

2.4.4.2.1.2 Undersaturation Method

Measurement of thorium solubilities by the undersaturation method were carried out at pH 6, 8 and 12. For each pH, 28 samples of thorium hydroxide precipitate were prepared as described in section 2.4.4.2.1.1 and were left for 28 days after which the samples were centrifuged at 6000 rpm for 30 minutes. The supernatant was then pipetted and kept for measurement of thorium concentration. 12 cm^{-3} of the test solution were then added to each precipitate. The test solutions were (i) sodium chloride, 0.1 mol dm^{-3}, at pH 3, (ii) sodium chloride (0.1 mol dm^{-3}), at the required pH of 6, 8 or 12, (iii) saturated calcium hydroxide solution at the required pH of 6, 8 or 12, (iv) ISA (2×10^{-2} mol dm^{-3}), in 0.1 mol dm^{-3} sodium chloride at the required pH, (v) ISA (2×10^{-3} mol dm^{-3}), in 0.1 mol dm^{-3} sodium chloride at the required pH, (vi) 1 % CDP and (vii) 10 % CDP, both at the required pH. 12 cm^{-3} of each solution were added to 4 sample tubes of the precipitated thorium. The pHs of these solutions

were then measured and, if needed, adjustments were made using 2 mol dm^{-3} sodium hydroxide or concentrated nitric acid. The solutions were left for 28 days after which they were filtered through pre-conditioned (0.1 mol dm^{-3} sodium chloride at the pH of the samples) centrifuge filters (10,000 Da MWCO). Concentrated nitric acid, 0.02 cm^{-3}, was then added to the filtered samples before the concentration of thorium in each solution was determined by ICP-OES analysis.

Kinetic investigations of the complexation of thorium with the organic ligands were conducted by setting up further samples and measuring the thorium solubilities after 2, 7, 14, 21 and 28 days.

2.4.4.2.2 Oversaturation

Measurements of thorium solubilities by the oversaturation method were carried out at pH 6, 8 and 12. As an example of the procedure used, a pH of 6 will be described throughout this section. Each test solution (12 cm^{-3}), as described in 2.4.4.2.1.2, was added to 4 centrifuge vials. 0.1 cm^{-3} of a stock thorium nitrate solution (0.814 mol dm^{-3}), were then added to each vial. The pH of the solutions were adjusted to the required pH using carbonate free sodium hydroxide (2 mol dm^{-3}), and concentrated nitric acid. The solutions were left for 28 days before filtering them through pre-conditioned (0.1 mol dm^{-3} sodium chloride at the pH of the samples) centrifuge filters. The filtered samples were then acidified by adding concentrated nitric acid (0.02 cm^{3}), before the concentration of thorium in each solution was determined by ICP-OES analysis.

Kinetic investigations of the complexation of thorium with the organic ligands were conducted by setting up further samples and measuring the thorium solubilities after 2, 7, 14, 21 and 28 days.

2.5 Thorium Complexation in CDP

The samples used for this analysis were similar to those made up for the thorium solubility experiments but with a few modifications.

2.5.1 LC-ICP-MS

Thorium nitrate (0.05 cm^3 of 0.814 mol dm^{-3}), in DI water, was added to 10 cm^3 of test solution. The test solutions were deionised water, saturated calcium hydroxide, ISA (1 x 10^{-2} mol dm^{-3}) in water, ISA (1 x 10^{-2} mol dm^{-3}) in saturated calcium hydroxide solution and 10% CDP. The pH of all the solutions, except the thorium in water, were adjusted to approximately 7 with carbonate free sodium hydroxide (2 mol dm^{-3}), or concentrated hydrochloric acid. A pH of 7 was chosen as it needed to be high enough for the thorium to precipitate but within the range of the reversed phase HPLC column. The solutions were left for 48 hours before filtering through 10,000 Da MWCO filters, (one per sample, preconditioned with sodium hydroxide at the pH of the samples). The samples were then ready for analysis. Standards of formic, lactic and acetic acid were also run to see how their retention time had differed using the new HPLC conditions. These standards were made up as in section 2.3.2.1.

2.6 Metal ISA Interactions

The complexes were formed by making 1:1 mixtures of M:ISA at a concentration of 0.05 mol dm^{-3}. The solution was then left in desiccators to evaporate and solidify. Many of the samples did not solidify properly and formed a gel like substance. In these cases the samples could not be used. The metals used were nickel, iron, cobalt, cadmium and europium all used in the chloride form.

2.6.1 Solid State NMR Studies

A number of different techniques were used on the SS MNR instrument including basic carbon NMR, dipolar dephasing, different spinning speeds and cadmium NMR.

2.6.1.1 ^{13}C NMR Studies

Details are outlined in section 2.1.1.

2.6.1.2 Dipolar Dephasing

The dipolar dephasing was carried out by changing the d7 delay in the pulse sequence from 2 μs to 50 μs. The pulse sequence used is shown in Figure 8.
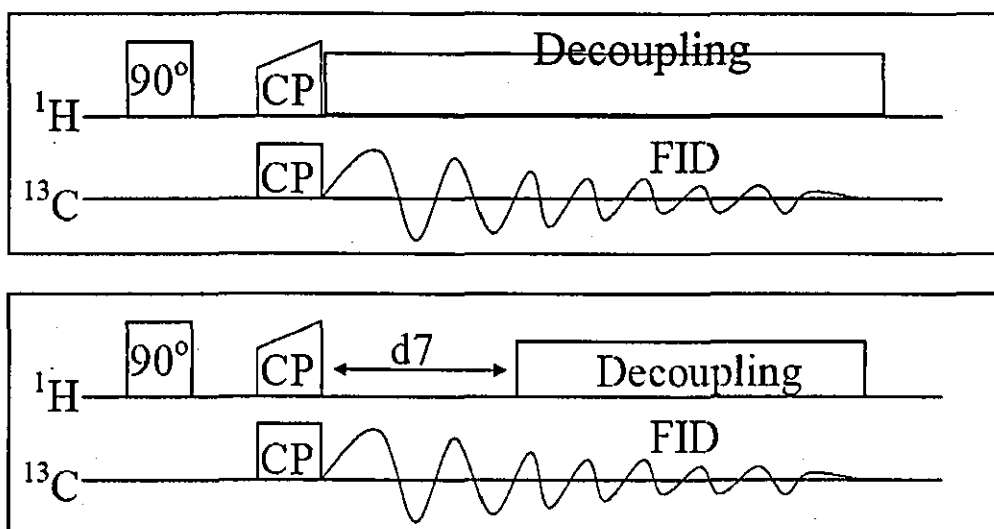
Figure 8 Pulse programme for a standard ^{13}C CP MAS solid state NMR run (top) and one using dipolar dephasing (bottom)

2.6.1.3 CSA

The same parameters as outlined in section 2.1.1 but the spinning speed was varied from 1 – 2 kHz.

2.6.2 XRD

See section 2.1.1

2.6.3 Cadmium NMR

The same parameters were used as outlined in section 2.1.1 but the X nucleus was cadmium instead of carbon.

2.6.4 Gaussian Modelling

The position of the metal bound to the ligand for the modelling of these complexes can be seen in Appendix 4.

2.6.4.1 Structure A
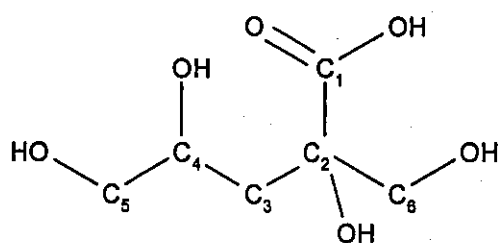
2.6.4.1.1 1:1 Metal:ISA monodentate

The input parameters for the calculations can be seen below. The top line of each set of input data was changed according to the complex being calculated. The other information was kept the same. Each structure was optimised then the NMR calculations were performed.

Optimisation of the complex structure

%chk=CRH_ISA_metal_Cd_1_OH.chk

%mem=52MW

%nproc=1

opt b3lyp/3-21g* geom=connectivity

(then would follow the optimisation data which would be taken from the drawn structure)

NMR of optimised structure

%chk=CRH_ISA_metal_Cd_1_OH.chk

%mem=52MW

%nproc=1

nmr=printeigenvectors b3lyp/3-21g* geom=checkpoint

Title Card Required

0 1

The inputted structure had cadmium bonded to the carbonyl oxygen on carbon 1 and the hydroxyl oxygens on carbons 1, 2, 4, 5 and 6. The formula was $Cd(ISA)(H_2O)_3(OH)_2$ when the cadmium was bound to the carboxyl group and $Cd(ISA)(H_2O)_4(OH)$ when the cadmium was bound to a hydroxyl group.

2.6.4.1.2 2:1 Metal ISA

One cadmium was always bonded to the carboxyl oxygen on carbon 1, the other was bound to the hydroxyl oxygens on carbons 1, 2, 4, 5 and 6. The formula was $Cd_2(ISA)(H_2O)_7(OH)_3$, or $Cd(OH)_2(H_2O)_3(ISA)Cd(OH)(H_2O)_4$.

2.6.4.1.3 1:1 Metal ISA Bidentate

The cadmium always had one bond with the carboxyl oxygen on carbon 1 then the other bond was to the hydroxyl oxygen on carbons 1, 2, 4, 5 and 6. The formula was $Cd(ISA)(H_2O)_3(OH)$.

2.6.4.2 Structure B

As with structure A, the position of the metal bound to the ligand for the modelling of these complexes can be seen in Appendix 4.
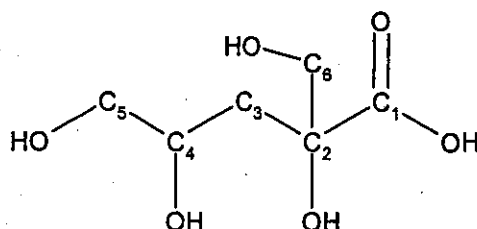
2.6.4.2.1 1:1 Metal:ISA monodentate

See section 2.6.4.1.1. The only change was that the starting structure of ISA was structure B.

2.6.4.2.2 2:1 Metal:ISA

See section 2.6.4.1.2. The only change was that the starting structure of ISA was structure B.

2.6.4.2.3 1:1 Metal:ISA Bidentate

See section 2.6.4.1.3. The only change was that the starting structure of ISA was structure B.

3 RESULTS AND DISCUSSION

The aim of this work was to analyse CDP and determine the effect of the products on the solubilities of radionuclides as well as studying the complexation mechanisms involved. This section discusses the characterisation of CDP along with solubility studies carried out with various metals, in particular the tetravalent actinide thorium and also the complexation studies of ISA, the main product of CDP.

3.1 Characterisation of ISA

The ISA used throughout this work was characterised by a series of analytical techniques. FTIR and NMR spectra and HPLC chromatograms of the ISA are shown in Appendix 1. The spectra and chromatograms were compared to those obtained previously (referred to later as the standards), at Loughborough University [93].

3.1.1 FTIR

The absorption peaks recorded from the ISA used during the investigations described in this thesis compared favourably to the standard.

3.1.2 NMR

The NMR absorption spectra and the assignment of the peaks recorded from the sample of ISA used throughout this work compared favourably to the standard.

3.1.3 HPLC

The retention time of the sodium ISA peak was identical to that observed from previous batches which were analysed on the same day under the same conditions and, apart from a peak that also was present in the blank, no extra peaks were observed. When the ISA was made up in a saturated calcium hydroxide solution there were two peaks present, see Figure 9 and Figure 10. Two peaks have been observed before for ISA in a study by Greenfield et al. [43]. The study reported the two peaks to be due to the lactone and the open chain form although in this case only the open chain form should have been present as the pH was at 12.

There is a possibility that the second peak could be the other isomer of ISA as another study by Greenfield et al.[6] has shown that using sodium or calcium hydroxide to prepare the ISA can have an effect on the proportions of the α or β, also called erythro and threo, isomers produced. Because of this discrepancy, only the first larger peak eluting for the ISA was used in determining concentrations and comparing results. This is also because the second peak which is also present in the CDP solutions is often small and overlapped with other peaks as it is not as clearly resolved as the faster eluting peak. The two retention times in all the CDP samples will always be reported.
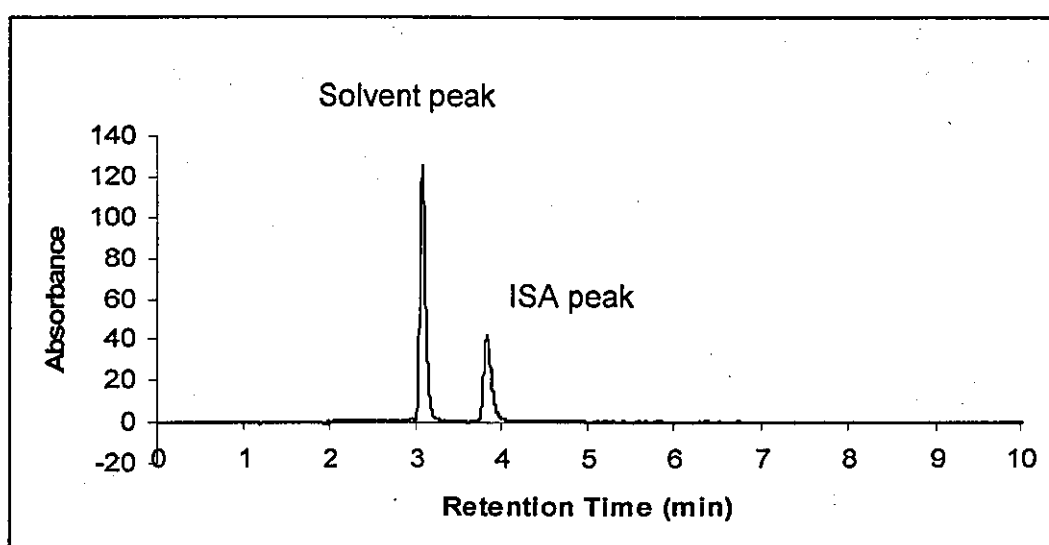
Figure 9 ISA in sodium hydroxide – The peak at 3.1 minutes was in the blank. The absorbance shown is milli absorbance
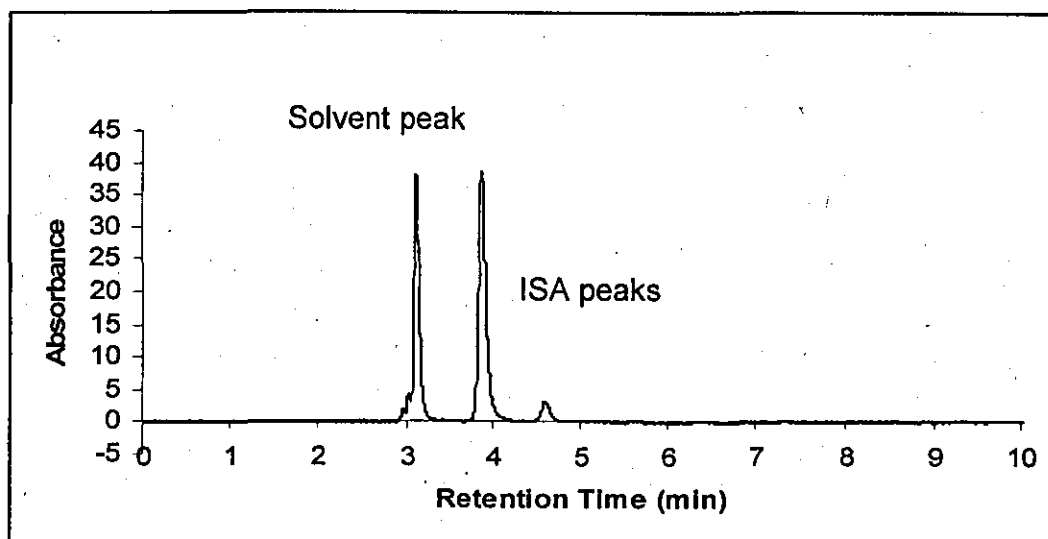
Figure 10 ISA made up in calcium hydroxide – The peak at 3.1 minutes was in the blank. The absorbance shown is milli absorbance

3.2 Cellulose Degradation Products

The CDP were characterised using HPLC and the main peaks were identified by comparing retention times with known standards. Initially the method of making the CDP involved using NRVB cement. The first set of solubility experiments involving different cations besides thorium used CDP from this batch. The method then evolved into using calcium hydroxide instead of the NRVB material to save time and for ease of use. The CDP made using calcium hydroxide were used for the thorium solubility work. This section includes the characterisation of both of these types of CDP. A final method of producing CDP was then employed which used another type of cement whose proposed use was for encasing plutonium contaminated material waste. This was investigated to see if there were any major differences in the CDP components depending on which cement was used. Different cellulose loadings were also investigated using the PCM grout and NRVB grouts to look at the production of ISA in the CDP.

3.2.1 Characterisation

The first step was to identify the main components present in the different solutions of CDP and calculate the ISA concentrations as this was needed in later solubility studies.

3.2.1.1 CDP using NRVB grout

The CDP made with NRVB grout were used in the solubility experiments discussed in section 3.3.1, 3.3.2 and 3.3.3. The concentration of ISA in the CDP was 6.13×10^{-4} mol dm^{-3}. The chromatogram of the CDP and the retention times of the main components present can be seen in Figure 11 and Table 8. There was some water loss associated with this particular batch which may have contributed to the slightly lower ISA concentration than expected. The effect of different cellulose loadings was investigated using this method of CDP production and the chromatograms from this analysis can be seen in Appendix 2 and the results are discussed in more detail in section 3.2.2.
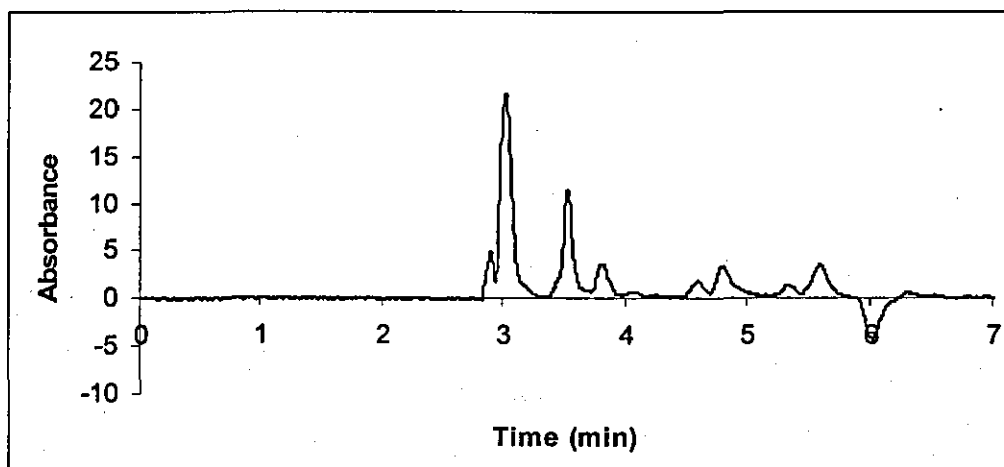
Figure 11 Chromatogram of the 10% CDP solution made using NRVB grout. The absorbance shown is milli absorbance

Table 8 Retention times of the main components present in 10% CDP made using NRVB grout

Carboxylic Acid	Retention time
Formic Acid	3.53
ISA	3.81 and 4.60
Lactic Acid	4.80
Acetic Acid	5.62

The different concentrations of ISA produced from different cellulose loadings can be seen in Table 9. These results were obtained in a separate study which is why another 10% CDP sample is present with a slightly different ISA concentration to that previously reported of 6.13×10^{-4} mol dm^{-3}.

Table 9 ISA concentrations in CDP with different cellulose loadings, made in the presence of NRVB grout

CDP Loading	ISA concentration (mol dm^{-3})	ISA Peak Area
1 %	0.19×10^{-2}	30.75
10 %	1.64×10^{-2}	264.41
20 %	2.04×10^{-2}	327.90
50 %	5.14×10^{-2}	828.69
100 %	5.59×10^{-2}	900.23

3.2.1.2 CDP using Calcium Hydroxide

The CDP created using calcium hydroxide were used for the thorium solubility experiments and method development work discussed in section 3.3.4. This study used CDP at 1% and 10% although only the 10% chromatogram is shown here in Figure 12 and the retention times of the main components are in Table 10. As this CDP was used for a large solubility study, 2 batches had to be prepared, the chromatograms for the second batch can be found in Appendix 2 along with the 1% CDP solution data for both batches.
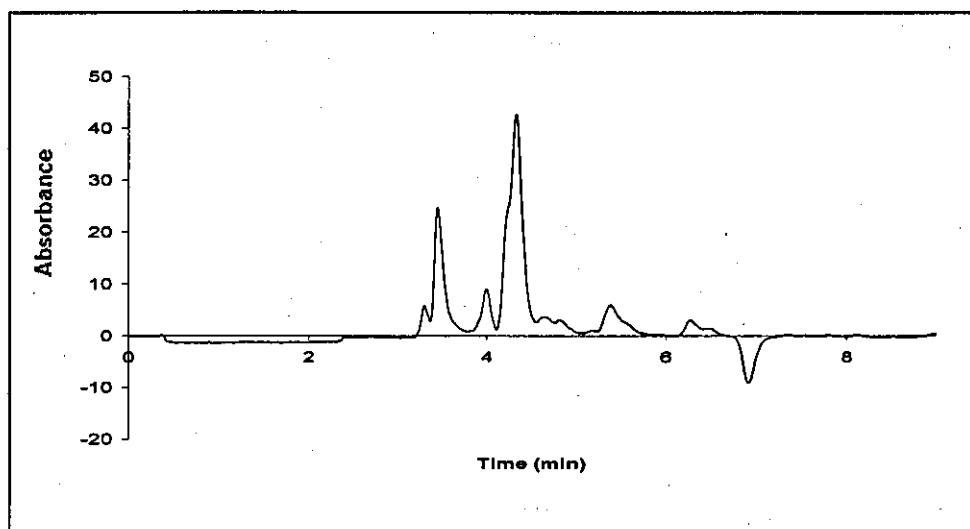
Figure 12 Chromatogram of the 10% CDP solution made using Ca(OH)$_2$, batch 1. The absorbance shown is milli absorbance

Table 10 Retention times of the main components present in 10% CDP made in the presence of Ca(OH)$_2$

Carboxylic Acid	Retention time (min)
Formic Acid	4.05
ISA	4.40 and 5.12
Lactic Acid	5.43
Acetic Acid	6.29

The retention times differed to the previous batch of CDP as a new column was used because of column degradation. The concentration of ISA found in both batches and with the different cellulose loadings can be seen in Table 11.

Table 11 ISA Concentration in each CDP batch and loading used, made in the presence of Ca(OH)₂

CDP Batch number	Cellulose Loading	ISA concentration (mol dm^{-3})
1	1 %	7.22×10^{-5}
	10 %	0.0101
2	1 %	3.40×10^{-4}
	10 %	0.007

3.2.1.3 CDP using PCM grout

The CDP generated using the PCM grout material were used to investigate whether different cements cause changes in the CDP fingerprint or concentrations of components in the CDP. These data were compared to the NRVB data and are discussed in more detail in section 3.2.2. Chromatograms for the different loadings of cellulose in the presence of PCM grout are in Appendix 2. The chromatogram for a 10% loading of CDP is shown in Figure 13. The figure does not include the whole of the first peak as this meant a clear view of the rest of the chromatogram was not possible if the initial peak was shown in full. As with the NRVB solutions, different cellulose loadings were made up in the presence of PCM grout and analysed, see Table 13.

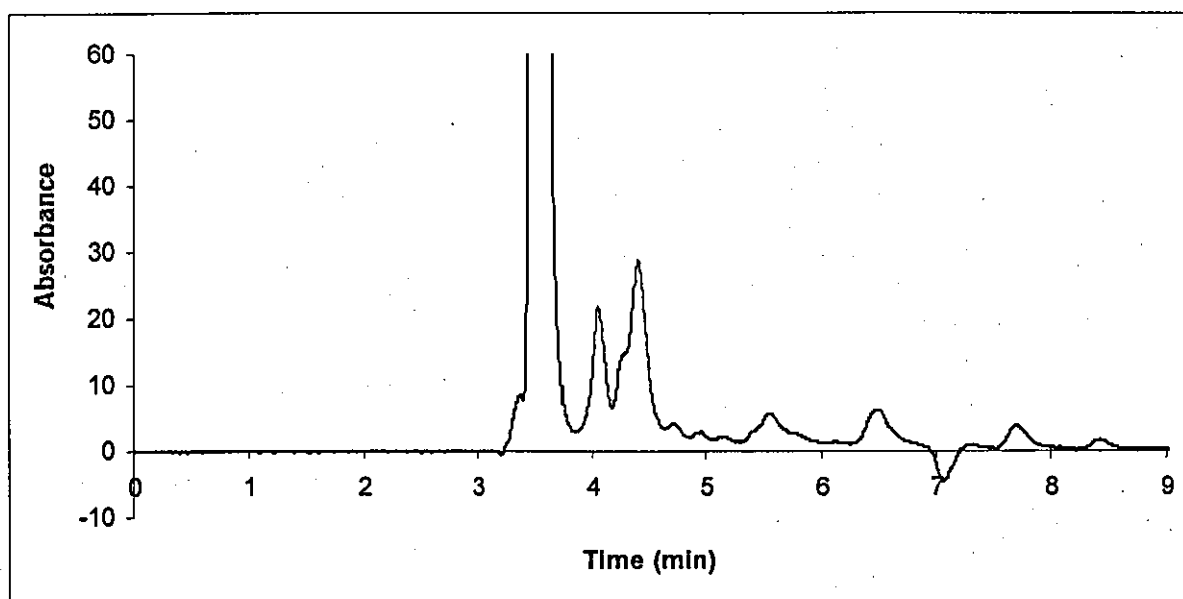**Figure 13** Chromatogram of the 10% CDP solution made in the presence of PCM grout. The absorbance shown is milli absorbance

Table 12 Retention times of the main components present in 10% CDP made in the presence of PCM grout

Standard	Retention Time (min)
Formic Acid	4.12
ISA	4.43 and 5.43
Lactic Acid	5.59
Acetic Acid	6.45
Unknown	11.16

Table 13 ISA Concentration in each CDP loading used with PCM grout

Cellulose Loading	ISA Concentration (moldm^{-3})	ISA Peak Area
1%	2.9 x 10^{-4}	12.04
10%	5.9 x 10^{-3}	242.55
20%	5.1 x 10^{-3}	211.34
50%	5.6 x 10^{-3}	229.55
100%	5.8 x 10^{-3}	239.79

3.2.2 PCM/NRVB/Ca(OH)$_2$ Comparisons

There appeared to be no significant differences between the 10% loadings of cellulose from the three different materials used in terms of the identity of the products produced. There was some variation with the concentrations of ISA present but when looking at the peak areas of the rest of the components in the solution this was thought to be due to some evaporation of the sample affecting all the species concentrations in the mixture. These results indicate that the cement involvement in the degradation of cellulose is to provide a high pH environment but it does not strongly influence the main species formed in the degradation process or their concentrations.

3.2.2.1 NRVB different loadings

The effect of cellulose loadings was studied to determine if any major differences were apparent in the CDP mixture when different amounts of cellulose were present. This obviously has a great importance in the safety assessment of a repository as there could easily be areas of different cellulose loadings present throughout. The concentration of ISA produced was of particular interest as this is the main component produced in the degradation process and also is used in solubility studies discussed later.

3.2.2.1.1 ISA Concentrations

Figure 14 shows the increase in ISA concentration with increased cellulose loadings of 1, 10, 20, 50 and 100 % (w/w). The concentration appeared to tail off when a higher cellulose loading was used indicating that a maximum ISA concentration from the degradation of cellulose was being reached.
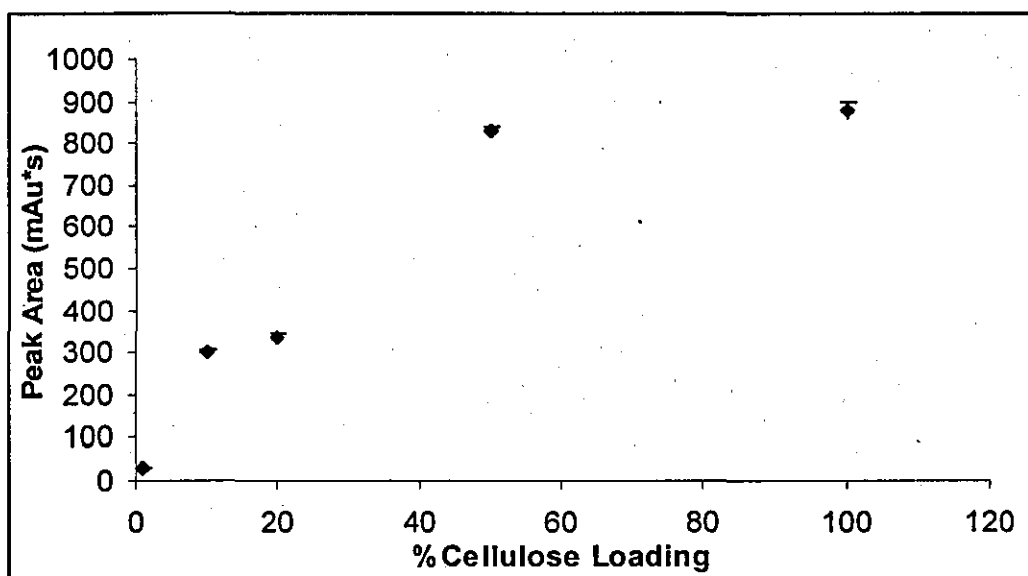
Figure 14 Graph of Peak area of ISA against cellulose loading

This effect was also noticed in the production of the lactic acid and acetic acid. The concentrations in solution are increasing with increased cellulose loading but not as quickly as their initial rate of formation, see Figure 15. Formic acid was not plotted on this graph as it was suspected that the peak was overlapped with other unretained components eluting at the beginning of the column. Another interesting point to note is that at a 20% cellulose loading there is a dip in the concentration of ISA produced and this is also seen in the formation of the other carboxylic acids.
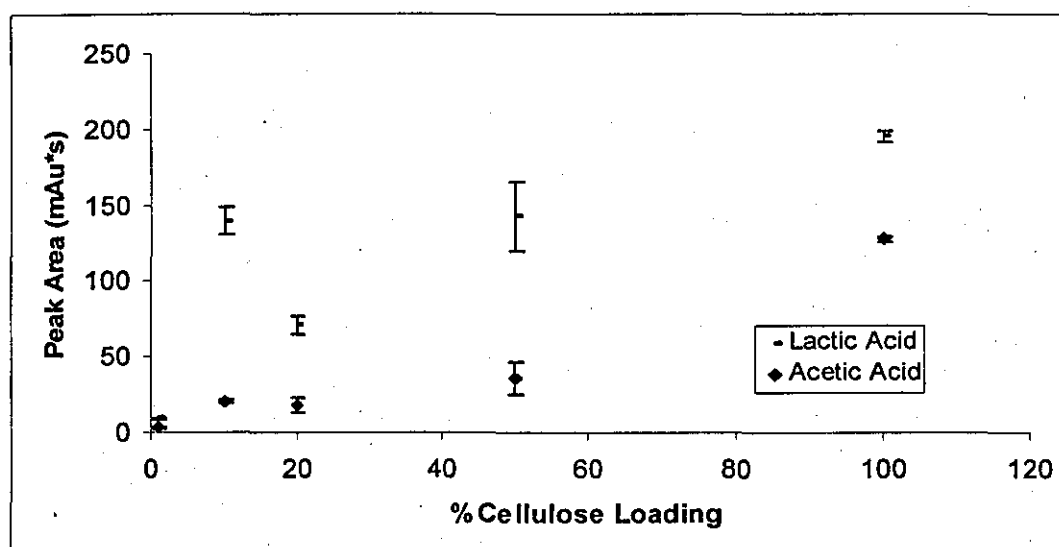
Figure 15 Graph of Peak area of lactic and acetic acid against cellulose loading

The results suggested that after a cellulose loading of approximately 50 %, no further ISA was produced. Interestingly other components were produced as the loading increased indicating that the degradation of cellulose was not complete, just the production of ISA which complies with previous studies that the degradation of cellulose is a very long process. This indicates that other products were produced or the ISA itself was degrading to produce new species, see Table 14.

Table 14 Number of components present in CDP using different cellulose loadings

Cellulose Loading	Number of components
1 %	5
10 %	8
20 %	5
50 %	5
100 %	10

3.2.2.2 PCM different loadings

Different cellulose loadings were prepared as described in section 2.3.2, using PCM grout instead of NRVB to investigate whether this caused any differences in the components produced or concentrations of the products. This is an important comparison because, if the PCM grout causes higher concentrations of complexing ligands to be produced, this needs to be accounted for in the safety assessment of the disposal of PCM. The chromatograms, along with peak retention times and areas, can be found in Appendix 2.

3.2.2.2.1 ISA Concentrations

For consistency the ISA concentrations in the PCM solutions were calculated, Table 13, and compared to the NRVB data, Table 9. The results indicated that a maximum concentration of ISA was produced from a 10% loading of cellulose, and that further increases in cellulose loading did not increase the quantity of ISA produced by the degradation of cellulose, Figure 16.
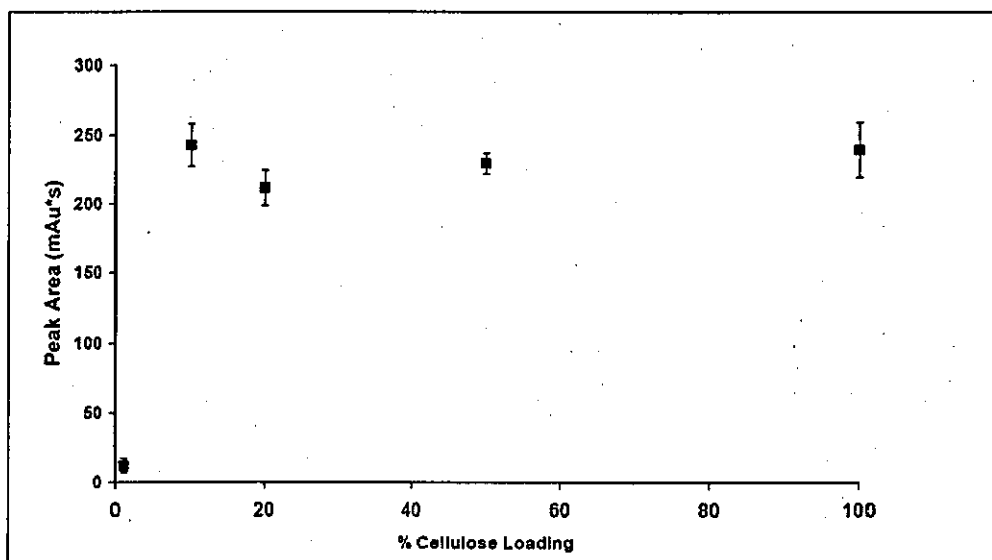
Figure 16 ISA peak area as a function of cellulose loading

When the peak areas of the other main components present in the CDP mixture were analysed, although there was considerable scatter in the results, it could be seen that as in the case of ISA, the maximum concentrations of the three organic acids were produced by a 10% cellulose loading. An increase in cellulose loading did not produce significantly more acetic,

lactic or formic acids, Figure 17 . The same affect is seen at a 20% cellulose loading as with the NRVB material where there is an apparent drop in the concentration of carboxylic acids produced.
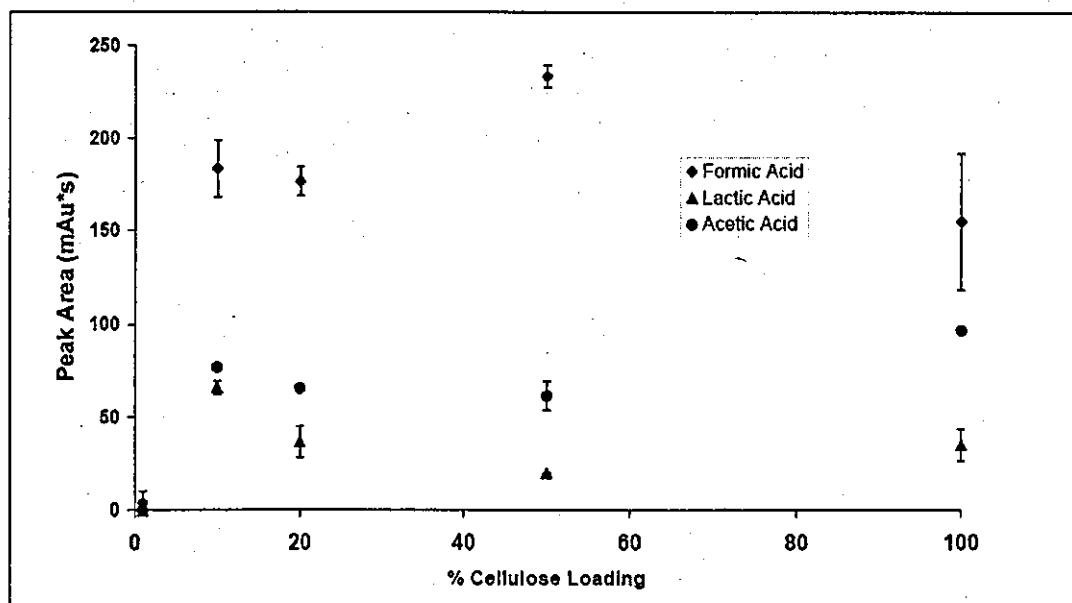
Figure 17 Peak areas of identified species as a function of cellulose loading

Despite the lack of change in the production of ISA, and the three simple organic acids with increased cellulose loading above 10%, it was clear that the fingerprint of the CDP became more complicated with higher cellulose loading. There were many more components present in the 100% loading sample than the 1% for example. The results are shown in Table 15. At present the components responsible for these peaks remain unidentified.

Table 15 Number of components present in CDP using different cellulose loadings

Cellulose Loading	Number of components
1 %	5
10 %	14
20 %	14
50 %	18
100 %	18

These data indicated that the degradation of cellulose is a complex process with new species being formed at higher cellulose loading, but with other species either being produced in a lower quantity, or being degraded themselves. Species with longer retention times are likely to be less polar and larger than the carboxylic acids identified above which may provide some indication as to their identity.

3.2.3 Discussion

The main products from the alkaline anaerobic degradation of cellulose have been identified as ISA, formic acid, lactic acid and acetic acid which correlates well to previous research [43]. No significant differences in the products produced were apparent when a different material was used to create the alkaline environment indicating that this material was only present to create the high pH environment. There were some differences in the number of different products produced at different cellulose loadings and in the presence of different cementitious materials. At cellulose loadings of 1 and 10 % the concentration of ISA in all three solutions (NRVB, PCM grout and calcium hydroxide,) was similar. The differences become apparent when looking at Figure 14 and Figure 16 where the maximum concentration of ISA produced in relation to cellulose loading is shown. With the PCM material a maximum concentration of ISA was reached at approximately 10% cellulose loading and there was no significant increase in the ISA concentration after this point. With the NRVB material this occurred at approximately 50% cellulose loading.   Studies have shown that ISA can sorb onto cementitious materials and this could be occurring [95]. The sorption of ISA onto the NRVB

could be higher than the sorption onto the PCM material resulting in a lower concentration of ISA present at the lower cellulose loadings. It may not be until a 50% cellulose loading is used that no more ISA can sorb onto the NRVB material so more is detected in the solution. It is also possible that the differences found are due to the grinding up of the cementitious material as it would be impossible, unless machinery were used, to get the same surface area of cement each time a solution was set up.

There were some differences observed with the number of components present when the two different materials were used although this is most likely because of HPLC column degradation. When the NRVB samples were analysed by HPLC, the resolution between the peaks in the solution was not as good as previous analyses with the PCM grout data. The cause was suspected to be column degradation. This would mean that not as many solution species could be detected as their peaks overlapped. Because of this, no further conclusions could be drawn from this part of the investigation.

When the cellulose loading was increased in both solutions, even though the maximum concentration of ISA had been reached by a 50% cellulose loading, the number of components in the mixture carried on increasing. This implies that either the ISA was degrading to form some other products or new products were being produced which may mean that over a longer time period the ratios of all the species present may be different. As previously mentioned, the sorption of some species onto the cementitious materials may also be occurring which would mean that when the cellulose concentration is increased more components may be detected as the sorption sites on the cement are being filled or saturated. A study could be carried out to actually determine the pore size of the different cementitious materials used to see if there is a large difference between cements which may cause differences in terms of the sorption of ISA. The degradation of the ISA itself is a possibility as has been studied by Askarieh et al. [31]. Askarieh's study suggests that the microbial degradation of complexing agents produced form the degradation of cellulose is possible although the chances are small and the microbes present to degrade the compounds would usually need time to evolve which is unlikely to happen after just 30 days.

Cellulose degradation is complicated and the mechanisms involved are not fully understood [6]. The main product is always reported as ISA but the nature of the degradation means that

many different products can be produced depending on the exact conditions employed. In a review of the mechanisms of alkaline degradation, Greenfield et al. state that the products from the alkaline degradation of cellulose can be interpreted in terms of the Nef-Isbell theory[6]. Under alkaline conditions cellulose can be considered as a glucose unit, substituted by the rest of the chain at the 4-position, present as both pyranose and acyclic forms. The acyclic form can undergo an epimerisation where the carbonyl functionality migrates via a series of endinols. A dicarbonyl species can then be created by elimination of a hydroxide or alkoxide ion to the endinol followed by a rearrangement. This then undergoes a benzilic acid rearrangement to form the saccharinic acid. All the steps previous to the benzilic rearrangement are reversible. All of the steps involved in the Nef-Isbell reactions and the reversibility means that a number of different products can be produced which makes the analysis and identification of all the products quite complex. The rates of this process are also greatly dependant on the conditions as a study by Ziderman and Bel-Ayche [96] proved when the rate of the peeling reaction increased as the pH was raised from 8 to 10.5. As the pH in the solutions studied throughout this work was determined by the cementitious material used this could affect the rate of the reaction. Temperature can also have an affect [97] although any differences in results throughout this study should not have been changed by this as the temperature remained constant for all the different batches prepared.

Although the same make of tissues were used throughout, the purity was never investigated and differences in the results could come from different batches of tissues used.

3.3 Solubility studies

The solubilites of various cations were studied in the presence of CDP and different ISA concentrations. The aim was to determine whether these ligands have an effect on the metal solubility and if so, to what degree. Previous studies have shown that the solubility of some metals is increased in a solution of CDP over that expected from ISA at the same concentration. The cations studied were nickel, cadmium, copper, and thorium. Examples of di and tetravalent metals were studied as they are all expected in the repository and the solubility is likely to be affected in varying amounts depending on the valency of the metal. The experiments were also carried out with europium, iron (III) and tin but no reproducible results could be obtained. As thorium is a tetravalent cation and the biggest increase in solubility has been found with such actinides, its solubility was looked at in greater detail including method development for the solubility studies.

3.3.1 Nickel Solubility

The expected solubility for nickel in solutions at high pH is approximately 10^{-8} mol dm-3 according to the CHESS database [98]. In CDP the solubility has previously been found to be 2×10^{-4} mol dm^{-3} [7]. The solubility found in different ligand solutions in this study can be seen in Table 16. The concentration of ISA present in the CDP was 6.13×10^{-4} mol dm^{-3}.

Table 16 Solubility of Nickel in the presence of different complexing ligands

Ligand solution	Metal Solubility (mol dm^{-3})	Standard deviation of Grand Mean
ISA 1×10^{-3} mol dm^{-3}	2.12×10^{-6}	5.95×10^{-7}
ISA 1×10^{-4} mol dm^{-3}	1.87×10^{-7}	3.37×10^{-8}
CDP 10% loading containing 6.13×10^{-4} mol dm^{-3} ISA	2.85×10^{-5}	2.56×10^{-5}

The solubility of nickel in CDP was an order of magnitude lower than previous results. The baseline solubility of nickel in NRVB equilibrated water was 1.2×10^{-7} mol dm^{-3}. The solubility in all the ligand solutions except the ISA at 1×10^{-4} mol dm^{-3}, had risen above the baseline as expected and the metal was at least 10 times more soluble in CDP than ISA of a comparable concentration. The ISA alone increased the metal solubility by a factor of 10 above the baseline when 1×10^{-3} mol dm^{-3} concentrations of ISA were studied. The difference found between these results and previous studies could be due to the fact that the concentration of ISA in the CDP used previously was 10^{-3} mol dm^{-3} whereas the solution of CDP used in this work only contained 6×10^{-4} mol dm^{-3}. This could have a large effect on the metal solubility as ISA alone increased the solubility of the metal.

3.3.2 Cadmium Solubility

According to the CHESS database [98] the solubility of cadmium is approximately 3×10^{-7} mol dm^{-3} under alkaline conditions. This was calculated assuming the production of the crystalline solid though if the amorphous precipitate is formed as expected then the solubility could be higher than this. The results from these solubility studies can be seen in Table 17.

Table 17 Cadmium solubility in the presence of different complexing ligands

Ligand solution	Metal Solubility (mol dm^{-3})	Standard deviation of Grand Mean
ISA 1×10^{-3} mol dm^{-3}	4.74×10^{-6}	8.06×10^{-7}
ISA 1×10^{-4} mol dm^{-3}	8.4×10^{-7}	1.76×10^{-7}
CDP 10% loading containing 6.13×10^{-4} mol dm^{-3} ISA	7.95×10^{-6}	2.75×10^{-8}

The concentration in a solution of NRVB equilibrated water was 2.93×10^{-8} mol dm^{-3}. The solubility in ISA at 1×10^{-4} mol dm^{-3} concentration is close to the baseline solubility at high pH with no ligands present. In the CDP solution the solubility is approximately twice that of

ISA at a similar concentration. These results indicated that there is something else present in the degradation products increasing the metal solubility as with the nickel. The ISA alone increases the solubility by a factor of approximately 10.

3.3.3 Cobalt Solubility

The calculated solubility of cobalt at high pH is 5×10^{-12} mol dm^{-3} using the CHESS database [98]. Other studies have found the solubility to be 2.9×10^{-6} mol dm^{-3} at high pH and 25 °C [99]. This difference could again be due to the crystallinity of the solid phase formed during precipitation as the CHESS database assumes the crystalline solid is formed and calculates this solubility. The solubility results can be seen in Table 18.

Table 18 Cobalt solubility in the presence of different complexing ligands

Ligand solution	Metal Solubility (mol dm^{-3})	Standard deviation of Grand Mean
ISA 1×10^{-3} mol dm^{-3}	2.35×10^{-8}	2.06×10^{-9}
ISA 1×10^{-4} mol dm^{-3}	1.77×10^{-8}	1.52×10^{-10}
CDP 10% loading containing 6.13×10^{-4} mol dm^{-3} ISA	2.16×10^{-6}	1.59×10^{-8}

The cobalt solubility in NRVB equilibrated water was 2.8×10^{-8} mol dm^{-3}. The ISA did not affect the solubility of the cobalt significantly as the concentration in solution is very similar to the baseline concentration detected. The CDP however increases the solubility approximately 100 times above background and the ISA solutions.

3.3.4 Thorium Solubility

Thorium is often used as an analogue for plutonium as plutonium may exist in the 4+ state. Solubility experiments carried out previously have often reported different results. The solubility of thorium is of importance in the performance safety assessment of a nuclear waste repository and so it is essential to gain accurate, reproducible data. For these reasons some method development was carried out into how best to measure thorium solubility.

3.3.4.1 Measurement of Thorium

The techniques used were liquid scintillation counting, gamma spectrometry and ICP-MS. It was determined that the latter was the most accurate method to detect and measure thorium although the high salt content of the samples used in the solubility experiments meant that ICP-OES was a more suitable method for analysing those samples.

3.3.4.1.1 Liquid Scintillation Counting

This was a relatively simple technique but it was not known whether it would provide enough sensitivity to get to such low levels of thorium expected at high pH. The solubility in a number of different solutions was tested as listed in the following sections.

3.3.4.1.1.1 Thorium Solubility in Water

The first solution measured was prepared from thorium nitrate obtained from Fluka, batch 1, in water, where all the thorium should be in solution and therefore there is no precipitation. When the thorium nitrate was added to water the pH drops to approximately 2. The resulting spectra showed two peaks present, Figure 18. It was a possibility that from the outset that two batches of thorium would have to be used in this study due to the large number of samples needed and the small amount of thorium available of one batch. As a test the same experiment was carried out on the second batch of thorium nitrate, obtained from Hopkins and Williams (a much older stock), Figure 19. It was clear that there are differences between the two spectra, mainly that the older batch, batch 2, has only one peak present. The counts from these experiments can be seen in Appendix 3.
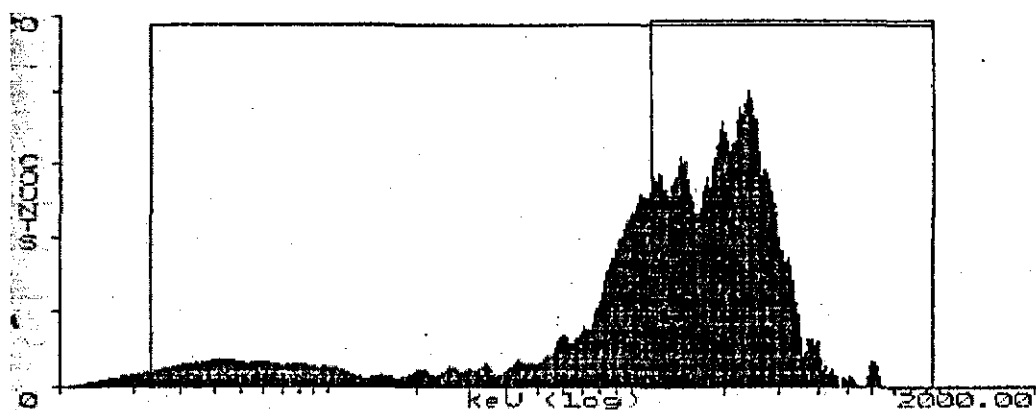
Figure 18 Liquid scintillation spectra for thorium nitrate in water, Fluka batch 1
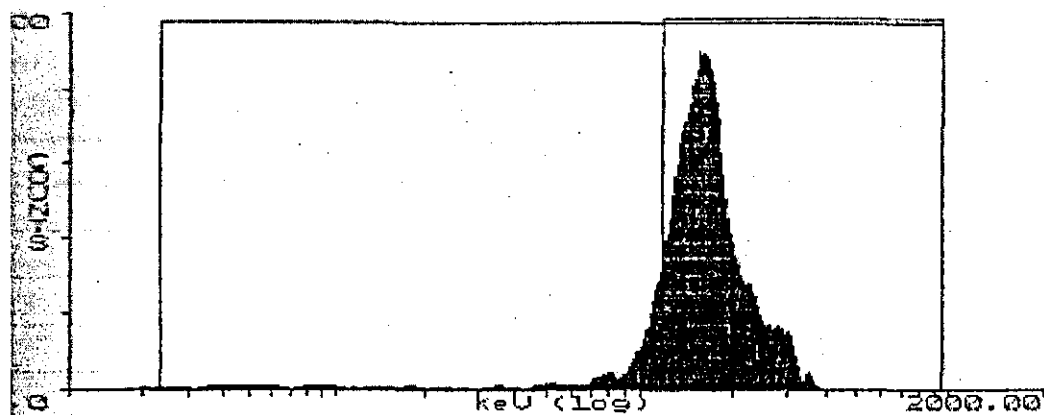

Figure 19 Liquid scintillation spectra for thorium nitrate in water, Hopkins and Williams batch 2

Originally it was thought that the different peaks were due to the ^{232}Th and a daughter or daughters of thorium. To try and identify the peaks some standards were counted, the spectra can be seen in Appendix 3. ^{241}Am, ^{233}U and ^{228}Th were analysed. Each standard has two main alpha energies at 5.48 and 5.44, 4.82 and 4.77, and 5.4 and 5.3 MeV respectively. From the positions of the peaks it was determined that the first peak present in batch 1 – Fluka was from the ^{232}Th as the expected energy of this would be 4 MeV, and the second must be from the daughters which have a higher energy than the thorium as shown in Table 19.

Table 19 Daughter products of Th ^{232} and their associated energies

Radionuclide	Half Life	Energy (MeV)
^{232}Th	1.4×10^{10} years	α 4.0, γ 0.06
^{228}Ra	6.7 years	β 0.01
^{228}Ac	6.1 hours	β 2.2-0.25, γ 1.6-0.06
^{228}Th	1.9 years	α 5.4, 5.3, γ 0.08
^{224}Ra	3.6 days	α 5.7, γ 0.24
^{220}Em	52 seconds	α 6.3
^{216}Po	0.16 seconds	α 6.8
^{212}Pb	10.6 hours	γ 0.41-0.11, β 0.59, 0.36
^{212}Bi	61 minutes	γ 2.2-0.04, β 2.3, α 6.1, 6.0
^{212}Po	3×10^{-7} seconds	α 8.8
^{208}Tl	3.1 minutes	β 1.3-2.4, γ 2.62-0.28
^{208}Pb	stable	

It is possible that batch 2 thorium nitrate was purified and the daughters removed which is why only one peak remains in the spectrum. There were no records available with this sample so this could not be confirmed without trying to purify the batch 1 sample for a comparison.

3.3.4.1.1.2 Thorium in Calcium Hydroxide

The solution of thorium in calcium hydroxide would be the baseline solubility result for thorium at high pH as calcium hydroxide was present in the CDP solutions. The thorium was prepared in calcium hydroxide to see if the method was sensitive enough to use for such low levels of thorium as expected at high pH. Figure 20 shows the spectra obtained for both batches. Interestingly there was no longer a difference between the two batches and both showed the same peak present which was in the same position as the second peak that was

present in batch 1, thorium in water. The counts were not close to background which was not
expected as at high pH there should be very little thorium present in the solution.
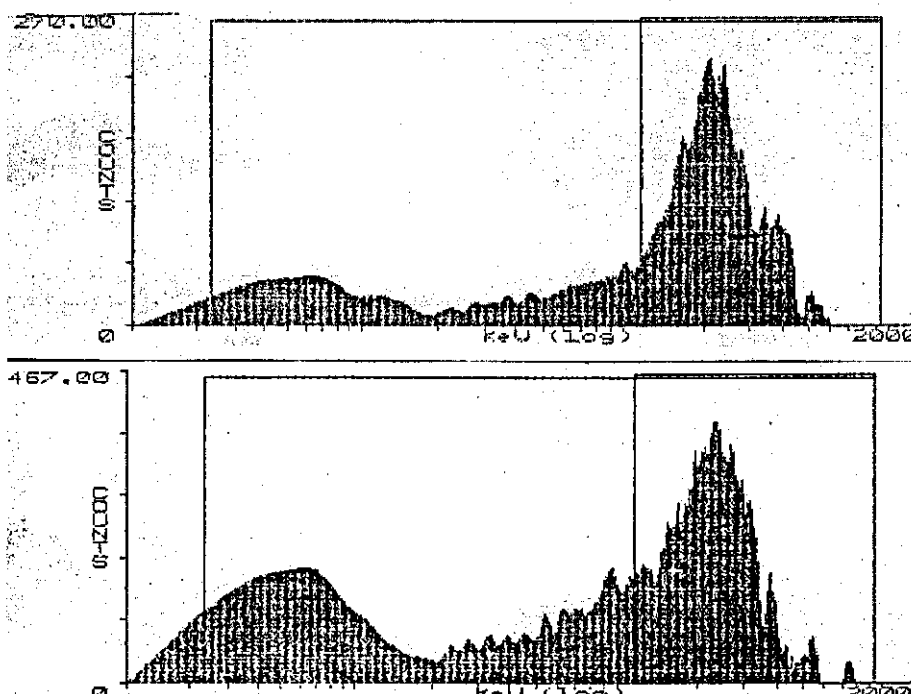

Figure 20 Thorium in calcium hydroxide top – batch 2, bottom – batch 1

Tests were carried out to see if the extra counts were coming from chloride or carbonate
complexes that may have been formed. It is possible that the calcium hydroxide would have
these components present and if they formed strong complexes with the thorium or daughters,
it could increase their solubility. The results from these experiments where thorium was in
the presence of sodium carbonate and separately sodium chloride showed no significant
difference to the blank samples indicating that the presence of carbonate or chloride were not
responsible for the increased counts observed in the calcium hydroxide solution. See
Appendix 3 for counts recorded for all these experiments.

3.3.4.1.1.3   Colloid interferences

Thorium is known to form colloids [100] so a test was carried out to see if the high counts observed were from thorium colloids. Figure 21 shows the results from filtering the solutions three times to see whether there was a significant drop in counts. There was an obvious drop in counts initially after filtering once which could be due to colloids but could also be because of sorption of thorium onto the filters. After filtering once there is no further change in the number of counts in solution although the counts remain higher than expected so the extra activity observed cannot be solely because of colloids.
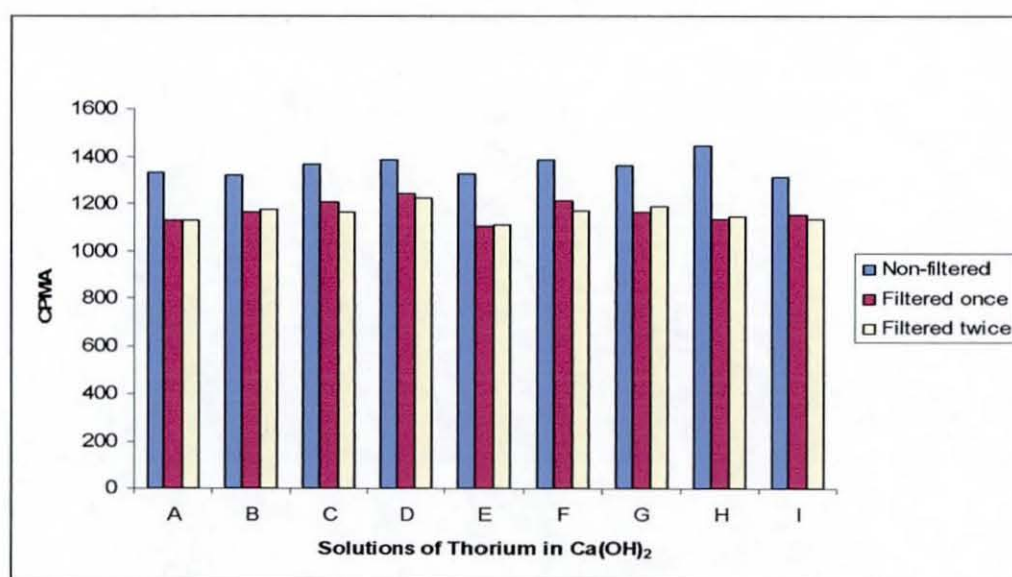

Figure 21   Graph of counts per minute, channel A, against different solutions of thorium in Ca(OH)$_2$ after being filtered for different time periods

3.3.4.1.1.4   Thorium in fresh calcium hydroxide

An experiment was carried out on the thorium in fresh calcium hydroxide to see whether ageing i.e. sorption of carbon dioxide in the calcium hydroxide, had any effect on observed counts. This test had no effect on the counts observed or the spectra seen for the thorium solubility in calcium hydroxide.

3.3.4.1.1.5 Thorium in Sodium Hydroxide

The solubility of thorium in sodium hydroxide at pH 13 was investigated to determine whether the presence of calcium was affecting the thorium or if the same peak was present. The results showed only background counts. This meant that the technique may not have a low enough LOD to use in these solubility studies even if the problem of extra counts could be resolved, although a difference in solubility above background could be determined. It also meant that there was definitely something present in the calcium hydroxide increasing the thorium or daughters solubility as this would not result from just a pH effect or instrumental error.

3.3.4.1.1.6 Thorium in NRVB

The solubility studies needed to be carried out in a solution of NRVB as some of the CDP used was made in the presence of this cementitious material. This analysis could also have helped in determining if the extra counts observed in the presence of calcium hydroxide came from an interference or contaminant in the calcium hydroxide used. Similar results were obtained to those for thorium in calcium hydroxide, Figure 22. Again there was only one peak present and it was at the same position as previously observed. This implied that a contaminant was not present in the calcium hydroxide but that there was something in both this and the NRVB that enhances thorium or its daughters solubility.
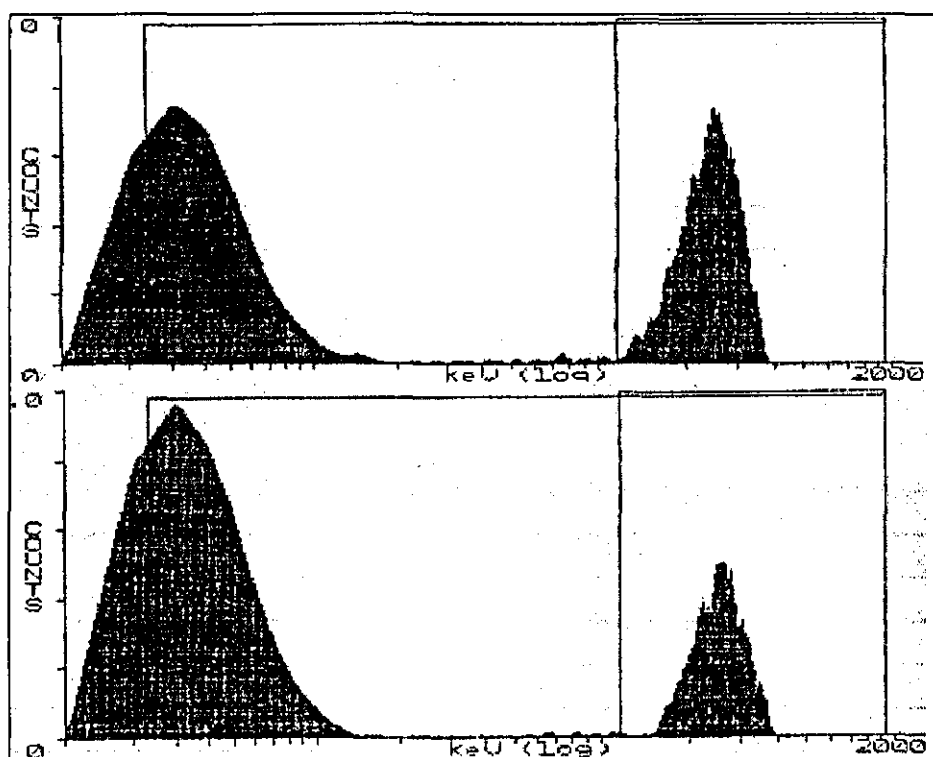
Figure 22 Thorium solubility in NRVB solutions, top – batch 2, bottom – batch 1

3.3.4.1.2 Gamma Spectrometry Analysis of Thorium

To try and understand what was causing the extra peaks in the calcium hydroxide samples, gamma spectrometry was carried out to try and identify whether it was the daughters. If the active component producing the extra counts in solution could be identified, it would help with understanding what else was present in the calcium hydroxide increasing this components concentration. Table 20 shows the radionuclides detected in the gamma spectrum of the thorium in water and calcium hydroxide. There were many unidentified peaks present but it was clear that there were daughters present in both batches of thorium and in the calcium hydroxide samples. The thorium in sodium hydroxide was also analysed but had background results as expected. The counts from the daughters were reduced significantly when looking at data from both solutions, acidic and high pH, so some had precipitated out but not all. This indicates that the daughter solubility in calcium hydroxide is higher than expected but why the daughters were not seen in sodium hydroxide is still unclear.

Table 20 Thorium daughters, their gamma photon energies and observed counts for the corresponding energies

Radionuclide	γ photon energy (keV)	Thorium in Water		Thorium in Ca(OH)₂	
		Batch 1 counts	Batch 2 counts	Batch 1 counts	Batch 2 counts
²¹²Pb	239	43728	17886	1450	677
	300	3101	1261	789	0
²⁰⁸Tl	2615	0	0	0	0
	583	9573	3562	373	189
	511	3587	1327	0	0
	861	1123	391	0	0
	277	2598	0	0	0
²²⁸Ac	911	5066	2379	1441	1009
	969	3083	1405	867	528
	338	7684	3664	2430	1553
	965	1081	779	0	0
	463	2270	1042	663	401
	795	1129	513	310	187
	209	5603	2617	1666	1029
	270	3622	1632	1027	654
	1588	417	0	0	0
	328	2737	1323	786	465
	129	6030	2926	1637	1017
²¹²Bi	727	2165	880	0	0
²²⁴Ra	241	43728	17886	1450	677

3.3.4.1.3 ICP-MS Analysis of Thorium

To try and determine exactly what was in the solution of thorium in calcium hydroxide, ICP-MS scans were performed on the samples. The sample of thorium in water, which should have contained everything in solution and all the daughters in equilibrium with each other, showed only thorium and possibly thorium oxide present. This could be because the concentration of daughters individually in the solution was so low that the ICP-MS didn't detect them.

3.3.4.2 Discussion

This discussion area is split into two main sections, the solubility of nickel, cadmium and cobalt and then the solubility measurement issues with thorium. The cations besides thorium all exhibit an increase in their solubility in the presence of CDP when compared to the same concentration of ISA. Cadmium exhibits the smallest increase of at least 2 times, then nickel whose solubility is increased by approximately 10 times and then the cobalt has an enhancement of at least 200 times. These results alone pose two questions, i) why the solubility of some cations increased over others and ii) what else was in the CDP which caused solubility increases above those observed from similar concentrations of ISA?

When investigating how a metal binds to a ligand it is important to understand the processes involved in the complexation reaction. The complexation can be best described by the hard/soft acid/base, HSAB theory. The basics behind the theory is that hard acids will react faster and form stronger complexes with hard bases, and the same for soft acids with soft bases. The affinity for hard acids and bases to react with each other is mainly ionic, for the soft species it's predominantly covalent. ISA would be classed as a hard base because of its hydroxyl groups and carboxyl group. Nickel and cobalt are both borderline lewis acids but the cadmium is a soft lewis acid. This implies that for the solubility of the cadmium to be increased less than the nickel or cobalt that the other ligands present could be hard bases as they are not forming strong complexes with the cadmium. The extra complexing agents present are likely to be hard bases like ISA as previous studies always suggest that the other components have similar functional groups to ISA and are other small carboxylic acids. The bonding involved can also be thought of in terms of molecular orbitals, in general, electron

pairs occupy the highest occupied molecular orbital's, HOMO, of the ligand. The HOMO of the ligand should have an energy that makes overlap with the lowest unoccupied molecular orbital, LUMO, of the cation preferential. As ISA is a weak field ligand, Hund's rules will apply. To use this theory to explain what is happening in the complexes of M:ISA and other complexing ligands with the metals the metals themselves need to be looked at.

Nickel has an electronic configuration of $[Ar]4s^2 3d^8$. This configuration means it is likely to form strong complexes by accepting electrons from an element on the ligand such as oxygen, to fill the d orbital. Cobalt has a similar electronic configuration to nickel of $[Ar]4s^2 3d^7$. This should cause the complexation reactions of these two cations to be similar. Cadmium on the other hand has an electronic configuration of $[Kr]5s^2 4d^{10}$ which means it has a full d orbital. This makes the bonding process with ligands such as the ISA much harder to explain and is a likely reason for the complex not forming as strongly as the other two cations present.

When analysing what else may be present in the CDP mixture it is important to consider what makes a good ligand and why a ligand would bind preferentially to a cation more than another similar ligand. The stability of the complexes formed is also an important consideration as obviously the more stable complexes will be formed over less stable ones. This stability can be defined thermodynamically in terms of equilibrium constants for the formation of the complexes. When a complex is formed the energy change involved can be expressed as:

$$\Delta G^0 = -RT \ln K$$

Where ΔG^0 is the standard reaction Gibbs function, R is the gas constant, T is the temperature in Kelvin and K is the equilibrium constant for the formation of the complex. The stability of the products depends on ΔG^0. The more negative this function is, the more thermodynamically stable the complex will be. The size of the equilibrium constant of the complex will therefore also affect the stability. Under near field conditions the radionuclides present are likely to be in the form of solid oxides or hydroxide phases which would dissolve in the cement porewater entering the repository to form mainly aqueous hydrolysis species.

The equilibrium constant for the dissolution reaction shown below is called the solubility product, Ksp.

$$M(OH)_{n(s)} = M^{n+}_{(aq)} + {}_nOH^-_{(aq)}$$
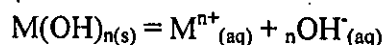
When complexing organic ligands are present in solution they could potentially stabilise the metal ion in solution, driving the dissolution reaction to increase the radionuclides solubility.

To make a good ligand the complexing agent usually has elements such as oxygen or nitrogen that when complexed with a metal ion can donate electrons. The electron donating ability of these elements will depend on their environment within the ligand. As a general rule, the greater the electron-donating ability of the ligand, the stronger the complex that is created. Steric factors can also play an important role in the complexation process so need to be considered when trying to determine what else could be complexing in the CDP solution.

When studying the results from the thorium solubility method development work it is hard to draw any firm conclusions. The main findings showed that one batch of thorium, batch 1, gave two peaks when LSC analysis was carried out when the thorium was in acidic conditions and batch 2 gave only one peak. When the thorium was added to a saturated solution of calcium hydroxide, and the solution filtered, both batches exhibited only one peak. When the thorium was in a solution of sodium hydroxide at high pH, no peaks or counts were observed with either batch of thorium. This was initially thought to be because the daughter isotopes of thorium were present. When the thorium was in acidic conditions the two peaks present were most likely to be thorium and a daughter or mixture of daughters with a similar energy. Batch 2 could have been purified prior to dispatching it to Loughborough and the daughters could have been removed. When the thorium was in calcium hydroxide the thorium precipitated out leaving the daughters in solution although this explanation does not account for the peak still observed in the thorium batch which may have been purified. This theory also does not explain why the calcium hydroxide leaves the daughters in solution and not the sodium hydroxide. Although work was carried out to try and see if there was a contaminant in the calcium hydroxide no changes in the results were found when freshly made calcium hydroxide was prepared and used. The effect of more counts than expected was also seen

with the NRVB water sample so it is unlikely that there is a contaminant in both the calcium hydroxide and the NRVB. This indicates that the phenomenon is definitely because of the presence of calcium although the tests in calcium chloride and calcium carbonate showed background counts.

The gamma spectroscopy supports the theory that the daughters were present and were having an effect as they were identified in both of the batches of thorium. Interestingly one batch of thorium, batch 2, the batch that only had one peak in the original sample in acid, always had lower counts than batch 1. This lower activity could mean that there were daughters present in the acidic thorium sample but they may have been at lower levels which the instrument could not detect.

Colloids, carbonate and chlorides were all investigated to see whether the remaining peak in the samples was still thorium with its solubility increased by something in the calcium hydroxide. All these tests resulted in background counts. The most likely explanation for these results is that the extra counts were a combination of all the effects studied above.

3.3.4.3 Comparison of Thorium Solubility Methods

ICP-MS was proven to be a good method for analysing thorium when in acidic conditions. When the thorium is at high pH, most of the actinide precipitates out of solution leaving very low levels in the samples for detection. The high pH of the samples was problematic for ICP-MS due to high salt concentration. The salt content meant that dilutions of at least 100 times had to be used before the samples could be analysed by this method. This caused the concentration of thorium in solution at high pH after dilutions to be very close to the LOD of the ICP-MS. Because of these problems ICP-OES was chosen as the method of analysis for this high pH work as the matrix of the samples shouldn't be such a problem for this and only ^{232}Th will be detected so the daughters shouldn't affect the results if present. Different methods of oversaturation and undersaturation were used to try and produce reproducible, accurate values for the solubility of thorium at a pH 6, 8 and 12 and the kinetics were also investigated.

3.3.4.3.1 Undersaturation

The undersaturation section was split into two parts, the kinetics of thorium precipitation and the solubility of thorium in the presence of different ligands.

3.3.4.3.1.1   Kinetic Studies

The first stage of the undersaturation method was to precipitate thorium hydroxide, centrifuge the sample and remove the supernatant. Thorium solubilities after 2, 7, 14, 21 and 28 days, at three different pHs of 6, 8 and 12 are shown in Figure 23, Figure 24 and Figure 25.
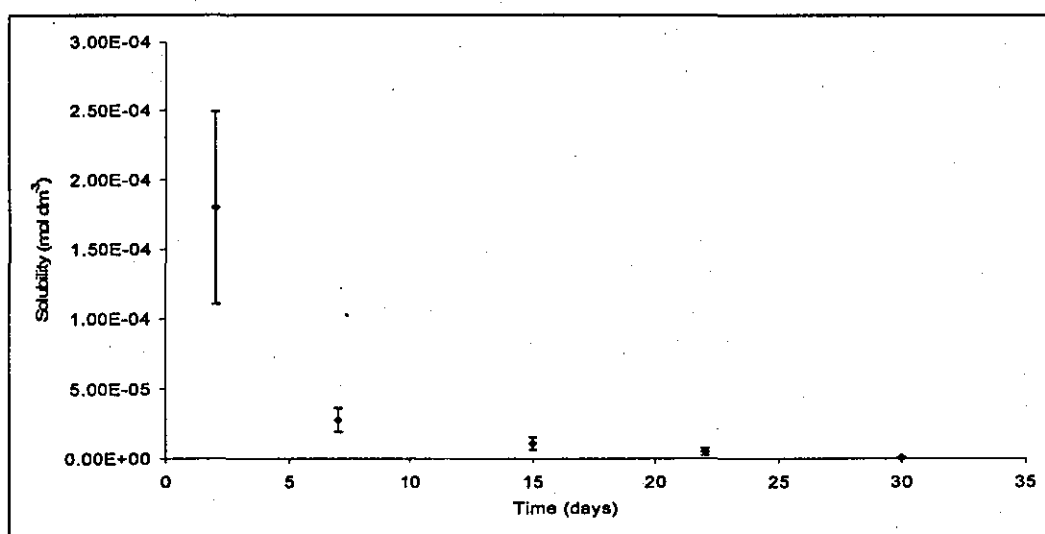

Figure 23 Thorium solubility at pH 6 as a function of time

It should be noted that the samples were not shaken during the kinetic studies and therefore are diffusion controlled.
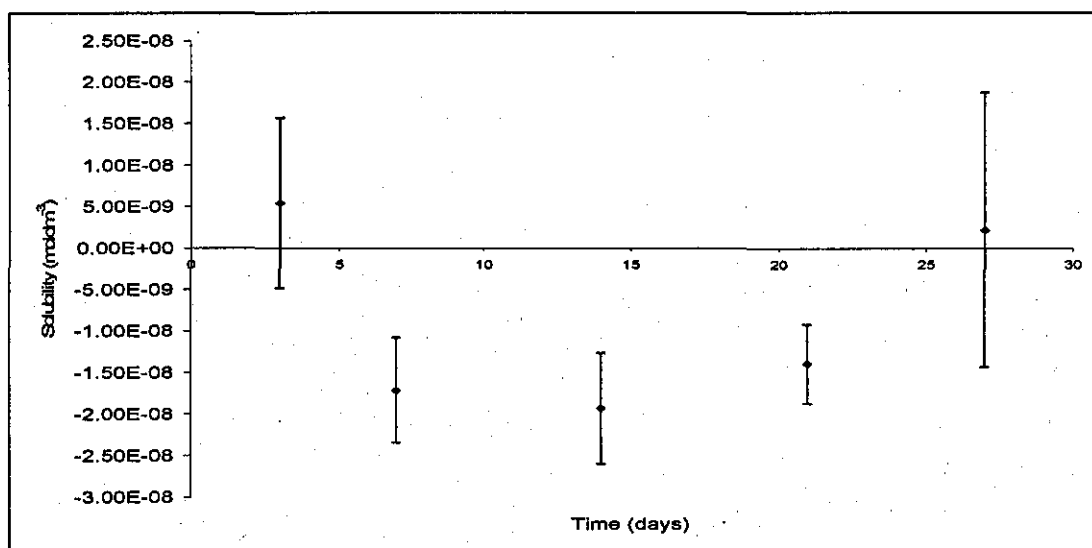
Figure 24 Thorium solubility at pH 8 as a function of time
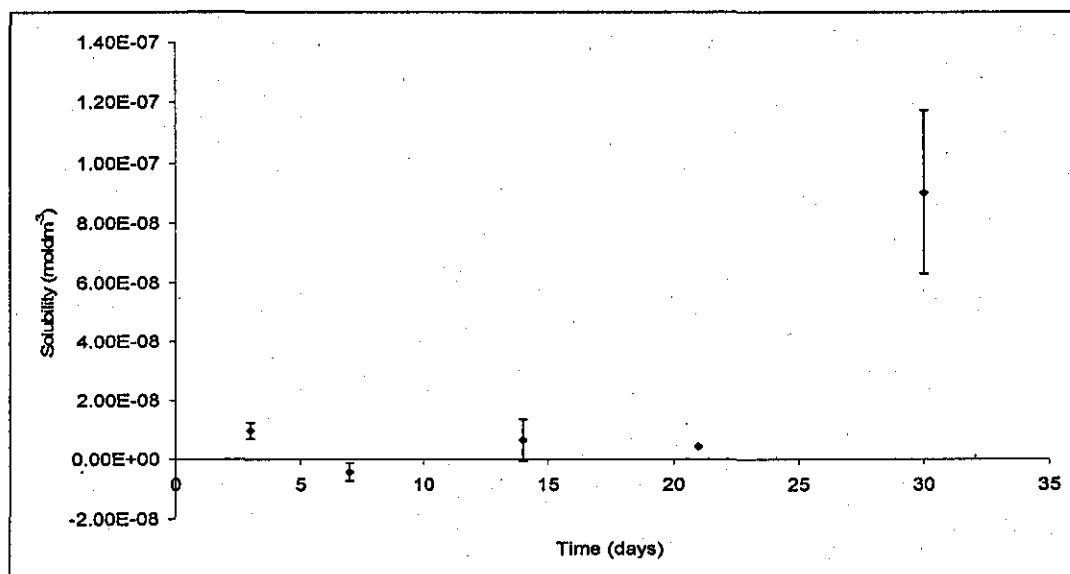
Figure 25 Thorium solubility at pH 12 as a function of time

The samples at pH 6 appeared to reach equilibrium (i.e. constant thorium solubility) after a period of approximately 15 days. After 2 days the samples at pH 8 were at baseline levels, which was the expected solubility (10^{-8} to 10^{-9} mol dm^{-3}) of the thorium at a pH above 7. The large amount of scatter associated with these results was probably because the solubility was

close to the minimum detectable amount of thorium for the instrument which is reported as 1 ppb. The samples were set up at a pH of 8 but the final pH of all of them was recorded as approximately 9.

At pH 12, equilibrium was reached after 2 days. There was an anomalous result at 30 days but the scatter associated with this measurement was large when compared to the other points so this value could be disregarded.

3.3.4.3.1.2 Undersaturation Method

After preparing the thorium hydroxide precipitates, each sample was left at least 28 days before the addition of the test solution. The solubilities of thorium, measured by using the undersaturation method, are shown in Table 21. Errors for these data are in Appendix 3.

Table 21 Thorium solubilities from the undersaturation approach

Sample	Thorium solubilities (mol dm^{-3}) in CDP or ISA solutions						Enhancement factor CDP 10% / ISA 10^{-2} mol dm^{-3}
	ISA 10^{-2} mol dm^{-3}	CDP 10%	ISA 10^{-3} mol dm^{-3}	CDP 1 %	NaCl	Ca(OH)$_2$	
pH 12 3 day	5.27E-08	3.65E-05	2.4E-08	-3.7E-08	1.7E-07	7.5E-09	692
pH 12 6 day	3.11E-06	5.23E-05	2.2E-06	5.36E-07	2.93E-06	1.59E-06	17
pH 12 17 day	5.94E-07	6.16E-05	1.9E-07	2.1E-07	8.43E-07	2.07E-07	104
pH 12 20 day	3.77E-07	5.66E-05	1.4E-07	1.08E-08	4.43E-08	6.12E-08	150
pH 12 30 day	2.48E-07	6.61E-05	2.4E-07	2.45E-07	1.29E-07	5.05E-08	266
pH 8 3 day	3.12E-07	5.42E-07	9.3E-08	1.91E-07	2.88E-07	4.7E-08	1.7
pH 8 6 day	6.88E-08	3.58E-08	2.3E-08	-6.7E-08	4.01E-08	-3.7E-08	0.5
pH 8 15 day	2.24E-07	1.66E-07	3.1E-06	1.88E-07	3.92E-07	4.56E-07	0.7
pH 8 20 day	3.22E-09	4.84E-08	3.1E-06	6.45E-09	3.87E-08	-1.4E-08	15
pH 8 28 day	7.2E-08	1.1E-07	5.6E-08	6.77E-08	3.7E-07	-9.7E-09	1.5
pH 6 2 day	1.82E-06	1.65E-06	2.1E-07	-2.3E-08	3.87E-08	4.3E-09	0.9
pH 6 6 day	1.04E-06	3.75E-07	4.7E-07	1.29E-08	3.73E-07	3.29E-07	0.4
pH 6 15 day	4.93E-07	1.19E-06	2.1E-07	-6.9E-08	2.22E-05	5.37E-08	2.4
pH 6 20 day	5.2E-07	6.88E-08	1.9E-08	-1.1E-07	1.15E-08	-3.4E-08	0.1
pH 6 28 day	4.97E-07	6.36E-07	8E-08	3.91E-07	1.63E-07	-7.2E-10	1.3
28 days (non kinetic)							
pH 12	5.93E-07	3.93E-05	2.8E-07	3.04E-07	2.11E-07	7.17E-07	66
pH 8	1.34E-07	6.1E-08	2.6E-08	-8.9E-08	1.74E-07	1.92E-08	0.5
pH 6	5.89E-08	6.65E-08	5.6E-08	-9.5E-08	1.14E-07	-3.4E-08	1.1
Supernatant							
pH 12	4.58E-06	4.68E-06	3.5E-06	3.09E-05	1.52E-05	9.16E-06	
pH 8	1.75E-05	5.44E-05	1.1E-05	4.95E-05	5.15E-05	2.18E-05	
pH 6	7.94E-06	2.32E-05	5.5E-06	1.21E-05	1.28E-05	0.000534	

Results for the thorium solubility measurements at pH 6 and 8 showed that the thorium solubility in CDP was similar to that in ISA samples if the ISA concentrations are the same in both solutions. At pH 12, large differences in thorium solubilities were observed. The thorium solubility enhancement factor of 692 measured after 3 days appeared to be anomalous and the high value was because of the low concentration of thorium measured in the 10^{-2} mol dm^{-3} ISA solution.

At all the pHs, the 1% CDP and ISA at 1×10^{-3} mol dm^{-3} had little affect on the thorium solubility. The low solubilities of thorium measured at pHs 6 and 8 in CDP and ISA solutions meant that kinetic studies at these pHs were not investigated. Kinetic investigations conducted at pH 12 suggested that solutions should be left for at least 28 days before measurement of thorium concentration as is shown in Figure 26 for the 10% CDP solution.
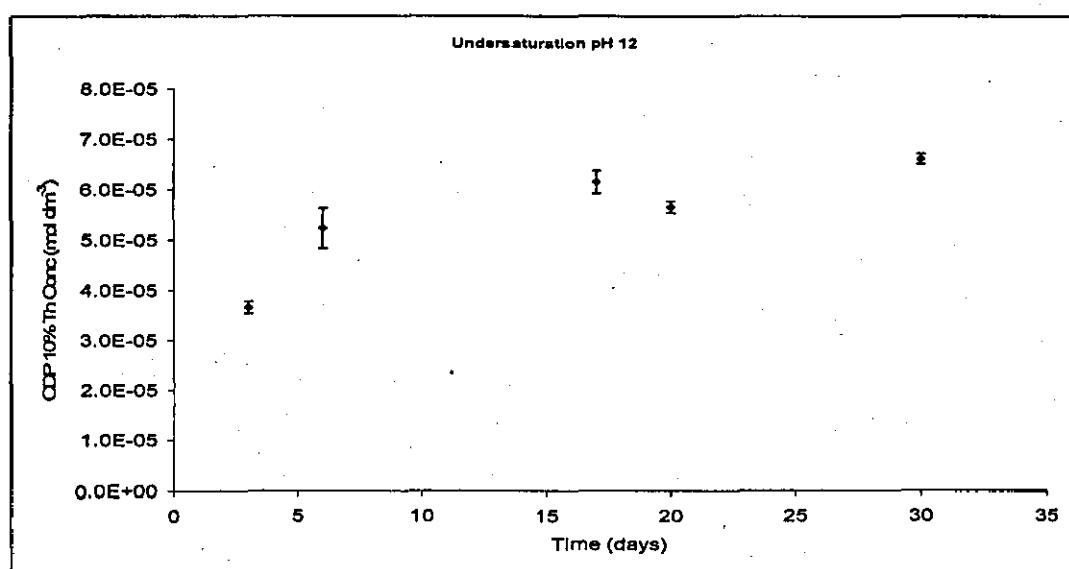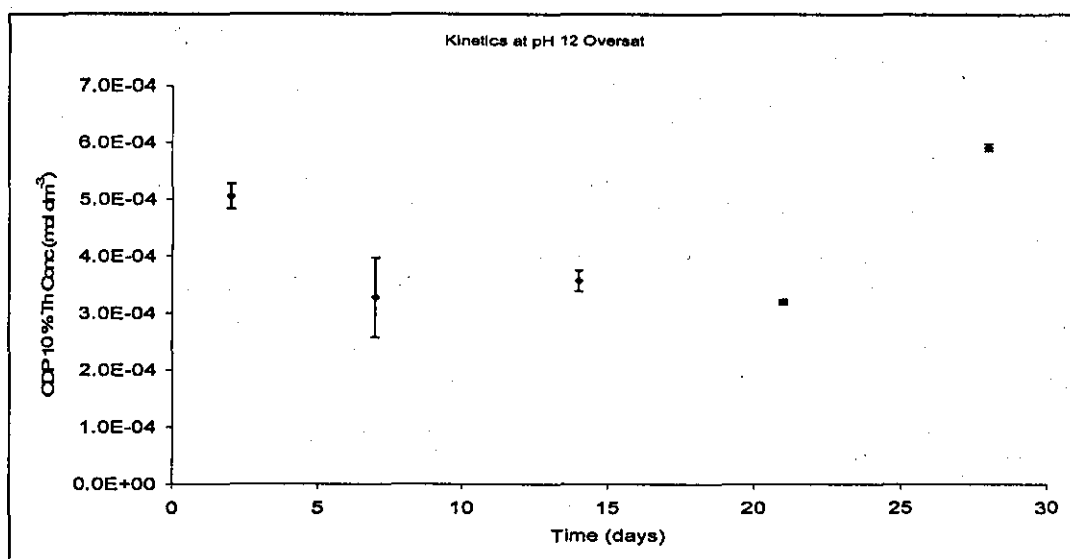

Figure 26 Thorium solubility in a 10% CDP solution as a function of time at pH 12 using the Undersaturation approach

3.3.4.3.2 Oversaturation

The results from the oversaturation experiments at pH 6, 8 and 12 over different time periods of 2, 7, 14, 21 and 28 days are shown in Table 22. Errors for these data are in Appendix 3.

Table 22 Thorium solubilities form the Oversaturation approach

Sample	Thorium solubility in ISA and CDP solutions						Enhancement factor
							CDP 10%
	ISA 10^{-2} mol dm^{-3}	CDP 10%	ISA 10^{-3} mol dm^{-3}	CDP 1 %	NaCl	Ca(OH)$_2$	ISA $^{-2}$ mol dm^{-3}
pH 12 2 day	2.73E-05	5.04E-04	2.27E-07	3.00E-06	2.38E-07	9.44E-07	18
pH 12 7 day	1.74E-05	3.27E-04	4.27E-09	1.89E-04	4.27E-09	-5.87E-08	19
pH 12 14 day	2.08E-05	3.57E-04	2.57E-07	-1.19E-07	-8.53E-09	-5.23E-08	17.
pH 12 21 day	5.17E-06	3.20E-04	6.40E-08	-1.17E-07	8.53E-09	-4.80E-08	62
pH 12 28 day	1.49E-05	5.92E-04	1.44E-07	1.45E-07	5.06E-07	3.52E-08	40
pH 8 2 day	1.83E-06	6.74E-06	4.44E-08	6.66E-07	2.58E-07	3.30E-07	3.7
pH 8 7 day	3.96E-06	2.16E-06	1.17E-08	-1.53E-07	-2.56E-08	-6.83E-08	0.5
pH 8 14 day	5.94E-07	1.32E-06	2.33E-07	-1.23E-07	1.61E-07	-5.01E-08	2.2
pH 8 21 day	7.47E-07	6.59E-07	-1.49E-08	-1.34E-07	1.07E-09	-4.37E-08	0.9
pH 8 28 day	8.47E-07	1.98E-06	3.44E-08	-8.60E-08	5.91E-08	-7.52E-09	2.3
pH 6 2 day	5.46E-05	2.73E-05	1.27E-06	4.61E-07	1.06E-06	9.17E-07	0.5
pH 6 7 day	1.51E-05	9.58E-06	3.86E-05	-1.46E-07	7.05E-07	5.44E-08	0.6
pH 6 14 day	3.70E-06	1.37E-05	-4.16E-08	-1.05E-07	1.88E-07	-3.31E-08	3.7
pH 6 21 day	3.65E-05	2.31E-05	-3.20E-08	-3.52E-08	1.89E-06	3.63E-08	0.6
pH 6 28 day	1.95E-05	2.67E-05	2.11E-06	1.35E-07	2.88E-06	1.48E-06	1.4
28 days, non kinetic							
pH 12	1.23E-05	5.69E-04	7.69E-08	6.41E-08	2.51E-07	5.23E-08	46
pH 8	1.72E-07	1.00E-06	1.71E-08	-1.04E-07	5.67E-05	6.18E-08	6
pH 6 (29 days)	4.64E-05	3.09E-05	6.27E-07	-2.03E-08	2.02E-06	4.36E-07	0.7

As with the undersaturation method there were only small differences in the solubilities of thorium in CDP solution (10%) and ISA solution (1 x 10^{-2} mol dm^{-3}) at pH 6 and 8. However, there were differences in thorium solubilities at pH 12. Although the enhancement factor was lower than the undersaturation method for the thorium solubilities at pH 12, the values were less scattered. These enhancement factors were much closer to previous values reported where an enhancement factor of 21.7 was observed when the solubility of thorium was determined in 10% CDP and ISA solutions [7].

At all the pHs, the 1% CDP and ISA at 1×10^{-3} mol dm^{-3} had little affect on thorium solubility. Figure 27 shows that there was little variation in thorium solubility in 10% CDP as a function of time. These results suggest that a steady thorium solubility was reached quickly when the oversaturation method was used.

Figure 27 Thorium solubility in a 10% CDP solution as a function of time at pH 12 using the Oversaturation approach

3.3.4.3.3 Comparison of Over and Undersaturation methods

The thorium solubilities in CDP and in ISA solutions using the oversaturation and undersaturation methods are compared in Table 23. At all the pHs, thorium appeared to be more soluble in the presence of 10% CDP and ISA x 10^{-2} mol dm^{-3} when the oversaturation method was used. There were only minor differences in thorium solubilities in the other solutions at pHs 8 and 12, probably due to these measurements being close to background measurements. Thorium solubilities at pH 6 suggest that there was more thorium in solution when the oversaturation method was used for the sodium chloride and ISA solutions at 10^{-3} mol dm^{-3}, but these results were higher than expected because of a drift in pH. These solutions were at a lower pH than 6 resulting in higher thorium solubilities. The concentration of thorium in solutions of 10% CDP and ISA (10^{-2} mol dm^{-3}) using the

oversaturation method was always approximately ten times higher or more when compared to the undersaturation method.

Table 23 Comparison of thorium solubilities from the over and undersaturation methods. All data are taken from the 28 day kinetic samples

Sample ID	Thorium Solubilities (moldm^{-3})		Enhancement Factor
pH 12	Oversaturation	Undersaturation	(Over/Under)
ISA -2	1.49E-05	2.48E-07	60
CDP 10%	5.92E-04	6.61E-05	9
ISA -3 M	1.44E-07	2.38E-07	0.6
CDP 1 %	1.45E-07	2.45E-07	0.6
NaCl	5.06E-07	1.29E-07	4
Ca(OH)$_2$	3.52E-08	5.05E-08	0.7
pH 8			
ISA -2	8.47E-07	7.20E-08	11.8
CDP 10%	1.98E-06	1.10E-07	18
ISA -3 M	3.44E-08	5.59E-08	0.6
CDP 1 %	-8.60E-08	6.77E-08	-1.27
NaCl	5.91E-08	3.70E-07	0.2
Ca(OH)$_2$	-7.52E-09	-9.67E-09	0.8
pH 6			
ISA -2	1.95E-05	4.97E-07	39
CDP 10%	2.67E-05	6.36E-07	42
ISA -3 M	2.11E-06	8.02E-08	26
CDP 1 %	1.35E-07	3.91E-07	0.4
NaCl	2.88E-06	1.63E-07	18
Ca(OH)$_2$	1.48E-06	-7.17E-10	-2071.85

The differences in thorium solubilities measured by the two methods were almost certainly because of the differences in the kinetics of the reactions. The undersaturation method is diffusion controlled as the thorium is in a solid form when the CDP or ISA solutions were added. The samples were not shaken so it is likely that it would take more time for the thorium to become solubilised. In the oversaturation method, the thorium was added to the CDP or ISA solutions in a liquid form and then the pH was adjusted so the complexing ligands present in these solutions would react with thorium before, or as the thorium hydroxide precipitate was formed. This hypothesis is supported by the results shown in Figure 26 and Figure 27.

3.3.4.4 Thorium Solubility Protocol

The work presented in section 3.3.4 has demonstrated the need for a standard protocol to be used when investigating the solubility of thorium. As a result of the work in this thesis, the following protocol is put forward using the oversaturation method.

Samples are prepared in replicates of 4. Test solutions are prepared which include experimental controls and the complexing ligands of interest. Each test solution (12 cm^{-3}), is added to 4 centrifuge vials. 0.1 cm^{-3} of a stock thorium nitrate solution (1 mol dm^{-3}), is then added to each vial. The pH of the solutions is adjusted to the required pH using carbonate free sodium hydroxide (2 mol dm^{-3}), and concentrated nitric acid. The solutions are left shaking for a minimum of 7 days before filtering them through pre-conditioned (0.1 mol dm^{-3} sodium chloride at the pH of the samples) centrifuge filters, 10 000 Da MWCO. The filtered samples are then acidified by adding concentrated nitric acid (0.02 cm^{3}), before the concentration of thorium in each solution is determined by ICP-OES analysis.

3.3.5 Discussion

There were three main differences observed during this work. These were the differences between thorium solubilities

(i)   at pHs 6, 8 and 12,

(ii)   in CDP and ISA and,

(iii)   when using the undersaturation or oversaturation methods.

Throughout this study keeping pH constant at a certain value was difficult, particularly at the lower values of 6 and 8, despite the samples being prepared and stored in a nitrogen atmosphere glove box. The pH usually rose, sometimes from 6 to 8 and 8 to 10, so either the pH had to be adjusted or, in extreme cases, the experiments were repeated. Other studies have found that this rise in pH is a function of ageing of the thorium hydroxide precipitate but the conclusions drawn offer little explanation as to why this might occur [101]. The ageing of the precipitate would involve the transformation of Th(OH)$_4$ (am) on the surface of the precipitate formed to the more stable ThO$_2$ (cr) but solid transformations are usually slow compared to hydrolysis and solid-liquid interactions [9]. The predominant species present at

pH greater than 7 is $Th(OH)_4$ [9]. At pH 6 however there may still be significant amounts of other thorium complexes present, particularly $Th(OH)_3^+$ which could affect the results [82]. Small variations in pH around 6 have been shown to produce significantly large differences in thorium solubility which would explain the problems of reproducibility in the measurements observed in this work. One study found the concentration of thorium in solution to fall from $10^{-7.4}$ to $10^{-9.5}$ when the pH changed from 6.18 to 6.63 [9].

Another important factor that needs to be considered with changing pH is the pKa of the complexing ligands present in the CDP solution and also the fact that the ISA changes structure from a lactone form at pH < 6 to a open chain form at pH > 10. From pH 6 to 10 both lactone and open chain forms of ISA are expected to be present in solution as discussed previously [51]. These changes would affect the experiments conducted by using the oversaturation method more as the pH is adjusted in these experiments whereas in the undersaturation experiments the ligand solutions are already at the required pH before being added to the thorium hydroxide precipitate so changes in ISA structure should not occur. These changes in structure will almost definitely change the complex formed with thorium and therefore could affect the solubility. Previous work, reported by Rai et al. has demonstrated the importance of the lactone form of the ISA when determining the solubility of Np(IV) at pH's ranging from 5 to 14 [56]. With the changes in structure, the availability of the groups involved in complexation will change. Rai et al. also reported that their studies indicated that deprotonation of some of the hydroxyl groups on the ISA could be induced at lower pHs than expected due to the presence of a metal. This hypothesis is supported in a study of the coordination of aldonic acids to copper [68]. Depending at which pH deprotonation occurred, this could greatly affect the complexes formed at the pHs used in this work. The pKa of the carboxylate group on the ISA has been reported as 3.87 and has been found to be almost completely deprotonated at pH ≥5.3 so deprotonation of this group should be well defined at the pHs used during this work [74], [52]. Even if the hydroxyl group wasn't deprotonated, as the pH increased the deprotonation of the carboxylate group could initiate a change in the conformation of the ISA molecule, which could affect the hydrogen bonding environments of some of the hydroxyl groups. One possible structure that could be formed has been presented in previous work where there is an insertion of a hydrogen bond between the carboxylate anion and the hydroxyl group on the secondary alcohol. This would create a

four carbon ring, which is not dissimilar to the lactone structure, but a hydrogen bond closes the ring as apposed to a covalent ester linkage [52]. This change was noticed as the pH was increased from 5-13 and was observed by looking at the change in proton NMR chemical shifts as a result of increasing pH.

An additional consideration which could also affect the formation of complexes of thorium and ISA is the presence of calcium which can affect the stoichiometry of the M:ISA complexes formed and/or form complexes in which calcium is incorporated into the complex. The formation of these complexes could explain the measured differences between the solubilities of thorium in CDP and in ISA solution. At high pH a 1:1 Th:ISA complex is formed in the absence of calcium but, in the presence of Ca, a 1:2:2 Th:Ca:ISA or a 1:1:2 Th:Ca:ISA complex is formed [88],[54]. At pH 8 studies have found that in the absence of calcium three isosaccharinate ligands were found to be involved in the complexation with thorium [67]. All the above explanations could explain why there is a difference in the measured CDP and ISA thorium solubilities at the different pH's but at pH 12 there is still a higher solubility of thorium in the 10% CDP solution when compared to thorium solubility in ISA solution as observed with the other metals studied previously. The increase in thorium solubility in CDP when compared to thorium solubility in ISA solution suggests that there is a component, or components, other than ISA present in CDP which is responsible for the increased solubility as discussed previously. The increased solubility is probably because of the presence of a number of complexing ligands which have an accumulative effect on increasing thorium solubility. Investigations into complexing ligands other than ISA present in CDP found only ligands in small concentrations, none of which increased the solubility of thorium significantly on their own [7].

Although the solutions were left for at least 28 days before the concentrations of thorium were measured in the undersaturation and oversaturation methods the differences in measured solubilities may be because the solutions in the undersaturation method were not left long enough to allow a steady state to develop. Previous work has found that an equilibration time of at least 2 months for an undersaturation experiment was needed to maintain constant steady state thorium and H^+ concentrations [10].

3.4 Thorium Complexation in CDP

The solubility of thorium has been shown to increase in the presence of CDP. Some of this solubility increase was due to the main component of CDP, ISA. As the solubility of the metal was higher in CDP than an equivalent concentration of ISA, there must be other complexing agents present in CDP. This preliminary work was carried out to try and elucidate what else was binding with the thorium by identifying which peak on an HPLC analysis of the CDP solution the thorium was associated with. Previous studies have shown that LC-ICP-MS can be a useful analytical method in separating out and determining carboxylic acids in complex mixtures [102].

A HPLC method had already been established for the analysis of CDP [43] but this had to be adapted for use with the ICP and LC-MS. This caused some changes in the retention times of the main species present. Table 24 shows the new retention times of the standards as run previously. The aim of this work was to separate out the main components in CDP using reversed phase LC and then run these on the ICP-MS. When the samples were run on the ICP, thorium was detected and its retention time recorded. It was hoped that the retention time on the ICP could be matched with a peak retention time on the LC to determine where the thorium is binding.

Table 24 Retention times of standards using new conditions on the HPLC for LC-ICP-MS analysis

Peaks Present	Retention time on the HPLC (min)
Unretained	2.19
Formic Acid	3.27
ISA	3.57, 4.13
Acetic Acid	In background as used in the mobile phase
Lactic Acid	3.90

Figure 28 shows the ICP-MS spectra from thorium in calcium hydroxide, thorium in CDP and thorium in ISA. There was a problem with carry over of the thorium on the column so it was

difficult to obtain a completely clean baseline from one thorium run to another as more time would be needed on the instrument. This did have an effect on the results as it was difficult to state whether a certain peak was definitely from the samples just run or from the previous analysis; However looking at peak areas some conclusions could still be drawn. The very small peak at approximately 2.2 minutes was most likely due to unretained thorium which is supported by the spectra shown in Figure 29 when the thorium was in an acidic solution. Unfortunately the graphs could not be overlaid with each other as the thorium in water peak overlaps everything else due to the high concentration in solution. The peaks at 3.3 and 5.1 minutes are due to the ISA. There were two other small peaks present in the CDP sample at 4 minutes and 9.5 minutes. These peaks remained unidentified.
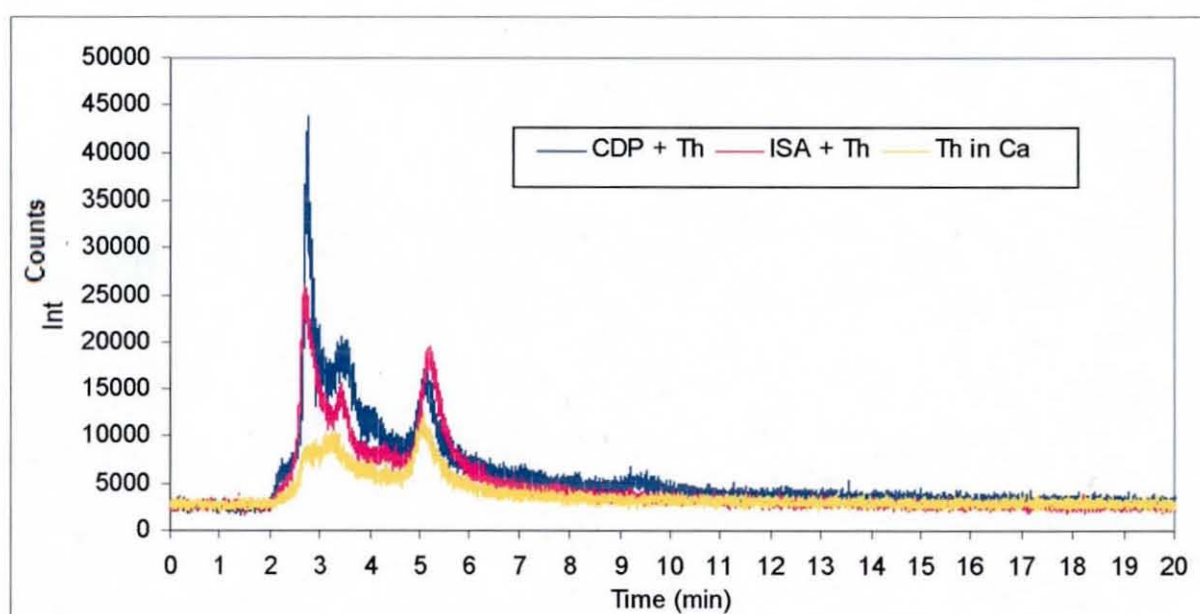
Figure 28 Graph of peak intensity against time for thorium in CDP, ISA and Ca(OH)₂, on the ICP-MS
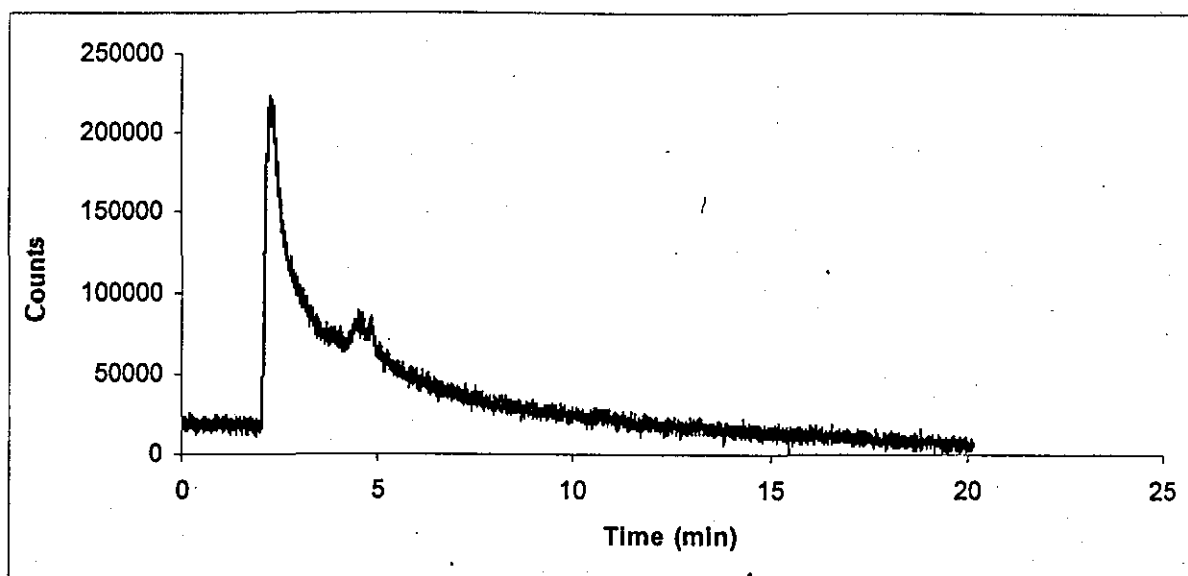
Figure 29 Graph of peak intensity against time for thorium in water, unretained, on the ICP-MS

It was difficult to make any firm conclusions from these results as even the thorium in calcium hydroxide had a small peak where the ISA peak was. As mentioned previously this is most likely to be due to the carry over issues. The results indicate that a lot of the thorium was being complexed to a species or a number of species which eluted at 2.7 minutes on the ICP-MS. This retention time matches most closely with the formic acid peak on the LC but this could also be a mixture of other species eluting at the same time which remain unidentified.

Figure 30 shows the CDP chromatogram with the new HPLC conditions used for this analysis. The solvent front was at 2.5 minutes, formic acid was the first large peak followed by ISA, the second ISA peak and then an unidentified peak at 4.4 minutes. There did not appear to be any lactic acid although the retention times for this standard and the second ISA peak were close so a small amount may not be detected. The resolution between peaks needed to be improved for any further conclusions to be made.
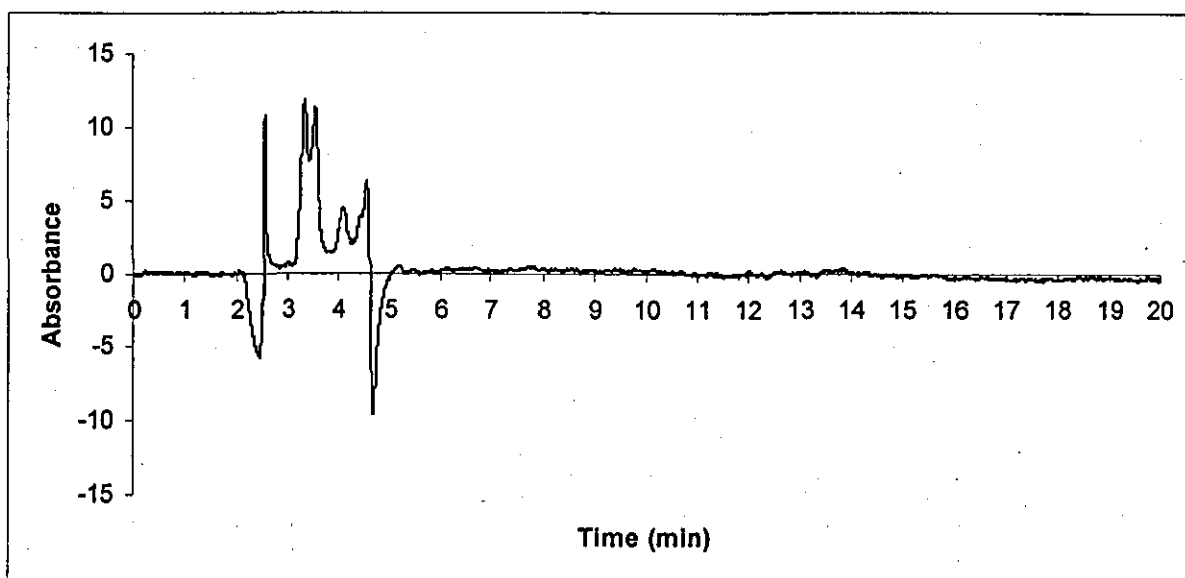
Figure 30 Graph of UV absorbance against time for CDP on the HPLC

3.4.1 Discussion

As this work only includes preliminary studies, few firm conclusions could be made on the results obtained so far. The technique of LC-ICP-MS has been shown to effectively separate out the main components of CDP with thorium complexed to them and has shown that thorium can be successfully detected as the free and bound species. One interesting point is that there is little free thorium present in any of the samples other than the sample which contained thorium in water. This supports previous theories that the thorium is in the $Th(OH)_4$ form at high pHs [9] (or a similar complex) or it is actually complexed with ligands in the solutions. It does seem that the spectra for the thorium in calcium hydroxide is very similar to that of the thorium in ISA and CDP so it could be argued that what was observed from these results was just the hydroxide complexes of the thorium and not the ligand complexation. To solve this problem the relative peak areas of the spectra could be noted as there are larger peak areas for the thorium in ISA and CDP than the thorium in calcium hydroxide so a background subtraction could be carried out on these peaks in future work. These results support the theory that the main complexing agent in CDP is the ISA as there are only two extra peaks in the CDP sample, both of which show very small peaks. However

it could be that other complexing agents are overlaid by the ISA thorium peaks. The technique shows promise but more work is needed if this method is to provide useful and reliable results.

3.5   Metal:ISA Interactions

The way in which ISA interacts and binds with metals has been studied to gain a greater understanding of the complexation mechanisms occurring. This may enable the outcome of M:ISA interactions, in terms of stoichiometry and coordination, to be predicted using modelling and reasons as to why ISA complexes with certain metals over others may be established.

3.5.1   Solid State NMR Studies

As the environment in a nuclear waste repository is unlikely to be homogeneous, it is possible that there will be solid and liquid forms of different materials present. For this reason SS NMR is being used to look at M:ISA interactions in the solid state. This work is also leading on from some solution NMR research which was inconclusive as to where the metal is bound to an ISA ligand so it was thought that SS NMR may provide more information on the process involved [103]. When characterising a solid it is also important to use more than one method of analysis so this study also set out to prove that SS NMR can be used as an extra tool for solid state characterisation of complexes. SS NMR uses a technique called Cross Polarisation Magic Angle Spinning, CP-MAS. This enables ^{13}C spectra that would normally have poor signal to noise ratios and long relaxation times due to the nuclei being of low abundance, to be recorded clearly and relatively quickly. The magnetisation is transferred from the abundant proton spins in the sample to the ^{13}C spin via the dipolar coupling between the two nuclei.

3.5.1.1 ^{13}C

The labelling of the carbon atoms in the ISA ligand can be seen in Figure 31. The ^{13}C atoms in the spectra were assigned using the solution NMR data carried out previously, as solution NMR had a lot of extra techniques such as DEPT and COSY available to aid assignment [103]. The chemical shifts of the carbons should not change significantly when comparing solution to SS NMR and this comparison has been carried out before in studies to assign SS NMR peaks [77].
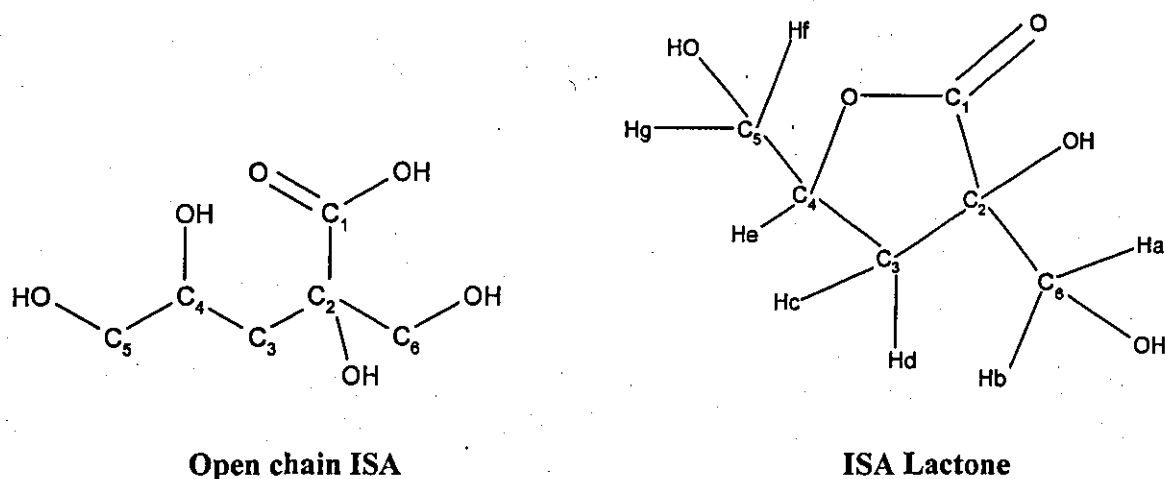
Figure 31 Labelling of carbons in gluconic acid, gluconolactone, isosaccharinic acid and isosaccharinolactone for the assignment of NMR peaks

The ^{13}C spectra for ISA and ISA lactone can be seen in Figure 32. The two different structures were analysed because at pH 7 some of the lactone form is expected whereas at higher pHs the open chain will dominate. The assignment of the peak chemical shifts can be seen in Table 25. It was clear from the spectra and peak assignments that there were differences between the open chain and lactone forms which were expected due to the different environments of the carbons in the structures.
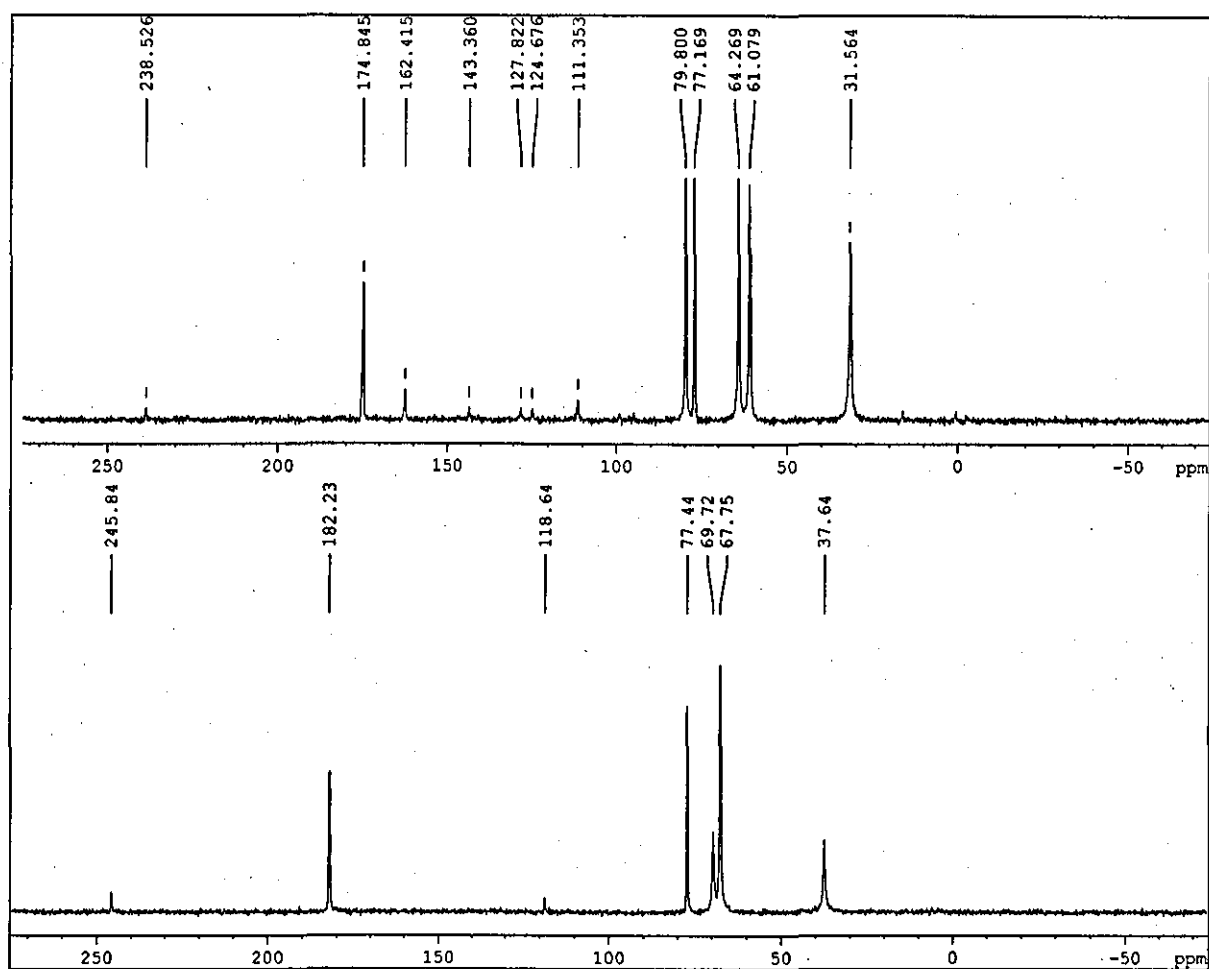
Figure 32 Carbon spectra for ISA lactone (top) and ISA open chain (bottom)

The ISA peak chemical shifts were difficult to assign as two of the peaks in the open chain arrangement were overlapped. This indicated that two carbons in this structure were in very similar chemical environments. When this was compared to the solution NMR work, carbons 4 and 6 were very close in chemical shift at 68 ppm so the peak at 69.72 ppm in the solid state spectra was assigned to both these carbons. This assignment does mean that when discussing carbons 4, 5 and 6, it should be remembered that these were only tentative assignments. This also applies to carbons 5 and 6 for the lactone structure. Looking at the differences produced from the open chain ISA and lactone ISA carbon chemical shifts, carbon 2 showed the smallest change and carbon 4 the largest. This is likely to be because the ring actually formed through carbon 4 whereas carbon 2 had little change in its chemical environment.

Table 25 Peak assignments for ISA open chain and ring formation from C^{13} NMR solid state spectra

^{13}C	Open Chain	Lactone
1	182.23	174.84
2	77.44	77.17
3	37.64	31.56
4	69.72	79.80
5	67.75	61.08
6	69.72	64.27

The lactone structures were studied as some of the samples analysed were made at pH 7. As fore mentioned, at this low pH some of the lactone form of the ISA was expected to be present so this could change the complexation mechanisms of the M:ISA as different steric effects would be involved.

3.5.1.1.1 Variation of chemical shift with pH

Samples of ISA were prepared at pH 7, 10 and 13. This was to enable accurate comparisons of the spectra to the metal ISA spectra at the correct pH. It is clear from Figure 33 that there were no significant changes in the ISA spectrum at the different pHs leading to the conclusion that the major component in each sample was an identical species. The extra peaks in the spectra at pH 13, 165 – 175 ppm, were thought to be impurities in the sample as they did not correlate to any other peaks seen before and were of low intensity. All the spectra, regardless of pH, showed the same carbon chemical shifts as the open chain ISA. In solution it has been shown that at pH 7 the lactone form should be present but these results indicate that when the sample solidifies the ring structure is broken and the open chain dominates[51]. It is possible that the pH could have drifted during solidification but all the samples were made up at the same time under the same conditions so the same effect would be expected when the metal is present which was not the case as discussed later.
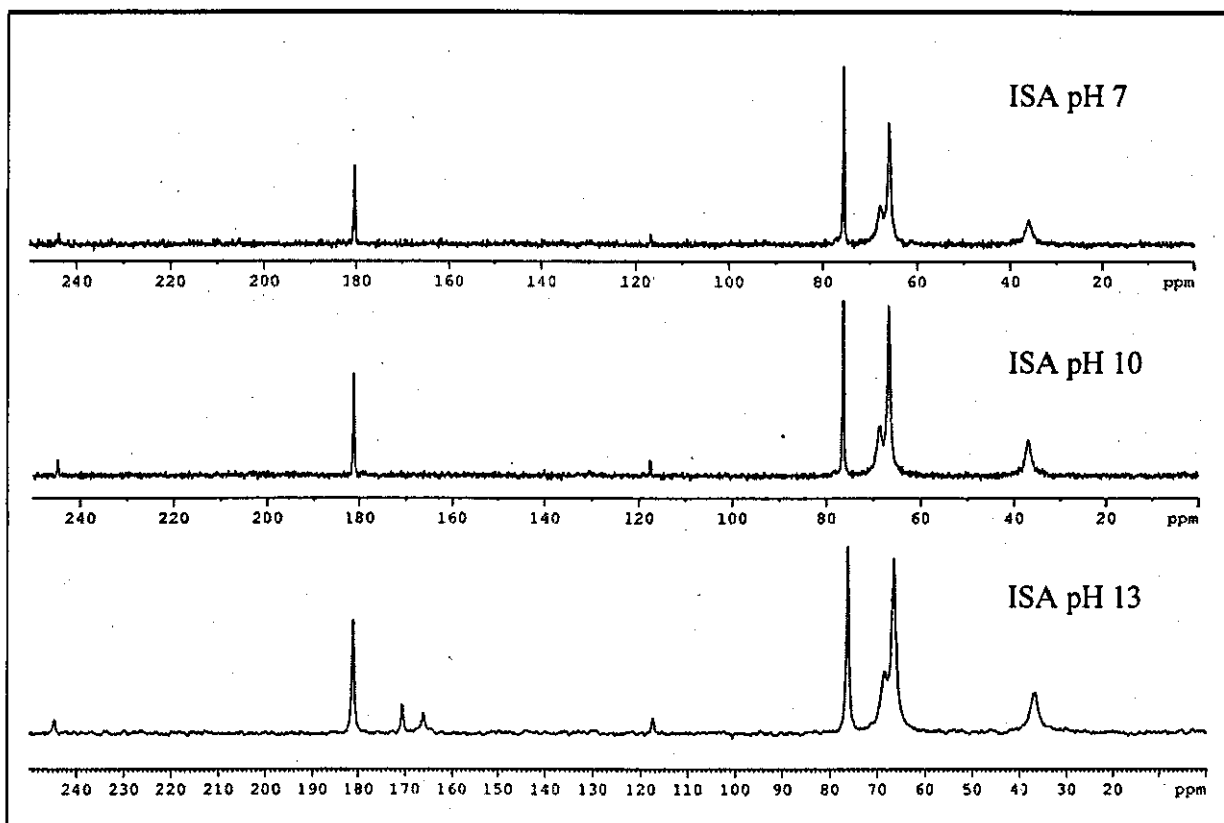
Figure 33 C^{13} solid state NMR spectra of ISA at pH 7, 10 and 13

Various metal ligand complexes using metals cadmium, europium, iron and nickel, were studied and the changes in carbon chemical shifts were recorded when there was a metal added. The samples were analysed at pH 7, 10 and 13. The results can be seen in Table 26 and the spectra can be found in Appendix 4. Some of the spectra had a number of peaks present, more than the number of carbons in the ISA ligand. In these cases it is believed that some of the peaks represent the lactone form and some the open chain so in Table 26 both sets of peaks have been assigned to these different structures. Where there are blank boxes in the table, this was where no peaks were seen which could be due to the sample not solidifying fully before analysis.

Table 26 Peak assignments for the C^{13} NMR spectra of ISA in the presence of different metals. L = Lactone form, S = Open chain form. The numbers in the headings represent the pH each complex was prepared at.

C^{13}	Metal complex analysed and the C^{13} chemical shift (PPM)										
	Cd 7	Cd 10		Cd 13	Eu 7	Eu 10		Fe(II) 7	Fe(II) 10		Ni 7
	L	L	S	S	L	L	S	L	L	S	L
1	174.97	174.89	179.19	179.71	174.6	174.6	181.59	175.12	174.45		174.63
2	77.16	77.28	77.28	77.99	77.76	76.78	79.39	77.15	76.63		76.78
3	31.54	31.65	39.78	39.9	31.14	31.1	36.94	31.59			31.15
4	79.79	79.92	69.65	68.88	79.38	79.39	76.78	79.72			79.41
5	61.04	61.14	66.75	66.87	60.65	60.62	67.12	61.19			60.63
6	64.22	64.37	67.24	68.04	63.83	63.8	69.04	64.1			63.83

The assignment of these peaks to the relevant carbons became more difficult as the pH of the samples increased due to an increasing number of peaks appearing. Despite this there were some differences in carbon chemical shifts observed, Table 27. For some complexes there were no significant changes in chemical shift of any of the carbon atoms, for example the complexes at pH 7 when compared to the lactone forms, but there were other differences which may be worth considering in future work. These were changes in the relative peak intensities, peak widths or the CSA of the complex which may provide further information. For this study the main focus was on the chemical shift changes.

Table 27 Chemical shift differences for the C^{13} NMR spectra of ISA in the presence of different metals. L = Lactone form, S = Open chain form. Samples at pH 7 were compared to ISA lactone, samples at pH 10 were compared to both forms, samples at pH 13 were compared to the open chain ISA. The numbers in the headings represent the pH each complex was made up at.

C	Metal complex analysed and the C^{13} chemical shift difference (ppm)										
	Cd 7	Cd 10		Cd 13	Eu 7	Eu 10		Fe(II) 7	Fe(II) 10		Ni 7
		L	S			L	S		L	S	
1	0.13	0.05	3.04	2.52	0.24	0.24	0.64	0.28	0.39		0.21
2	0.01	0.11	0.16	0.55	0.59	0.39	1.95	0.02	0.54		0.39
3	0.02	0.09	2.14	2.26	0.42	0.46	0.7	0.03			0.41
4	0.01	0.12	0.07	0.84	0.42	0.41	7.06	0.08			0.39
5	0.04	0.06	1.00	0.88	0.43	0.46	0.63	0.11			0.45
6	0.05	0.1	2.48	1.68	0.44	0.47	0.68	0.17			0.44

One major difference in the M:ISA spectra compared to the ISA spectra in the absence of metal is that there is no longer an overlapped peak. Another point of interest is that, at pH 7 there is one set of peaks present, at pH 10 there seems to be two, and at pH 13 further peaks appear. pH 7 could be the lactone form of ISA, even though this was not the main form present in the absence of metal. pH 10 could have both lactone and open chain forms displaying both sets of peaks. At pH 13, only the open chain form should be present so this indicates there is another affect occurring at high pH. These differences can be seen visually in Figure 34. Another hypothesis is that the lactone form is not being observed at all, instead a similar ring type structure is being formed when the ligand complexes to the metal at the lower pHs.
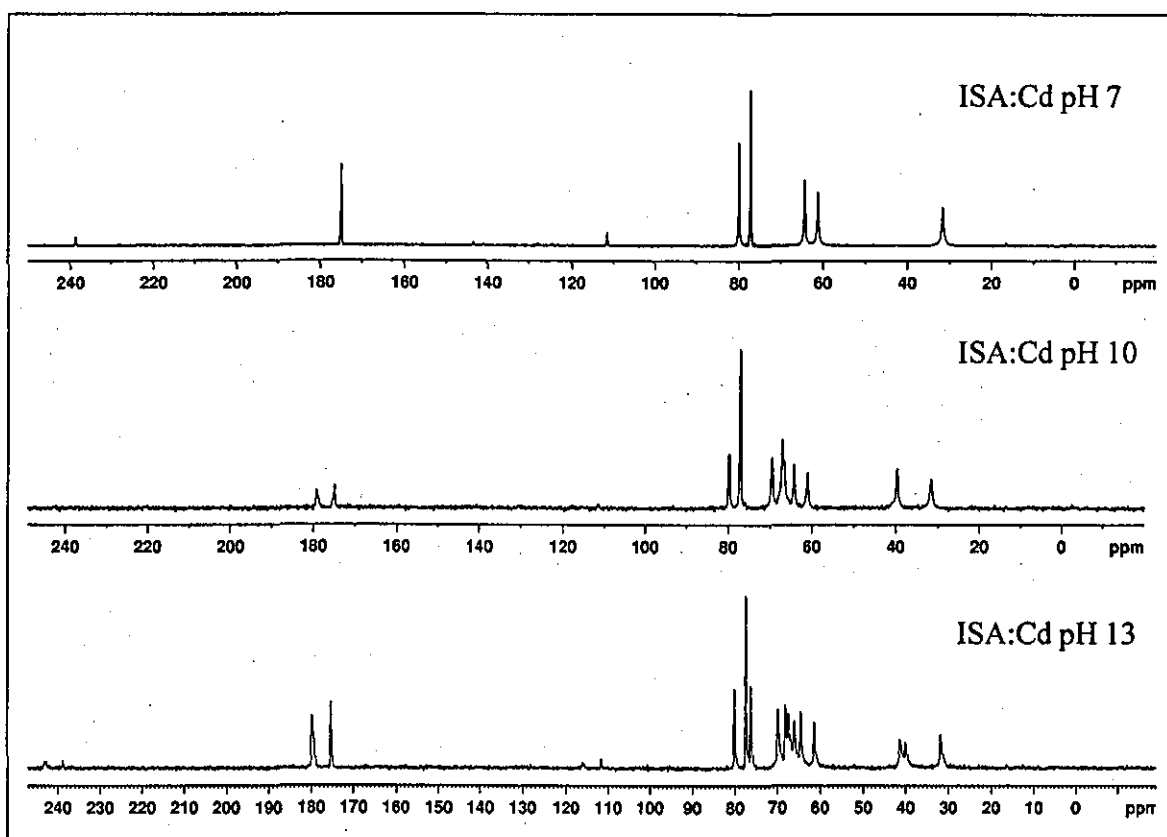
Figure 34 Cd:ISA spectra at pH 7, 10 and 13

If any of the complexes at pH 7 are compared to the open chain ISA at pH 7 then there are some large differences in the chemical shifts of most of the carbons. As the spectra of the M:ISA complexes at pH 7 are so similar to the lactone shifts it is more likely that, in the presence of a metal and when the complex solidifies, the sample stays in the lactone form, or a similar structure, not the open chain. It is apparent that the extra peaks seen in the M:ISA spectra at pH 10 and 13 must be due to the addition of the metal itself as they are not pH effects.

For the complexes Cd-7, Eu-7, Fe-7, Ni-7 and Cd-10, Eu-10 (the lactone peaks) there is little variation with the chemical shifts. In the instances where all the chemical shifts for a particular complex vary by similar amounts, it is likely to be due to changes in the instrument rather than significant experimental change. It is possible that the magnetic field could have changed slightly in between analyses. The only real differences that were apparent with these

complexes were for Cd-7 and Fe(II)-7 where carbon 1 differs from the other chemical shifts. If a metal were to complex to the lactone ISA, this is where it would be most likely due to the deprotonation and position of the carbonyl atom. As the changes in chemical shift are very small, it could be possible that, at low pH, the metal doesn't complex with the ligand at all but does cause the lactone structure to form.

For the Cd-10 and Cd-13 metal complexes the chemical shifts that show most variation are those for carbons 1, 3 and 6 when comparing the data from the open chain structure. When analysing this it seems quite feasible as it would place the metal at the carbonyl end of the ligand. If the assignments of the peaks for carbons 4, 5 and 6 were different, the proposed structure would not be quite as likely as the one suggested here so this supports the previous assignments made. Eu-10 showed the largest differences with carbons 2 and 4 which again is possible whereas swapping carbon 4 with carbon 5 or 6 to test the assignments would not be as likely because, with the latter arrangement, the oxygen groups are further away from each other. With the Fe(II)-10 there were actually only two peaks present. This could have been because the samples had not solidified properly but, even so, it shows the two peaks that have been least affected by the metals presence as they were still visible. These peaks represent carbons 1 and 2. All these results seem likely as it would not be expected for all the metals to show the same bonding due to differences in valency, size and coordination.

3.5.1.2 Dipolar Dephasing

The dipolar dephasing was used to see if the assignments of ^{13}C chemical shift to the different carbons present in the ISA structure could be confirmed, particularly carbons 4, 5 and 6 and also to try and identify the extra peaks appearing at high pH. Dipolar dephasing shows the change in signal intensity of the ^{13}C peaks with respect to how many protons they have attached. This technique applies an extra delay in the pulse sequence between starting to acquire the FID and turning the proton decoupling on, therefore, carbons with a different number of protons attached will be affected to varying degrees. Quaternary carbons are relatively unaffected by this technique, whereas carbons with two or three protons bonded will lose their peak intensity quickly. Figure 35 shows the spectra for ISA at pH 10 with delay times from 2 to 50 μs. When there is no delay, all the peaks are present as expected. At an intermediate delay of 32 μs, the peak at 37 ppm has dephased and has zero intensity and at

a delay of 50 µs, all the peaks except the quaternary carbons at 182 ppm and 77.44 ppm, are significantly reduced in height. This indicates that the peak on the far right can be assigned as CH_2, confirming previous assignments. Dipolar dephasing has confirmed that the peak at 182 ppm is from carbon 1, the peak at 77 ppm is from carbon 2 and the peak at 37 ppm is carbon 3. The data does indicate that the peaks at 67 ppm are likely to be CH_2 i.e. carbon 5 as previously labelled because the peaks disappear at a similar rate to the carbon 3 peaks.
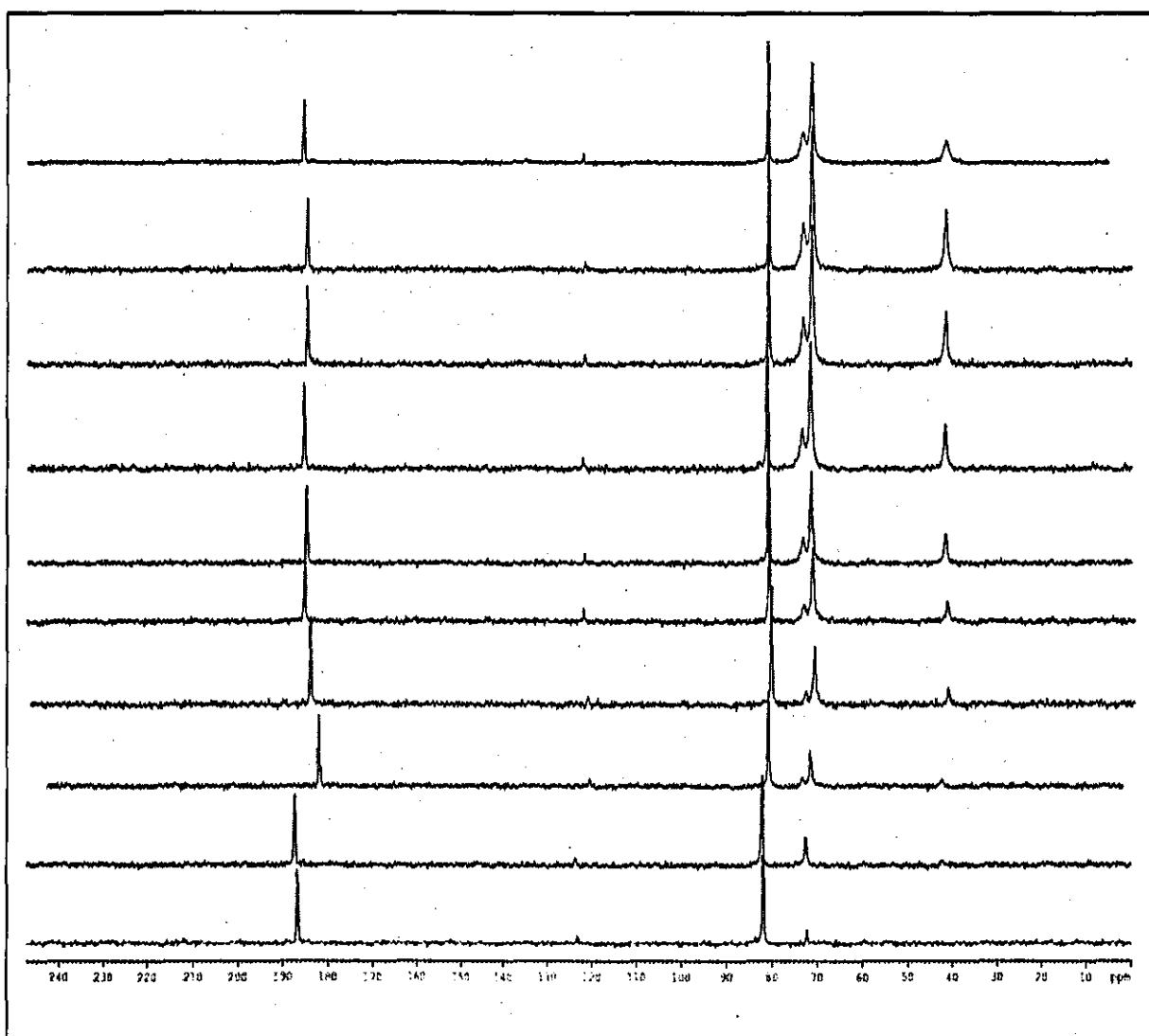
Figure 35 ISA at pH 10 C^{13} spectra. The difference in spectra id the change in D7 delay from 0, 2, 6, 10, 14, 22, 26, 32, 40 and 50 µs going from the top spectra to the bottom.

All the spectra of the Cd:ISA complexes at the different pH's support previous assignments, see Appendix 4. The spectra also support the theory that the extra peaks appearing as the pH of the complexes is increased are from the different ISA forms present as the related peaks i.e. the ones with very similar ppm values are affected in the same way by dipolar dephasing, indicating that they have the same number of protons bonded but are in slightly different environments. For Cd:ISA at pH 13 the ^{13}C spectrum is more complicated with evidence of a third component in the mixture, despite there being no lactone form present, Figure 36. There are also four signals left on the very last spectrum as appose to three for the pH 10 complex again indicating that there are more species present at pH 13 than at 10 or 7.
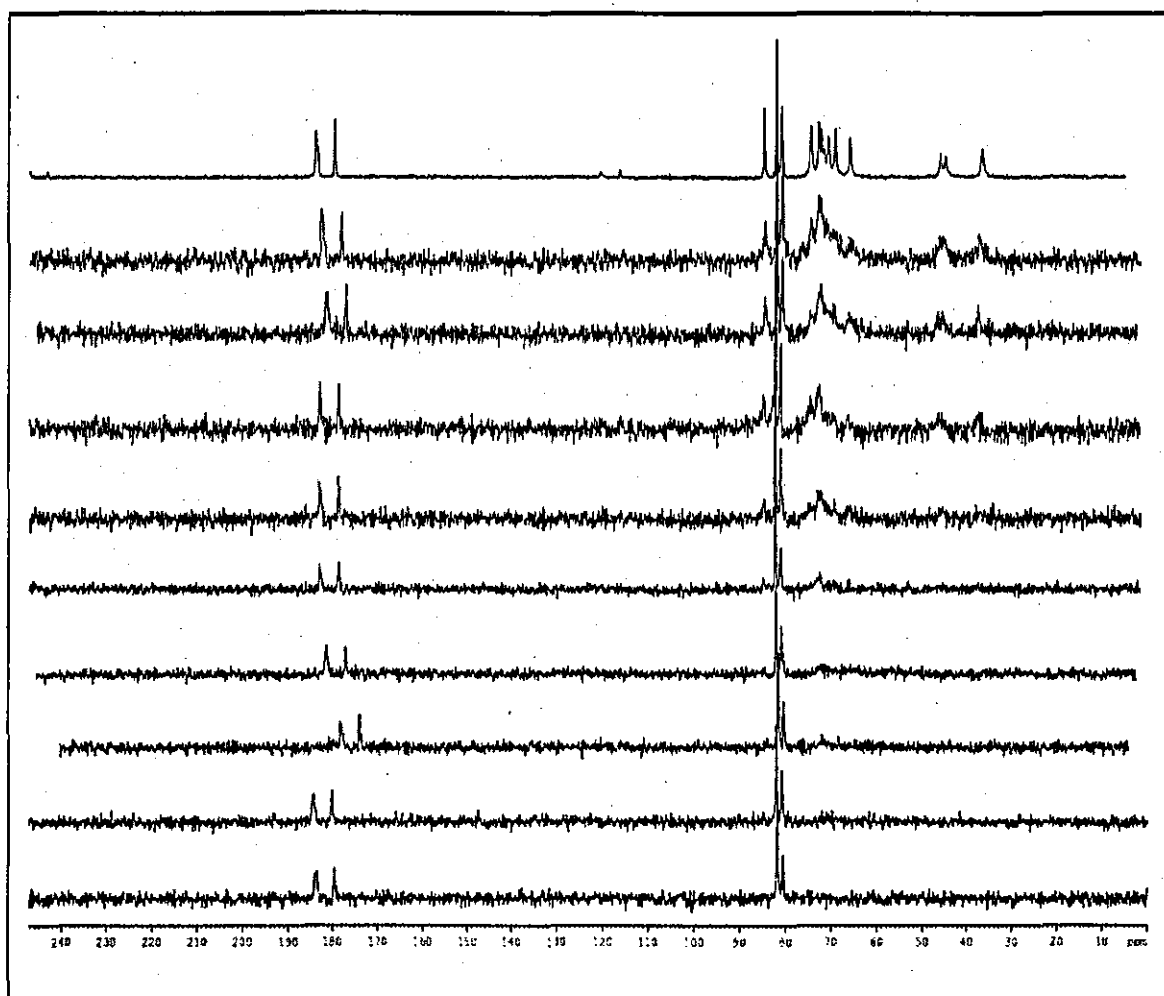
Figure 36 Cd:ISA at pH 13 C^{13} spectra. The difference in spectra id the change in D7 delay from 0, 2, 6, 10, 14, 22, 26, 32, 40 and 50 μs going from the top spectra to the bottom.

3.5.1.3 CSA

Chemical shift anisotropy can tell us more about a carbons orientation in space by producing spinning side bands, SSBs. The relative intensities of these bands give an indication as to the orientation of nuclei with respect to its surrounding atoms. An example of some CSA patterns can be seen in Figure 37. Each chemical shift seen in a ^{13}C spectrum is made up from the sum of the shielding tensors XX, YY and ZZ along the three axes of the 3D nuclei. When an atom is completely symmetrical in orientation, then no CSA or SSBs are observed. When one or two of these shielding tensors differs to the others then SSBs are seen and they appear equidistance from the main peak on opposite sides but will be of different intensities depending on the orientation of the nuclei being analysed. Previously the samples were spun at 8 kHz to reduce the number of SSBs so they didn't get confused with actual carbon peaks. The faster the sample is spun the less CSA is seen. The CSA spectra for the ISA spun at different speeds can be seen in Appendix 4.

Figure 37 ISA, pH 10 ^{13}C spectra, 1 kHz spinning speed
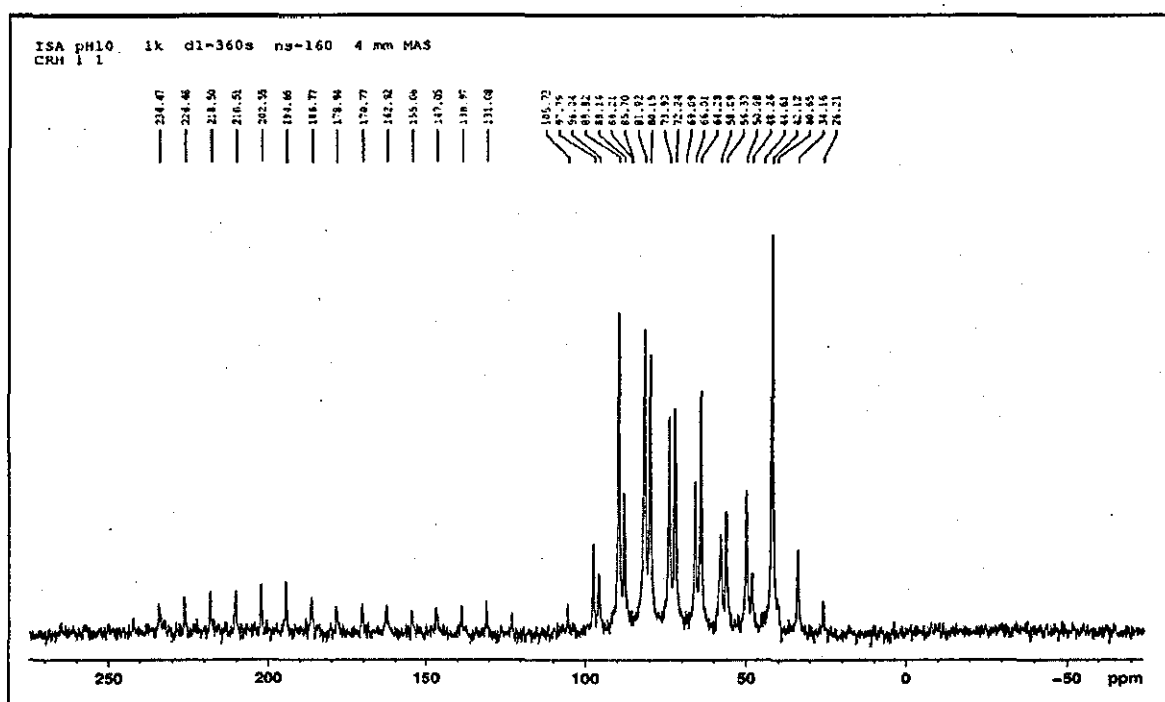
Results become more difficult to interpret when looking at the peaks from 100 to 0 ppm. In this region a lot of the CSA spinning side bands are overlapped. Because of this overlapping the CSA in this case cannot provide much more useful information about the structures. It is possible though to compare this experimental CSA with calculated CSA patterns using Gaussian modelling. This would mean that, when two ^{13}C signals have the same pseudo-isotropic chemical shift, they may have different CSA values that could be diagnostic and this could be found out by comparing the two techniques. This would obviously be important for the pH 10 and 13 samples where there are a lot of extra, unidentified peaks present. The main data to draw from the CSA in the ISA sample at this stage is that the peak from carbon 3 at ~ 42 ppm has very little anisotropy as few SSB are observed. The other carbons present appear to have more anisotropy than carbon 3 but less that carbon 1. Until any extra experimental or modelling is carried out to accompany this work, no further conclusions can be drawn from this analysis.

3.5.2 XRD

The XRD study was carried out to determine if a more complete structure of the ISA could be gained to help the assignment of peaks in the NMR work. The results from the XRD support the SS NMR experimental investigation, Figure 38, and the four samples show clear differences in crystallinity, particularly at high pH. The spectra show again that different forms of ISA are present at the three different pH values studied. As the samples are not very crystalline (hence why NMR studies were carried out initially) the spectra produced have a noisy baseline and they don't have many clear defined peaks.
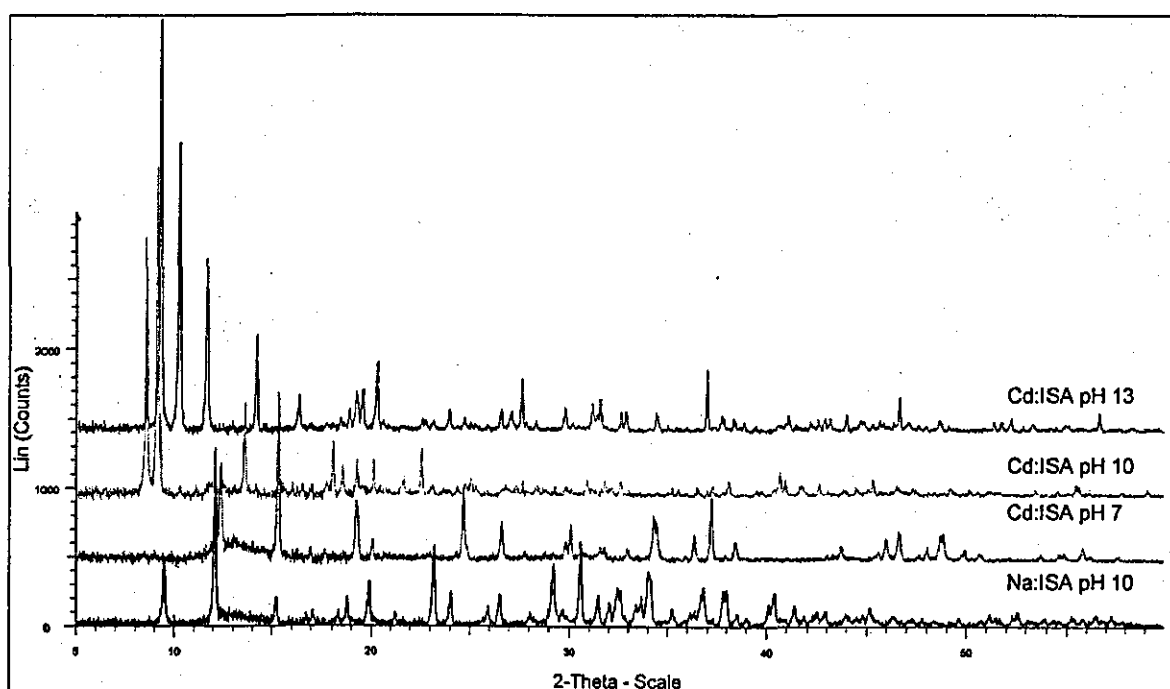
Figure 38 XRD of Cd:ISA at different pH's

3.5.3 Cd NMR

The Cd NMR spectra exhibit the same patterns as the metal ISA complexes where there is one set of peaks present for the M:ISA complex at pH 7, two at pH 10 and then three at pH 13. What is interesting is that a tiny amount of the peak at pH 7 is present in the pH 10 sample but none is present in the pH 13 sample. Then the second peak produced at pH 10 remains in the pH 13 sample, see Figure 39.
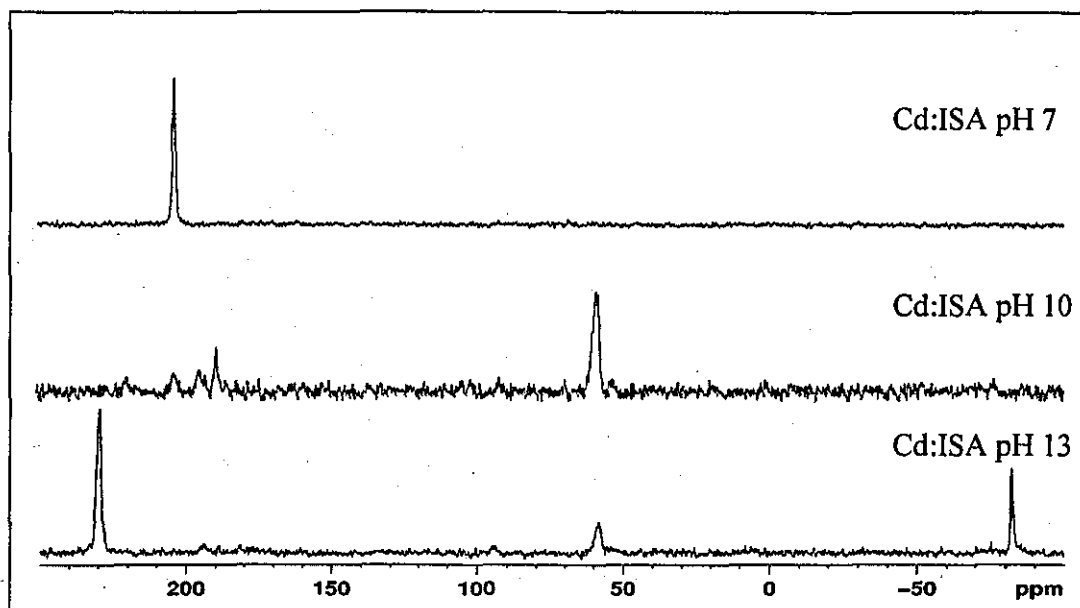
Figure 39 Cd NMR spectra for Cd:ISA complexes at pH 7, 10 and 13

This supports the theory that the second set of peaks present at pH 10 are from the same structure or form of ISA as present at pH 7. However the pH 7 structure does not seem to be present at pH 13.

3.5.4 Gaussian Modelling

Gaussian modelling [91] is a suite of computer programmes that allows the optimisation of a structure such as ISA, Figure 40. It has been shown in previous studies that experimental ^{13}C chemical shifts similar to those from ISA, correlate well to Gaussian modelling data [80],[81]. The software uses electronic structure theory to perform the calculations and this enables the model to compute the energy of a particular molecular structure. For example the spatial arrangement of atoms or nuclei and electrons are used to perform geometry optimisations by locating the lowest energy molecular structure, and the vibrational frequencies of the molecules resulting from interatomic motion within the molecule can then be obtained [104]. Once an optimised structure has been obtained the software can calculate NMR shifts and shielding tensors as shown in Figure 41.
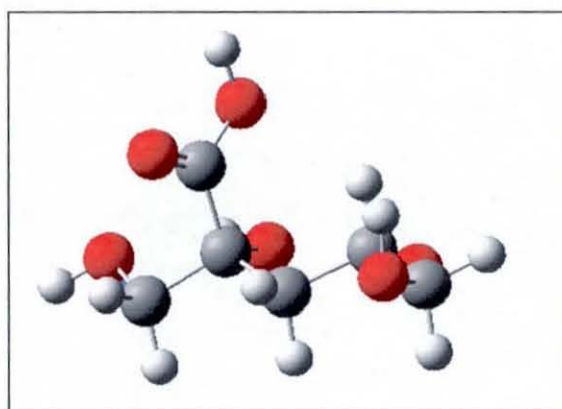
Figure 40 Structure drawn into the Gaussian modelling programme for ISA open chain
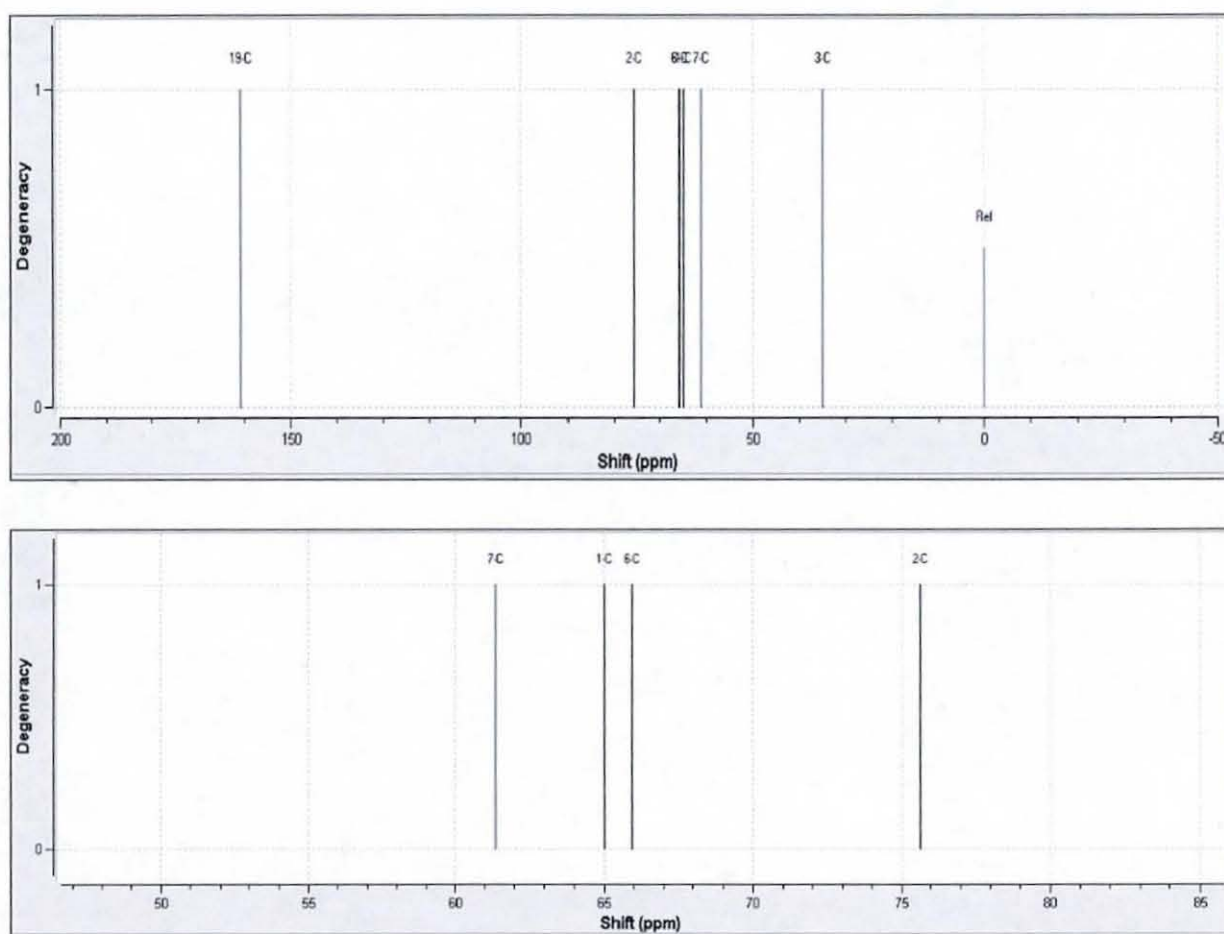
Figure 41 Calculated NMR ^{13}C spectra from the optimised Gaussian structure in Figure 40. Top spectrum is the total scale, bottom spectrum is a zoomed in version showing the peaks at 60 to 80 ppm more clearly.

The NMR calculated chemical shifts were used to compare to the experimental work to see if any matches were present.

3.5.4.1 Structure A

There were two different conformations of the ISA ligand that were analysed, the first being shown in Figure 40. This is the expected structure of ISA with the carboxyl group branching off the main carbon backbone [55]. The order of peaks from the calculated and experimental data has been compared to see if the correct assignments are being made, Table 28. The calculated data supports the previous experimental assignments of carbons 4 and 6 being the overlapped ones.

Table 28 Gaussian chemical shift assignments for ^{13}C NMR spectra verses previous experimental assignments

Order	Gaussian Order	Previous assumption from this work
Highest ppm	1	1
	2	2
	4	6 + 4
	6	
	5	5
Lowest ppm	3	3

Despite the modelling supporting the previous assignments of chemical shifts to the different carbons, comparisons will be made assuming the overlapped peaks are carbons 4 and 6 at 69.72 ppm, carbons 5 and 6 at 67.75 ppm and carbons 4 and 5 at 69.72 ppm just to ensure all conformations are covered. There were always differences between the modelled and experimental chemical shifts, even when no metal was present, so, to carry out this analysis, the differences between the ligand with no metal and ligand in the presence of metal were looked at. These differences were worked out within the experimental and calculated data and then the final values were compared. As the modelled structures were only the open

chain forms of the ISA, only data from the open chain forms at pH 10 and 13 experimental work was used to compare to calculated shifts. All the graphs drawn for comparison purposes can be seen in Appendix 4.

3.5.4.1.1 1:1 Metal:ISA Monodentate

The first set of modelled data was carried out with one metal binding to the ligand through only one bond. It has been shown in previous studies that 1:1, 2:1 and 3:1 M:ISA complexes can exist at the range of pHs looked at in this study [72]. The results for the differences in calculated carbon chemical shifts can be seen in Table 29.

Table 29 Table of Gaussian calculated carbon chemical shift differences where ISA was complexed with one metal at different positions. The differences are between the chemical shift of the ISA with no metal present and the chemical shifts when a metal is bound.

C No	Carbon chemical shifts (ppm) and where the metal was bound					
	Sugar + M 1 (C=O)	Sugar + M 1 (OH)	Sugar + M 2	Sugar + M 4	Sugar + M 5	Sugar + M 6
1	58.8032	7.018	16.033	15.158	6.594	17.355
2	19.7424	12.8486	7.9589	14.049	12.1084	23.0375
3	13.4064	9.2804	17.3789	7.9678	15.5824	13.2081
4	17.1419	8.5209	12.1882	13.7044	9.6689	18.1229
5	14.8854	14.4566	13.8454	9.6988	14.5588	10.9044
6	16.2951	16.3091	14.1699	14.4384	15.9835	23.9591

There were no clear matches with the experimental and calculated data. There are many possible explanations for this, the main one being that there are so many different possible combinations of ways in which the metal could bind to the ligand in terms of the denticity and geometry that a lot more structures need to be modelled. There could also be more than one type of complex present at any one time so modelling of a few structures together should be carried out.

3.5.4.1.2 2:1 Metal:ISA

As no firm conclusions about the structure of these complexes could be drawn from the 1:1 calculated data, a 2:1 M:ISA structure was modelled and the results in chemical shift differences are shown in Table 30.

Table 30 Table of Gaussian calculated carbon chemical shift differences where ISA was complexed with two metals both attatched by one bond at different positions. The differences are between ISA shifts with no metal and shifts whne the metal was present.

| C No | Carbon chemical shifts (ppm) and where the metal was bound | | | | |
	Sugar + 2M C1 – C1	Sugar + 2 M C1 - C2	Sugar + 2 M C1 – C4	Sugar + 2 M C1 – C5	Sugar + 2 M C1 – C6
1	23.984	18.213	17.593	18.336	23.538
2	-34.9973	-38.4419	-36.4837	-36.1864	-35.7405
3	7.9238	5.193	1.0865	3.1674	2.2756
4	-3.8555	-2.3225	2.09	-3.4096	-0.8828
5	-5.1541	-10.2847	-8.1269	-6.7891	-9.9105
6	1.8897	4.0312	6.4975	7.2407	6.7948

There was one graph from these results that seemed to have a closer match, when comparing the differences in chemical shifts, than any of the others. This was from the pH 13 open chain experimental spectra (when the peaks for carbon 5 and carbon 6 were thought to be the overlapping peaks at 67 ppm) and it had a similar pattern of differences to the modelled data for 2 metals, bound to the ISA at carbon 1 (C=O) and carbon 4, see Figure 42. These are the closest matches seen so far, but they are still not exactly matched.
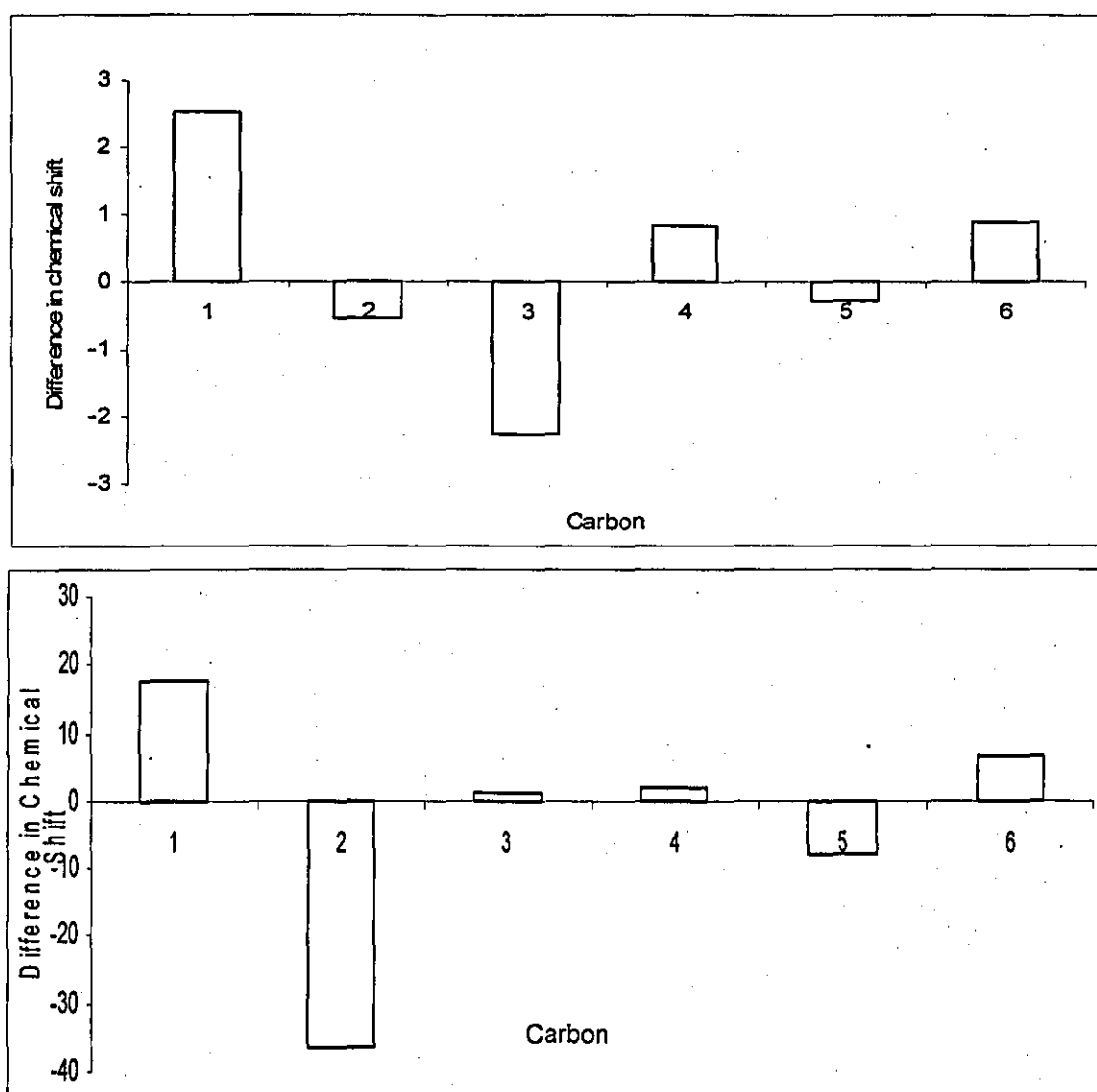
Figure 42 Comparison of graphs for 2 metals bound to ISA each through single bonds. Top is experimental, bottom is calculated.

Carbon 2 is still not quite matched and, as the structures which give these matches are not very likely in terms of the overlapped peaks, further analysis is needed.

3.5.4.1.3 1:1 Metal:ISA Bidentate

Still no definite structures of these complexes has been elucidated so a 1:1 M:ISA structure was modelled again, but this time the metal was bound to two oxygen's on the ligand, one of

which is always bound to the carbonyl group as this is most likely to be where the metal is always attached. Table 31 shows the chemical shift differences for the carbons with these conformations.

Table 31 Table of Gaussian calculated carbon chemical shift differences where ISA was complexed with one metal, bidentately bound, at different positions. Differences calculated between the ISA shifts with no metal and the ISA shifts with metal present.

| C No | Carbon chemical shifts (ppm) and where the metal was bound | | | | |
| | Sugar + M | Sugar + 2M | Sugar + M | Sugar + M | Sugar + M |
	C1 – C1	C1 - C2	C1 – C4	C1 – C5	C1 – C6
1	15.386	20.952	14.775	18.038	18.34
2	-39.1256	-36.4294	-31.9262	-37.3755	-39.2272
3	4.596	-0.6116	3.3682	1.8297	5.0704
4	-1.5442	-3.537	-4.1754	-1.0314	-2.7238
5	-7.3595	-15.4702	-9.0608	-7.0864	-9.9637
6	10.2566	1.3276	7.443	7.9839	5.4031

As with the first modelled structure there were no significant matches between all the graphs.

3.5.4.2 Structure B

As no firm matches were seen with the Gaussian calculations for structure A ISA and the experimental, a different structure for ISA was proposed. This is the structure, shown in Figure 43, with the carboxyl group at the end of the carbon backbone.
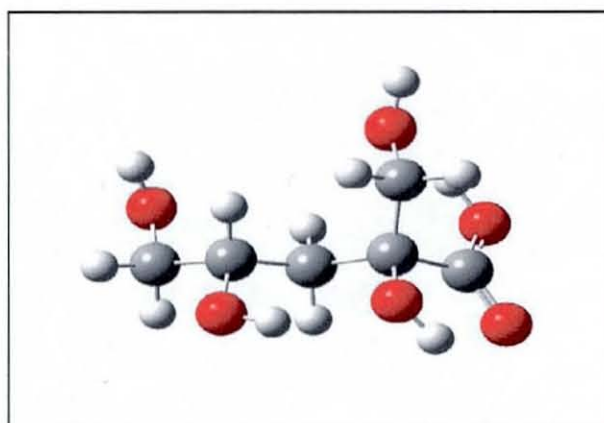
Figure 43 Structure drawn into the Gaussian programme for ISA open chain, structure B.

Table 32 contains the order of results for the calculated peak assignments compared to the experimental. From this comparison it looks like carbons 5 and 6 may have been assigned incorrectly. This is possible, as mentioned previously the two nuclei are in very similar chemical environments and there was always an uncertainty with these carbon assignments. Because of this difference, the calculated results will be compared with the experimental as for structure A, where carbons 4 and 6 are the overlapped peaks at 69.72 ppm, as previously assigned, and where carbons 5 and 6 are the overlapped peaks at 67.75 ppm. A comparison was also made with the possibility of carbons 4 and 5 being the overlapped pair at 69.72 again to cover all eventualities.

Table 32 Gaussian chemical shift assignments for ^{13}C NMR spectra verses previous experimental assignments – Structure B ISA

Order	Gaussian Order	Previous assumption from this work
Highest ppm	1	1
	2	2
	4	4 + 6
	5	
	6	5
Lowest ppm	3	3

All the comparison graphs can be seen in Appendix 4. Data were analysed as previously by comparing the differences between the uncomplexed ligand chemical shifts with the shifts when the metal is present. Again, as the lactone structure has not yet been modelled only the data from pH 10 and 13 is being compared

3.5.4.2.1 1:1 Metal:ISA Monodentate

As before the first structure modelled was a 1:1 M:ISA configuration. Table 33 shows the carbon chemical shift differences of all the modelled data for this structure.

Table 33 Table of Gaussian calculated carbon chemical shift differences where ISA was complexed with one metal at different positions – Structure B ISA

C No	Carbon chemical shifts (ppm) and where the metal was bound					
	Sugar + M 1 (C=O)	Sugar + M 1 (OH)	Sugar + M 2	Sugar + M 4	Sugar + M 5	Sugar + M 6
1	8.835	12.167	5.62	-1.82	-3.17	-1.68
2	11.64	19.3417	8.13	3.12	8.98	2.87
3	2.43	18.3948	3.3	9.07	5.4	2.88
4	5.59	18.8345	7.01	6.71	5.74	4.33
5	3.92	17.1106	5.47	6.56	6.18	3.1
6	3	18.2043	10.29	7.76	2.95	5.94

There were no close matches in either the pH 10 or pH 13 data. This could be because the structure of ISA is different or could be due to reasons mentioned previously.

3.5.4.2.2 2:1 Metal:ISA

As no firm matches were made with the 1:1 M:ISA modelled structure a 2:1 formation was modelled. The data from the chemical shift differences can be seen in Table 34.

Table 34 Table of Gaussian calculated carbon chemical shift differences where ISA was complexed with two metals both attached by one bond at different positions – Structure B ISA

C No	Carbon chemical shifts (ppm) and where the metal was bound				
	Sugar + 2M C1 – C1	Sugar + 2 M C1 - C2	Sugar + 2 M C1 – C4	Sugar + 2 M C1 – C5	Sugar + 2 M C1 – C6
1	15.776	11.883	4.858	9.659	9.279
2	10.1839	11.4687	11.5295	9.45	11.4466
3	4.8933	2.0959	5.0131	5.0283	4.0576
4	4.407	6.1851	6.1129	4.557	6.1147
5	7.7044	5.0954	3.4064	4.037	6.4071
6	3.1248	6.1975	8.5089	4.1935	9.2508

Again no clear similarities were seen. There are so many different conformations that could be formed when a metal complexes with ISA that further work is needed to be put in to try and model all the possible outcomes.

3.5.4.2.3 1:1 Metal:ISA Bidentate

This was the final conformation modelled in this particular study where the metal is bound to the ISA via two bonds. One of the bonds is always through the carbonyl group. The chemical shift differences can be seen in Table 35.

Table 35 Table of Gaussian calculated carbon chemical shift differences where ISA was complexed with one metal, bidentately bound, at different positions – Structure B ISA

	Carbon chemical shifts (ppm) and where the metal was bound				
	Sugar + M	Sugar + M	Sugar + M	Sugar + M	Sugar + M
C No	C1 – C1	C1 - C2	C1 – C4	C1 – C5	C1 – C6
1	8.986	4.909	0.134	-8.554	1.092
2	11.3374	7.4233	15.7097	8.7322	8.6985
3	1.9741	1.8544	8.9928	2.9659	0.7864
4	6.1892	3.1315	5.7549	7.7142	8.5015
5	3.3188	7.2621	9.6937	-2.1346	-0.45
6	8.5771	9.6281	6.1424	12.7553	3.9076

Although there were still no absolute matches with the modelled and experimental data, there was one graph which matched better than any others seen previously. This match was found when the metal was bound at the carbonyl group, carbon 1, and at carbon 5, Figure 44. As these groups are the furthest away from each other in the ISA chain, this may indicate that the ISA must bend round the metal for this conformation to occur.
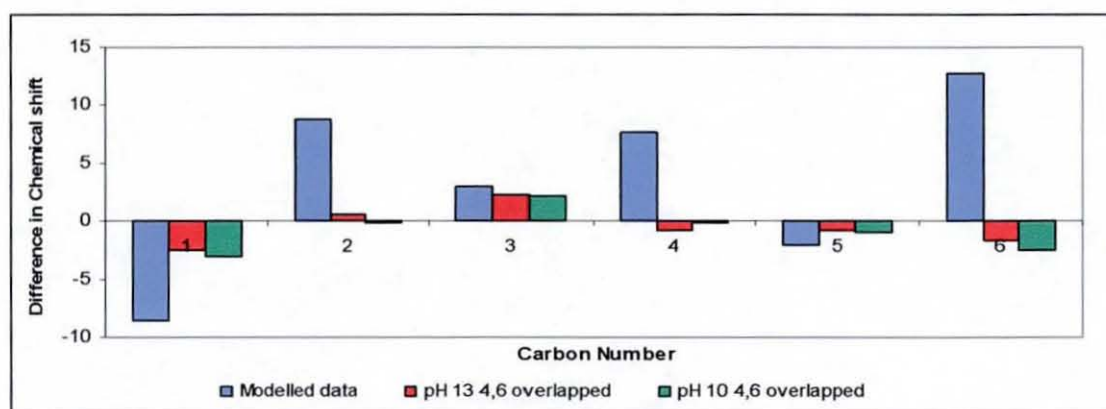
Figure 44 Graph of difference in C^{13} chemical shift when metal is present or absent for modelled data and experimental at pH 10 and 13.

Carbons 4 and 6 are still not exactly matched.

3.5.5 Discussion

Within this section there are two main areas of focus, the differences in the experimental results when there is a metal present or not, and the differences between the modelled and experimental results. The first area (experimental results) can be divided further into the various changes observed in the spectra obtained at different pHs and changes seen when a metal was present:

i)   There was no significant change in the ligand spectra in the absence of metal at the different pHs

ii) The lactone spectra, or a similar closed ring structure, was seen at pH 7 when metals were in the reaction mixture.

iii) At pH 10 and 13 extra peaks were visible which correlated well with the Cd NMR spectra and the XRD data

As discussed previously in section 3.3.4.2, the HSAB theory can be applied to try and determine the most likely M:L bonding combinations and what groups or elements the metal is prone to bond to. The metals studied here are both hard and soft acids, Cd being soft whilst Fe and Eu are hard and Ni is borderline and the ligand ISA is a hard base. It is important to remember other compounds could be formed in the mixtures, for example, chloride which will be present as a hard base and sodium as a hard acid. Another possibility that should be considered is the possibility that outer sphere complexes could be formed which wouldn't necessarily show significant changes in the NMR chemical shifts of the carbons. These complexes are always a possibility when the metal and ligand have opposite charges and it could mean that at pH 7, for example, an outer sphere complex is formed and the NMR shifts unchanged as there is no metal directly bonded to the ligand.

The changes in the chemical shifts of the carbons are generally shifted upfield (a lower chemical shift), indicating that they are being more shielded than previously. This is reasonable since the electrons from the cadmium must be having a shielding effect on the carbon nucleus when it is bonded.

The first point of discussion above was to explain why there is no change in the ligand spectra at the different pHs and why they are all the open chain structure. This finding is supported by another study where gluconic acid, often used as an analogue for ISA, was studied at different pHs [64]. This indicates that this pH range causes no significant conformational changes in ISA, and any changes observed when a metal is present must come from the complexation itself. Above pH 7 there are only small amounts of lactone present usually, so it is possible that they are still present but not at high enough concentrations to give peaks in the NMR spectra.

The second main point of discussion is to explain why at pH 7 the ISA either solidifies as the lactone form, and has little or no complexation with the metal, or it complexes with the metal but in a ring formation very similar to that of the lactone conformation. Many studies in this area suggest the involvement of the hydroxyl groups as well as the carboxyl to form bonds whether directly [69] or through hydrogen bonds [52] with the metal. In the absence of a metal a high pH is required for the deprotonation of the hydroxyl groups [60], but metal induced deprotonation can occur at much lower pH [68]. The structure formed can then take a ring conformation. The first point could also be valid though, where no complexation is observed. This could be because the ligand will stay preferentially bound to the sodium or chloride as they are both hard acid/bases but the first explanation is supported more in the literature.

The deprotonation of some of the hydroxyl groups on the ISA molecule means that a number of different complexes could be formed, which could in turn produce the extra peaks that are being seen at the higher pHs, particularly at pH 13 as this would increase the amount of deprotonation present. The extra lines observed have been noticed in a study by Cho et al. [52], but at a much lower pH and without any metal being complexed. Even so similar explanations were given, as in this thesis, where extra peaks seen in the spectra (other than the six main peaks for the six carbons in ISA), could be due to the lactone form being present as well as the open chain. Interestingly the study also suggests that, at the pH used in the investigations described in this thesis, the lactone form is unlikely to be present which would support the theory that it is actually a ring structure formed with the metal at pH 7. Although the study is observing the complexation of Na and Ca with ISA, it also finds that at high pH, i.e. 13, the cation is more closely associated with one of the hydroxyl groups than with the carboxylate, this is a structural conformation also proposed by Vicedomini et al. [69] when

studying Pb complexation reactions with gluconate ions. This would mean a new complex is formed at pH 13 which is exactly what the results in this thesis are suggesting. A study by Ramos et al. [64], also indicated that at high pH the metal is complexed through the deprotonated hydroxyl groups and 2:1 M:L complexes were formed which backs up the stoichiometries of the modelled data calculated previously. Gajda et al. [68], also detected new complexes formed above pH 12. To further support this theory different analytical techniques would need to be employed to prove the appearance of new complexes. Another possible explanation for the extra peaks at pH 13 could be the formation of mixed hydroxyl complexes, such as those reported by Borsari [105] when studying Cd:EDTA complexes above pH 13.8. A final explanation of the extra peaks could also be that at high pH there is expected to be more than one stoichiometry present [72],[68]. Other work involving divalent cations and gluconate have shown that, at high pH, dimers can be formed [70]. This again would show a different form of the ISA in the NMR spectra.

All the explanations given above need to be added to information on the metals involved themselves for any accurate hypothesis to be given as to the complexation that may be occurring. Cadmium's most common oxidation state is 2+ and when complexed this can have coordination numbers of 4 to 8 so the coordination number will dominate the geometry of the complex. The cation has an ionic radius of 1.14 $\text{Å}^{[106]}$ with the electronic configuration of $1s^2 2s^2 2p^6 3s^2 3p^6 3d^{10} 4s^2 4p^6 5s^2 4d^{10}$. As significant changes in three of the carbon chemical shifts have been observed when looking at the ISA spectra, with and without Cd, a coordination number of three could be assumed. This is a rare coordination number for the transition elements but can occur for d^{10} elements and also large bulky ligands, both of which are present in this case. If this is the coordination number then the most likely geometry of the complex formed would be trigonal planar or possibly trigonal pyramidal. When looking at any steric issue in the two complexes proposed the trigonal planar looks feasible so this could be what is present. These data need to be put together with the results of the stoichiometry work to get a more accurate assignment. Cd:ISA complexes were found to form in a 1:1 and 3:1 complex at pH 10 and 1:1 at pH 13. For the sample at pH 13 this would indicate that all the changes in chemical shift come from just one metal bonding with one ligand at three sites. The sample at pH 10 could be slightly different as one of the stoichiometries found was 3:1 M:L indicating that it could be three different metal cations

bonding at carbon 1, 3 and 6 separately. When comparing solid state work to solution, similarities should be made with caution as it has been shown that the coordination number of cadmium in complexes can change when in solution, solid or gaseous state [105]. A study by Chung and Moon also showed that the carboxylate to cadmium ratio can affect the chemical shift of the cadmium so, when comparing previous work to these results, this should be remembered [107].

Europium's most common oxidation state is the 3+ ion and has varying coordination numbers of 3 to 12. Its ionic radius is 0.95 Å [106] and the electronic configuration is $1s^22s^22p^63s^23p^63d^{10}4s^24p^64d^{10}5s^25p^66s^24f^7$. Lanthanide 3+ ions have large ionic radii. They are typical hard Lewis acids and the bonding in their complexes is electrostatic and non-directional. As a result, steric factors govern the coordination geometry of lanthanide complexes. Coordination numbers are generally high (>6) and coordination geometries are often irregular. This could explain why the europium seems to complex at the carbon 2 and 4 positions as it avoids the steric effects of the carbonyl group on carbon 1. This conformation was more difficult to determine as only two carbons seemed to be affected by the bonding of the metal and yet the literature suggests that europium has coordination numbers starting from 3 not 2. The stoichiometry data for this complex at pH 7 and pH 13 indicate that it is only a 1:1 complex that is formed [72]. It should also be noted that europium is often used in NMR as a lanthanide shift reagent which should significantly move the chemical shifts of the carbons. As this has not occurred to any large extent in this work it is possible that the metal isn't complexed at all to the ligand.

Fe(II) is in the 2+ oxidation state and has coordination numbers of 4, 6 or 8. The ionic radius is 0.74 Å [106] and the electronic configuration is $1s^22s^22p^63s^23p^64s^23d^6$. Again as with both other metals discussed the geometry will depend on the coordination number which is hard for us to determine without knowing more about the ligand. As with the europium this does not fit in entirely with the coordination numbers usually exhibited by this metal. This could be because the ^{13}C spectra obtained for Fe(II) were quite distorted and the peak shapes were not good so the results could have been misinterpreted or there could be differences that cannot clearly be seen due to the bad peak shapes and extra peaks. As with the europium the stoichiometry data from this complex at pH 10 was not carried

out but pH 7 indicates a 1:1 complex forming. This would imply that both the bonds to carbons 1 and 2 were coming from the same metal cation.

The second main question that arose from this work was why there are no clear matches with the modelled and experimental data. Gaussian is a molecular model which essentially uses electronic structure theory to operate [104]. This enables the model to compute the energy of a particular molecular structure, i.e. the spatial arrangement of atoms or nuclei and electrons, perform geometry optimisations by locating the lowest energy molecular structure, and compute the vibrational frequencies of molecules resulting from interatomic motion within the molecule. Electronic structure methods use the laws of quantum mechanics rather than classical physics for their computational calculations. The basis for the calculations comes from solving the Schrödinger equation:

$$H\Psi = E\Psi$$

Where Ψ = wavefunction , H = the Hamiltonium operator and E = Eigen value, or energy for the system.

The Schrödinger equation however, cannot provide exact solutions to larger systems as they are not computationally practical. To get round this the model uses a number of approximations in its calculation of which there are two major types; semi-empirical methods and ab initio methods. Semi empirical methods use parameters obtained from experimental studies to simplify the computation. Ab initio computations are based solely on the laws of quantum mechanics, the first principles, and on a small number of physical constants such as the speed of light. These approximations could mean that differences are seen between the experimental and calculated data. Gaussian also uses a third set of electronic structure methods called density functional methods, DFM. DFM are useful as they include the effects of electron correlation i.e the fact that electrons react to other electrons motion in the same system and as a result will repel each other.

The other main explanation as to why the data doesn't match could be because there may be a large number of different complexes present which haven't been modelled and also

there are many more different conformations and stoichiometries that need to be modelled which has been demonstrated in many other studies, discussed previously.

4 CONCLUSIONS AND FURTHER WORK

4.1 Cellulose degradation products

Cellulose degrades under alkaline anaerobic conditions, such as those likely to be found in a nuclear waste repository, to yield a number of complexing ligands in solution. The main products from the degradation of cellulose have been identified as formic acid, ISA, lactic acid and acetic acid. Of these, the main component was ISA which had a concentration in a 10% cellulose loading of approximately 0.01 mol dm^{-3}. Different cementitious materials (NRVB, PCM grout and calcium hydroxide), were used to create the CDP to see if this had any effect on the products produced or the ISA concentration. When comparing the solutions from a 10% cellulose loading in the presence of these cementitious materials, there were no significant differences in terms of what species were present. Small changes were observed in the concentrations of ISA but this was likely to be due to some evaporation of the solution when heated for 30 days. Different cellulose loadings were then investigated of 1, 10, 20, 50 and 100 % w/w using PCM grout and NRVB. When comparing the solutions with the different cellulose loadings some differences were observed. In the presence of PCM grout a maximum concentration of ISA was produced at a 10% cellulose loading. This occurred at a loading of approximately 50 % with the NRVB solutions. The difference in maximum ISA concentration is possibly due to sorption of the ISA onto cement or the grinding of the cementitious material prior to adding the water and cellulose. The differences in grinding of the cement would result in significant differences in surface area available which would alter the sorption processes of any ligands to the cement. Interestingly, even though this affect was also observed with the other standards of formic acid, lactic acid and acetic acid, there were still more species being formed as the cellulose loadings increased when both NRVB and PCM grout was used. The formation of these new products implies that either new species are formed directly from the cellulose degradation when higher loadings are present, or, the initial products produced are degrading to yield new species. The number of individual components showed slight differences when comparing the PCM grout and NRVB results but this was thought to be due to HPLC column degradation as the resolution of many of the peaks from the NRVB samples was not as good as previously reported.

4.1.1 Further Work

The results from the HPLC analysis of CDP using NRVB grout need to be repeated on a new column to determine whether any differences observed were in fact from column degradation and not from experimental changes. To further this study the kinetics of the ISA production could be looked at in more detail studying loadings at more frequent intervals. As the identification of cellulose degradation products can help the understanding of the degradation process but also the solubility studies performed throughout this study, the other components produced at the higher cellulose loadings could be identified by a number of different techniques such as LC-MS or ICP-MS.

4.2 Solubility Studies

The solubility of metals in the presence of different complexing ligands at high pH was carried out to determine if CDP had an effect on the solubility above that of ISA at the same concentration. The metals studies were nickel, cobalt and cadmium, chosen as they may be present in intermediate level wastes but also they can be used as analogues for other cations.. Method development was carried out on how to determine thorium solubility accurately as previous studies show discrepancies within the results. Oversaturation and undersaturation methods were investigated and the solubility of thorium was determined in the presence of CDP and different ISA concentrations as with the other metals. This study also investigated the solubility of thorium at three different pHs of 6, 8 and 12 and looked at the kinetics of the reaction.

4.2.1 Nickel Solubility

The expected solubility of nickel in sodium hydroxide was 10^{-8} mol dm^{-3} and in CDP 10^{-4} mol dm^{-3}. The solubility of nickel in basic conditions was 5×10^{-8} mol dm^{-3} which was close to the expected level. Expected trends were observed with the solubility in different concentrations of ISA where the concentration of nickel in solution increased with increasing ISA concentration. The solubility of nickel in CDP was increased by approximately ten times over that of ISA of approximately the same concentration.

4.2.2 Cadmium

The expected concentration of cadmium in a high pH solution was 10^{-7} mol dm^{-3}. The solubility of cadmium in the high pH solutions was 6×10^{-7} mol dm^{-3}. The expected trends were observed with the ISA at different concentrations where the metal solubility increased with increasing ISA concentration. The solubility in the presence of CDP was only twice that of the ISA solution.

4.2.3 Cobalt

The expected solubility in samples at pH 12 is 3×10^{-6} mol dm^{-3} although other reported solubilities have been at 5×10^{-12} mol dm^{-3}. As with nickel and cadmium, the solubility of the metal increased as ligand concentration increased. The solubility in CDP was higher than ISA by two orders of magnitude.

4.2.4 Thorium Solubility Method development

Previous studies on the solubility of thorium have produced different solubility values. Work was carried out in this thesis to determine a suitable method to determine the solubility of thorium accurately and reliably. The methods of analysis were also investigated and first method chosen was liquid scintillation counting. Two batches of thorium were studied. When samples of thorium nitrate were prepared in acidic conditions, batch 2 gave one peak when analysed by liquid scintillation counting and batch 1, two peaks. The first peak present in batch 1 was thought to be thorium and from calibration standards it was assumed that the second peak was due to daughters of thorium. When the thorium was added to a saturated solution of calcium hydroxide, both batches showed only one peak, believed to be the daughter peak. No peaks were observed when both batches were made up in sodium hydroxide and only background counts were obtained. It was thought that batch 2 could have been purified and, therefore had the thorium daughters removed, prior to being sent to Loughborough which was why no second peak was observed on the LSC. This theory does not explain however why a peak occurs in the presence of calcium hydroxide. There was definitely a complexing component in the calcium hydroxide increasing the solubility of something in the thorium solution, most likely a daughter product, but tests were inconclusive to determine what this was. Gamma spectrometry was used to try and identify where the

extra counts and activity were coming from. The gamma spectrometry results supported the theory that daughter radionuclides were present causing an extra peak to be seen in the LSC spectra but again this doesn't provide answers for why calcium hydroxide has an effect on this and why only one peak was seen initially for batch 2.

The explanation for why there was a peak in the calcium hydroxide solution of both batches, but not with sodium hydroxide, was thought to be due to carbonate interference but, when the effect of calcium carbonate on the solubility of thorium was investigated only background counts were obtained. Tests were carried out for chloride interferences, colloid effects and contaminant effects from the calcium hydroxide and, although none of these tests provided firm conclusions as to what is occurring in the samples, it is possible that the effect seen is a combination of all of these issues and alone their effects cannot be studied effectively. ICP-MS analysis of the thorium solutions showed only thorium present and no other metals. This could be because the concentration of any other metals present was not high enough to detect. Because these results were inconclusive, ICP was chosen as the method of choice for the analysis of thorium in future work as the daughters, if present, could be detected separately from the thorium. ICP-OES was thought to be the best method for this high pH study because the high salt content of the samples could interfere with the ICP-MS.

4.2.5 Over and Undersaturation study

The solubility of thorium was measured in (i) 0.1 mol dm^{-3} sodium chloride at pH values of 6, 8 and 12 at ambient temperature, (ii) saturated calcium hydroxide solutions at pH values of 6, 8 and 12 at ambient temperature, (iii) ISA concentrations of 1 x 10^{-3} mol dm^{-3} and 1 x 10^{-2} mol dm^{-3} at pH values of 6, 8 and 12 at ambient temperature in sodium chloride, (iv) 1% CDP solution at pH values of 6, 8 and 12 and (v) 10% CDP solution at pH values of 6, 8 and 12 at ambient temperature. Thorium solubilities were measured by using the undersaturation and oversaturation methods. The kinetics of both methods were investigated by measuring thorium solubilities after 2, 7, 14, 21 and 28 days.

The undersaturation experiments showed little change in the thorium solubilities at pH 6 and 8 in the presence of either CDP or ISA. At pH 12, 10% CDP showed a significant increase in thorium solubility when compared to ISA solution which had a similar concentration of ISA to that of the CDP. This indicates that there are other complexing agents present in the CDP

solution in addition to ISA and these are responsible for the increased solubility of the thorium as with the other metals studied. Kinetic studies of thorium hydroxide precipitation showed that 28 days is sufficient for a steady state to be achieved, but more time may be needed for a steady state to be reached after the addition of the ligand solution to the precipitate. A considerable amount of scatter was evident in these results.

The oversaturation experiments displayed less scatter and were more reproducible. The thorium solubility in ISA solution (1×10^{-3} mol dm^{-3}) and 1% CDP were comparable to background values at all pHs. Solubilities of thorium increased at all pHs when the ISA concentration increased to 1×10^{-2} mol dm^{-3}. Differences between thorium solubilities in CDP (10%) and in ISA (1×10^{-2} mol dm^{-3}) solution were only observed at pH 12. The solubility was approximately 46 times higher in the CDP when compared to the ISA. A study of the kinetics of complexation reactions suggested that a steady state was attained after 7 days.

Overall the oversaturation experiment appears to be the favoured method to use as the results were less scattered and contained less anomalies than the results obtained from the undersaturation method.

4.2.6 Further work

It has been proved that there is something else other than ISA present in the CDP which increases the solubility of metals at high pH. Further metals could be studied but it would be more beneficial to try and determine what else is present in the CDP which increases metal solubility. If other components could be determined and their stability constants for their complexes with metal calculated then the results could be modelled. This modelling could determine if the increase in solubility is a result of many small components all increasing the solubility slightly and the accumulative effect of all of the complexing ligands produces a large overall increase in metal solubility. Further methods for identifying the CDP products are discussed in section 4.3.1. The problem associated with the thorium solubility methods (oversaturation and undersaturation) was pH drift, and the use of a buffer should be investigated before future work is initiated. If the undersaturation method was to be repeated, a longer equilibration time should be investigated.

4.3   Thorium complexation in CDP

Thorium complexation studies were carried out to determine which species in the CDP the thorium was complexing with. This complexation study was only a preliminary experiment to see if there was any separation on the ICP-MS of thorium peaks. The work has found that free thorium prepared in acid, uncomplexed, elutes straight away and is unretained by the column as expected. This result indicates that most of the thorium in the CDP is complexed and is not in the free form. The ISA seems to complex most of the thorium although due to carryover in the column when the higher pH samples were analysed, it was difficult to determine differences between thorium in calcium hydroxide and thorium in ISA.

4.3.1   Further Work

If the LC-ICP-MS work is to be extended then the problem of carryover needs to be resolved. The carryover appeared as soon as the high pH samples were run as no significant carryover was noticed from the acidic thorium solutions. This carryover indicates that thorium binds strongly to the column material and not just the stainless steel of the column and inlet or outlet lines. This needs to be removed before each subsequent sample otherwise the spectra obtained would be very difficult to interpret. This would mean using the instrument for prolonged periods of time which was not available at the time of this study.

The resolution of the peaks from the CDP on the LC could be improved as although the main peaks can be detected, they are not as fully resolved as previously when using the other conditions with the phosphate buffer mobile phase. There are many different methods of improving the resolution of the carboxylic acid species which have been looked into such as LC-ICP-MS with dervitisation of the acids [102], ion exchange chromatography [108],[109], diffusion dialysis [110] or capillary electrophoresis [111]. These methods could then be followed by ICP-MS or LC-MS to identify other species present in the CDP.

4.4 Metal:ISA Interactions

The complexation of metals to ISA was studied using a range of solid state NMR techniques and Gaussian modelling. The aim was to determine where the metal would bind to the ISA ligand. The results have shown that NMR has the potential to be a very useful tool in determining the method of binding of radionuclides to organic molecules such as ISA at high pH. The ISA complexes showed little change in the carbon chemical shifts at pH 7, with or without the metal present, as the lactone structure of the ligand seems to prevent complete complexation of the metal or, when complexed, the metal is causing the ISA to form a ring structure very similar to that of ISA lactone. For the samples at pH 10 or 13, cadmium had the greatest effect on the chemical shift at carbons 1, 3 and 6 which correlates with the solution NMR work carried out previously at Loughborough. Europium showed changes for carbon 4 and carbon 2 which again almost matches the solution NMR work, with the exception of carbon 5, and with iron the largest effect was seen on carbons 1 and 2. All these results suggest that the metal is binding to the ligands prepared at higher pH in a bi or tri dentate complex and not bonding via all the hydroxy groups.

The work carried out with the uncomplexed ISA at different pHs showed no significant differences in the spectra; they all had the open chain peak chemical shifts. This implies that, regardless of pH, when the samples are left over a long period of time to solidify they form the open chain structure. When there is a metal present differences were observed. At pHs 7 and 10 there was evidence of the lactone form being present. At pH 7 the ISA appears to be completely in the lactone form. This may mean that when a metal is present, it makes it harder for the lactone ring to be opened when solidifying. Alternatively it could mean that the metal is binding to the oxygens on carbons 1 and 4 causing a very similar structure to the lactone to be formed which would give a similar NMR spectrum.

The dipolar dephasing technique to identify carbons with a different number of protons bound supported previous assignments, but did not add any more information to that already obtained. Due to the rate of dipolar dephasing it could be assumed for Cd:ISA at all the pHs that the peak at approximately 179 ppm is carbon 1, as it is a quaternary carbon, the peak at 77.27 ppm is carbon 2, as it is also quaternary, the peak at 31 ppm is carbon 3, because it is a

CH_2 group, and then the peaks at 61 and 64 ppm disappear at the same rate as the peak at 31 ppm so, in theory, should also be CH_2's.

The slow spinning ^{13}C CP-MAS experiments give more information about the CSA values of the carbon nuclei but, due to overlapping peaks, not much else can be drawn from this work until the modelling is looked into further, and more experimental data are obtained as it is a useful comparative technique.

The Gaussian modelling revealed a very similar pattern of peaks to the experimental data when no metal was present. There were few matches between the modelled and experimental data for the M:ISA complexes but any matches found indicated that the metal was bound at the carboxyl end of the ISA molecule as expected. More modelling needs to be carried out to examine this further.

4.4.1 Further work

To complete this section of work and be certain of the complexation involved in these compounds, more experimental and modelling needs to be carried out. Experimentally there is more data that can be obtained from the CSA and SSBs of the SS NMR spectra which could aid the final assignment of all of the peaks as well as providing useful information on the complexes formed with the ligand and metals. More techniques can also be used to assign the peaks fully such as MQ-DEPT, which was used for the solution NMR work but now could be applied to the solid state work and 2D ^{13}C-^{13}C INADEQUATE, (Incredible Natural Abundance DoublE QUAntum Transfer Experiment). This technique can determine which signals are arising from neighboring carbons. A study by Ramos et al. [64], which was very similar to the work carried out in this thesis, used the intensity of the peaks in the NMR to determine the number of metal ions present producing that particular peak. This could be employed in this work also in order to help with the stoichiometry data. Extra techniques are needed to determine exactly what is being looked at as there are too many different conformations of ligand and metal to attempt to model them all. Techniques such as electrochemical studies [70], or REDOR spectroscopy could be used as has been before for similar studies [76]. With regards to the modelling, there are many other structures that could

be inputted, mainly the lactone form of ISA, and further stoichiometries of the metal and ISA, especially 1:2 M:ISA.

REFERENCES

[1] Defra, *http://www.defra.gov.uk/environment/radioactivity/mrws/index.htm*, accessed on 27/07/08.

[2] Nirex., *Nirex Safety Assessment research Programme, Proceedings of the Royal Society of Chemistry/Nirex Symposium: The Chemistry of Deep Disposal of Radioactive Waste*, S/98/008 (1998)

[3] Nirex, *The viability of a phased geological repository concept for the long-term management of the UK's radioactive waste*, Nirex Report no. N/122 (2005)

[4] CoRWM, *Managing our radioactive waste safely, CoRWM's recommendations to the government*, CoRWM Doc 700 (2006)

[5] Hicks T.W, Baldwin T.D, Hooker P.J, Richardson P.J, Chapman N.A, Mckinley I.G, Neall F.B., *Concepts for the geological disposal of Intermediate-level radioactive waste*, Galson Sciences Ltd, 0736-1, version 1.1 (2008)

[6] Greenfield B.J., Harrison W.N., Robertson G.P., Somers P.J., Spindler M.W., *Mechanistic Studies of the Alkaline Degradation of Cellulose in Cement*, NSS/R272, AEA-D&R-0219 (1993)

[7] Greenfield B.F., Hurdus M.H., Spindler M.W., Thomason H.P., *The Effects of the Products from the Anaerobic Degradation of Cellulose on the Solubility and Sorption of Radioelement's in the Near Field*, NSS/R376 (1997)

[8] Glaus M.A, Van Loon L.R, Achatz S, Chodura A, Fischer K., *Degradation of cellulosic materials under the alkaline conditions of a cementitious repository for low and intermediate level radioactive waste Part I: Identification of degradation products*, Analytica Chimica Acta, 398, 111 (1999)

[9] Neck V, Altmaier M, Muller R, Bauer A, Fanghanel Th, Kim J.I., *Solubility of crystalline thorium dioxide*, Radiochimica Acta, 91, 253 (2003)

[10] Neck V, Muller R, Bouby M, Altmaier M, Rothe J, Denecke A, Kim J.I., *Solubility of amporphous Th(IV) hydroxide – application of LIBD to determine the solubility product and EXAFS for aqueous speciation,* Radiochimica Acta, 90, 485 (2002)

[11] NuSAC, RWMAC, *Review of the regulation of nuclear safety and the management of radioactive materials and radioactive waste within the United Kingdom ('The NuSAC/RWMAC joint regulatory review'), Structures and principles of the regulation of the nuclear licensed sites HSE,* Health & Safety Executive (2003)

[12] Department of Trade and Industry, *Managing the Legacy, a Strategy for Action,* Presented to Parliament by the Secretary of Trade and Industry by command of her Majesty, cm5552 (2002)

[13] NDA, TECHNICAL NOTE, A Proposed Framework for Stage 4 of the MRWS Site Selection process, Number: 8150715 (2008)

[14] NDA, The 2007 UK Radioactive Waste Inventory, Main Report, Defra/RAS/08.002, NDA/RWMD/004 (2007)

[15] UK Patent Office, *Repository for Radioactive Waste – Vault Backfill,* UK Patent GB 2 295 263 B (1997)

[16] Francis A.J., Cather R., Crossland I.G., *Development of the Nirex Referenc Vault Backfill; report on current status in 1997,* Nirex Report, S/97/014 (1997)

[17] Glasser F.P., *Fundemental aspects of Cement Solidification and Stabilisation,* Journal of Hazardous Materials, 52, 151 (1997)

[18] Aggarwal S, Angus M.J, Ketchen J, *Sorption of Radionuclides onto Specific mineral phases present in repository cements,* AEA Report, NSS/R312, AEA-D&R-0395 (2000)

[19] Proceedings of the Royal Society of Chemistry/UK-Nirex Symposium, *The Chemistry of deep disposal of radioactive waste,* Loughborough University, December (1997)

[20] Baston G.M.N, Berry J.A, Bond K.A, Brownsword M, Linklater C.M., *Effects of Organic Degradation Products on the Sorption of Actinides,* Radiochimica Acta, 58/59, 349 (1992)

[21] Berry J.A, Bond K.A, Ferguson D.R, Pilkington N.J., *Experimental Studies of the Effects of Organic Materials on the Sorption of Uranium and Plutonium,* Radiochimica Acta, 52/53, 201 (1991).

[22] Arthur J.C., *Reactions induced by high energy radiation: Cellulose and cellulose derivatives,* Volume V of High Polymers; 2nd Edition, London, UK, Wiley-Interscience (1971)

[23] David C, Van den Bergh M.A., *Utilisation of Waste Cellulose, II. Gamma irradiation and alkaline hydrolysi,.* Cellulose Chemistry and Technology, 16, 153 (1982)

[24] Greenfield B.F., Roesvear A., Williams S.J., *Review of the Microbiological, Chemical and Radiolytic Degradation of Organic material likely to be present in Intermediate Level and Low Level Radioactive Wastes,* AEA-D&R-0120, DOE/HMIP/RR/91/002 (1990)

[25] Bradshaw S, Gaudie S.C, Greenfield B.F, Long S, Spindler M.W, Wilkins J.D. *Experimental studies on the chemical and radiation decomposition of intermediate level wastes containing organic materials,* UK AEA Report AERE – R 12223, Didcot, UK, UKAEA (1986)

[26] Bradshaw S, Gaudie S.C, Greenfield B.F, Lyon C.E, Rees J.H, Spindler M.W, Wilkins J.D., *Preliminary experimental studies on the chemical and radiation degradation of combustible plutonium contaminated material,* UKAEA Report AERE-R 12223, Didcot, UK, UKAEA (1986)

[27] Rai D, Rao L, Xia Y.X., *Solubility of crystalline calcium isosaccharinate,* Journal of Solution Chemistry, 27, 1109 (1998)

[28] Burns W.G, Lyon C.E, Walters W.S, Wilkins J.D., *α-irradiation of combustible plutonium contaminated material,* UKAEA Report AERE R11696 (1985)

[29] Colasanti R, Coutts D, Pugh SYR, Rosevear A., *Microbiology and radioactive waste disposal; review of the Nirex research programme – January 1989,* Nirex Report NSS/R131, Didcot, UK:Nirex (1990)

[30] Rosevear A., *A Review of national research programmes on the microbiology of radioactive waste disposal,* Nirex Report NSS/R263, Didcot, UK:Nirex (1991)

[31] Askarieh M.M., Chambers A.V., Daniel F.B.D., FitzGerald P.L., Holtom G.J., Pilkington N.J., Rees J.H., *The Chemical and Microbial Degradation of Cellulose in the near field of a repository for radioactive wastes.* Waste Management 20, 93 (2000)

[32] Pilkington N.J., *The Solubility of Technetium in the Near-Field Environment of a Radioacyive Waste Repository,* Journal of Less Common Metals, 161, 203 (1990)

[33] Greenfield B.F, Spindler M.W, Woodwark D.R., *Summary of the effects of organic degradation products on near field radioelement chemistry,* Nirex Report, NSS/R298 (1997)

[34] Bourbon X., Toulhoat P., *Influence of Organic Degradation Products on the Solubilisation of Radionuclides in Intermediate and Low Level Radioactive Wastes,* Radiochimica Acta, 74, 315 (1996)

[35] Blazej A, Kosik M., *Cellulose and its Derivates: Chemistry, Biochemistry and Application,* Ellis Horwood limited, New York (1985)

[36] Theander O., *Advances in Carbohydrate Chemistry and Biochemistry,* R Academic Press, San Diego, 46, 273 (1988)

[37] Ziderman I.I, Belayche J., *Specific Ion Hydroxide Catalysis of the Endwise Depolymerisation of Cellulose,* Journal of Applied Polymer Science, 22, 711 (1978)

[38] Whistler R.L, BeMiller J.N., *Alkaline Degradation of Polysaccharides,* Advanced Carbohydrate Chemistry, 13, 289 (1958)

[39] Pavasars I, Hagberg J, Boren H, Allard B., *Alkaline Degradation of Cellulose: Mechanisms and Kinetics,* Journal of Polymers and the Environment, 11, 39 (2003)

[40] Van Loon L.R., Glaus M.A., Laube A., Stallone S., *Journal of Environmental Polymer Degradation,* 7, 41 (1999)

[41] Pavasars I., *Characterisation of Organic Substances in Waste Materials under Alkaline Conditions,* Linkoping Studies in Arts and Sciences, 196 (1999)

[42] Pourchez J, Govin A, Grosseau P, Guyonnet R, Guilhot B, Ruot B., *Alkaline stability of cellulose ethers and impact of their degradation products on cement hydration,* Cement and Concrete Research, 36, 1252 (2006)

[43] Greenfield B.F., Hurdus M.H., Pilkington N.J., Spindler M.W., Williams S.J., *Degradation of cellulose in the near field of a radioactive waste repository,* Materials Resource Society Symposium Proceedings 333 (1994)

[44] Motellier S, Richet C, Merel P., *Analysis of cellulose degradation products by capillary electrophoresis,* Journal of Chromatography A, 804, 363 (1998)

[45] Yun Yang B, Montgomery R., *Alkaline degradation of glucose: effect of initial concentration of reactants,* Carbohydrate research, 280, 27 (1996)

[46] Knill C, Kennedy J.F., *Degradation of cellulose under alkaline conditions,* Carbohydrate Polymers, 51, 281 (2003)

[47] Ilett D.J., Pilkington N.J., Tweed C.J., *Complexation of Radionuclides,* Nirex Science report S/98/008 (1998)

[48] Malin S, Berg M, Ifwer K, Sjoblom R, Ecke H., *The effect of isosaccharinic acid (ISA) on the mobilization of metals in municipal solid waste incineration (MSWI) dry scrubber residue,* Journal of Hazardous Materials, 144, 477 (2007)

[49] Allard S., *Investigations of α-D-isosaccharinate: Fundamental Properties and Complexation,* PhD Thesis, Department of Chemical and Biological Engineering, Chalmers University of Technology (2005)

[50] Sowden J.C., *The Saccharinic Acids,* Advanced Carbohydrate Chemistry, 12, 35 (1957)

[51] Ekberg S, Ekberg C, Albinsson Y., *Characterisation of α-Isosaccharinic Acid: Lactone and Carboxylic Conformations,* Journal of Solution Chemistry, 33, 5 (2004)

[52] Cho H, Rai D, Hess N.J, Xia Y, Rao L., *Acidity and Structure of Isosaccharinate in Aqueous Solution: A Nuclear Magnetic Resonance Study,* Journal of Solution Chemistry, 32, 8, 691 (2003)

[53] Van Loon L.R, Glaus M.A, Vercammen K., *Solubility Products of Calcium Isosaccharinate and calcium gluconate,* Acta Chemica Scandinavica, 53, 235 (1999)

[54] Vercammen K, Glaus M.A, Van Loon L.R., *Complexation of Calcium by α-isosaccharinic acid under alkaline conditions,* Acta Chimica Scandinavica, 53, 241 (1999)

[55] Bontchev R.P, Moore R.C., *Crystal structure of ammonium isosaccharate and aqueous solubility of ammonium and sodium isosaccharates,* Carbohydrate Research, 339, 2811 (2004)

[56] Rai D, Hess N.J, Xia Y, Rao L, Cho H.M, Moore R.C, Van Loon L.R., *Comprehensive Thermodynamic Model Applicable to Highly Acidic To Basic Conditions for Isosaccharinate Reactions with Ca(III) and Np(IV),* Journal of Solution Chemistry, 32, 8 (2003)

[57] Pointeau I, Hainos D, Coreau N, Reiller P., *Effect of Organics on selenite uptake by cementitious materials,* Waste Management, 26, 733 (2006)

[58] Van Loon L.R, Glaus M.A, Stallone S, Laube A., *Sorption of isosaccharinic acid, a cellulose degradation product, on cement,* Environmental Science and Technology, 31, 1243 (1997)

[59] Tits J, Wieland E, Bradbury M.H, Schaible A., *The uptake of Eu(III) and Th(IV) by calcite under hyperalkaline conditions,* PSI Report, PSI Bericht No 02-03 (2002)

[60] Mompean F.J, Illemassene M, Perrone J., *Chemical thermodynamics of compounds and complexes of U, Np, Pu, Am, Tc, Se and Zr with selected organic ligands,* Chemical Thermodynamics Volume 9, Elsevier (2005)

[61] Warwick P, Evans N, Hall T, Vines S., *Stability constants of uranium(IV)-α-isosaccharinic acid and gluconic acid complexes,* Radiochimica Acta, 92, 897 (2004)

[62] Warwick P, Evans N, Hall T, Vines S., *Complexation of Ni(II) by α-isosaccharinic acid and gluconic acid from pH 7 to 13,* Radiochimica Acta, 91, 233 (2003)

[63] Rai D, Rao L, Moore D.A., *The influence of Isosaccharinic Acid on the Solubility of Np(IV) Hydrous Oxide,* Radiochimica Acta, 83, 9 (1998)

[64] Ramos M.L, Caldeira M.M, Gil V.M.S., *NMR spectroscopy study of the complexation of D-gluconic acid with tungsten (VI) and molybdenum (VI),* Carbohydrate research, 304, 97 (1997)

[65] Carper W.R, Coffin D.B., *NMR Studies of Paramagnetic Metal Ion Interactions with Gluconate and 1,5-Glucanolactone,* Inorganica Chimica Acta, 167, 261 (1990)

[66] Bailey G.D., *NMR Investigations of metal-gluconate interactions,* PhD Thesis, Wichita State University (1991)

[67] Allard S, Ekberg C., *Complexing Properties of α-Isosaccharinate: Stability Constants, Enthalpies and Entropies of Th-complexation with Uncertainty Analysis,* Journal of Solution Chemistry, 35, 1173 (2006)

[68] Gajda T, Gyurcsik B, Jakusch T, Burger K, Henry B, Delpuech J.J., *Coordination chemistry of polyhydroxy acids: role of the hydroxyl groups,* Inorganica Chimica Acta, 275-276 (1998)

[69] Vicedomini M, Coccioli F., *On the dissociation of gluconate ions and their complex formation with lead (II) in alkaline solution,* Journal of Inorganic Nuclear Chemistry, 40, 2106 (1978)

[70] Bodini M, Willis L.A, Riechel T.L, Sawyer D.T., *Electrochemical and Spectroscopic studies of manganese(II), -(III), and –(IV) gluconate complexes. 1.Formulas and oxidation-reduction stoichiometry,* Inorganic Chemistry, 15 (1976)

[71] Rao L, Garnov A.Y, Dhupant R, Xia Y, Moore R.C., *Protonation and complexation of isosaccharinic acid with U(VI) and Fe(III) in acidic solutions: potentiometric and calorimetric studies,* Radiochimica Acta, 92, 575 (2004)

[72] Evans N.D.M., *Studies on metal alpha-isosaccharinic acid complexes in chemistry,* PhD Thesis, Loughborough University (2003)

[73] Tits J, Wieland E, Bradbury M.H., *The effect of isosaccharinic acid and gluconic acid on the retention of Eu(III), Am(III) and Th(IV) by calcite,* Applied Geochemistry, 20, 2082 (2005)

[74] Hagberg J, Duker A, Karlsson S., *Determination of dissociation Constants of Low Molecular Weight Organic Acids by Capillary Zone Electrophoresis and Indirect UV Detection,* Chromatographia, 56, 9/10 (2002)

[75] Duer M.J., *Solid State NMR Spectroscopy, principles and applications,* Oxford: Blackwell Science (2002)

[76] Chen Y.Y, Luo S.Y, Hung S.C, Chan S.I, Tzou D.L.M., *^{13}C Solid-state NMR chemical shift anisotropy analysis of the anomeric carbon in carbohydrates,* Carbohydrate Research, 340, 723 (2005)

[77] Tang H, Belton P.S, Davies S.C, Hughes D.L., *Solid State NMR and X-ray diffraction studies of α-D-galacturonic acid monohydrate,* Carbohydrate Research, 330, 391 (2001)

[78] Harper J.K, Grant D.M., *Enhancing Crystal-Structure Prediction with NMR Tensor Data,* Crystal Growth and Design, 6, 2315 (2006)

[79] Kaiser E, Simpson A.J, Dria K.J, Sulzberger B, Hatcher P.G, *Solid-State and Multidimensional Solution-State NMR of Solid Phase Extracted and Ultrafiltered Riverine Dissolved Organic Matter,* Environmental Science and Technology, 37, 2929 (2003)

[80] Diaz M, Jaballas J, Arias J, Lee H, Onak T., *^{13}C NMR Studies on Carboranes and Derivatives: Experimental/Calculational Correlations*, Journal of the American Chemical Society, 118, 4405 (1996)

[81] Zhang P, Klymachyov A.N, Brown S, Ellington J.G, Grandinetti P.J., *Solid State ^{13}C NMR investigations of the glycosidic linkage in α-α' trehalose*, Solid State Nuclear Magnetic Resonance, 12, 221 (1998)

[82] Hichung M, *Equilibrium Ultrafiltration of Hydrolyzed Thorium(IV) Solutions*, Bull. Korean Chemical Society, 10, 3, 270 (1989)

[83] Hyde E.K., National Acadamy of Sciences, National Research Council, *The Radiochemistry of Thorium*, Nuclear Science Series, U.S. Atomic Energy Commission, NAS-AS 3004 (1960)

[84] Dhanpat R, Felmy A.R., Moore D.A., Mason M.J., *The solubility of Th(IV) and U(IV) hydrous oxides in concentrated NaHCO3 and Na2CO3 solutions*, Materials Research Society Symposium Proceedings, 353 (Scientific Basis for Nuclear Waste Management XVIII, Pt 2), 1143-50 (1995)

[85] Neck V, Kim J.I., *Solubility and hydrolysis of tetravalent actinides*, Radiochimica Acta, 89, 1 (2001)

[86] Wierczinski B, Helfer S, Ochs M, Skarnemark G, *Solubility measurements and sorption studies of thorium in cement pore water*, Journal of Alloys and Compounds, 271-273, 272 (1998)

[87] Osthols E, Bruno J, Grenthe I, *On the influence of carbonate on mineral dissolution: III. The solubility of microcrystalline ThO$_2$ in CO$_2$-H$_2$O media*, Geochimica Cosmochimica Acta, 58, 613 (1994)

[88] Vercammen K, Glaus M.A, Van Loon L.R, *Evidence for the existence of Complexes between Th(IV) and α-Isosaccharinic Acid under Alkaline Conditions*, Radiochimica Acta, 84, 221 (1999)

[89] Kirk-Othmer Encyclopedia of Chemical Technology, *Thorium and Thorium Compounds*, John Wiley & Sons, Inc (2001)

[90] Holmes L, Pilvio R, *Determination of thorium in environmental and workplace materials by ICP-MS*, Applied Radiation and Isotopes, 53, 63 (2000)

[91] Gaussian.com, *Gaussian Product Information*, http://www.gaussian.com/g_brochures/g03_new.htm, accessed on 15/12/2006.

[92] Whistler R.L., BeMiller J.N., *α-D-Isosaccharino-1,4-Lactone, in Methods in Carbohydrate Chemistry Vol 2: Reactions of Carbohydrates*, Wolfrom M.L., Bemiller J.N., Editors., Wiley: New York (1963)

[93] Hallum R., *Analysis of Isosaccharinic Acid*, Loughborough University Report (2006)

[94] Cowper M, Myatt B.J., Williams S.J., *Further Studies of Plutonium Uptake by Non-aqueous Phase Liquids*, Serco Assurance Report, SA/ENV-0656 (2004)

[95] Van Loon L.R, Glaus M.A, Stallone S, Laube A., *Sorption of Isosaccharinic Acid, a Cellulsoe Degradation Product, on Cement*, Environmental Science and Technology, 31, 4, 1243 (1997)

[96] Ziderman I, Bel-Ayche J., *Specific hydroxide ion catalysis of the endwise depolymerisation of cellulose*, Journal of Applied Polymer Science, 22, 711 (1978)

[97] Haas D.W, Hrutfiord B.F, Sarkanen K.V., *Kinetic study on the alkaline degradation of cotton hydrocellulose*, Journal of Applied Polymer Science, 11, 587 (1967)

[98] Van der Lee J., *A Users Guide to CHESS, Another Speciation and Surface Complexation Computor Code*, Ecloe des Mines de Paris, Fontainebleau, France (1998)

[99] Ziemniak S.E, Goyette M.A, Combs K.E.S,. *Cobalt (II) Oxide Solubility and Phase Stability in Alkaline Media at Elevated Temperatures*, Journal of Solution Chemistry, 28, 7, 809 (1999)

[100] Rothe J, Denecke M.A, Neck V, Muller R, Kim J.I., *XAFS Investigation of the Structure of Aqueous Thorium(IV) Species, Colloids and Solid Thorium(IV) Oxide/Hydroxide,* Inorganic Chemistry, 41, 249 (2002)

[101] Prasad R, Dey A.K., *Electrometric Studies on the Precipitation of Thorium Hydroxide: Part II. Effect of Age on the pH of Thorium Chloride during the Progressice addition of Sodium Hydroxide,* Kolloid-Zeitschrift and Zeitschrift fur Polymere, Band 184. Heft 2 (1961)

[102] Marshall P.S, Leavens B, Heudi O, Ramirez-Molina C., *Liquid chromatography coupled with inductively coupled plasma mass spectrometry in the pharmaceutical industry: selected examples,* Journal of Chromatography A, 1056, 3 (2004)

[103] Evans N.D.M.E, Heath C, Edgar M., *An NMR Study of the Complexation of Various Metals with Gluconic and Isosaccharinic acids,* Report No. LBORO/NMR/NDME/1 (2006)

[104] Foresman J.B, Frisch A., *Exploring Chemistry with Electronic Structure Methods,* second edition, Gaussian Inc (1993)

[105] Borsari M., *Cadmium: Inorganic & Coordination chemistry,* Encyclopaedia of Inorganic Chemistry, University of Modena, Modena Italy

[106] Shannon R.D., *Revised effective ionic radii and systematic studies of interatomic distances in halides and chalcogenides,* Acta Crystallographica Section A, 32, 751 (1976)

[107] Chung K.H, Moon C.H., *Cadmium-113 nuclear magnetic resonance studies of cadmium(II)-carboxylate complexes in aqueous solution,* Journal of Chemical Society Dalton Transactions, 75 (1996)

[108] Hajos P, Nagy L., *Retention behaviours and separation of carboxylic acids by ion-exchange chromatography,* Journal of Chromatography B, 717, 27 (1998)

[109] Tanaka K, Chikara H, Hu W, Hasebe K., *Separation of carboxylic acids on a weakly acidic cation-exchange resin by ion-exclusion chromatography,* Journal of Chromatography A, 850, 187 (1999)

[110] Narebska A, Staniszewski M., *Separation of Carboxylic acids from Carboxylates by Diffusion Dialysis,* Separation Science and Technology, 43, 490 (2008).

[111] Schmitt-Kopplin Ph, Fischer K, Freitag D, Kettrup A., *Capillary electrophoresis for the simultaneous separation of selected carboxylated carbohydrates and their related 1,4-lactones,* Journal of Chromatography A, 807, 89 (1998)

Contents of Appendices

List of Figures

List of Tables

Appendix 1

1.1. *ISA Characterisation*

1.1.1. FTIR

Figure 1 FTIR Spectrum of ISA

Table 1 Peaks from the FTIR analysis of ISA

Major peaks (1/cm)	Corresponding functional groups
3296.1	O-H stretch
2920	C-H stretch
1596	Carboxylate salt C=O
1565.1	
1438.8	
1299	Carboxylate salt C=O
1220.9	
1116.7	Alcohol C-O
1069.5	" "
1025.1	" "
996.2	

1.1.2.   HPLC

The retention time for the ISA peak was at 4.55 minutes. The extra peak in the chromatogram at 3.5 minutes was also in the blank but as the retention times were not interfering this was not seen to be a problem.
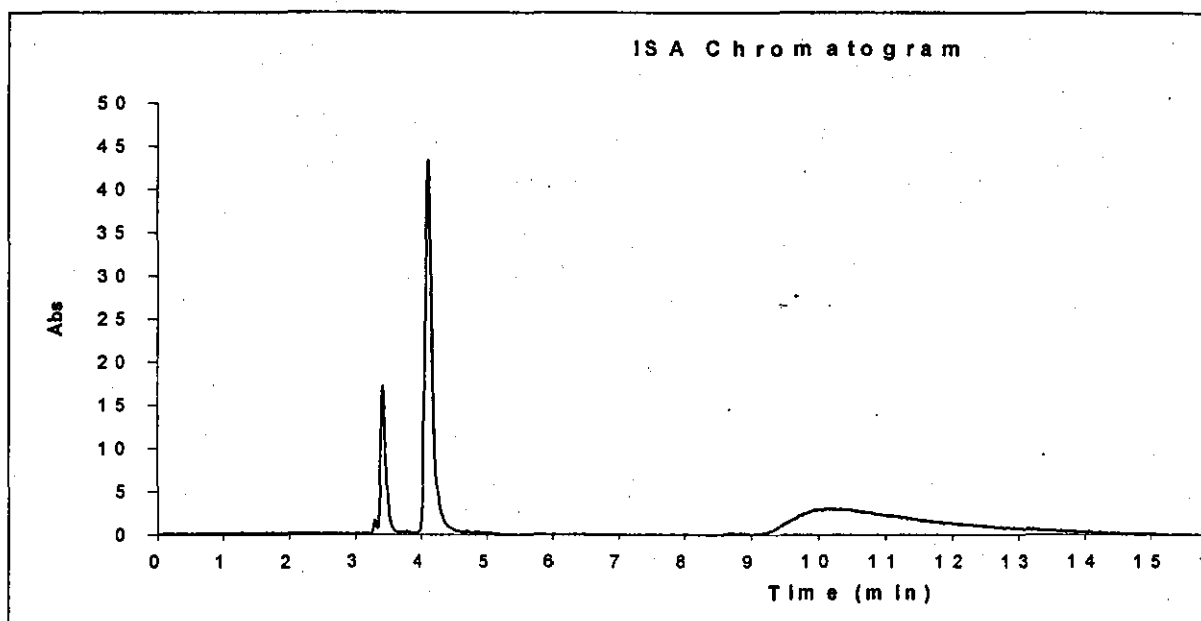
Figure 2 Chromatogram from the HPLC analysis of ISA. The absorbance shown is milli absorbance.

1.1.3.   NMR

The carbons and hydrogens in the ISA were numbered as shown in figure 3.
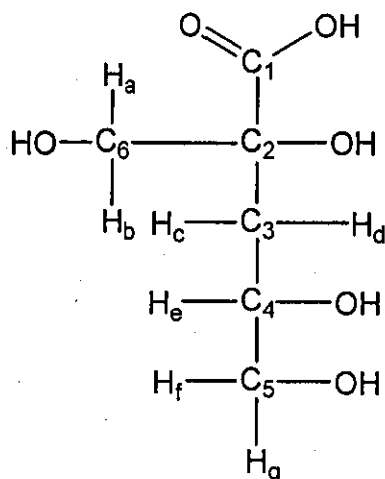
Figure 3 Isosaccharinic acid in the straight chain form

Table 2 Table of proton chemical shifts from the proton NMR analysis of ISA

Hydrogen	Shift (ppm)
a and b	3.577-3.513, 3.379-3.408
c and d	1.690-1.746, 1.533-1.581
e	3.779-3.721 multiplet
f and g	3.474-3.513, 3.306-3.353

Table 3 Table of carbon chemical shift values from the ^{13}Carbon NMR analysis of ISA

Carbon	Shift (ppm)
1	179.935
2	77.476
3	37.616
4	68.315
5	65.977
6	67.823

Figure 4 ^{13}C DEPT Spectra for ISA

Figure 5 Proton NMR Spectra for ISA

Appendix 2

1.2.   CDP Characterisation – Ca(OH)₂, NRVB and PCM

1.2.1.   CDP using NRVB

The following graphs were from an investigation testing the loadings of the CDP on

chromatograms produced so they were analysed on a different day to previous data,

new standard retention times can be seen below.

**Table 4 New Retention times of standards as run on a different day to previous
analysis**

Standard	Retention time
Formic Acid	3.502
ISA	3.608
Lactic Acid	4.208
Acetic Acid	4.643
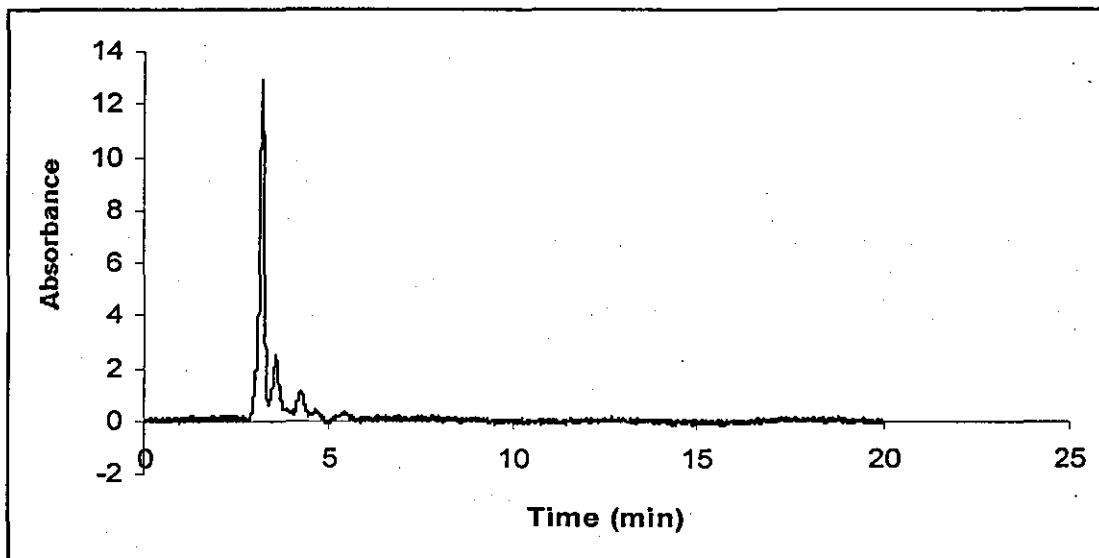
**Figure 6 HPLC Chromatogram of the 1% CDP sample used in the solubility
experiments. Prepared in the presence of NRVB. The absorbance shown is milli
absorbance.**

Table 5 Table of peak retention times and areas in the 1% CDP sample made using NRVB grout

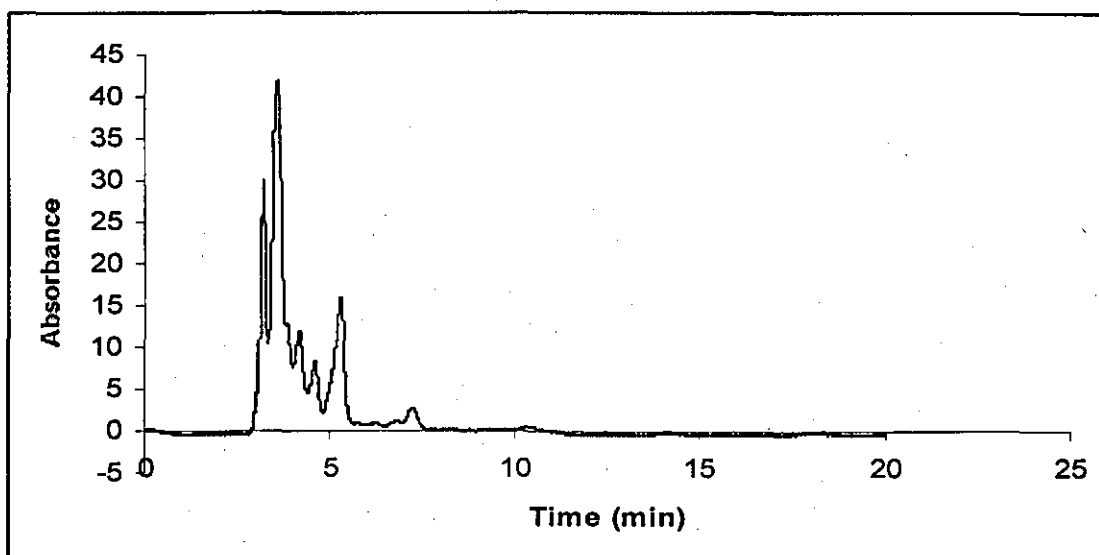| Retention time	Area (mAu*s)
3.17	118.00
3.55	30.74
4.24	10.12
4.66	3.10
5.40	7.31
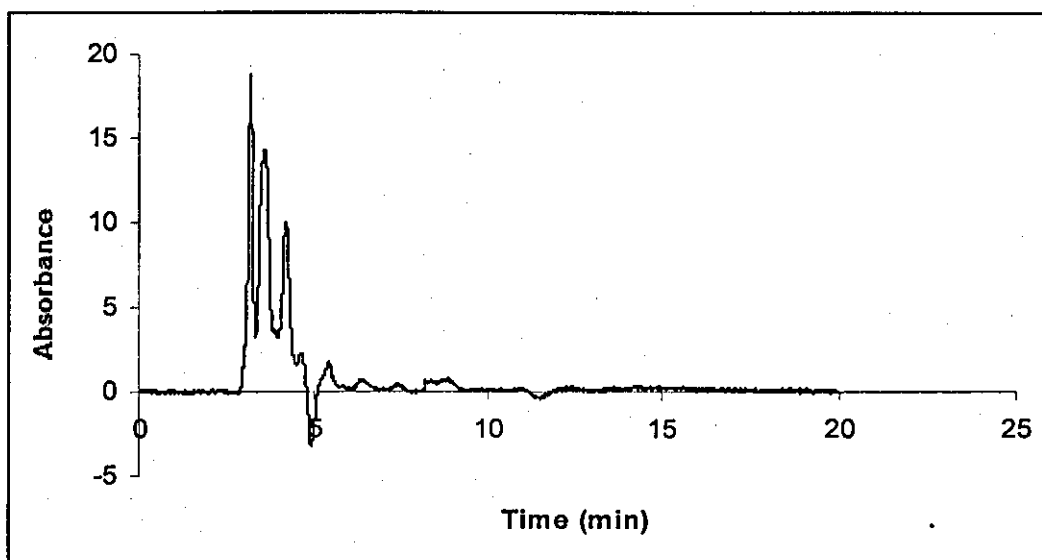
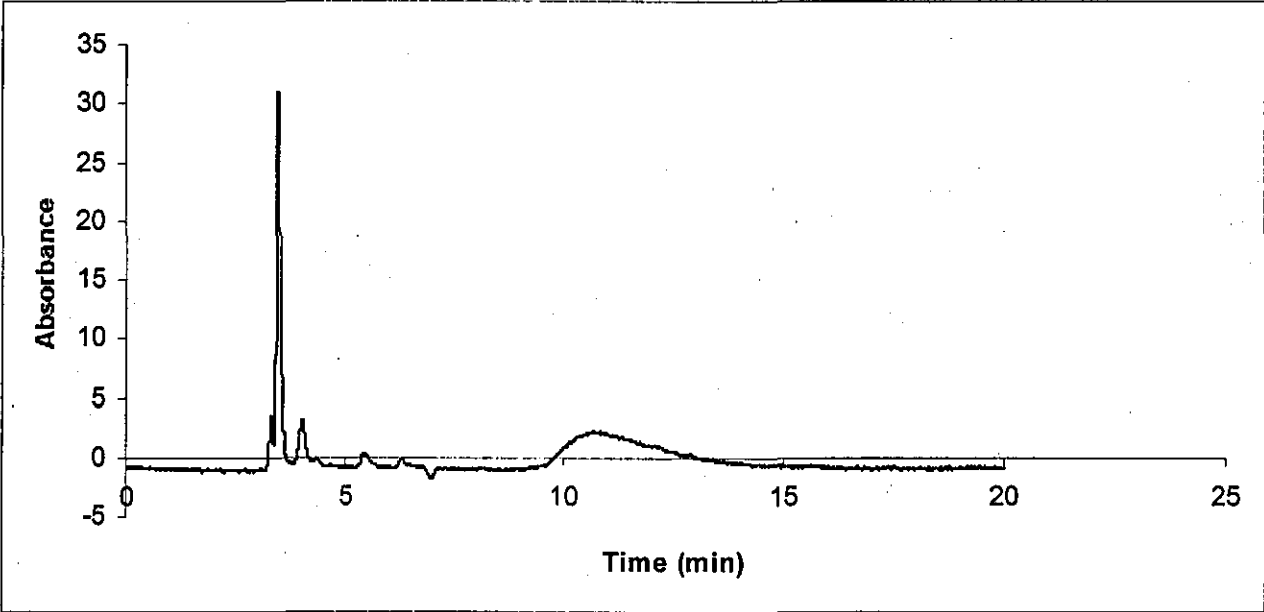**Figure 7 HPLC Chromatogram of the 10% CDP sample used in the solubility experiments. Prepared using NRVB. The absorbance shown is milli absorbance.**

Table 6 Table of peak retention times and areas in the 10% CDP sample made using NRVB grout

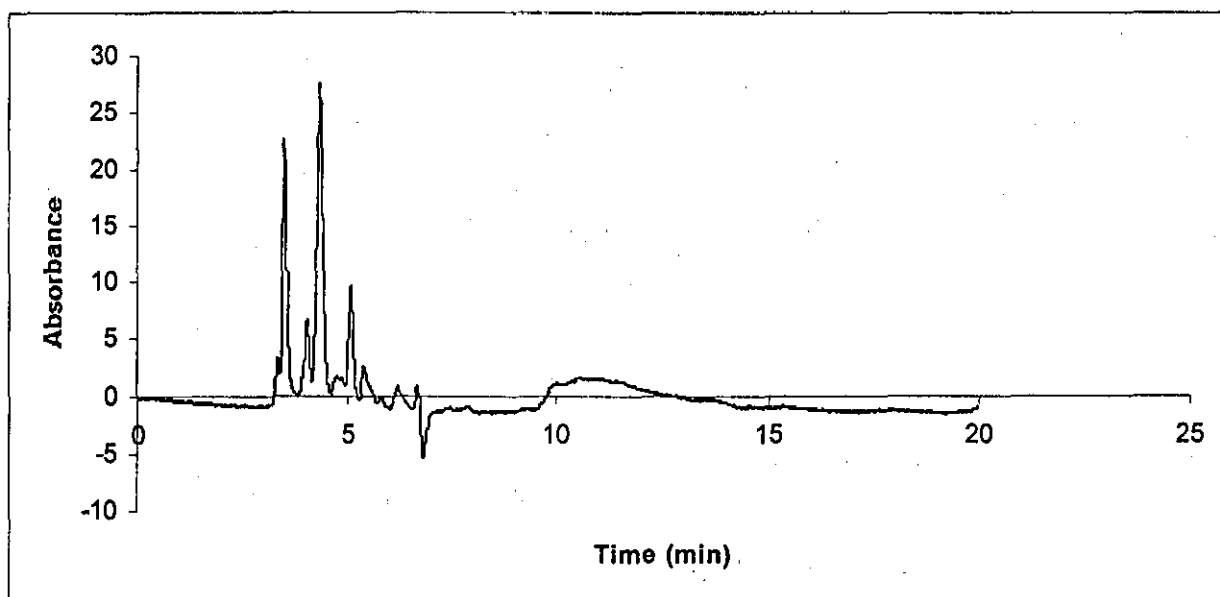| Retention time	Area (mAu*s)
3.16	179.91
3.59	264.41
3.79	48.19
4.17	142.87
4.61	22.12
5.39	28.12
6.40	14.19
7.36	4.83
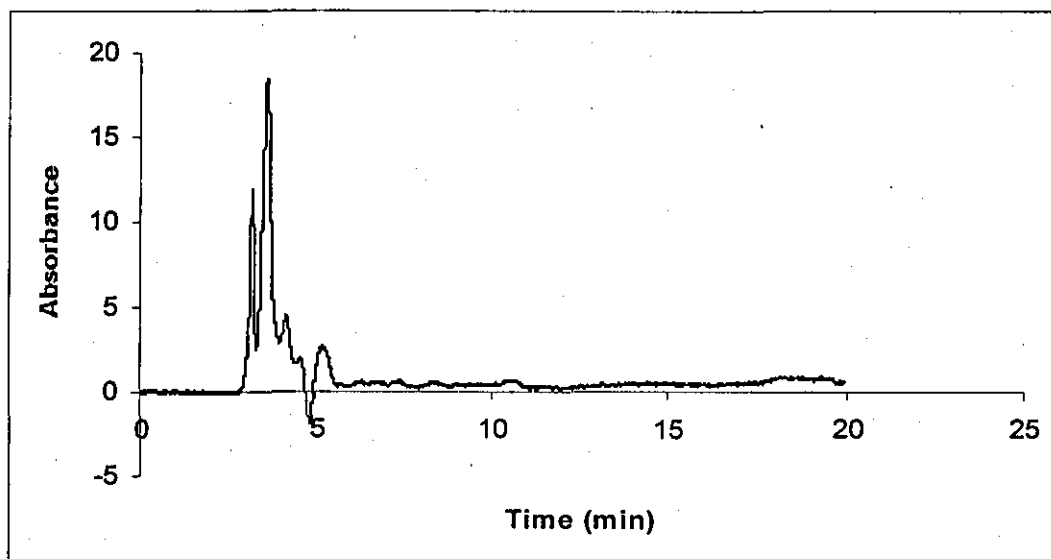
Figure 8 HPLC Chromatogram of the 20% CDP sample used in the solubility experiments, NRVB. The absorbance shown is milli absorbance.

Table 7 Table of peak retention times and areas in the 20% CDP sample made using NRVB grout

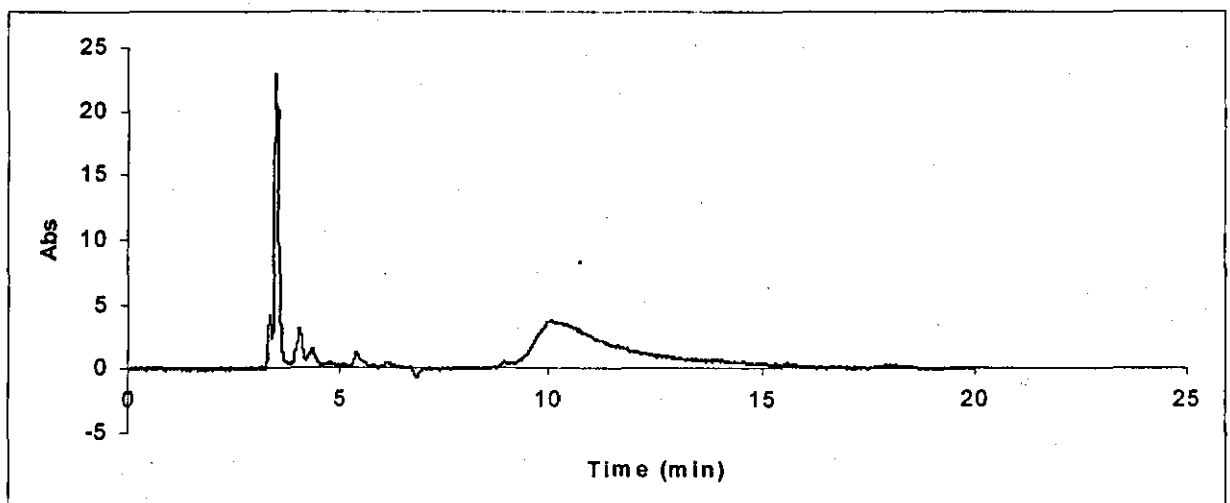| Retention time	Area (mAu*s)
3.169	117.94
3.59	327.89
4.12	76.45
4.52	19.24
5.15	49.36
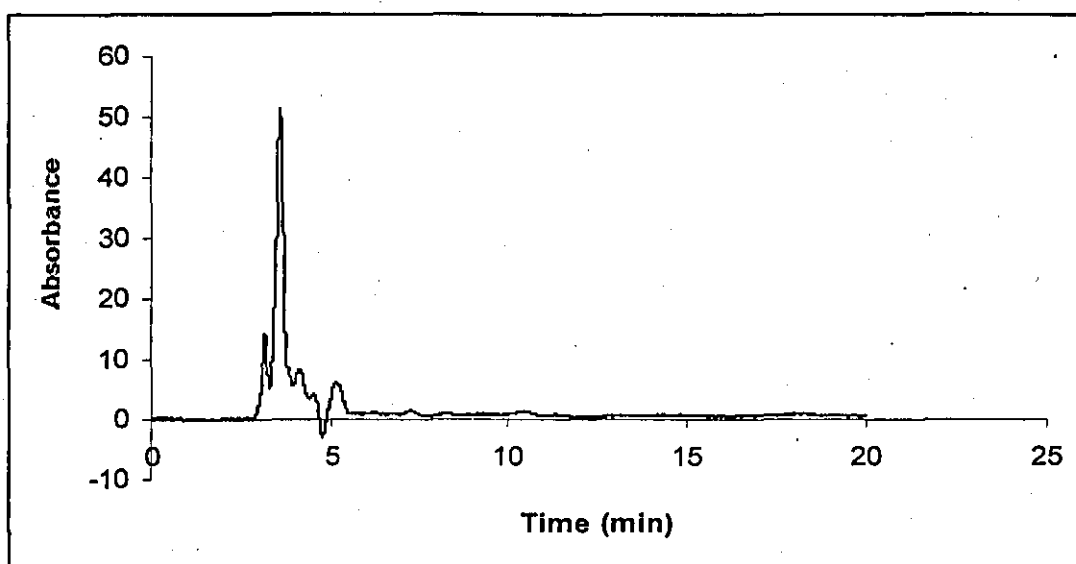
Figure 9 HPLC Chromatogram of the 50% CDP sample used in the solubility experiments. Prepared using NRVB. The absorbance shown is milli absorbance.

Table 8 Table of peak retention times and areas in the 50% CDP sample made using NRVB grout

Retention time	Area (mAu*s)
3.16	172.85
3.59	828.68
4.11	131.52
4.53	46.00
5.15	109.24

Figure 10 HPLC Chromatogram of the 100% CDP sample used in the solubility experiments. Prepared using NRVB. The absorbance shown is milli absorbance.

Table 9 Table of peak retention times and areas in the 100% CDP sample made using NRVB grout

Retention time	Area (mAu*s)
3.16	303.05
3.53	900.22
3.83	9.98
4.14	196.36
4.56	126.90
5.25	298.91
5.73	3.94
6.19	5.94
6.76	6.05
7.20	53.58

1.2.2.   CDP using Ca(OH)$_2$

Table 10 Table of peak retention times and areas in the 10% CDP sample made using Ca(OH)$_2$, batch 1

Retention time	Area (mAu*s)
3.30	31.34
3.46	262.77
4.33	476.28
4.64	38.67
4.81	26.37
5.38	61.93
5.53	15.05
6.27	28.74
6.49	9.70

Figure 11 HPLC Chromatogram of the 1% CDP sample used in the solubility experiments, batch 1, prepared using Ca(OH)$_2$. The absorbance shown is milli absorbance.

Table 11 Table of peak retention times and areas in the 1% CDP sample made using Ca(OH)₂ batch 1

Retention time	Area (mAu*s)
3.31	23.68
3.46	211.76
4.02	35.07
4.35	3.48
5.44	14.42
6.32	5.54
10.67	151.41

Figure 12 HPLC Chromatogram of the 10% CDP sample used in the solubility experiments, batch 2, Ca(OH)₂. The absorbance shown is milli absorbance.

Table 12 Table of peak retention times and areas in the 10% CDP sample made using Ca(OH)$_2$ batch 2

Retention time	Area (mAu*s)
3.34	19.66
3.47	159.19
4.02	52.89
4.33	268.12
4.74	12.42
4.85	12.54
5.07	80.07
5.39	31.60
5.55	1.12
5.77	4.65
6.21	24.38
6.68	9.16

Figure 13 HPLC Chromatogram of the 1% CDP sample used in the solubility experiments, batch 2, Ca(OH)$_2$. The absorbance shown is milli absorbance.

Table 13 Table of peak retention times and areas in the 1% CDP sample made using Ca(OH)₂ batch 2

Retention time	Area (mAu*s)
3.35	22.55
3.49	151.80
3.94	0.81
4.04	22.13
4.35	13.08
4.74	1.19
5.41	12.03
6.13	4.56

1.2.3.   CDP using PCM Grout
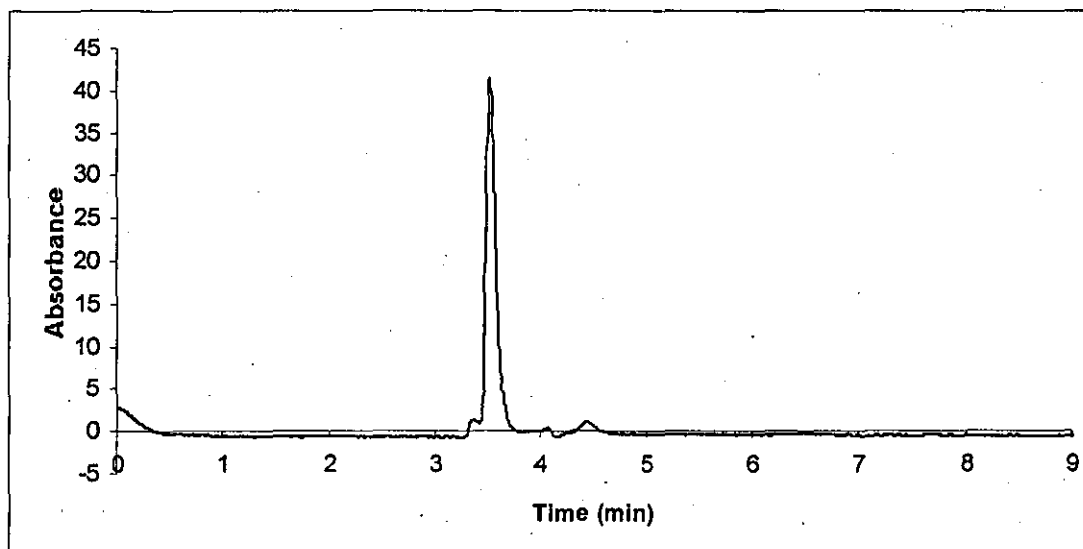
Figure 14 HPLC Chromatogram of the 1% CDP sample using PCM grout (there were no more species present after 8 minutes which is why the scale of the graph is less). The absorbance shown is milli absorbance.

Table 14 Table of peak retention times and areas in the 1% CDP sample made using PCM grout

Retention time	Area (mAu*s)
3.37	9.10
3.52	272.93
4.06	5.60
4.31	3.35
4.43	18.17
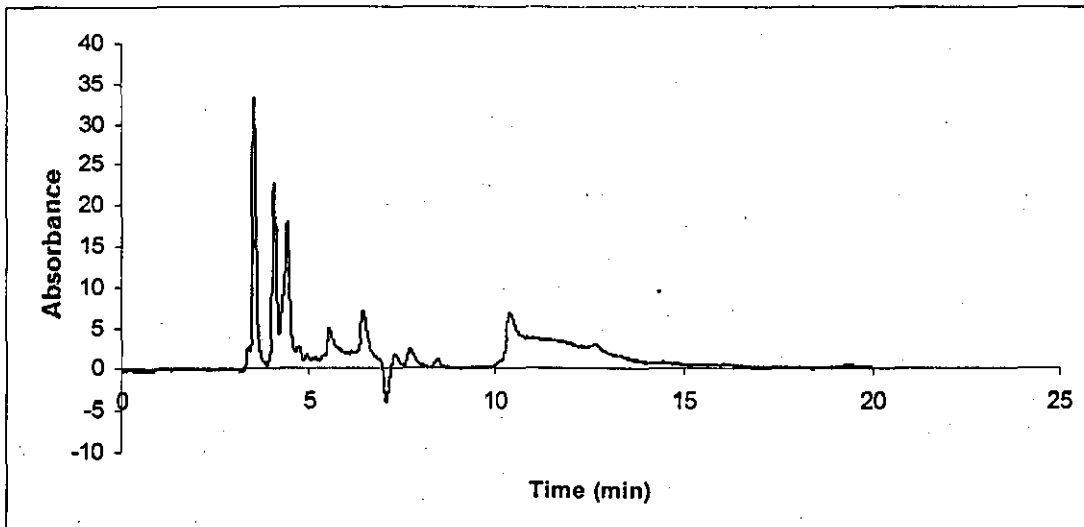
Figure 15 HPLC Chromatogram of the 20% CDP sample using PCM grout. The absorbance shown is milli absorbance.

Table 15 Table of peak retention times and areas in the 20% CDP sample made using PCM grout

Retention time	Area (mAu*s)
3.38	20.67
3.51	228.19
4.07	166.94
4.40	197.25
4.70	14.94
4.94	4.43
5.13	2.78
5.41	3.18
5.55	46.37
6.43	63.91
7.27	10.03
7.71	25.42
8.40	12.42
10.39	123.7128
12.65	13.78876
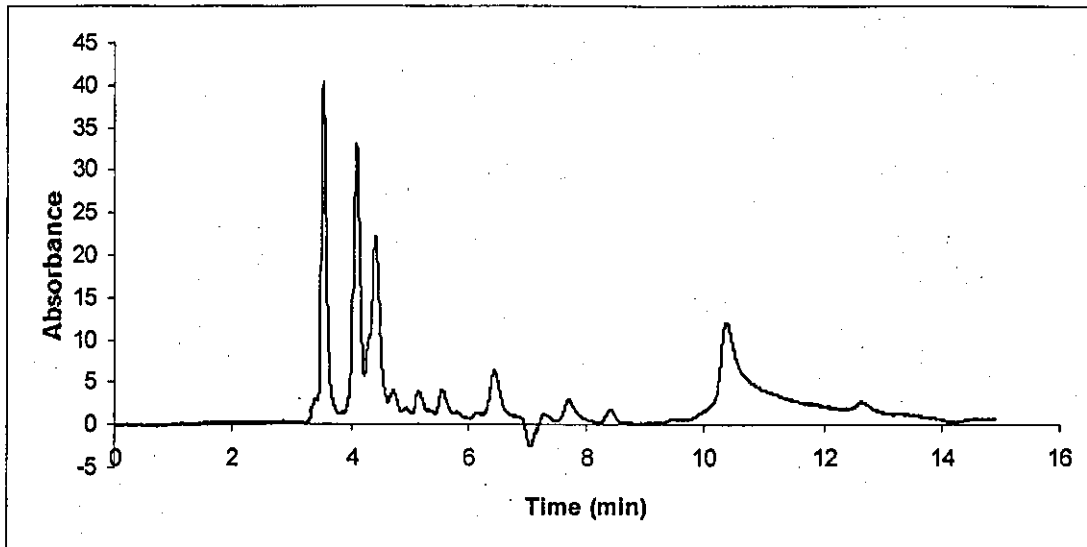
Figure 16 HPLC Chromatogram of the 50% CDP sample using PCM grout. The absorbance shown is milli absorbance.

Table 16 Table of peak retention times and areas in the 50% CDP sample made using PCM grout

Retention time	Area (mAu*s)
3.42	14.65
3.52	269.79
4.08	232.10
4.28	5.59
4.41	232.59
4.71	19.12
4.95	2.21
5.15	19.62
5.33	1.98
5.55	20.58
6.16	5.08
6.44	61.20
7.27	6.07
7.71	37.75
8.423373	19.13161
10.37405	291.3674
12.6475	16.24944
3.420132	14.65321
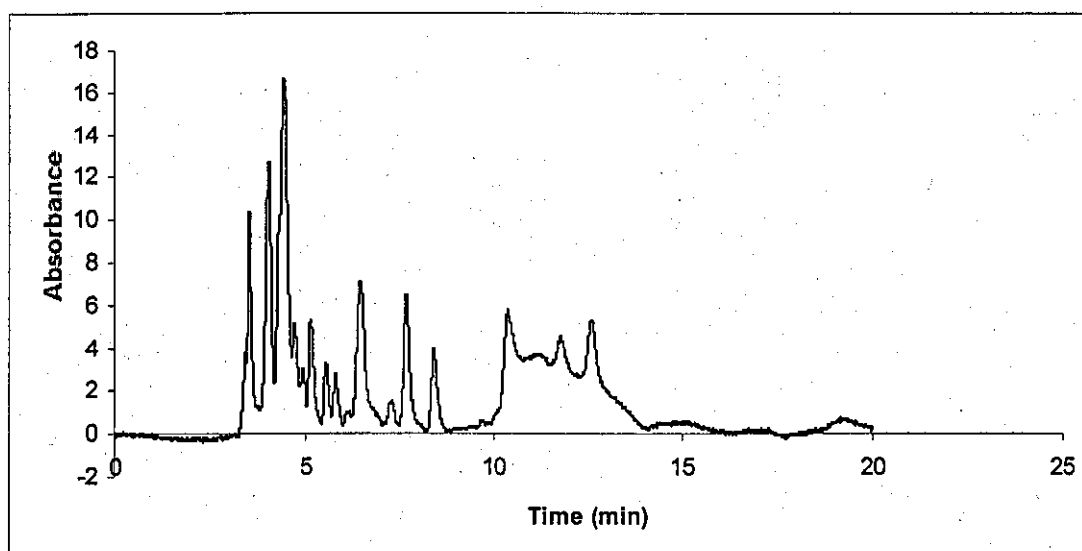
Figure 17 HPLC Chromatogram of the 100% CDP sample using PCM grout. The absorbance shown is milli absorbance.

Table 17 Table of peak retention times and areas in the 100% CDP sample made using PCM grout

Retention time	Area (mAu*s)
3.41	22.80
3.51	85.56
4.02	137.80
4.30	2.18
4.41	262.68
4.70	54.07
5.13	52.51
5.53	27.90
5.78	22.75
6.12	10.43
6.44	97.90
6.78	6.51
7.25	8.48
7.66	66.10
8.38	43.89
10.37	52.20
11.76	23.74
12.60	55.36

Appendix 3

1.3.   Thorium solubility Studies

1.3.1.   Liquid scintillation experiments

Table 18 Thorium counts in water (acidic conditions), batch 1 – Fluka, batch 2, Hopkins and Williams

Solution	CPMA	CPMB
Water	58.13	16.97
Water	57.52	17.08
Average	57.83	17.03
Th2a in water	4734.43	3916.51
Th2b in water	4798.09	4002.87
Average	4766.26	3959.69
Th1a in water	1252.32	811.89
Th1b in water	1032.82	693.60
Average	1142.57	752.75
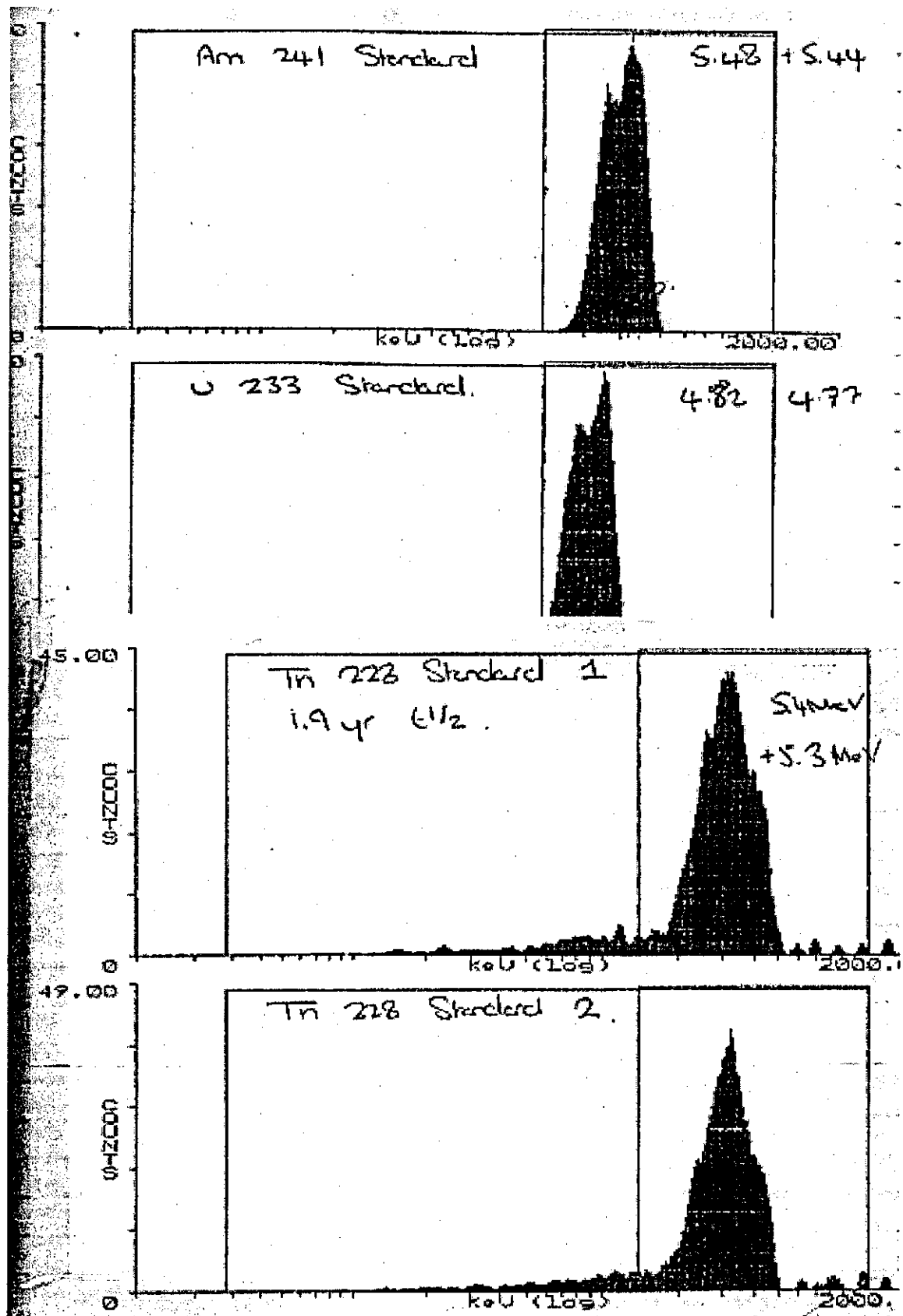
Figure 18 Standards from top to bottom of americium, uranium and thorium to try and identify the peaks in the thorium spectra

Table 19 Table of thorium in NaOH counts

Solution	CPMA	CPMB
Th2a in NaOH	68.18	25.25
Th2b in NaOH	63.95	22.05
Average	66.07	23.65
Th1a in NaOH	61.33	20.83
Th1b in NaOH	59.78	18.12
Average	60.56	19.48

Table 20 Table of thorium in Ca(OH)$_2$ counts

Solution	CPMA	CPMB
Th2a in Ca(OH)$_2$	1386.15	987.95
Th2b in Ca(OH)$_2$	1400.70	1000.84
Average	1393.43	994.40
Th1a in Ca(OH)$_2$	683.40	452.66
Th1b in Ca(OH)$_2$	686.08	452.54
Average	684.74	452.60

Table 21 Thorium in sodium carbonate and sodium chloride – all with batch 2 thorium

Solution	CPMA	CPMB
Th2a in NaCl	72.43	27.33
Th2b in NaCl	76.63	28.10
Average	74.53	27.72
Th2a in Na$_2$CO$_3$	46.00	12.00
Th2b in Na$_2$CO$_3$	69.12	25.77
Average	57.56	18.89

Table 22 Thorium in NRVB

Solution	CPMA	CPMB
Th2a in NRVB	2008.62	730.86
Th2b in NRVB	2104.41	795.80
Average	2056.52	763.33
Th1a in NRVB	1531.04	347.55
Th1b in NRVB	1597.60	377.96
Average	1564.32	362.76
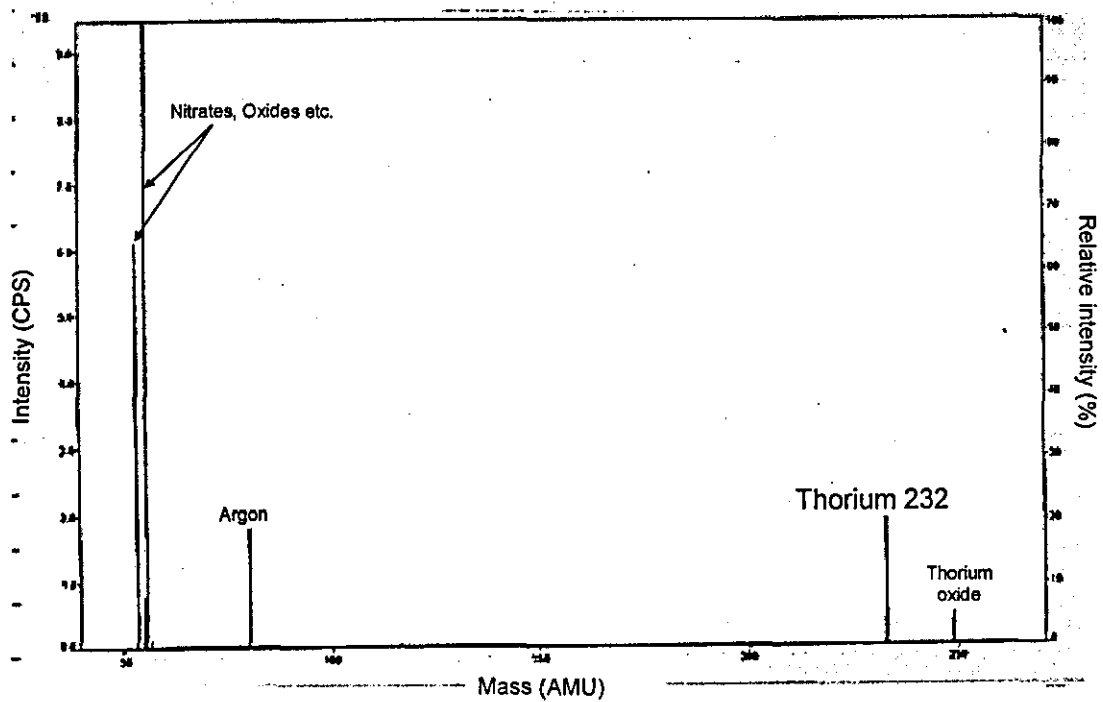
Figure 19 ICP-MS of batch 2 thorium in water
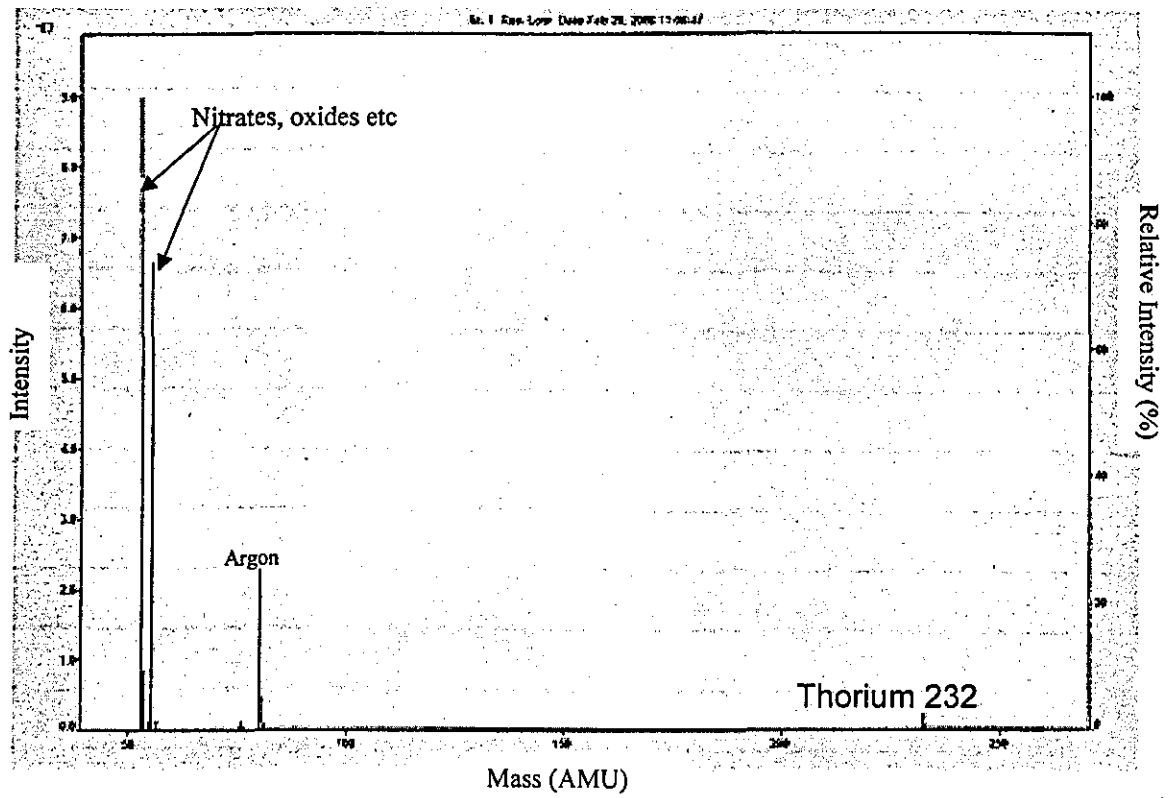
Figure 20 ICP-MS of Batch 1, thorium in water

1.3.2.   Oversaturation Data – Non Kinetics 28 days

Oversaturation pH 12 – non kinetic 28 days		
Sample	Average	St DEV of grand mean
Acidic	2.00E-03	1.10E-05
NaCl	2.51E-07	1.31E-07
CaOH	5.23E-08	3.46E-08
CDP 1 %	6.41E-08	6.83E-08
CDP 10 %	5.69E-04	1.94E-05
ISA -2	1.23E-05	7.56E-07
ISA -3	7.69E-08	1.10E-08
CaOH 10%	4.26E-09	1.41E-08

Oversaturation pH 8 non kinetic 28 days		
Sample	Average	St DEV of grand mean
Acidic	1.52E-03	5.06E-04
NaCl	5.67E-05	1.22E-05
CaOH	6.18E-08	6.64E-08
CDP 1 %	-1.04E-07	1.36E-08
CDP 10 %	1.00E-06	1.50E-07
ISA -2	1.72E-07	7.99E-08
ISA -3	1.71E-08	1.74E-08
CaOH 10 %	-6.63E-08	1.33E-08

Oversaturation pH 6 non kinetic 28 days		
Sample	Average	St DEV of grand mean
Acidic	2.10E-03	8.92E-06
NaCl	2.02E-06	1.03E-06
CaOH	4.36E-07	2.22E-07
CDP 1 %	-2.03E-08	5.62E-08
CDP 10 %	3.09E-05	1.44E-05
ISA -2	4.64E-05	1.90E-05
ISA -3	6.27E-07	4.49E-07
CaOH 10	6.37E-09	5.12E-08

Table 23 Oversaturation thorium solubility experiments, non kinetic, errors

1.3.3.   Oversaturation pH 12 Kinetics

Oversaturation 2 days pH 12		
Sample	Average	St DEV of grand mean
NaCl	2.38E-07	1.44E-07
CaOH	9.44E-07	8.91E-07
CDP 1 %	3.00E-06	2.13E-06
CDP 10 %	5.04E-04	2.21E-05
ISA -2	2.73E-05	1.78E-06
ISA -3	2.27E-07	1.57E-07

Oversaturation 7 days pH 12		
Sample	Average	St DEV of grand mean
NaCl	4.27E-09	2.01E-09
CaOH	-5.87E-08	2.04E-09
CDP 1 %	1.89E-04	1.82E-05
CDP 10 %	3.27E-04	6.99E-05
ISA -2	1.74E-05	1.45E-06
ISA -3	4.27E-09	1.45E-08

Oversaturation 14 days pH 12		
Sample	Average	St DEV of grand mean
NaCl	-8.53E-09	1.74E-09
CaOH	-5.23E-08	4.73E-09
CDP 1 %	-1.19E-07	0.00E+00
CDP 10 %	3.57E-04	1.85E-05
ISA -2	2.08E-05	5.50E-06
ISA -3	2.57E-07	2.23E-07

Oversaturation 21 days pH 12		
Sample	Average	St DEV of grand mean
NaCl	8.53E-09	5.23E-09
CaOH	-4.80E-08	3.64E-09
CDP 1 %	-1.17E-07	2.13E-09
CDP 10 %	3.20E-04	4.21E-06
ISA -2	5.17E-06	7.95E-07
ISA -3	6.40E-08	3.30E-08

Oversaturation 28 days pH 12		
Sample	Average	St DEV of grand mean
Acidic	2.72E-03	1.00E-04
NaCl	5.06E-07	2.07E-07
CaOH	3.52E-08	3.67E-08
CDP 1 %	1.45E-07	2.19E-07
CDP 10 %	5.92E-04	6.32E-06
ISA -2	1.49E-05	1.55E-06
ISA -3	1.44E-07	5.56E-08

Table 24 Oversaturation thorium solubility experiments, kinetic studies, pH 12, errors

1.3.4.   Oversaturation pH 8 Kinetics

Oversaturation 2 days pH 8		
Sample	Average	St DEV of grand mean
NaCl	2.58E-07	1.64E-07
CaOH	3.30E-07	2.32E-07
CDP 1 %	6.66E-07	5.96E-07
CDP 10 %	6.74E-06	1.02E-06
ISA -2	1.83E-06	1.20E-07
ISA -3	4.44E-08	1.65E-08

Oversaturation 7 days pH 8		
Sample	Average	St DEV of grand mean
NaCl	-2.56E-08	3.90E-09
CaOH	-6.83E-08	6.63E-09
CDP 1 %	-1.53E-07	2.04E-09
CDP 10 %	2.16E-06	2.18E-07
ISA -2	3.96E-06	4.12E-07
ISA -3	1.17E-08	8.77E-09

Oversaturation 14 days pH 8		
Sample	Average	St DEV of grand mean
NaCl	1.61E-07	1.10E-07
CaOH	-5.01E-08	4.73E-09
CDP 1 %	-1.23E-07	4.40E-09
CDP 10 %	1.32E-06	2.07E-07
ISA -2	5.94E-07	2.08E-07
ISA -3	2.33E-07	2.50E-07

Oversaturation 21 days pH 8		
Sample	Average	St DEV of grand mean
NaCl	1.07E-09	2.04E-09
CaOH	-4.37E-08	3.64E-09
CDP 1 %	-1.34E-07	2.13E-09
CDP 10 %	6.59E-07	1.77E-07
ISA -2	7.47E-07	1.01E-07
ISA -3	-1.49E-08	1.23E-09

Oversaturation 28 days pH 8		
Sample	Average	St DEV of grand mean
Acidic	2.92E-03	9.55E-06
NaCl	5.91E-08	8.84E-09
CaOH	-7.52E-09	1.43E-08
CDP 1 %	-8.60E-08	1.73E-08
CDP 10 %	1.98E-06	4.65E-07
ISA -2	8.47E-07	5.24E-08
ISA -3	3.44E-08	8.95E-09

Table 25 Oversaturation thorium solubility experiments, kinetic studies, pH 8, errors

1.3.5.   Oversaturation pH 6 Kinetics

Oversaturation 2 days pH 6		
Sample	Average	St DEV of grand mean
Acidic	2.90E-03	2.01E-05
NaCl	1.06E-06	8.21E-07
CaOH	9.17E-07	8.09E-07
CDP 1 %	4.61E-07	3.75E-07
CDP 10 %	2.73E-05	1.27E-05
ISA -2	5.46E-05	2.50E-05
ISA -3	1.27E-06	1.22E-06

Oversaturation 7 days pH 6		
Sample	Average	St DEV of grand mean
Acidic	2.81E-03	1.19E-05
NaCl	7.05E-07	5.00E-07
CaOH	5.44E-08	1.39E-07
CDP 1 %	-1.46E-07	6.60E-09
CDP 10 %	9.58E-06	4.36E-07
ISA -2	1.51E-05	5.52E-06
ISA -3	3.86E-05	8.54E-06

Oversaturation 14 days pH 6		
Sample	Average	St DEV of grand mean
Acidic	2.81E-03	7.08E-06
NaCl	1.88E-07	1.50E-07
CaOH	-3.31E-08	4.03E-08
CDP 1 %	-1.05E-07	4.66E-08
CDP 10 %	1.37E-05	1.98E-06
ISA -2	3.70E-06	5.77E-07
ISA -3	-4.16E-08	3.64E-09

Oversaturation 21 days pH 6		
Sample	Average	St DEV of grand mean
Acidic	2.82E-03	1.18E-05
NaCl	1.89E-06	1.51E-06
CaOH	3.63E-08	1.12E-07
CDP 1 %	-3.52E-08	1.10E-07
CDP 10 %	2.31E-05	6.09E-06
ISA -2	3.65E-05	1.31E-05
ISA -3	-3.20E-08	6.63E-09

Oversaturation 28 days pH 6		
Sample	Average	St DEV of grand mean
Acidic	2.90E-03	1.15E-05
NaCl	2.88E-06	2.28E-06
CaOH	1.48E-06	7.67E-07
CDP 1 %	1.35E-07	1.41E-07
CDP 10 %	2.67E-05	6.39E-06
ISA -2	1.95E-05	1.33E-05
ISA -3	2.11E-06	1.05E-06

Table 26 Oversaturation thorium solubility experiments, kinetic studies, pH 6, errors

1.3.6.   Undersaturation Non Kinetics – 28 days

Undersaturation pH 12 non kinetic – 28 days		
Sample	Average	St DEV of grand mean
Acidic	1.97E-03	1.07E-05
NaCl	2.11E-07	2.24E-08
CaOH	7.17E-07	2.46E-07
CDP 1 %	3.04E-07	8.13E-08
CDP 10 %	3.93E-05	9.44E-07
ISA -2	5.93E-07	2.20E-07
ISA -3	2.83E-07	1.50E-07

Undersaturation pH 8 non kinetic – 28 days		
Sample	Average	St DEV of grand mean
Acidic	1.90E-03	1.42E-05
NaCl	1.74E-07	2.24E-08
CaOH	1.92E-08	4.28E-09
CDP 1 %	-8.88E-08	7.72E-09
CDP 10 %	6.10E-08	3.30E-08
ISA -2	1.34E-07	6.03E-08
ISA -3	2.56E-08	7.80E-09

Undersaturation pH 6 non kinetic – 28 days		
Sample	Average	St DEV of grand mean
Acidic	1.82E-03	4.05E-05
NaCl	1.14E-07	3.97E-08
CaOH	-3.44E-08	1.75E-08
CDP 1 %	-9.55E-08	5.68E-09
CDP 10 %	6.65E-08	4.38E-08
ISA -2	5.89E-08	2.02E-08
ISA -3	5.56E-08	1.20E-08

Table 27 Undersaturation thorium solubility experiments, non kinetic studies, errors

1.3.7.   Undersaturation pH 12 Kinetics

Undersaturation 2 days pH 12		
Sample Name	Average	St DEV of grand mean
Acidic	2.94E-03	5.92E-05
NaCl	1.70E-07	7.76E-08
CaOH	7.50E-09	2.15E-08
CDP 1 %	-3.74E-08	3.88E-08
CDP 10 %	3.65E-05	1.21E-06
ISA -2	5.27E-08	2.07E-08
ISA -3	2.35E-08	8.99E-09

Undersaturation 7 days pH 12		
Sample Name	Average	St DEV of grand mean
Acidic	2.92E-03	2.26E-05
NaCl	2.93E-06	1.98E-06
CaOH	1.59E-06	9.31E-07
CDP 1 %	5.36E-07	2.47E-07
CDP 10 %	5.23E-05	3.99E-06
ISA -2	3.11E-06	1.78E-06
ISA -3	2.21E-06	8.69E-07

Undersaturation 14 days pH 12		
Sample Name	Average	St DEV of grand mean
Acidic	2.24E-03	8.79E-05
NaCl	8.43E-07	4.87E-07
CaOH	2.07E-07	6.51E-08
CDP 1 %	2.10E-07	1.03E-07
CDP 10 %	6.16E-05	2.22E-06
ISA -2	5.94E-07	1.97E-07
ISA -3	1.90E-07	1.16E-07

Undersaturaition 21 days pH 12		
Sample Name	Average	St DEV of grand mean
Acidic	1.90E-03	1.62E-04
NaCl	4.43E-08	2.39E-09
CaOH	6.12E-08	6.94E-08
CDP 1 %	1.08E-08	8.17E-08
CDP 10 %	5.66E-05	1.14E-06
ISA -2	3.77E-07	1.52E-07
ISA -3	1.35E-07	6.13E-08

Undersaturation 28 days pH 12		
Sample Name	Average	St DEV of grand mean
Acidic	2.29E-03	1.52E-05
NaCl	1.29E-07	5.81E-08
CaOH	5.05E-08	6.31E-08
CDP 1 %	2.45E-07	3.03E-07
CDP 10 %	6.61E-05	1.02E-06
ISA -2	2.48E-07	1.33E-07
ISA -3	2.38E-07	1.77E-07

Table 28 Undersaturation thorium solubility experiments, kinetic studies, pH 12, errors

1.3.8. Undersaturation pH 8 Kinetics

Undersaturation 2 days pH 8		
Sample Name	Average	St DEV of grand mean
Acidic	2.87E-03	7.32E-06
NaCl	2.88E-07	5.63E-08
CaOH	4.70E-08	3.64E-08
CDP 1 %	1.91E-07	3.06E-08
CDP 10 %	5.42E-07	1.34E-07
ISA -2	3.12E-07	1.35E-08
ISA -3	9.34E-08	3.90E-08

Undersaturation 7 days pH 8		
Sample Name	Average	St DEV of grand mean
Acidic	1.56E-04	1.24E-05
NaCl	4.01E-08	2.08E-08
CaOH	-3.65E-08	4.64E-09
CDP 1 %	-6.73E-08	2.39E-08
CDP 10 %	3.58E-08	1.90E-08
ISA -2	6.88E-08	3.47E-08
ISA -3	2.29E-08	1.22E-08

Undersaturation 14 days pH 8		
Sample Name	Average	St DEV of grand mean
Acidic	2.65E-03	3.58E-05
NaCl	3.92E-07	1.36E-07
CaOH	4.56E-07	2.22E-07
CDP 1 %	1.88E-07	9.84E-08
CDP 10 %	1.66E-07	4.97E-08
ISA -2	2.24E-07	6.04E-08
ISA -3	3.15E-06	2.03E-06

Undersaturation 21 days pH 8		
Sample Name	Average	St DEV of grand mean
Acidic	2.99E-03	8.91E-06
NaCl	3.87E-08	9.12E-09
CaOH	-1.40E-08	1.07E-08
CDP 1 %	6.45E-09	3.74E-08
CDP 10 %	4.84E-08	2.69E-08
ISA -2	3.22E-09	8.66E-09
ISA -3	3.14E-06	1.36E-06

Undersaturation 28 days pH 8		
Sample Name	Average	St DEV of grand mean
Acidic	2.99E-03	9.86E-06
NaCl	3.70E-07	2.44E-07
CaOH	-9.67E-09	1.45E-08
CDP 1 %	6.77E-08	9.26E-08
CDP 10 %	1.10E-07	2.24E-08
ISA -2	7.20E-08	1.55E-08
ISA -3	5.59E-08	2.86E-08

Table 29 Undersaturation thorium solubility experiments, kinetic studies, pH 8, errors

1.3.9.   Undersaturation pH 6 Kinetics

Undersaturation 2 days pH 6		
Sample Name	Average	St DEV of grand mean
Acidic	2.64E-03	6.44E-05
NaCl	3.87E-08	1.87E-08
CaOH	4.30E-09	2.21E-08
CDP 1 %	-2.26E-08	2.89E-08
CDP 10 %	1.65E-06	1.87E-07
ISA -2	1.82E-06	2.02E-07
ISA -3	2.12E-07	6.95E-08

Undersaturation 7 days pH 6		
Sample Name	Average	St DEV of grand mean
Acidic	6.61E-04	7.69E-05
NaCl	3.73E-07	1.13E-07
CaOH	3.29E-07	3.36E-07
CDP 1 %	1.29E-08	7.23E-08
CDP 10 %	3.75E-07	1.56E-07
ISA -2	1.04E-06	3.31E-07
ISA -3	4.72E-07	2.60E-07

Undersaturation 14 days pH 6		
Sample Name	Average	St DEV of grand mean
Acidic	9.43E-06	9.67E-06
NaCl	2.22E-05	1.00E-05
CaOH	5.37E-08	2.82E-08
CDP 1 %	-6.88E-08	7.65E-09
CDP 10 %	1.19E-06	7.46E-07
ISA -2	4.93E-07	2.15E-07
ISA -3	2.08E-07	8.96E-08

Undersaturation 21 days pH 6		
Sample Name	Average	St DEV of grand mean
Acidic	3.07E-03	7.08E-06
NaCl	1.15E-08	1.43E-09
CaOH	-3.44E-08	1.69E-08
CDP 1 %	-1.05E-07	1.03E-08
CDP 10 %	6.88E-08	3.66E-08
ISA -2	5.20E-07	5.00E-08
ISA -3	1.93E-08	9.69E-09

Undersaturation 28 days pH 6		
Sample Name	Average	St DEV of grand mean
Acidic	2.93E-03	6.34E-06
NaCl	1.63E-07	8.17E-08
CaOH	-7.17E-10	4.23E-08
CDP 1 %	3.91E-07	1.24E-07
CDP 10 %	6.36E-07	3.87E-07
ISA -2	4.97E-07	5.48E-08
ISA -3	8.02E-08	4.80E-08

Table 30 Undersaturation thorium solubility experiments, kinetic studies, pH 6, errors

Appendix 4

1.4.   NMR Studies

1.4.1.   ¹³C NMR Spectra
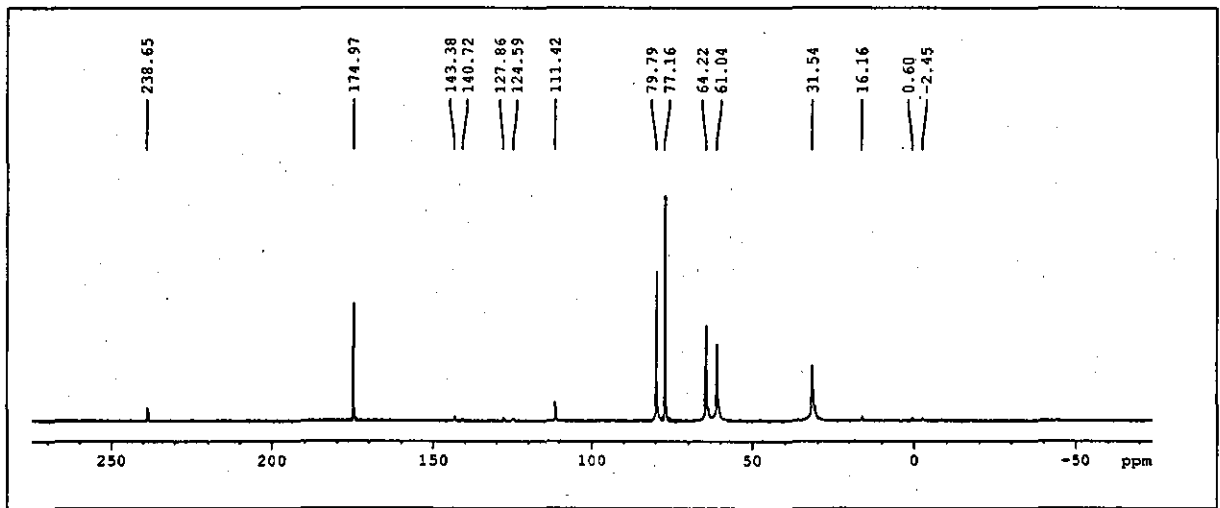
Figure 21 ¹³C NMR spectrum of ISA-Cd at pH 7
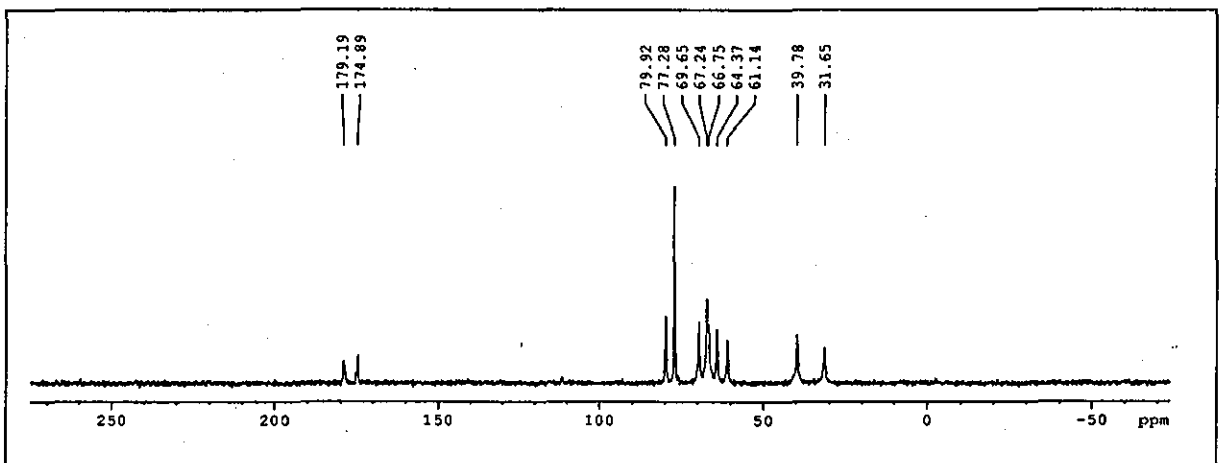
Figure 22 ¹³C NMR spectrum of ISA-Cd at pH 10
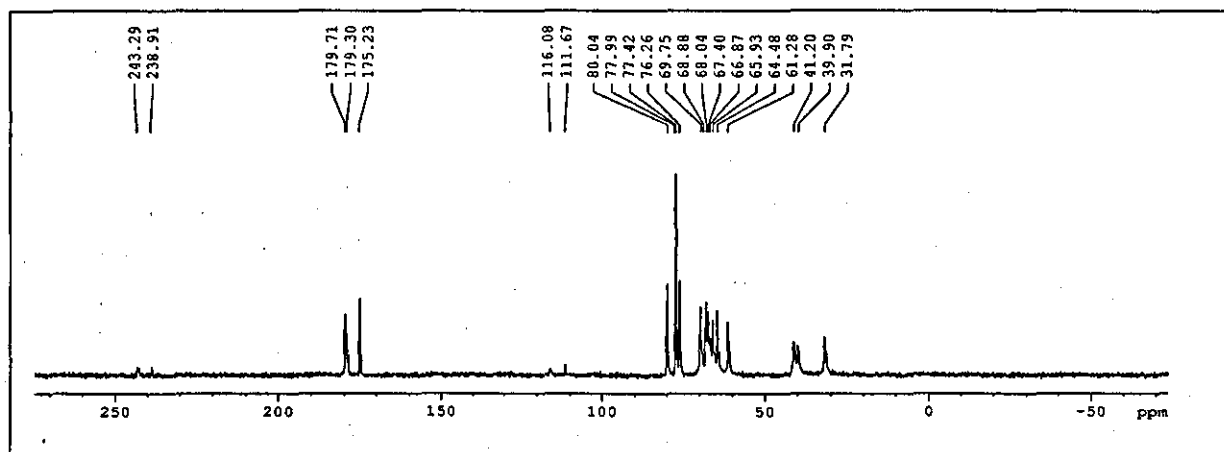
Figure 23 ^{13}C NMR spectrum of ISA-Cd at pH 13
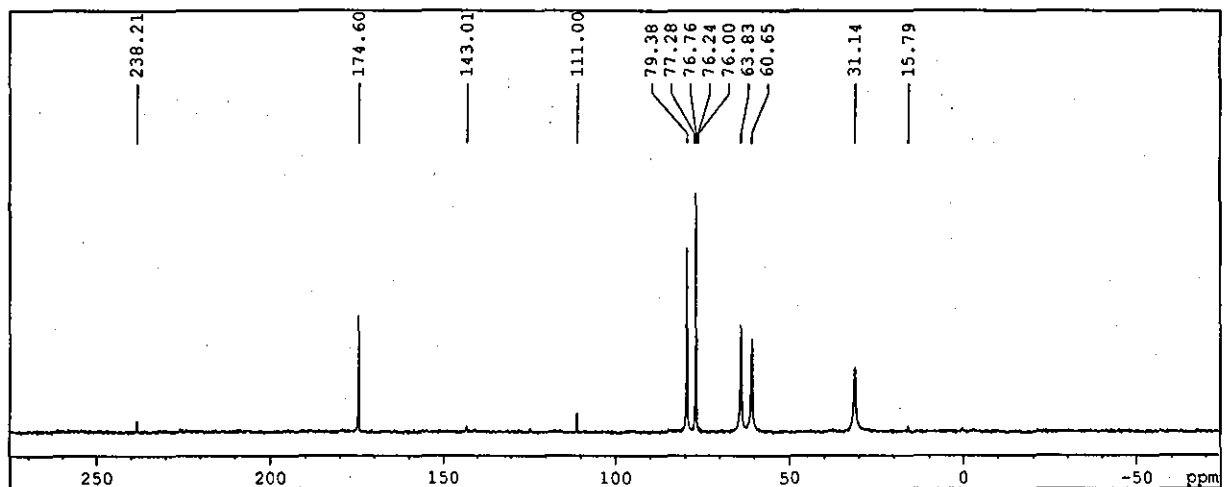
Figure 24 ^{13}C NMR spectrum of ISA-Eu at pH 7
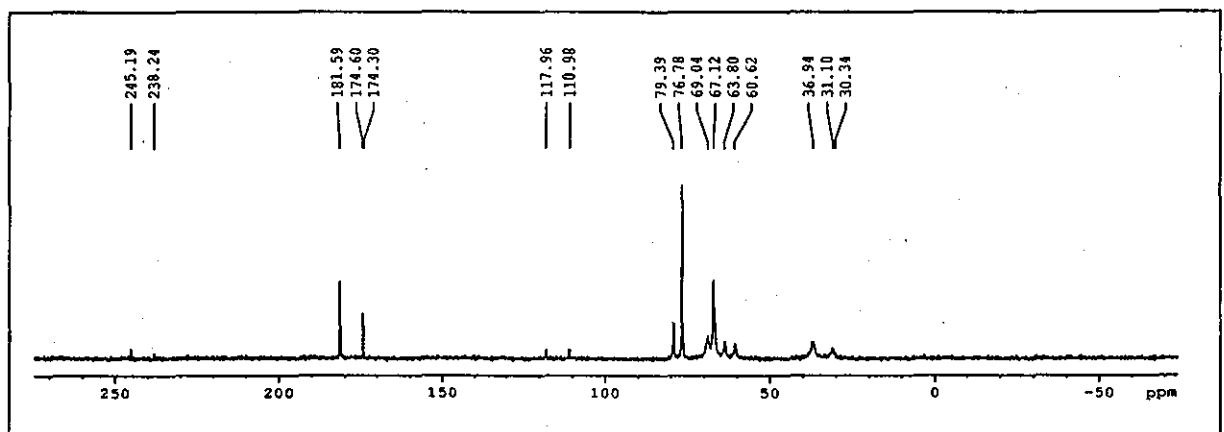
Figure 25 ^{13}C NMR spectrum of ISA-Eu at pH 10
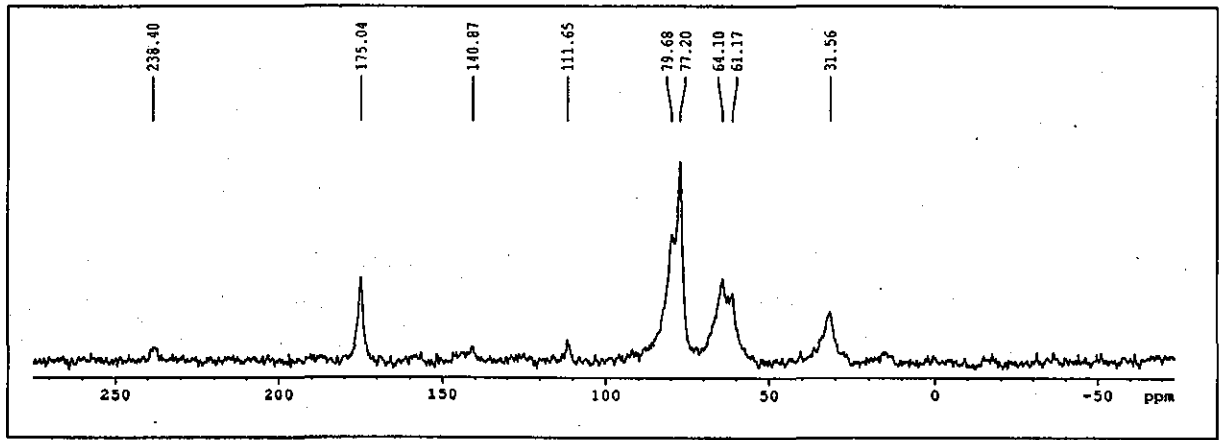
Figure 26 ^{13}C NMR spectrum of ISA-Fe at pH 7
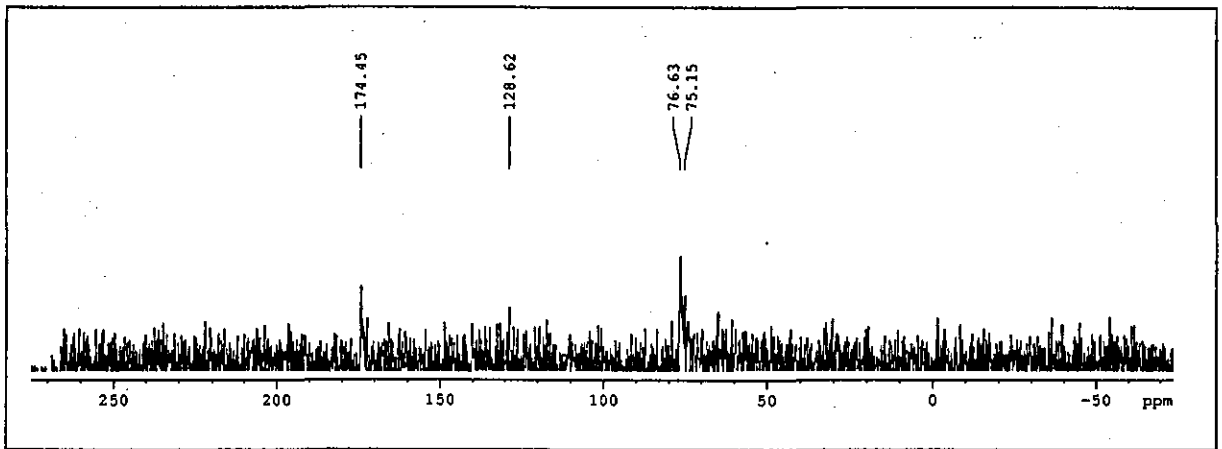
Figure 27 ^{13}C NMR spectrum of ISA-Fe at pH 10
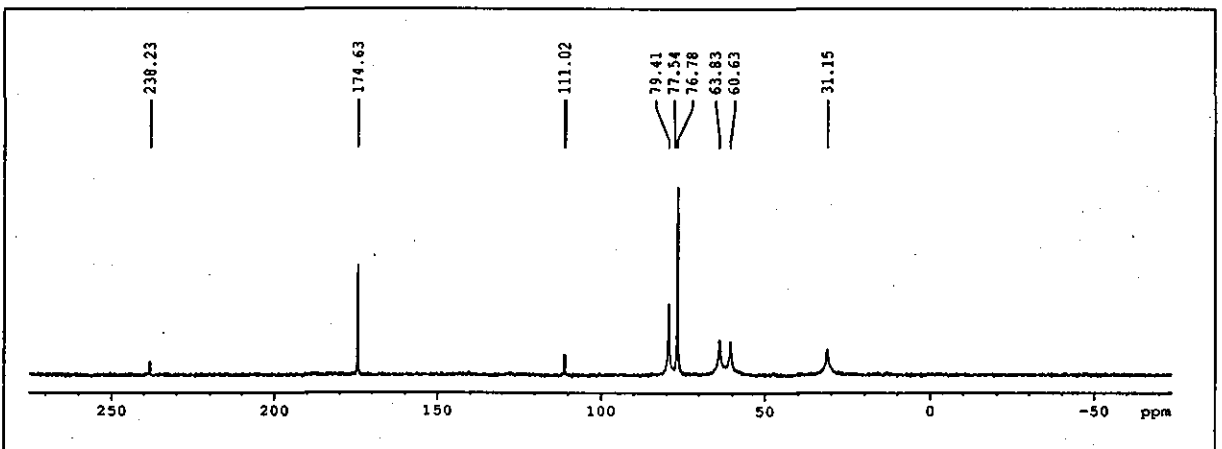
Figure 28 ^{13}C NMR spectrum of ISA-Ni at pH 7

1.4.2.   Dipolar Dephasing
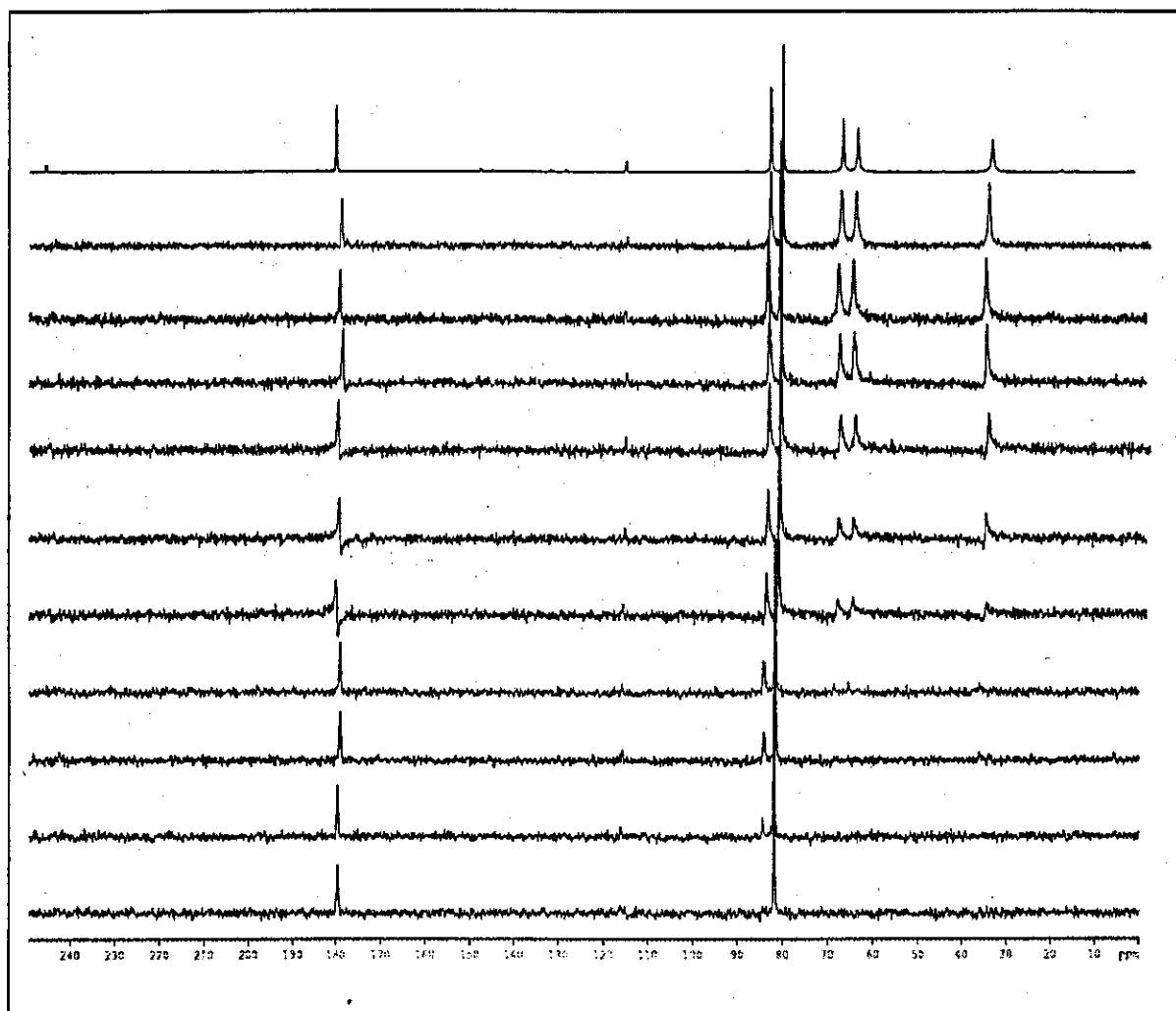
Figure 29 ISA-Cd pH 7, ^{13}C dipolar dephasing delays of 0, 2, 6, 10, 14, 18 , 22, 26, 32, 40, and 50 µs top to bottom
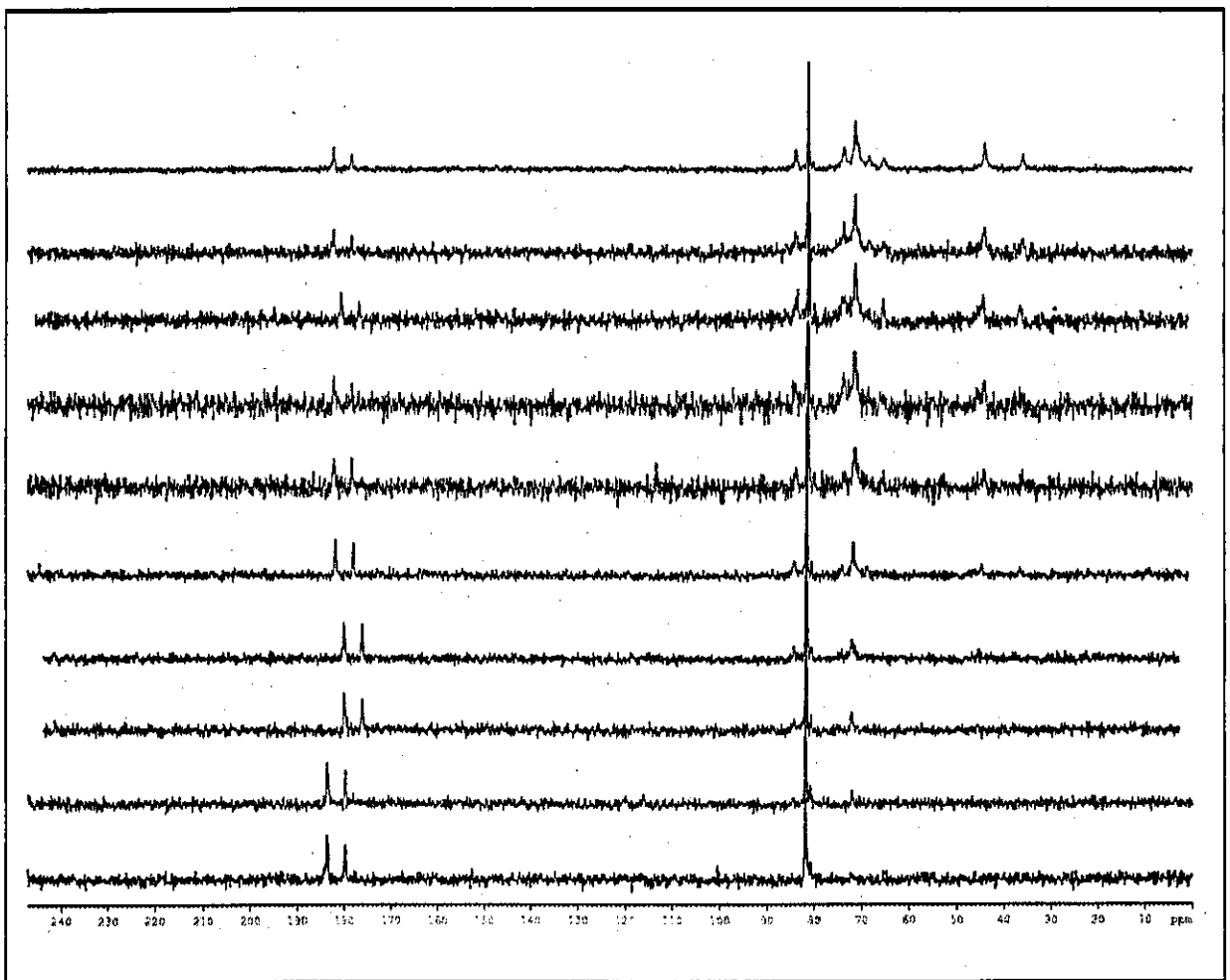
Figure 30 ISA-Cd ^{13}C dipolar dephasing pH 10, delays of 0, 2, 6, 10, 14, 18 , 22, 26, 32, 40, and 50 µs top to bottom

1.4.3.   CSA Investigations
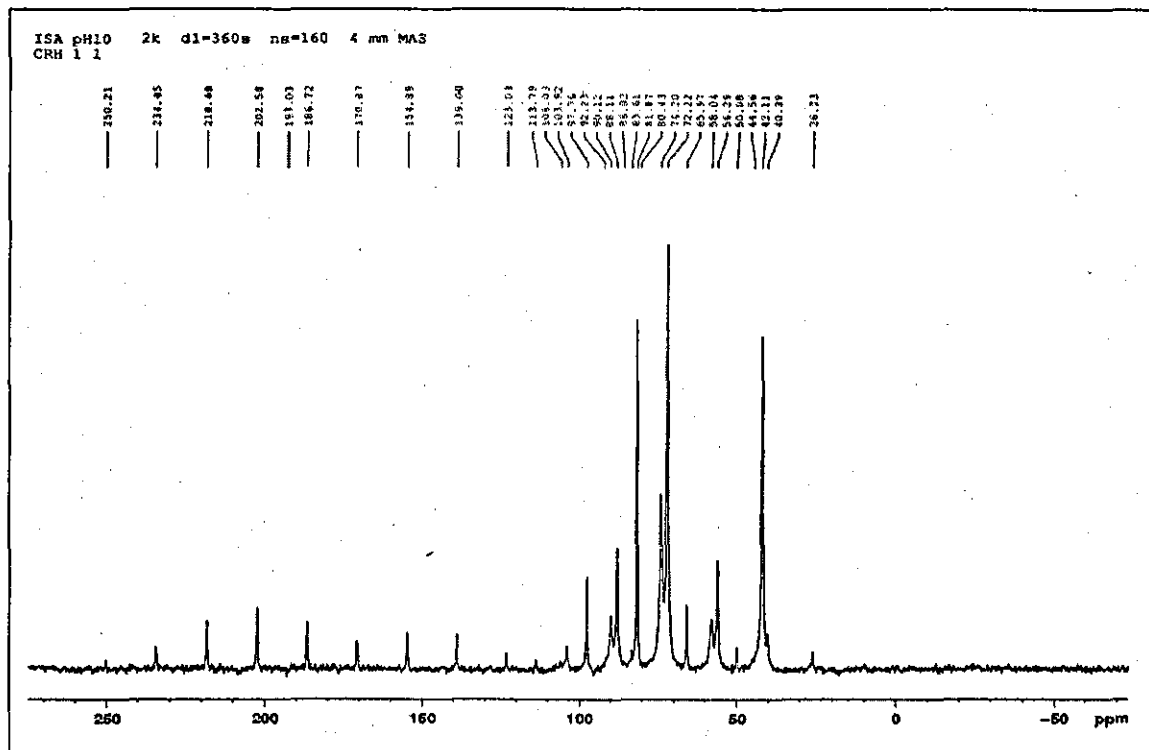
Figure 31 ISA pH 10, ^{13}C, 2 KHz Spinning Speed
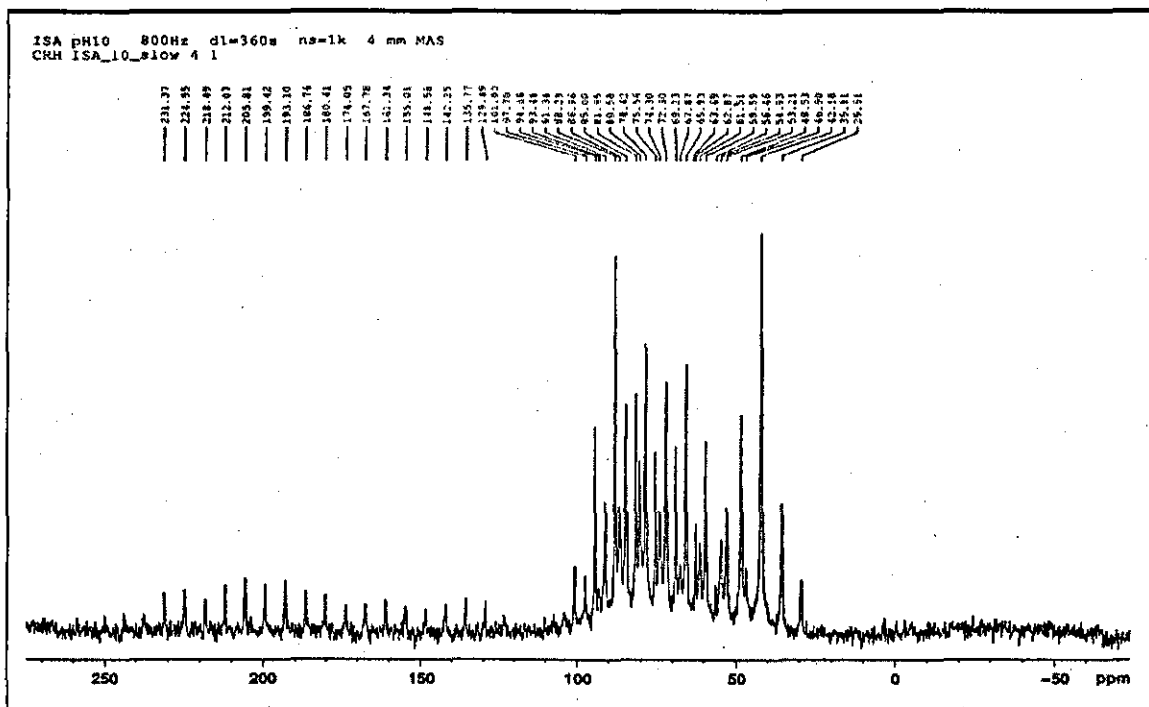
Figure 32 ISA pH 10, ^{13}C, 800 Hz Spinning Speed

1.5.   Gaussian Modelling

1.5.1.   Structure A - 1:1 Metal ISA
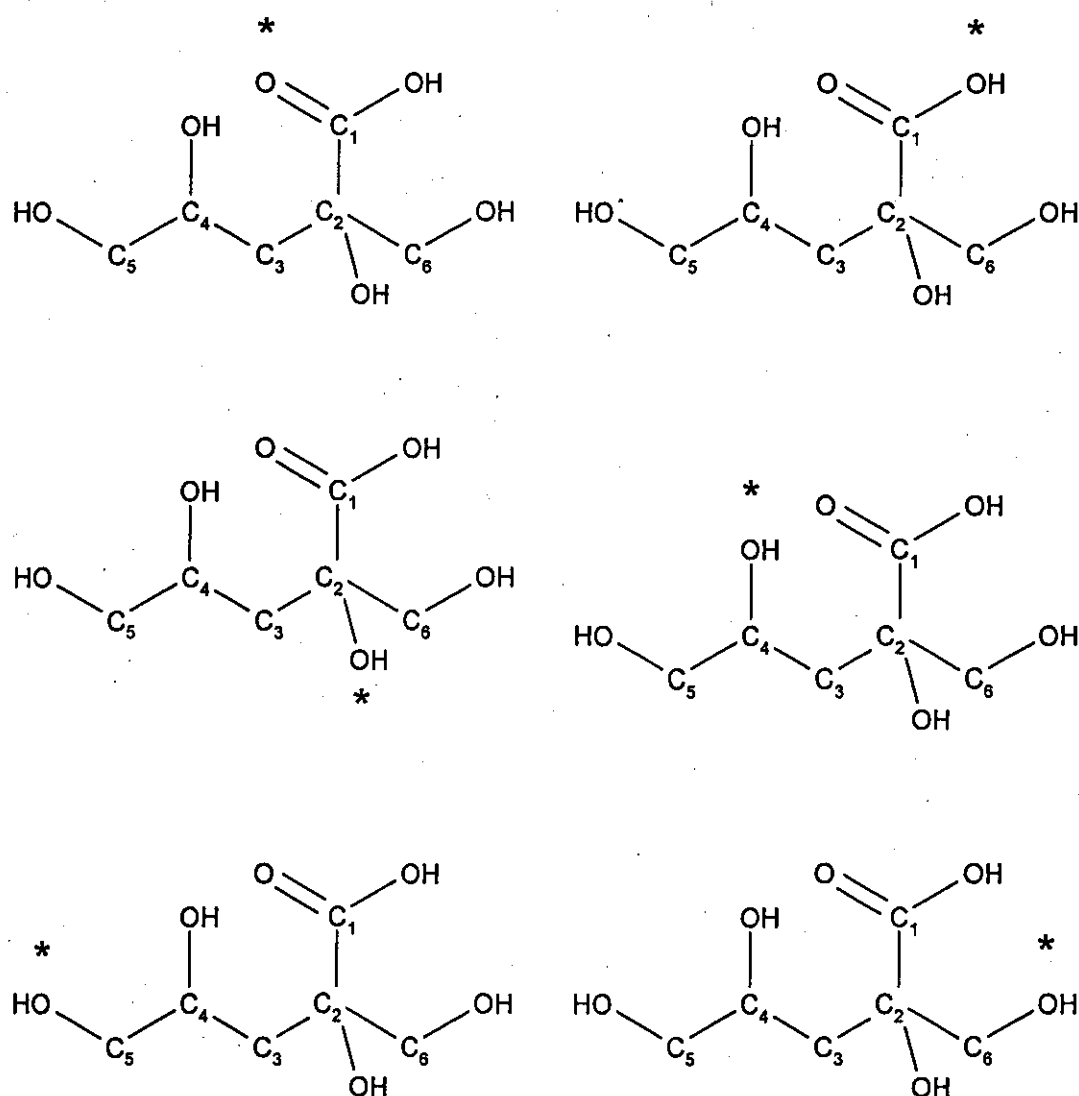
Figure 33 Inputted structure – The star indicates where the cadmium metal ion was
bound to the ligand

1.5.2.   Structure A - 2:1 M:ISA
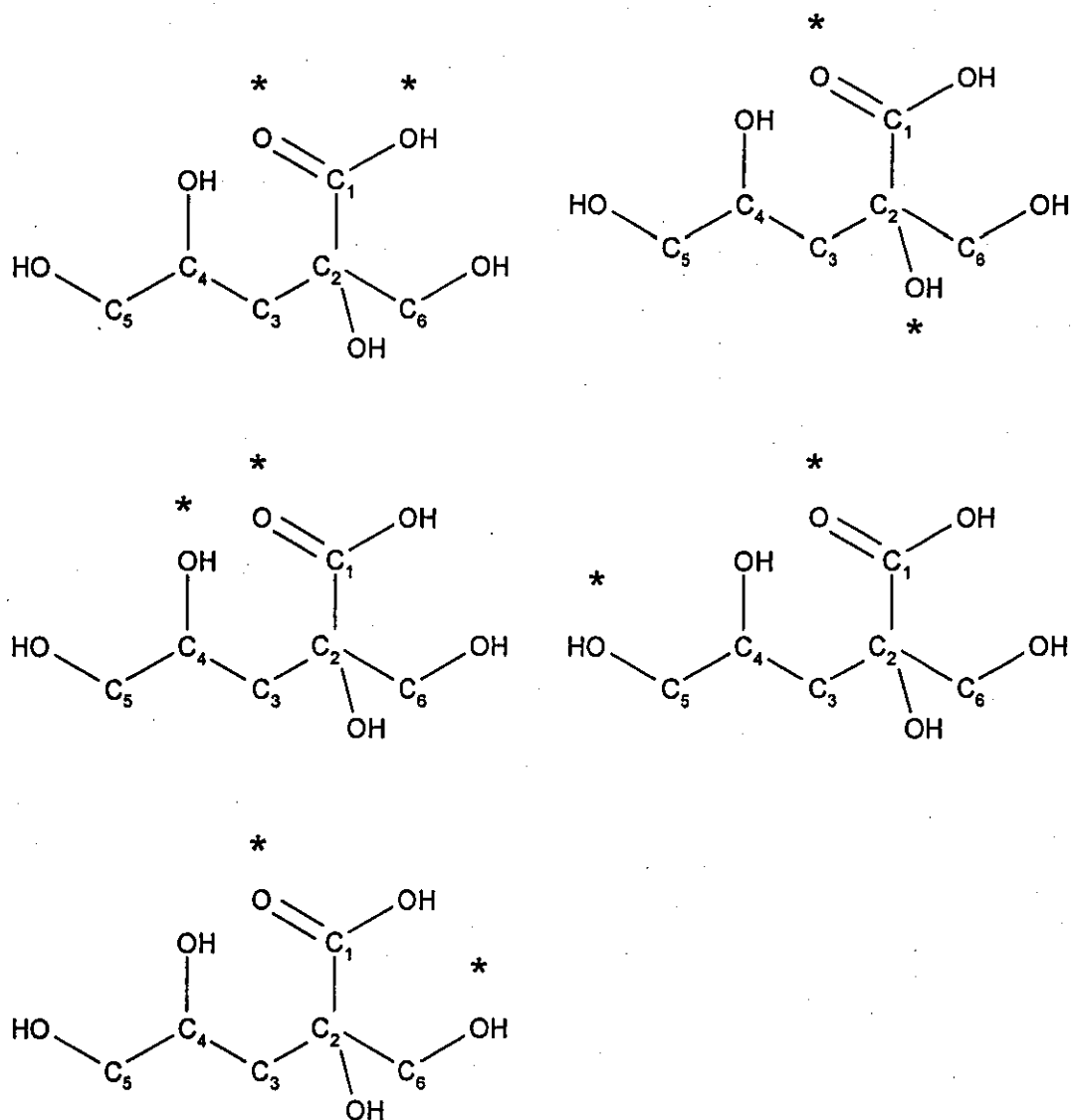
Figure 34 Inputted structure – The star indicates where the cadmium metal ion was bound to the ligand

1.5.3. Structure A - 1:1 Metal:Ligand – bidentate

The bonding is the same as the 2:1 complexes but instead of two metals its just one with two bonds to the ligand at the starred positions

1.5.4. Structure A - Chemical Shift Data

Table 31 Calculated chemical shifts 1:1 ISA:Metal monodentate

C No	Carbon chemical shifts (ppm) and where the metal was bound						
	Sugar - no metal Calculated	Sugar + M 1 (C=O)	Sugar + M 1 (OH)	Sugar + M 2	Sugar + M 4	Sugar + M 5	Sugar + M 6
1	157.85	99.04	150.83	141.81	142.69	151.25	140.49
2	72.61	52.86	59.76	64.65	58.56	60.50	49.57
3	32.06	18.65	22.78	14.68	24.09	16.48	18.85
4	62.93	45.79	54.41	50.74	49.23	53.26	44.81
5	58.32	43.44	43.87	44.48	48.62	43.76	47.42
6	62.01	45.71	45.70	47.84	47.57	46.03	38.05

Table 32 Calculated chemical shifts 1:2 ISA:Metal monodentate

C No	Carbon chemical shifts (ppm) and where the metal was bound					
	Sugar Calculated	Sugar + 2M C1 – C1	Sugar + 2 M C1 - C2	Sugar + 2 M C1 – C4	Sugar + 2 M C1 – C5	Sugar + 2 M C1 – C6
1	157.85	149.744	155.515	156.135	155.392	150.19
2	72.6109	58.1833	61.6279	59.6697	59.3724	58.9265
3	32.0648	12.5516	15.2824	19.3889	17.308	18.1998
4	62.9352	50.6028	49.0698	44.6573	50.1569	47.6301
5	58.3276	39.6036	44.7342	42.5764	41.2386	44.36
6	62.0137	48.8192	46.6777	44.2114	43.4682	43.9141

Table 33 Calculated chemical shift 1:1 ISA:Metal bidentate bonding

C No	Carbon chemical shifts (ppm) and where the metal was bound					
	Sugar Calculated	Sugar + M C1 – C1	Sugar + 2M C1 - C2	Sugar + M C1 – C4	Sugar + M C1 – C5	Sugar + M C1 – C6
1	157.85	158.34	152.77	158.95	155.69	155.38
2	72.61	62.31	59.61	55.11	60.56	62.41
3	32.06	15.87	21.08	17.10	18.64	15.40
4	62.93	48.29	50.28	50.92	47.77	49.47
5	58.32	41.80	49.91	43.51	41.53	44.41
6	62.01	40.45	49.38	43.26	42.72	45.30

1.5.5.   Structure A - Gaussian modelling and Experimental comparisons
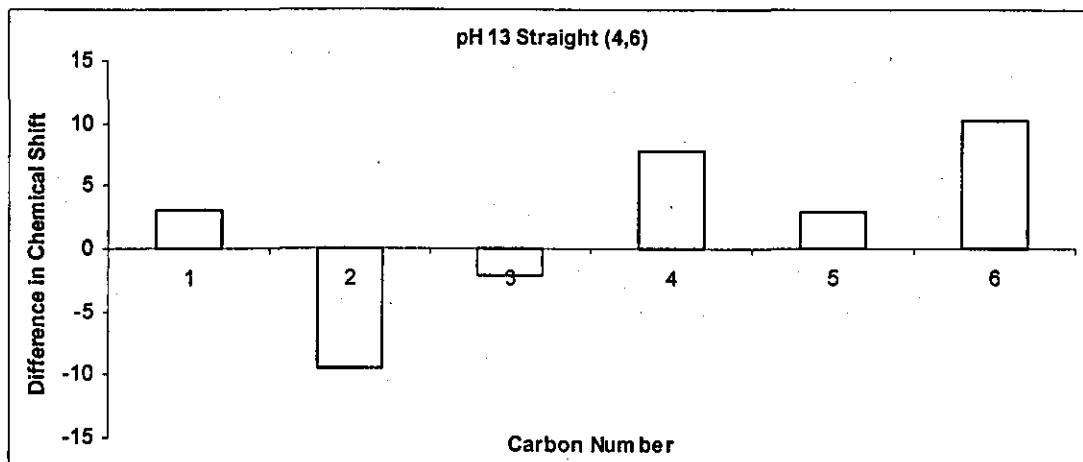
Figure 35 Experimental Differences, (carbon chemical shifts of ISA alone) – (carbon chemical shifts of ISA + M) for pH 13 with carbons 4 and 6 overlapped at 69 ppm
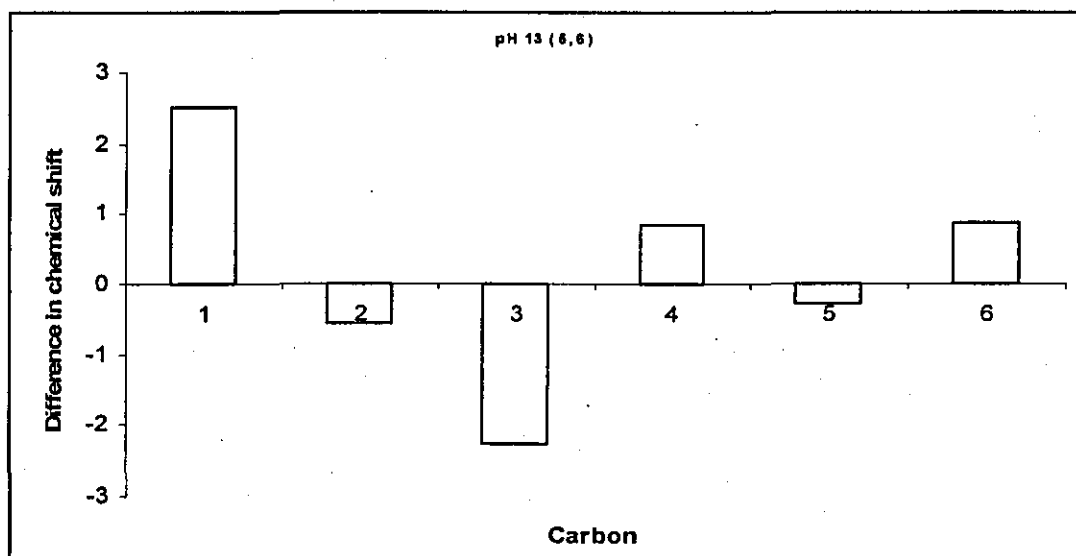
Figure 36 Experimental Differences, (carbon chemical shifts of ISA alone) – (carbon chemical shifts of ISA + M) for pH 13 with carbons 5 and 6 overlapped at 67 ppm
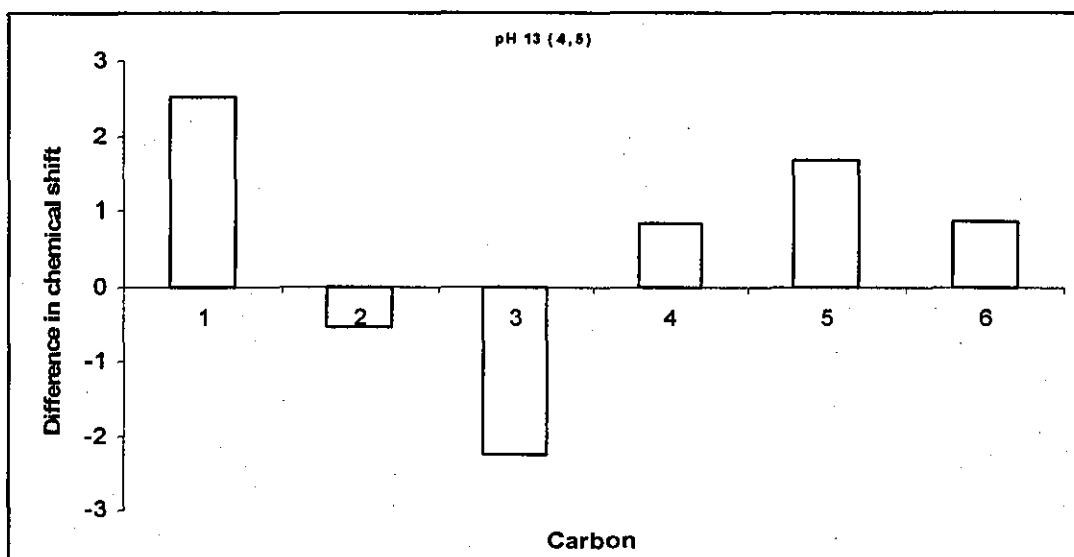
Figure 37 Experimental Differences, (carbon chemical shifts of ISA alone) – (carbon chemical shifts of ISA + M) for pH 13 with carbons 4 and 5 overlapped at 69 ppm
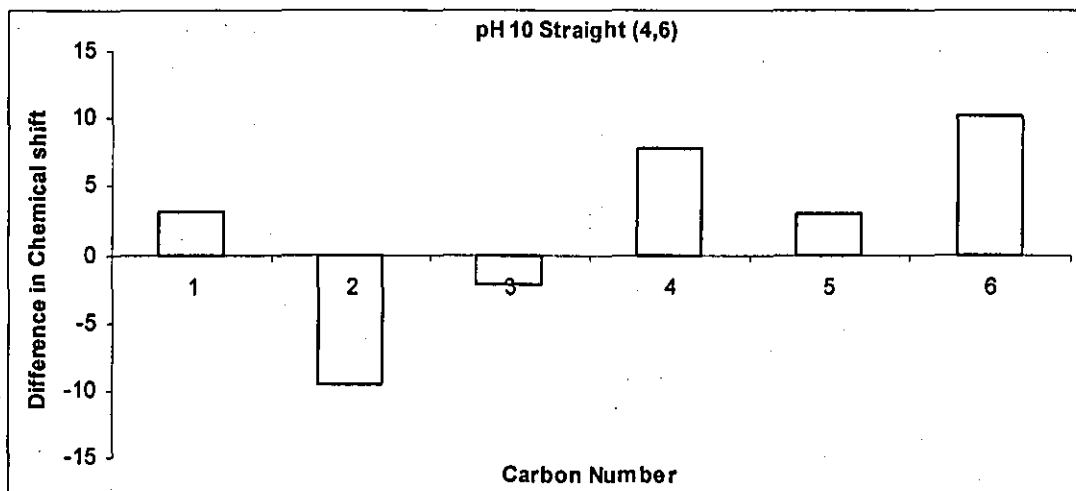
Figure 38 Experimental Differences, (carbon chemical shifts of ISA alone) – (carbon chemical shifts of ISA + M) for pH 10 with carbons 4 and 6 overlapped at 69 ppm
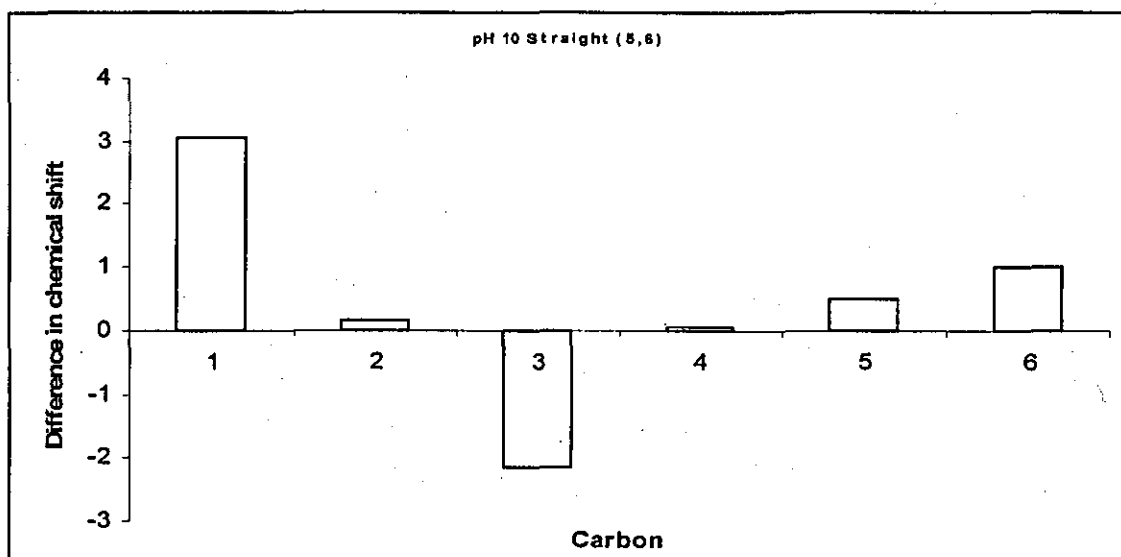
Figure 39 Experimental Differences, (carbon chemical shifts of ISA alone) – (carbon chemical shifts of ISA + M) for pH 10 with carbons 5 and 6 overlapped at 67 ppm
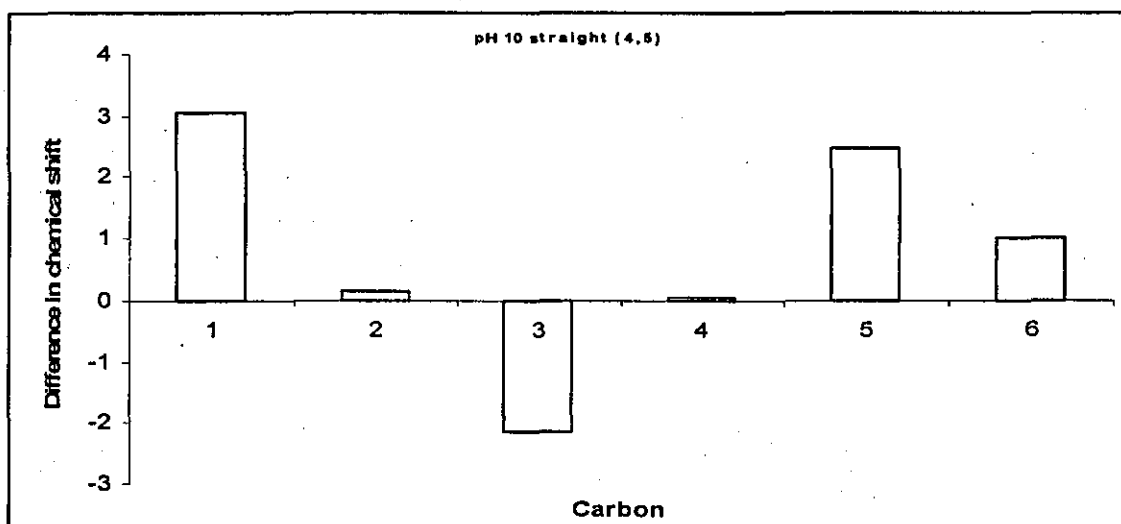
Figure 40 Experimental Differences, (carbon chemical shifts of ISA alone) – (carbon chemical shifts of ISA + M) for pH 10 with carbons 4 and 5 overlapped at 69 ppm
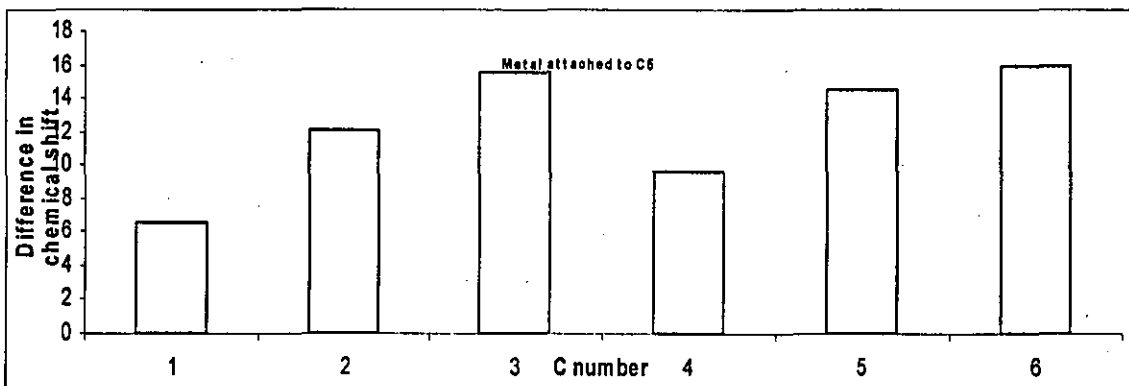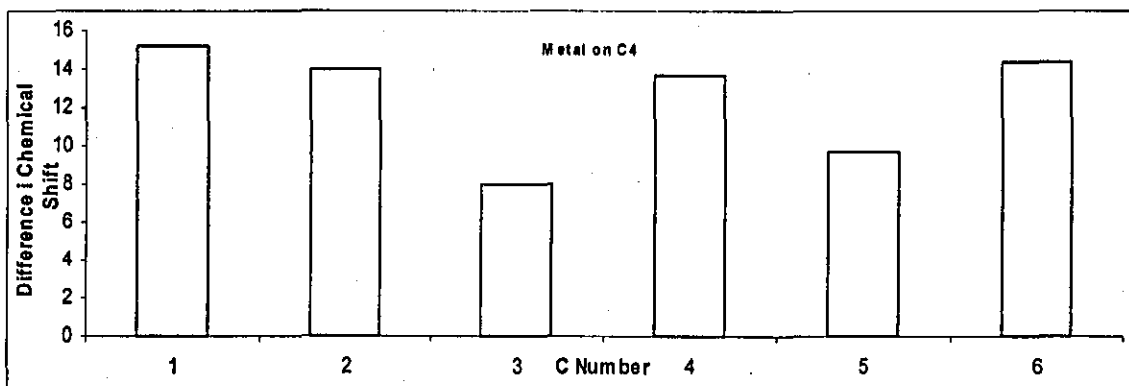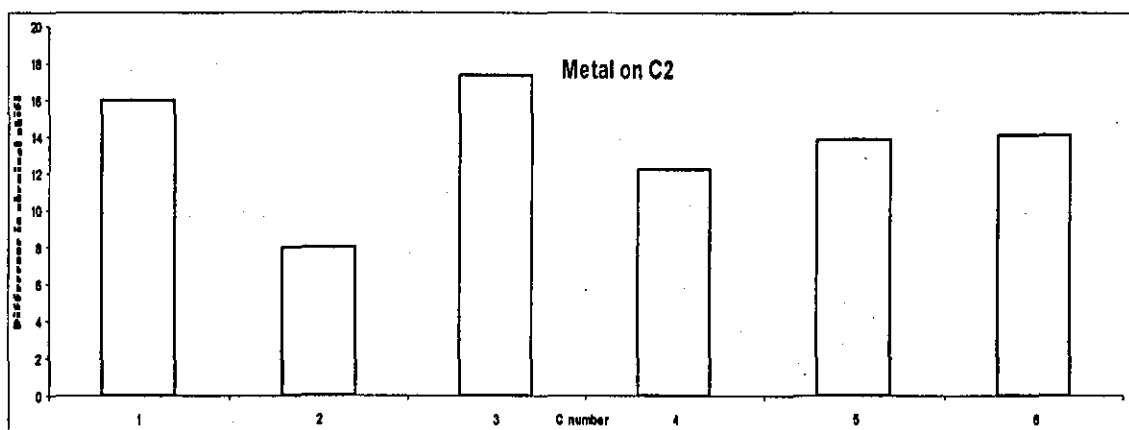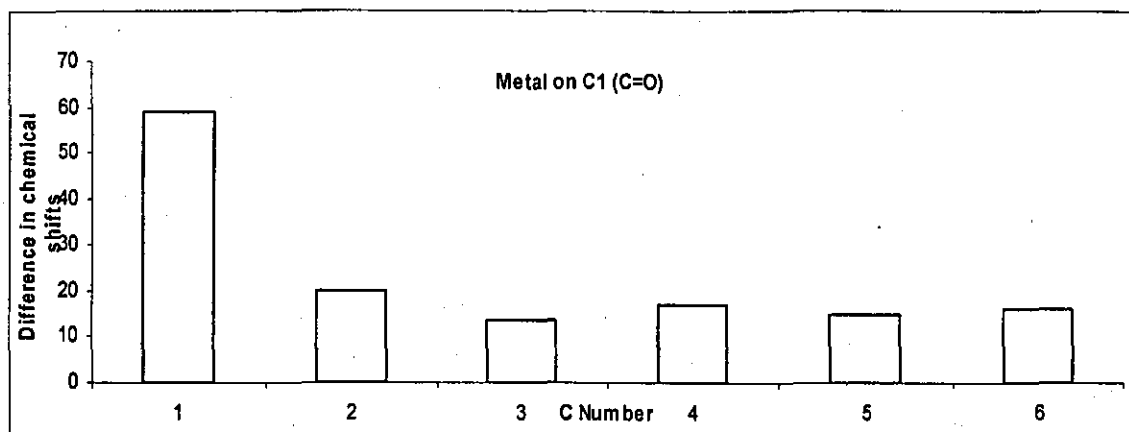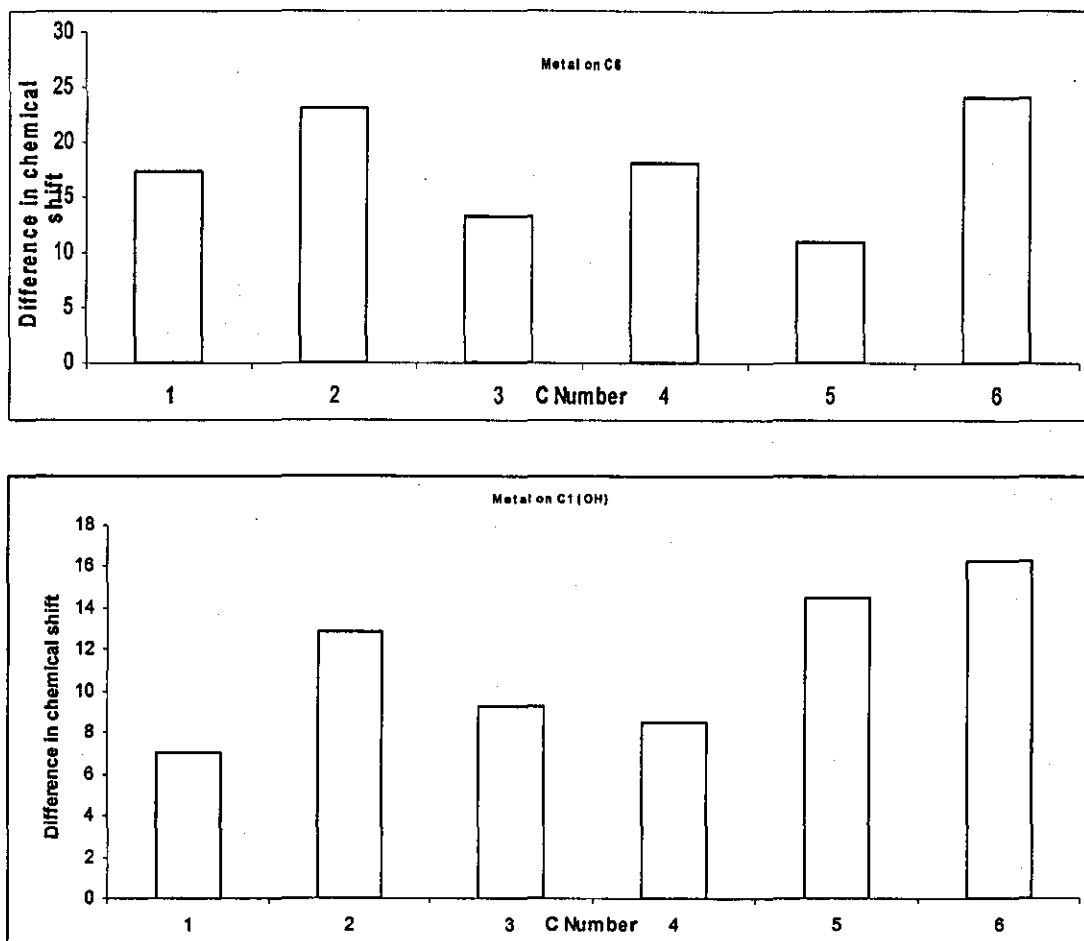
Figure 41 Structure A – 1:1 monodentate. Modelled differences, (carbon chemical shifts of ISA alone) – (carbon chemical shifts of ISA + M) The position of the metal for each complex is at the top of each individual graph
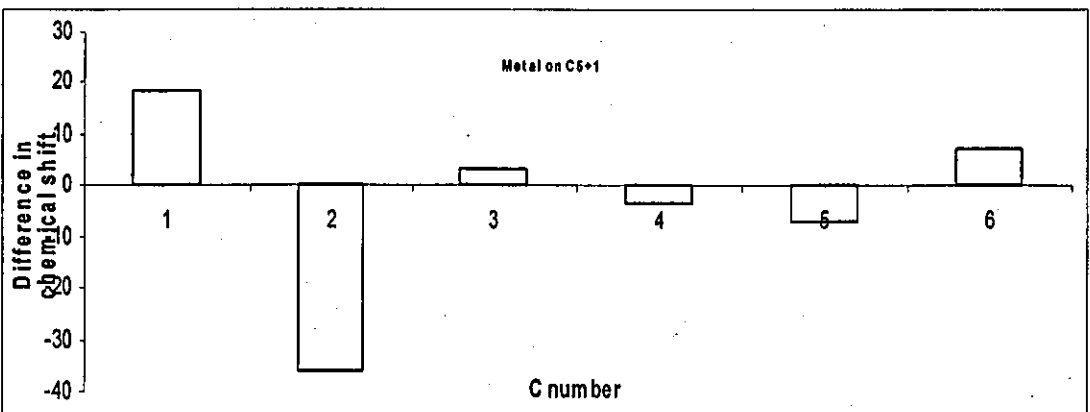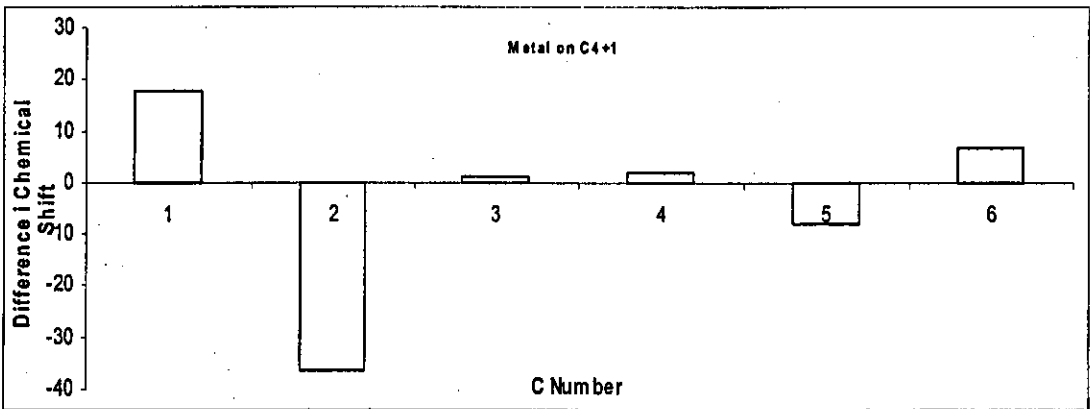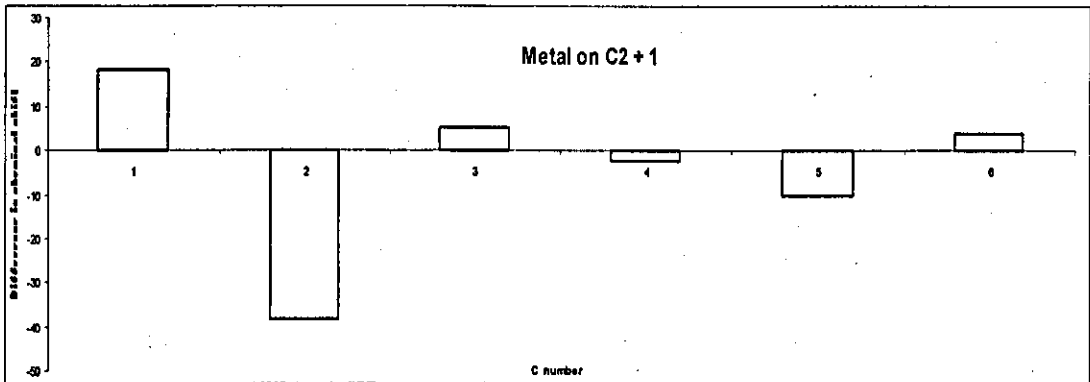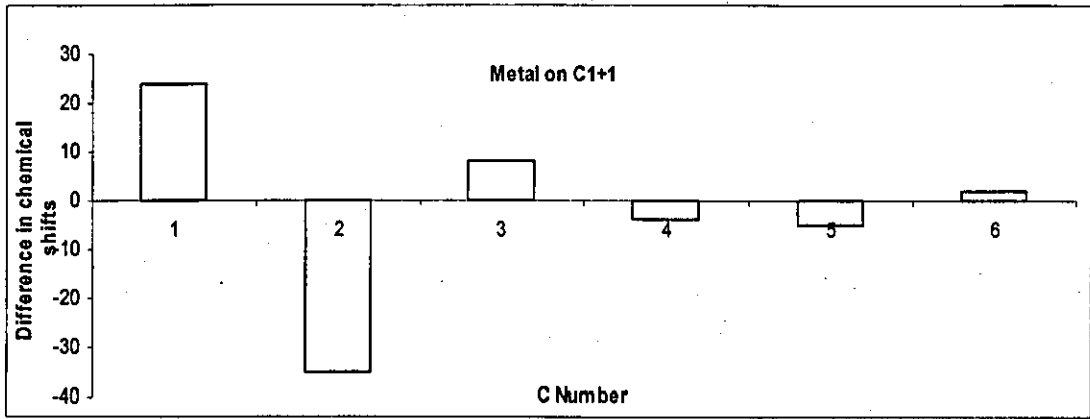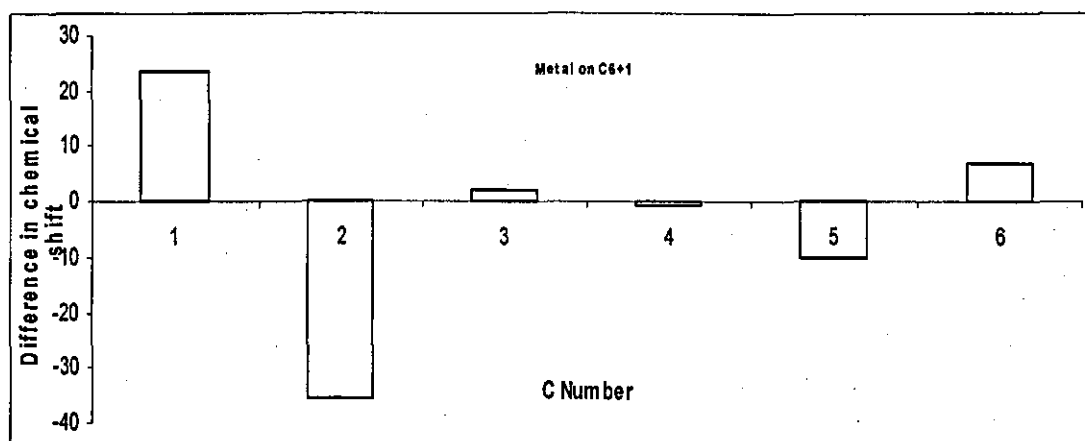
Figure 42 Structure A – 1:2 ISA:M monodentate. Modelled differences, (carbon chemical shifts of ISA alone) – (carbon chemical shifts of ISA + M) The position of the metal for each complex is at thetop of each individual graph
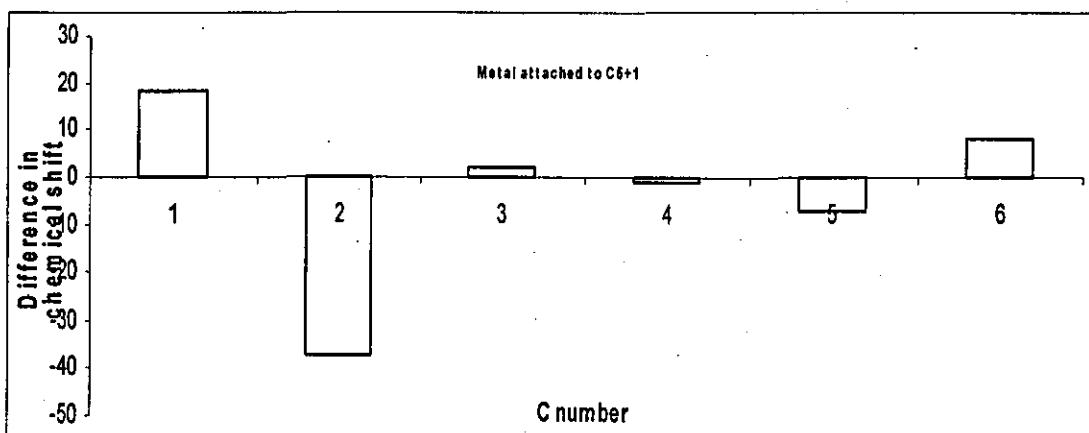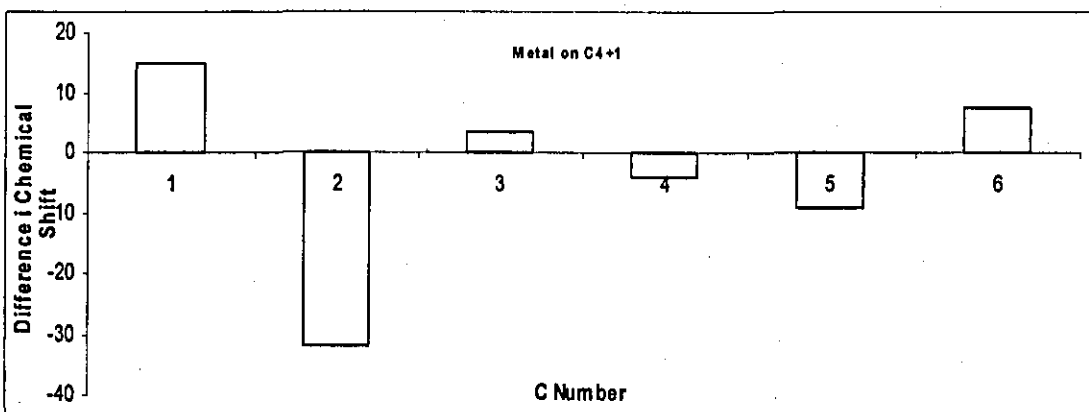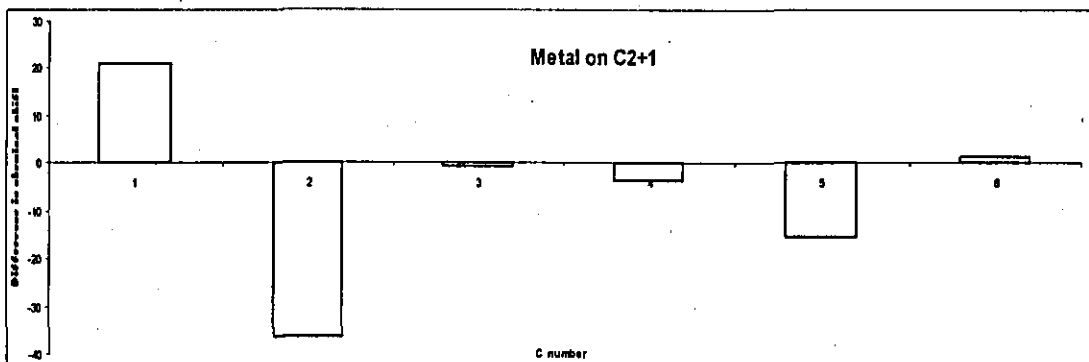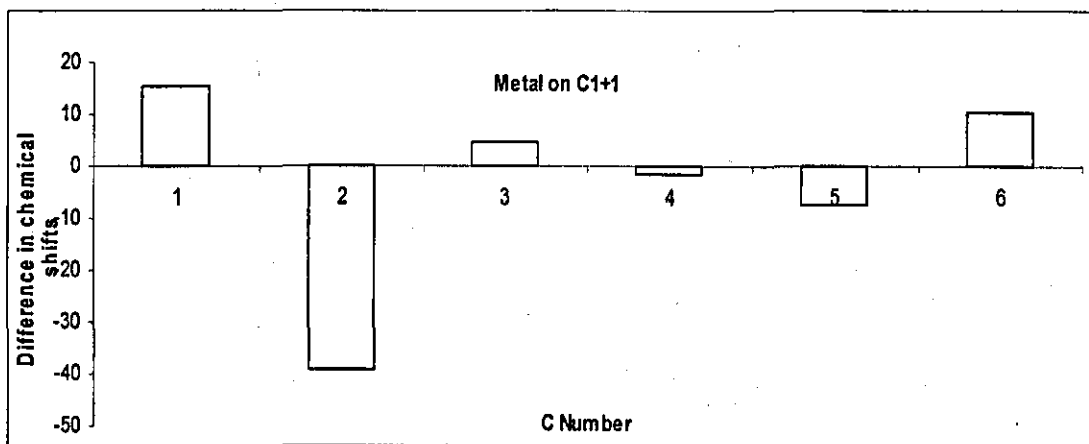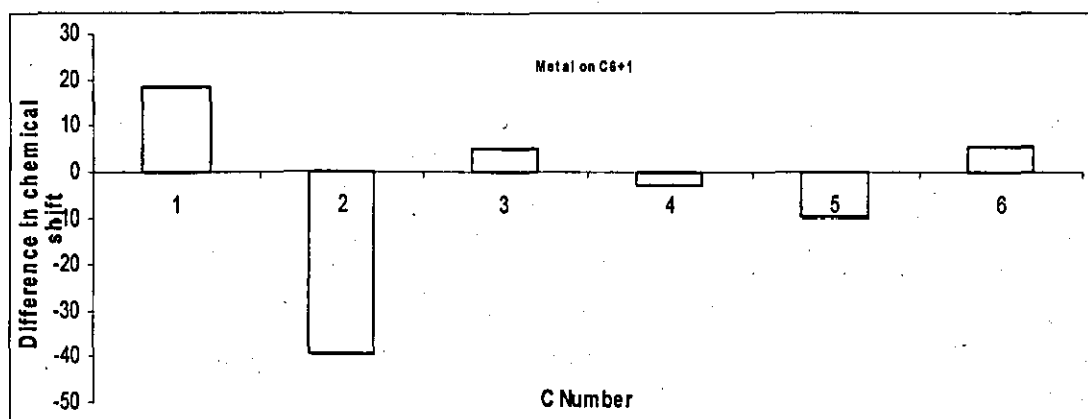
Figure 43 Structure A – 1:1 bidentate. Modelled differences, (carbon chemical shifts of ISA alone) – (carbon chemical shifts of ISA + M) The position of the metal for each complex is at thetop of each individual graph

1.5.6.   Structure B - 1:1 Metal ISA

Inputted structure – The star indicates where the cadmium metal ion was bound to the ligand
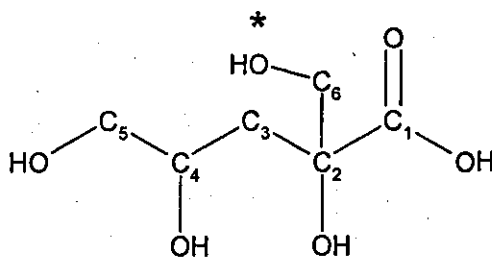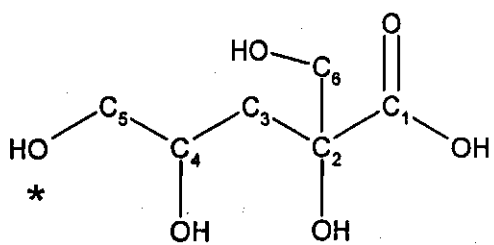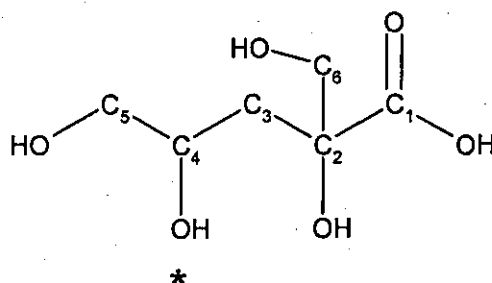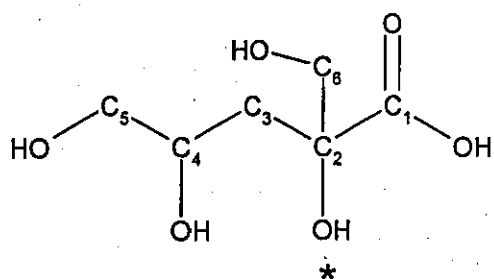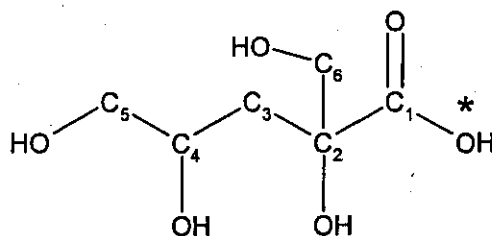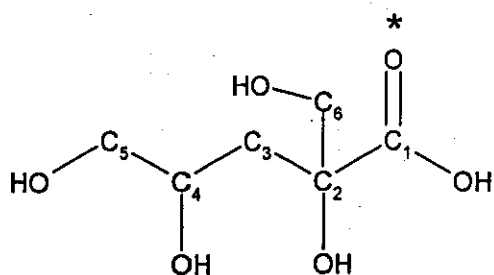
1.5.7.   Structure B - 2:1 Metal ISA
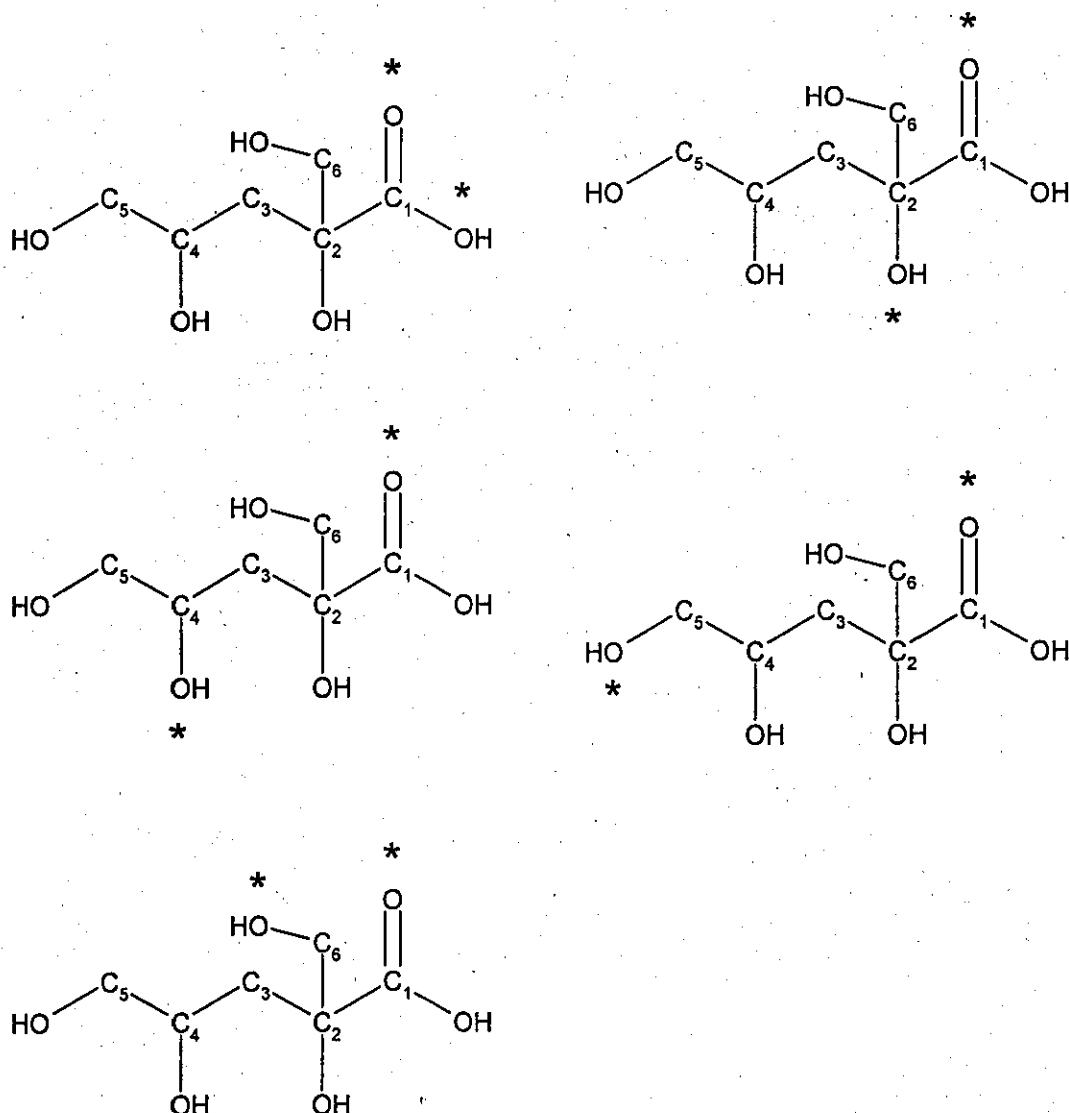
1.5.8.   Structure B - 1:1 Metal ISA - Bidentate

As above for the 2:1 complexes but instead of two metals its just one with two

bonds to the ligand at the starred positions

1.5.9. Structure B - Chemical Shift Data

Table 34 Calculated chemical shifts 1:1 ISA:Metal monodentate

C No	Carbon chemical shifts (ppm) and where the metal was bound						
	Sugar Calculated	Sugar + M 1 (C=O)	Sugar + M 1 (OH)	Sugar + M 2	Sugar + M 4	Sugar + M 5	Sugar + M 6
1	148.15	156.98	160.31	153.77	146.33	144.98	146.47
2	46.15	57.79	65.49	54.28	49.27	55.13	49.02
3	12.85	15.28	31.24	16.15	21.92	18.25	15.73
4	41.65	47.24	60.48	48.66	48.36	47.39	45.98
5	40.45	44.37	57.56	45.92	47.01	46.63	43.55
6	36.85	39.85	55.05	47.14	44.61	39.8	42.79

Table 35 Calculated chemical shifts 1:2 ISA:Metal monodentate

C No	Carbon chemical shifts (ppm) and where the metal was bound					
	Sugar Calculated	Sugar + 2M C1 – C1	Sugar + 2 M C1 - C2	Sugar + 2 M C1 – C4	Sugar + 2 M C1 – C5	Sugar + 2 M C1 – C6
1	148.15	163.92	160.03	153.00	157.80	157.42
2	46.15	56.33	57.61	57.67	55.6	57.59
3	12.85	17.74	14.94	17.86	17.87	16.90
4	41.65	46.05	47.83	47.76	46.20	47.76
5	40.45	48.15	45.54	43.85	44.48	46.85
6	36.85	39.97	43.04	45.35	41.04	46.10

Table 36 Calculated chemical shifts 1:1 ISA:Metal bidentate

C No	Carbon chemical shifts (ppm) and where the metal was bound					
	Sugar Calculated	Sugar + M C1 – C1	Sugar + M C1 - C2	Sugar + M C1 – C4	Sugar + M C1 – C5	Sugar + M C1 – C6
1	148.15	157.13	153.05	148.28	139.59	149.24
2	46.15	57.48	53.57	61.85	54.88	54.84
3	12.85	14.82	14.70	21.84	15.81	13.63
4	41.65	47.83	44.78	47.40	49.36	50.15
5	40.45	43.76	47.71	50.14	38.31	40
6	36.85	45.42	46.47	42.99	49.60	40.75

1.5.10.   Structure A - Gaussian modelling and Experimental comparisons
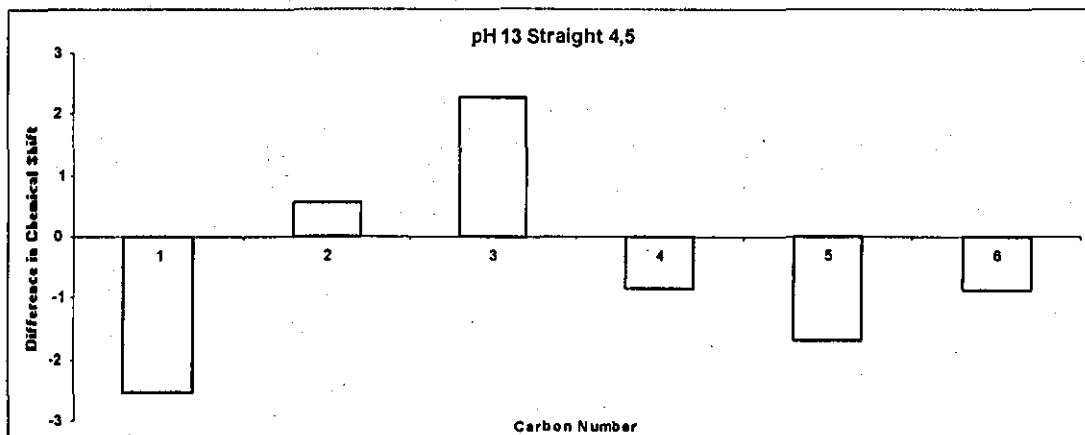
Figure 44 Experimental Differences, (carbon chemical shifts of ISA + M) – (carbon chemical shifts of ISA alone) for pH 13 with carbons 4 and 5 overlapped at 67 ppm
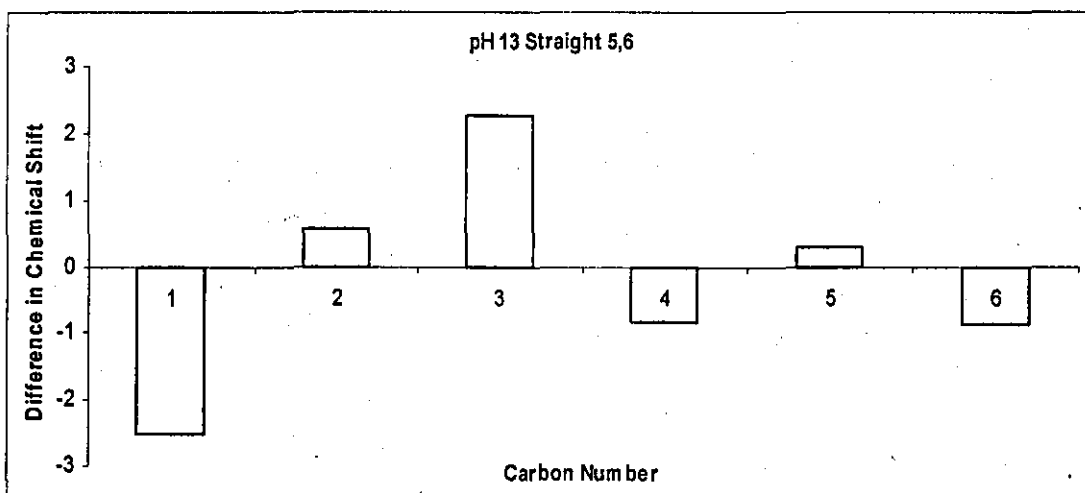

Figure 45 Experimental Differences, (carbon chemical shifts of ISA + Metal) – (carbon chemical shifts of ISA alone) for pH 13 with carbons 5 and 6 overlapped at 69 ppm
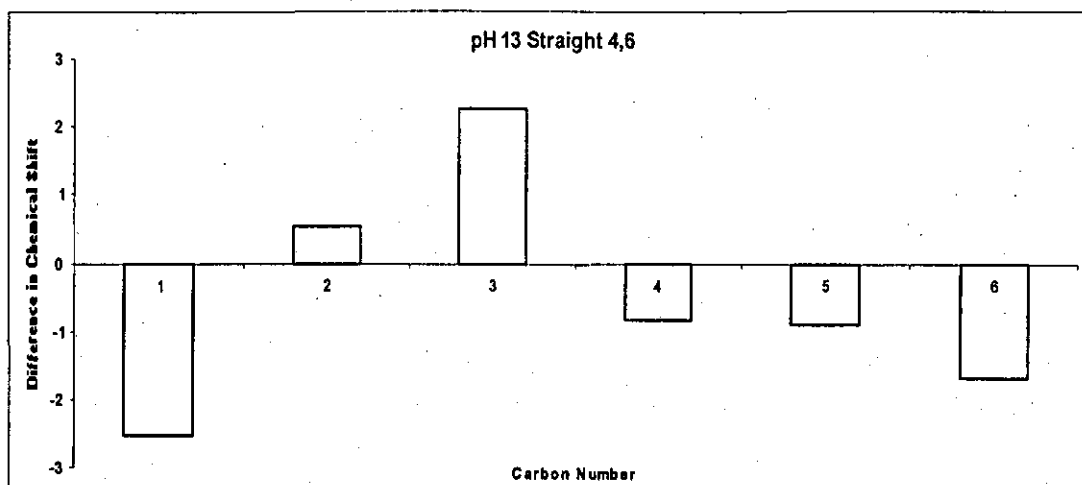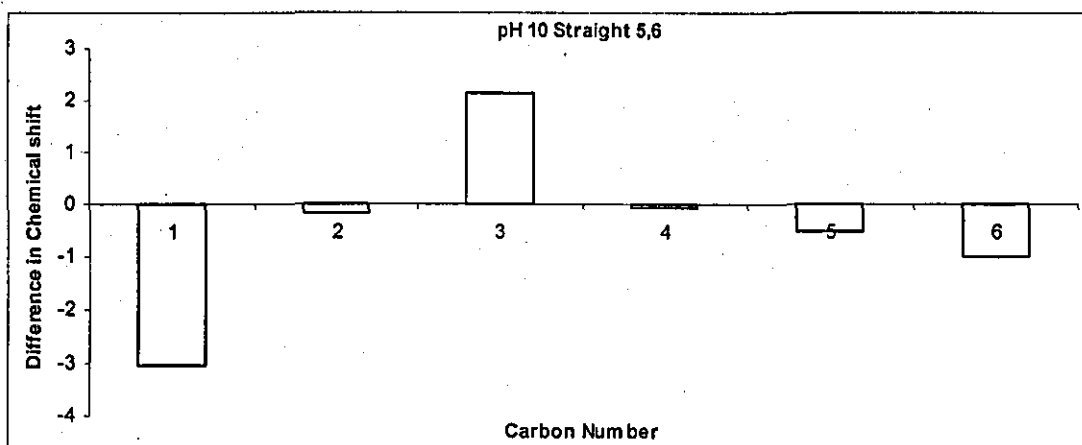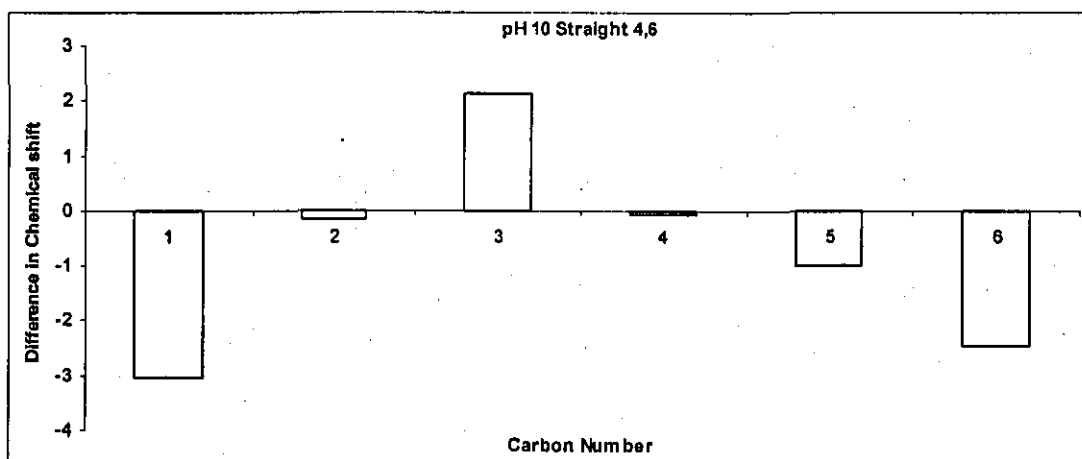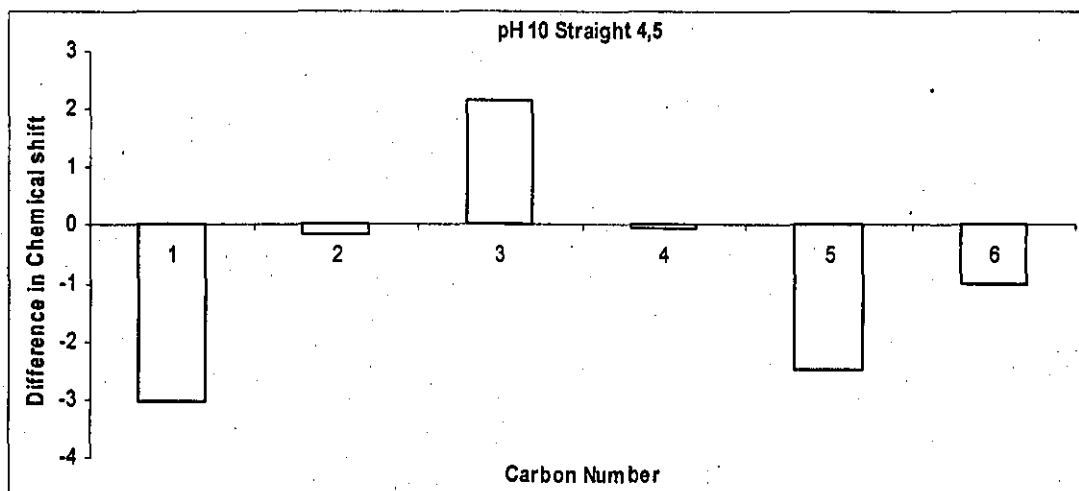
Figure 46 Experimental Differences, (carbon chemical shifts of ISA + Metal) – (carbon chemical shifts of ISA alone) for pH 13 with carbons 4 and 6 overlapped at 69 ppm

Figure 47 Experimental Differences, (carbon chemical shifts of ISA + Metal) – (carbon chemical shifts of ISA alone) for pH 10 with carbons 5 and 6 overlapped at 67 ppm

Figure 48 Experimental Differences, (carbon chemical shifts of ISA + Metal) – (carbon chemical shifts of ISA alone) for pH 10 with carbons 4 and 6 overlapped at 69 ppm

Figure 49 Experimental Differences, (carbon chemical shifts of ISA + M) – (carbon chemical shifts of ISA alone) for pH 10 with carbons 4 and 5 overlapped at 67 ppm
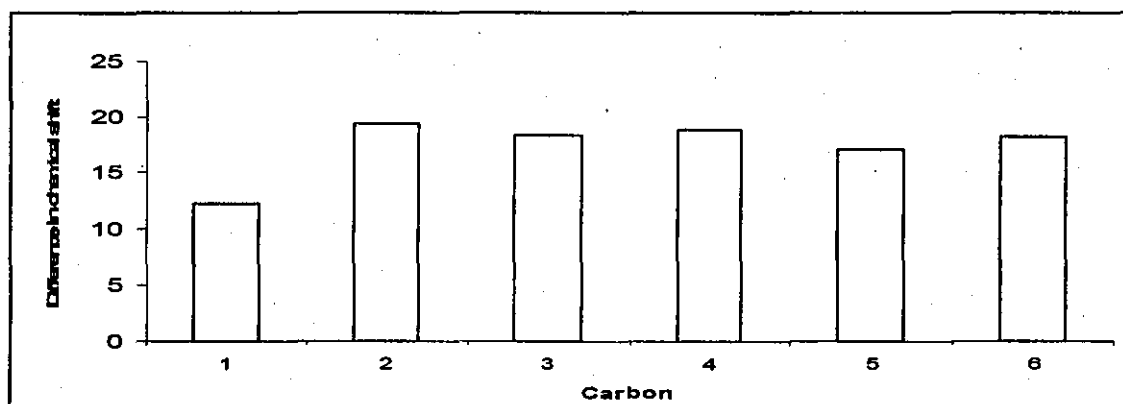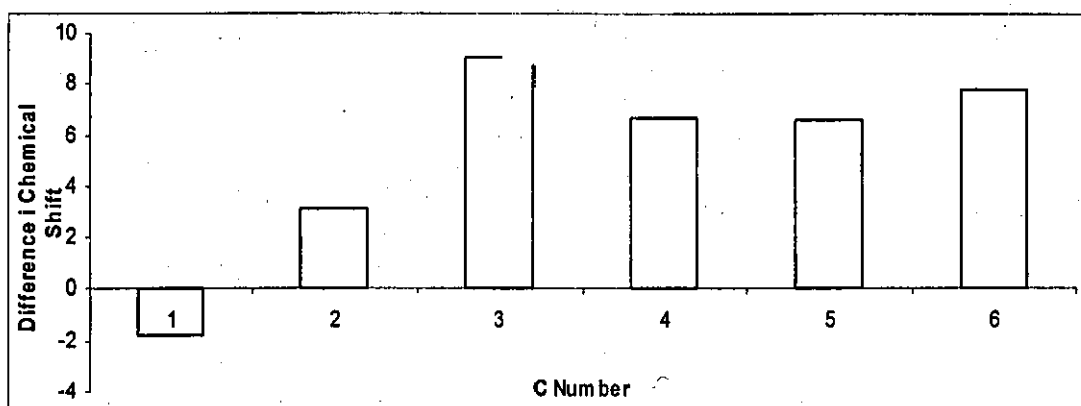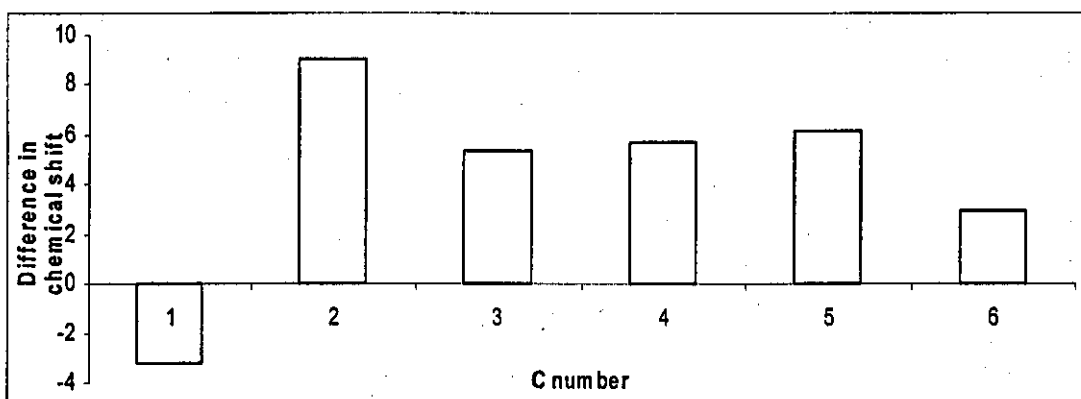

Figure 50 Structure B – 1:1 monodentate. Modelled differences, (carbon chemical shifts of ISA alone) – (carbon chemical shifts of ISA + M) Cd bonded to the hydroxyl group on carbon 1
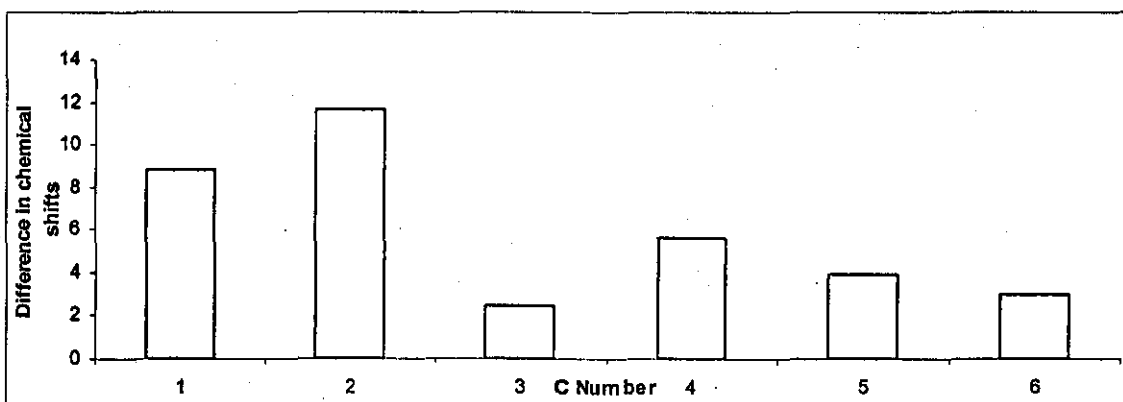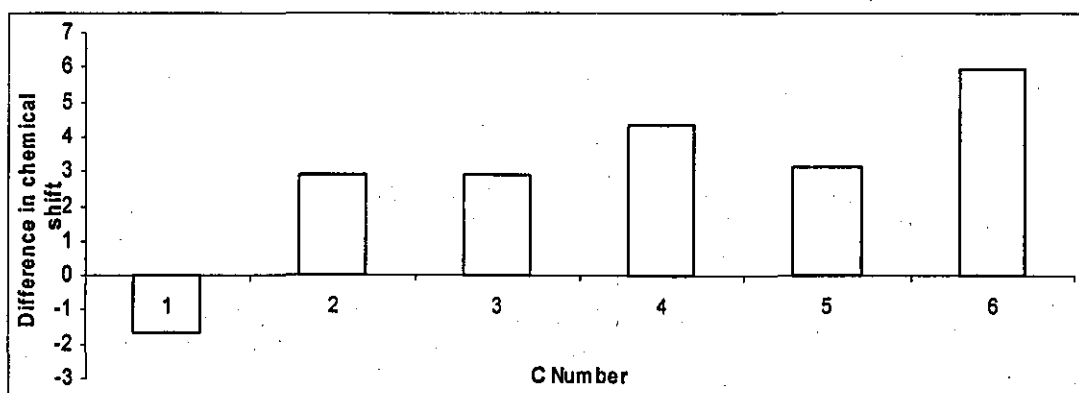

Figure 51 Structure B – 1:1 monodentate. Modelled differences, (carbon chemical shifts of ISA alone) – (carbon chemical shifts of ISA + M) Cd bonded to the carboxyl group on carbon 1
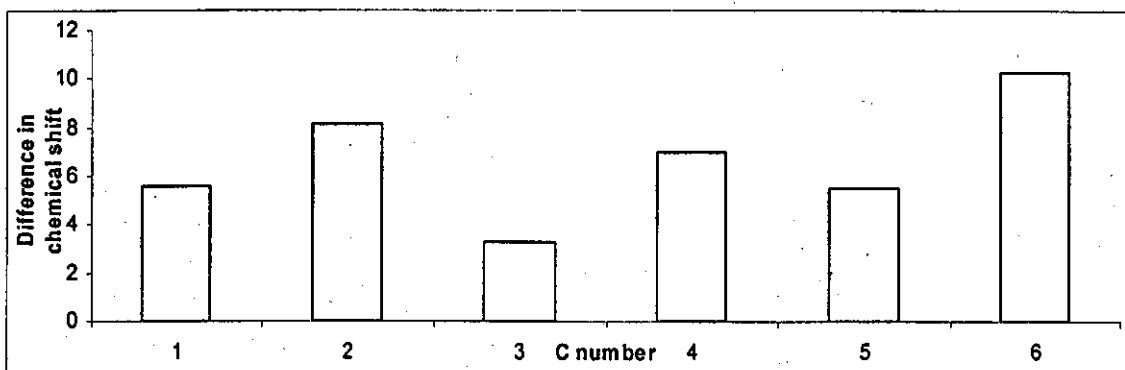
Figure 52 Structure B – 1:1 monodentate. Modelled differences, (carbon chemical shifts of ISA alone) – (carbon chemical shifts of ISA + M) Cd bonded to the hydroxyl group on carbon 2

Figure 53 Structure B – 1:1 monodentate. Modelled differences, (carbon chemical shifts of ISA alone) – (carbon chemical shifts of ISA + M) Cd bonded to the hydroxyl group on carbon 4

Figure 54 Structure B – 1:1 monodentate. Modelled differences, (carbon chemical shifts of ISA alone) – (carbon chemical shifts of ISA + M) Cd bonded to the hydroxyl group on carbon 5

Figure 55 Figure 56 Structure B – 1:1 monodentate. Modelled differences, (carbon chemical shifts of ISA alone) – (carbon chemical shifts of ISA + M) Cd bonded to the hydroxyl group on carbon 1
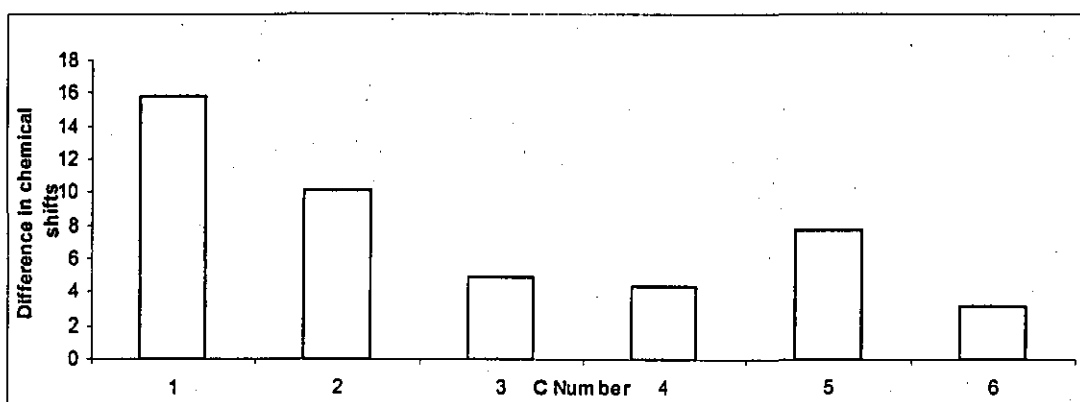

Figure 57 Structure B – 2:1 M:ISA. Modelled differences, (carbon chemical shifts of ISA alone) – (carbon chemical shifts of ISA + M) Cd bonded to carbon 1
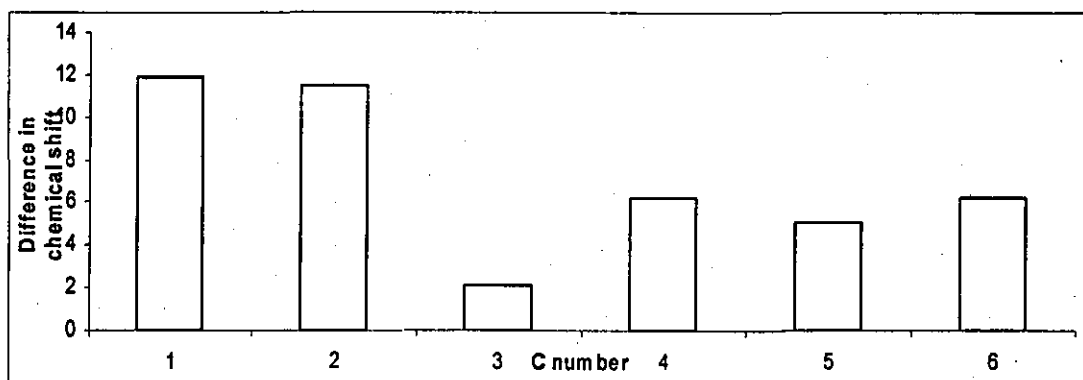

Figure 58 Structure B – 2:1 M:ISA. Modelled differences, (carbon chemical shifts of ISA alone) – (carbon chemical shifts of ISA + M) Cd bonded to carbon 1 (carboxyl group) and carbon 2 (hydroxyl)
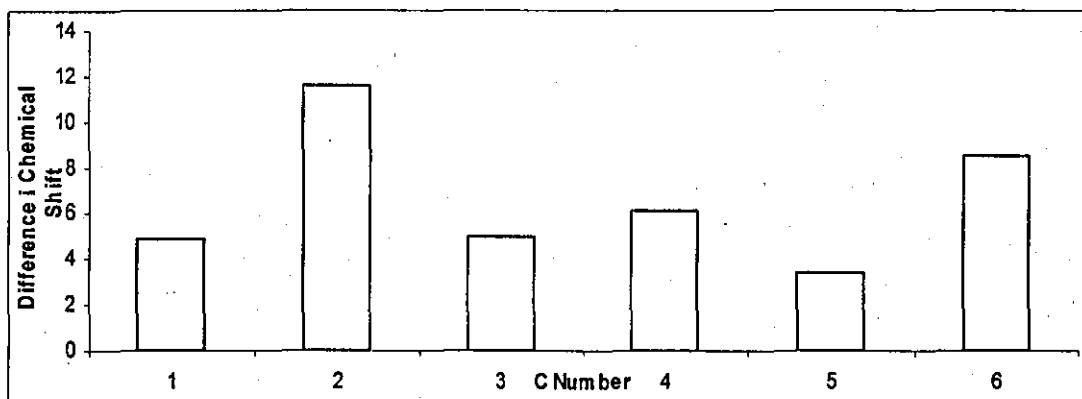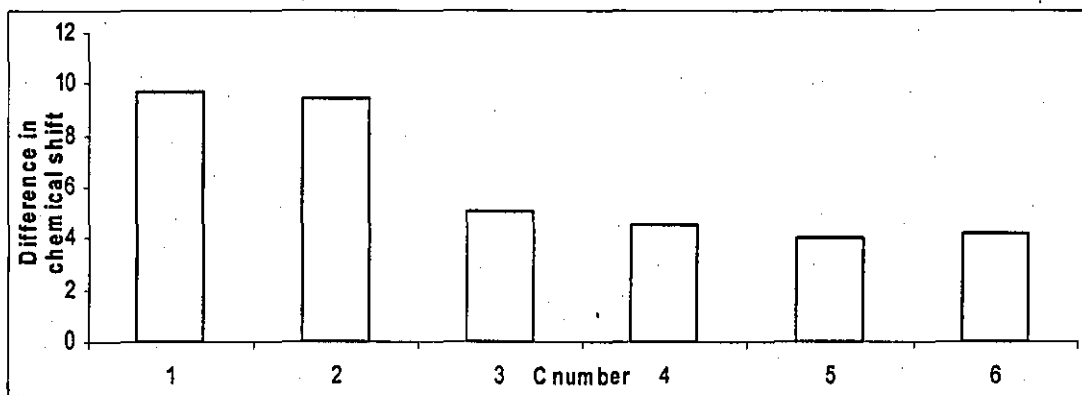
Figure 59 Structure B – 2:1 M:ISA. Modelled differences, (carbon chemical shifts of ISA alone) – (carbon chemical shifts of ISA + M) Cd bonded to carbon 1 (carboxyl group) and carbon 4 (hydroxyl)

Figure 60 Structure B – 2:1 M:ISA. Modelled differences, (carbon chemical shifts of ISA alone) – (carbon chemical shifts of ISA + M) Cd bonded to carbon 1 (carboxyl group) and carbon 5 (hydroxyl)
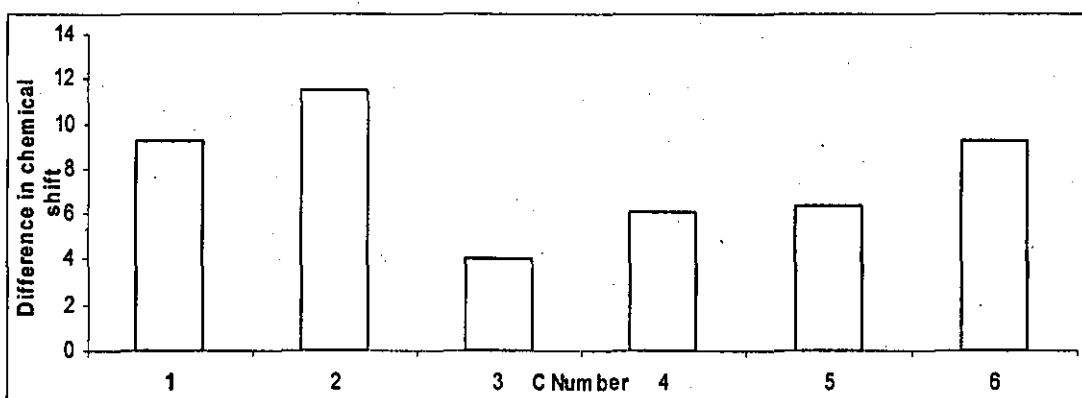

Figure 61 Structure B – 2:1 M:ISA. Modelled differences, (carbon chemical shifts of ISA alone) – (carbon chemical shifts of ISA + M) Cd bonded to carbon 1 (carboxyl group) and carbon 6 (hydroxyl)
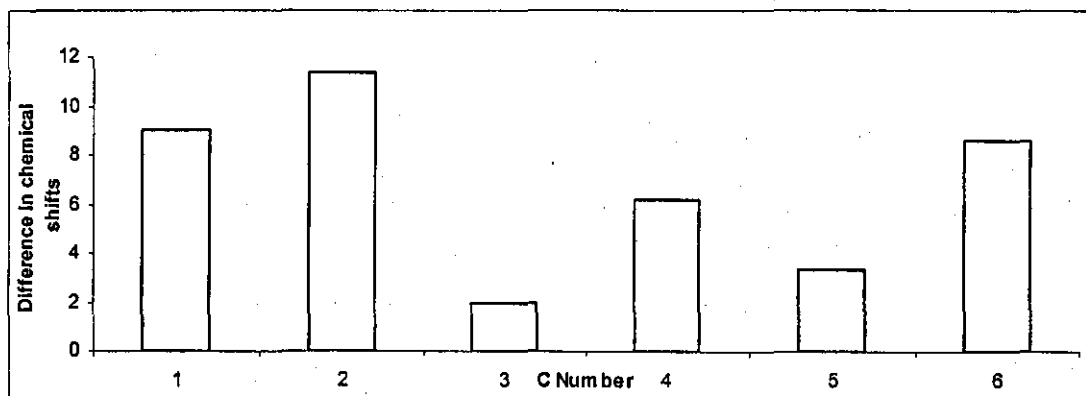
Figure 62 Structure B – 1:1 bidentate. Modelled differences, (carbon chemical shifts of ISA alone) – (carbon chemical shifts of ISA + M) Cd bonded to carbon 1
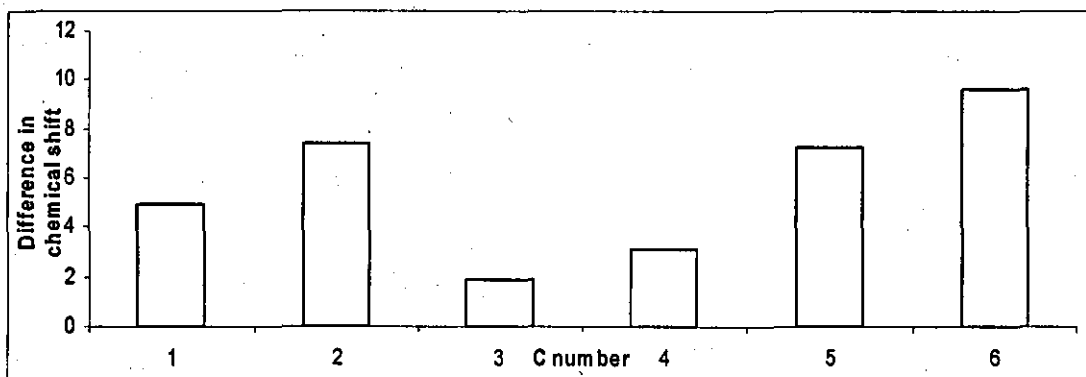

Figure 63 Structure B – 1:1 bidentate. Modelled differences, (carbon chemical shifts of ISA alone) – (carbon chemical shifts of ISA + M) Cd bonded to the carboxyl group on carbon 1 and the hydroxyl group on carbon 2

Figure 64 Structure B – 1:1 bidentate. Modelled differences, (carbon chemical shifts of ISA alone) – (carbon chemical shifts of ISA + M) Cd bonded to the carboxyl group on carbon 1 and the hydroxyl group on carbon 4
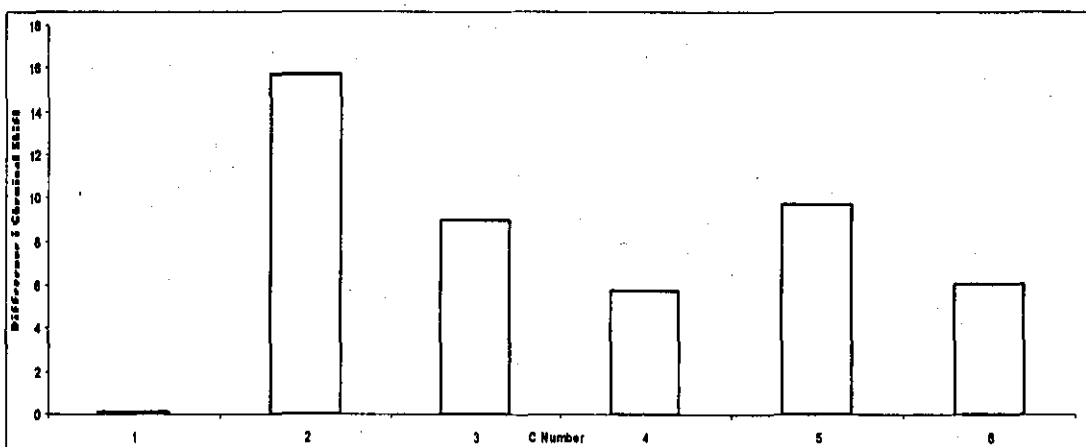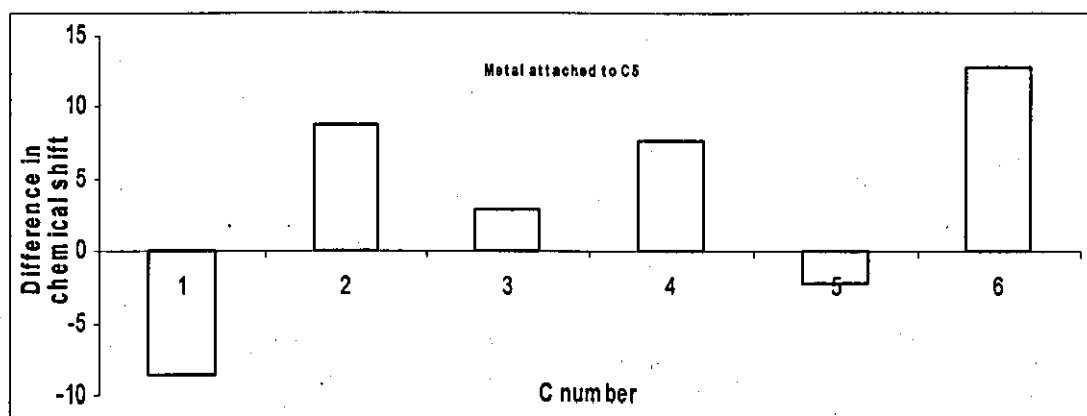
Figure 65 Structure B – 1:1 bidentate. Modelled differences, (carbon chemical shifts of ISA alone) – (carbon chemical shifts of ISA + M) Cd bonded to the carboxyl group on carbon 1 and the hydroxyl group on carbon 5

Figure 66 Structure B – 1:1 bidentate. Modelled differences, (carbon chemical shifts of ISA alone) – (carbon chemical shifts of ISA + M) Cd bonded to the carboxyl group on carbon 1 and the hydroxyl group on carbon 6
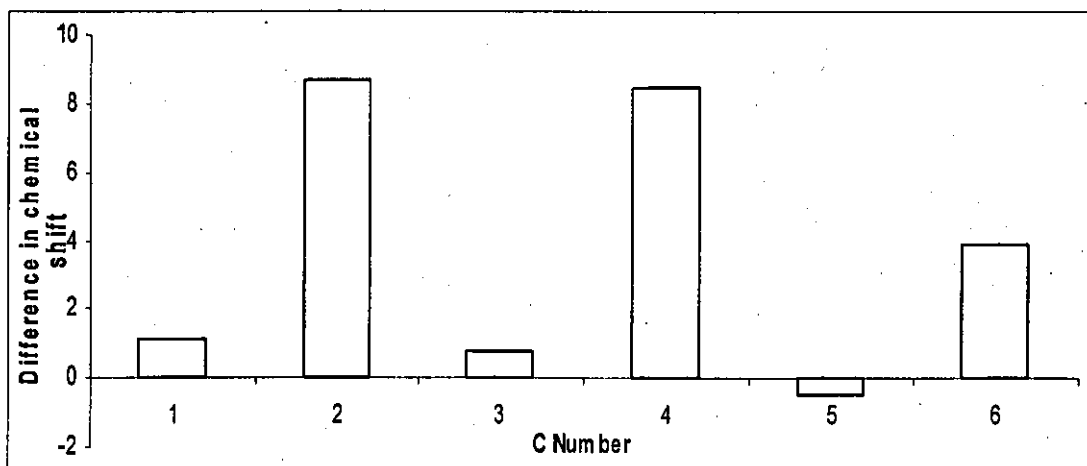
Professional Development Training

Date	Topic	Event and Lecturer
03/08/05	PhD induction day	Andrew Wilson, Brigette Vale, Jodie Clark, Rob Kirkwood.
06/09/05	Health and Safety	Dave Wilson
11/10/05	Presentation Skills	Ernie Mills
19/10/05	Reading for research	Jo Gilman
25/10/05	Chemistry friend of foe	David Lathbury, RSC Lecture at Loughborough University
08/11/05	Colloids	Aquanet conference Birmingham, various speakers
22/11/05	Tour of Sellafield Labs BFC	
23/11/05	Radiochemistry in Nuclear Cleanup – Exploring the Role of Chemistry and radiochemistry in the clean up and remediation of the UK's historic nuclear legacy.	Various Speakers
18/01/06	Materials for Nuclear Waste Management, An RSC Workshop.	Various Speakers
07/02/06	Young researchers meeting, Environmental Radiochemistry.	Various Speakers
09/02/06	Nirex Progress Meeting	Charlotte Heath, Nick Evans, Tara Lewis and Sturat Aldridge.
06-10/03/06	Advanced Topspin NMR Course	Bruker
30-31/03/06	EPSRC Solid-State NMR Service Training Course, Durham	Various Speakers
03-06/04/06	COGER 2006 Co-ordinating group on environmental radioactivity.	Various Speakers including myself
15-20/05/06	ThUL School 2003, Lille, Actinet. Designed to bring Theoreticians and experimentalists together.	Various Speakers
3-7/07/06	ACTINET Summer school on actinide migration	Various Speakers
29/11/06	RSC – Radiochemistry and radioactively Contaminated Land, Leeds	Various Speakers

8-9/02/07	Nexia Solutions – Underpinning Assesment Sciences Programme Symposia	Various Speakers including myself
17-19/04/07	COGER 2006 Co-ordinating group on environmental radioactivity.	Various Speakers
26-31/08/07	Migration Conference, Munich	Various Speakers and I presented a poster
21/11/07	RSC Materials Science Conference	Various Speakers
19/02/08	Nexia Solutions Conference	Various Speakers
2006-2008	Physical Chemistry 1st year lab demonstrator	
2006-2008	Radiochemistry Group Meetings	Various Speakers including myself for 5 formal presentations